UNIVERSITÀ
DEGLI STUDI
DI PADOVA

Sede Amministrativa: Università degli Studi di Padova

Dipartimento di Biologia

CORSO DI DOTTORATO DI RICERCA IN: BIOSCIENZE E BIOTECNOLOGIE
CURRICOLO: GENETICA E BIOLOGIA MOLECOLARE DELLO SVILUPPO
CICLO: XXIX

Peptidergic control of dormancy in *Drosophila melanogaster*

Tesi redatta con il contributo finanziario del progetto INsecTIME Marie Curie Initial Training Network, grant PITN-GA-2012-316790.

Coordinatore: Ch.mo Prof. Paolo Bernardi
Supervisore: Ch.mo Prof. Rodolfo Costa
Co-Supervisore: Ch.mo Prof. Gabriella Mazzotta

Dottoranda: DÓRA NAGY

TABLE OF CONTENTS

LIST OF FIGURES

LIST OF TABLES

ABSTRACT

Organisms, especially those living in temperate zones, are constantly exposed to the cyclical changes of environmental factors due to the alternating seasons. In order to increase their chances of survival, they evolved different adaptive mechanisms to withstand the stress of harsh periods. Among insects, diapause is the most commonly used strategy to achieve seasonal synchronization.

Diapause is a neuro-hormonally regulated state of dormancy that enables insects to switch to an alternative developmental program when external conditions are not suitable for normal development. In the fruit fly, *Drosophila melanogaster*, diapause is characterized by the arrest of the ovarian development at previtellogenic stages. Insulin-like signaling has been identified as a key regulator of dormancy in many organisms. The insulin producing cells (IPCs), located in the *Pars intercerebralis*, are crucial neurosecretory cells that are neuroanatomically connected to the neuroendocrine center that governs hormonal regulation of diapause. They are responsible for the production and release of different insulin-like peptides that have been found to act as diapause-antagonist hormones. Here we found that two neuropeptides, pigment dispersing factor (PDF) and short neuropeptide F (sNPF), produced in a small subset of neurons (ventrolateral clock neurons, LN_vs), modulate the diapause response of the flies, and this regulation is likely to exist via the IPCs. We discovered that an additional PDF-expressing neuron cluster in the tritocerebrum (PDF-Tri), previously shown to undergo apoptosis very early during adulthood, actually survives at cold temperatures and could be involved in cold-related functions. Interestingly, these PDF-Tri neurons were found to be synaptically connected to the IPCs in the cold.

Expression of genetically encoded sensors for the second messenger cAMP revealed that, IPCs respond to both synthetic neuropeptides PDF and sNPF. Surprisingly, they react with large cAMP increases to the co-application of the two peptides, raising the possibility of a synergistic effect between sNPF and PDF in controlling IPC activity. Since the detected cAMP responses are all abolished in PDF receptor mutant background, they seem to be regulated by PDFR. The study of two differently diapausing field lines highlighted marked differences between their PDF expression patterns, possibly related to diapause regulation.

When studying the general properties of *D. melanogaster* dormancy, we explored the relative relevance of some features of the experimental protocols used for diapause

assays. While in the standard protocol flies are raised at temperatures in the range 23-25°C and exposed to diapause-inducing conditions starting from the adult stage, we investigated the effects of lower growing temperatures on diapause levels. We documented changes in diapause levels due to these altered settings, highlighting their importance in controlling dormancy. Additionally, adopting semi-natural light-dark profiles that better mimic outdoor conditions, strong photoperiodic diapause was observed, which was not detectable when simple rectangular light-dark regimes were used. Our findings should be considered in designing new protocols for diapause studies.

RIASSUNTO

Gli organismi, soprattutto quelli che vivono in zone temperate, sono costantemente esposti a variazioni cicliche di fattori ambientali a causa dell'alternarsi delle stagioni. Si sono evoluti diversi meccanismi di adattamento che permettono di resistere e superare i periodi sfavorevoli. Tra gli insetti, la diapausa è la più comune strategia usata per raggiungere la sincronizzazione stagionale.

La diapausa è uno stato di dormienza, regolato a livello neurologico ed ormonale, che permette agli insetti di avviare un programma di sviluppo alternativo quando le condizioni ambientali non permettono un normale sviluppo. Nel moscerino della frutta *Drosophila melanogaster*, la diapausa si manifesta con l'arresto dello sviluppo delle ovaie nella frase previtellogenica. Segnali di tipo *insulin-like* sono stati identificati come regolatori chiave della dormienza in molti organismi. Le *insulin-producing cells* (IPCs) si trovano nella *Pars intercerebralis*, sono neuroanatomicamente connessi al centro neuroendocrino che controlla la regolazione ormonale della diapausa. Queste cellule sono responsabili della produzione e del rilascio di differenti *insulin-like peptides* che sono stati identificati come ormoni antagonisti della diapausa. Abbiamo scoperto che due neuropeptidi*, pigment dispersing factor* (PDF) e *short neuropeptide F* (sNPF), prodotti da un piccolo gruppo di neuroni chiamati *ventrolateral clock neurons*, regolano il processo della diapausa nei moscerini attraverso le IPCs.

Inoltre, abbiamo osservato che un altro gruppo di neuroni che producono PDF nel *tritocerebrum* (PDF-Tri) e che si ritenevano strutture rapidamente eliminate per apoptosi nell'adulto, in realtà sopravvivono e persistono nell'adulto a basse temperature, suggerendo quindi un loro coinvolgimento in funzioni correlate con la resistenza al freddo. L'espressione di sensori *genetically-encoded* per il secondo messaggero cAMP, ha rilevato che le IPCs reagiscono ad entrambi i neuropeptidi PDF e sNPF. Sorprendentemente reagiscono con grandi aumenti di cAMP alla somministrazione dei due peptidi, suggerendo un effetto sinergico tra sNPF e PDF nel controllo dell'attività delle IPCs. Dal momento che le risposte cAMP sono state abolite nel background mutante per il recettore PDF, sembrano essere regolate dallo stesso.

Lo studio di due diverse linee che manifestano differenze nel comportamento relativo alla diapausa ha evidenziato differenze marcate nell'espressione di PDF, potenzialmente collegata della regolazione della diapausa.

Studiando le proprietà generali della diapausa in *D. melanogaster*, abbiamo esplorato l'importanza relativa di alcuni aspetti dei protocolli sperimentali usati per i saggi di diapausa. Mentre nel protocollo originale i moscerini vengono fatti sviluppare a temperature comprese nel range 23-25^{o}C e quindi esposti a condizioni che inducono la diapausa solo a partire dallo stadio adulto, noi abbiamo studiato gli effetti sui livelli di diapausa dello sviluppo a temperature inferiori. Abbiamo documentato cambiamenti nei livelli di diapausa indotti da queste modifiche, sottolineando la loro importanza nel controllo della dormienza. Inoltre, adottando profili di luce-buio seminaturali, che mimano meglio le condizioni esterne, è stata osservata una diapausa altamente regolata dal fotoperiodo. Una risposta fotoperiodica non era stata rilevata in studi precedenti nei quali venivano utilizzati regimi di luce-buio rettangolari. I nostri risultati suggeriscono l'opportunità di disegnare nuovi protocolli, più rappresentativi delle condizioni naturali, per lo studio delle basi genetiche e fisiologiche della diapausa.

Abbreviations

AKH: adipokinetic hormone

Ast-A: allatostatin-A

Ast-C: allatostatin-C

CaLexA: calcium-dependent nuclear import of LexA

cAMP: cyclic adenosine monophosphate

CCh: carbamylcholine

CLK, *clk*: CLOCK protein, *clk* gene and mRNA

Crz: corazonin

CrzR: corazonin receptor

CRY: cryptochrome

CYC, *cyc*: CYC protein, *cyc* gene and mRNA

DILP1-8, *dilp1-8*: *Drosophila melanogaster* insulin-like protein 1-8 and their gene and mRNA

DLPs: dorsal-lateral peptidergic neurons

DN1, -2, -3: dorsal clock neurons (first, second and third cluster, respectively)

DTK: Drosophila tackhykinin

EPAC: exchange protein directly activated by cAMP

FRET: fluorescence resonance energy transfer

GFP: green fluorescent protein

GPCR: G protein-coupled receptor

Imp-L2: imaginal morphogenesis protein-Late 2

InR: insulin receptor

IPC: insuling producing cell

JH: juvenile hormone

LD cycle: light-dark cycle

l-LN_vs: large ventrolateral neurons

LN_ds: dorsal lateral neurons

LS-TIM, *ls-tim*: long (l) and short (s) forms of TIMELESS protein and gene

NFAT: nuclear factor of activated T cells

PDF: pigment dispersing factor

PDFR: pigment dispersing factor receptor (also called han)

PDF-Tri: PDF neurons in the tritocerebrum

PER, *per*: PERIOD protein, *period* gene and mRNA

PI3K: phosphatidylinositol 3-kinase

PI: *Pars intercerebralis*

PL: *Pars lateralis*

s-LN_vs: small ventrolateral neurons

S-TIM, s-*tim*: short form of TIMELESS protein and gene

sNPF: short neuropeptide F

sNPFR1: short neuropeptide F receptor

TIM, *tim*: TIMELESS protein, *timeless* gene and mRNA

TTX: tetrodotoxin

UAS: upstream activating sequence

1. Introduction

1.1. Biological rhythms

Living organisms are constantly exposed to cyclical changes of environmental factors, such as the alternation of day and night, the cycle of the seasons, as well as fluctuations in temperature and nutritional conditions. In order to achieve a life in harmony with their environment, they have evolved endogenous biological clocks that allow them to coordinate their physiology and behavior with the external world. Biological clocks function both as daily time measuring systems and as calendars that tell the time of the year.

The circadian clock is an endogenous time keeper that functions as a daily timer with an intrinsic period of approximately 24 hours. It helps the organisms to adapt to the daily changes of their surroundings, primarily to the predictable rhythms in light/dark and temperature cycles, which occur each day due to the earth's rotation about its axis. These internal circadian clocks regulate a wide range of biological processes: the body temperature, the sleep-wake cycle, the locomotion, the production of asexual spores (conidia) in fungi, as well as the movement of the leaves around the 24 h in several plants (Kreitzman & Foster 2009).

However, living creatures ought to have a flexible physiology suitable for facing not only the daily cyclical changes of the different environmental factors but also those happening seasonally as a consequence of the Earth's orbit around the Sun. Endogenous seasonal timers help the organisms to track the time of the year, serving as a seasonal clock machinery. With the shortening days and falling temperatures, migrating animals, like birds, escape the cold and travel in search of a new habitat to successfully survive the upcoming harsh season. Before bedding down, hibernating animals work hard in order to accumulate fat reserves that will provide them with energy during the dormant period. Before they take off, they run through a repertoire of behavioral and physiological changes, including an increase in appetite and food consumption (Kreitzman & Foster 2009). All of these adaptation mechanisms become extremely important when organisms have to bridge thermally stressful harsh winters or dry seasons, when food sources are poorly available and life conditions are not appropriate for normal development.

The first evidence for the existence of a so called "circannual biological clock" comes from the study conducted by Pengelly and Fisher (1957), who kept golden-mantled ground

squirrels in a highly controlled laboratory environment (12 hours on/off and constant temperature) with the attempt to study how their hibernation pattern was influenced when all external cues were excluded. Surprisingly, even when kept in these artificial conditions, the squirrels hibernated from October to April (Pengelly & Fisher 1957). Wild birds kept in captivity (12 hours on/off and constant temperature) still showed annual rhythm of migratory behavior (Gwinner 1986). These studies clearly indicate that both hibernation and migration are influenced by an internal circannual clock, since the animals tested could not rely on prior experience.

Among insects, diapause is a major strategy to achieve seasonal synchronization (Tauber et al. 1986). With the onset of winter, diapausing individuals switch to an alternative developmental pathway by entering a dormant state. Diapausing animals are characterized by accumulated energy stores and metabolic depression, and go through numerous developmental and hormonal changes, all of which supporting successful survival.

1.2. Diapause - a state of developmental arrest

Diapause is an overwintering strategy widely used by insects in order to survive adverse seasons. It refers to a form of developmental arrest/slow-down, analogous to hibernation in mammals. With an upcoming harsh season, diapausing animals manage to "escape in time" by shifting their energy-expensive processes to more favorable periods of the year when many nutrients are available. Diapause also means remarkable changes in patterns of gene expression: numerous genes are silenced during the dormant state, while others are highly upregulated, revealing the complexity in the regulation of this phenomenon at the molecular level (Denlinger 2002; Williams et al. 2006; Kubrak et al. 2014; Kučerová et al. 2016; Schiesari et al. 2016; Liu et al. 2016; Zhao et al. 2016).

It is important to emphasize that diapause is not identical to quiescence, which is an alternative form of insect dormancy. The most important difference between these two forms of animal dormancy is that, while quiescence is an immediate response to an unpredictable environmental change, diapause is a much more complex, pre-programmed developmental arrest: an anticipated dormant state induced by predictable, seasonally recurring changes of the environment (Poelchau et al. 2013). In case of quiescence, the

normal activity of the organism resumes once the environmental conditions become favorable. By contrast, in the diapause-destined insects the diapause program starts long before the advent of the severe conditions, allowing the organisms to get prepared for the stressful period by switching to another metabolic pathway and store additional energy reserves (Hahn & Denlinger 2011).

Photoperiod (i.e. changes in the length of the day) is believed to be the most important environmental signal that can trigger the initiation of diapause. Though it shows marked changes between the different seasons, its value on a given date repeats year after year. Therefore, it provides a reliable indicator of the time of year that organisms can measure to get seasonal information from their external environment (Tauber et al. 1986; Kreitzman & Foster 2009). The critical photoperiod, which refers to the photoperiod that induces diapause response in 50% of the individuals, varies widely among species. The other diapause-initiating environmental stimulus is a drop in temperature (thermoperiod). However, it cannot be considered as a stable seasonal indicator, since it might vary from year to year (Tauber et al. 1986; Kreitzman & Foster 2009).

Diapause can happen at any developmental stage of an insect life cycle (egg, larvae, pupae, and adult). It is always triggered in a single specific stage ("sensitive stage") of the life cycle, however can be manifested in another stage ("diapausing stage") (Denlinger 2002). For instance, the silkworm *Bombyx mori* exhibits a maternally controlled embryonic diapause, induced in the maternal generation and exhibited in the egg stage (Hasegawa 1951).

The drosophilid fly *Chymomyza costata* enters diapause at the larval stage in response to short-day signals sensed by the third larval stage (Riihimaa et al. 1988) (*Figure 1*). When reared under short days, Chinese oak silk moth *Antheraea pernyi* goes to a dormant state at pupal stage. Interestingly, in this species there is a transparent patch of cuticle over the pupal brain functioning as a photoperiod-sensitive organ, which plays an important role in diapause regulation (Williams & Adkisson 1964) (*Figure 1*). Adult females of the linden bug *Pyrrhocoris apterus* initiate the diapause program when experience short-day photoperiods and low temperatures. The ovarian development of diapausing females is arrested/slowed-down at previtellogenic stages during the period of dormancy (Hodek 1971) (*Figure 1*).

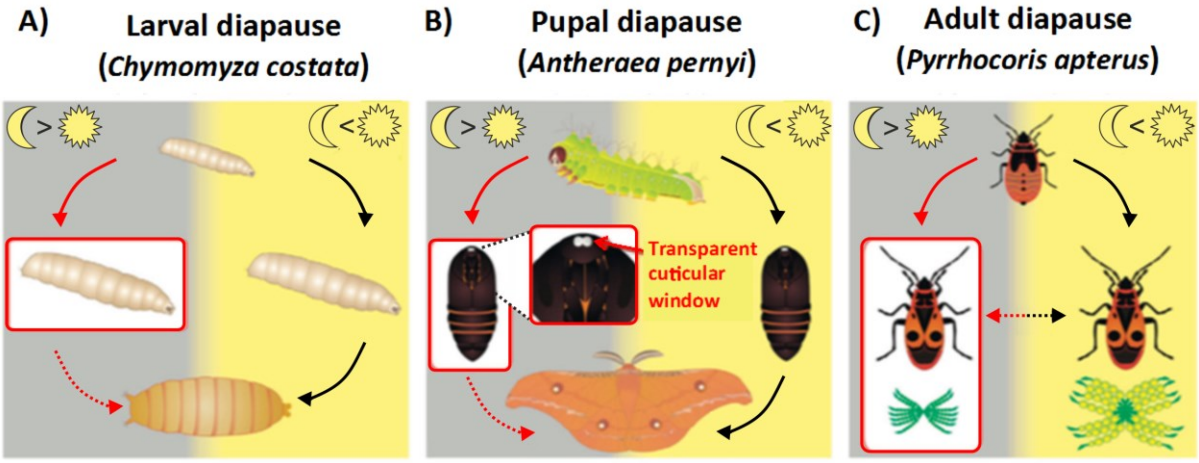

Figure 1. Schematic illustration of insect species entering diapause at different stages. Based on photoperiodic information experienced by the sensitive stage, the developmental program can be switched from reproductive state to diapause. (A) In the drosophilid fly *Chymomyza costata* diapause occurs in larval stage. (B) *Antheraea pernyi* enters diapause at the pupal stage, and this process is modulated by a transparent patch of cuticle directly over the brain. (C) The linden bug *Pyrrhocoris apterus* overwinters in a state of adult reproductive dormancy, characterized by suspended ovarian maturation. The diapausing stage is highlighted in red square. The figure is modified from Dolezel 2015.

Many insects have been tested to study diapause and discover the exact molecular mechanisms that lead to this developmental arrest. The fruit fly *Drosophila melanogaster* has been an excellent model for genetic studies for more than 100 years. It is considered a powerful model organism to study a large number of biological processes including genetics and inheritance, embryonic development, learning, behavior, and aging. It has several advantages as a model organism, for instance its cost-effective maintenance, short generation time (10 days at 25^{o}C), and numerous available genetic mutants and genetic tools for targeted gene expression (Beckingham et al. 2005). Saunders et al. described the first diapause experiments with *Drosophila melanogaster*, exposing newly eclosed females to a range of photoperiods at low temperature, thereby mimicking the shortening days and falling temperatures of upcoming winters (Saunders et al. 1989). When maintained under these conditions, females displayed reproductive diapause characterized by marked reduction in the ovarian maturation (Saunders et al. 1989; Saunders et al. 1990). While non-diapausing females initiate vitellogenesis and complete ovarian development, the ovaries of diapausing flies are arrested in previtellogenic stages (Saunders et al. 1989; Saunders et al. 1990) (*Figure 2*). In *D. melanogaster*, the development of the egg chamber is divided into 14 stages (St 1-14), among which stage 8 is a phase when oocytes begin to largely increase in volume due to yolk protein synthesis and uptake (*Figure 2*).

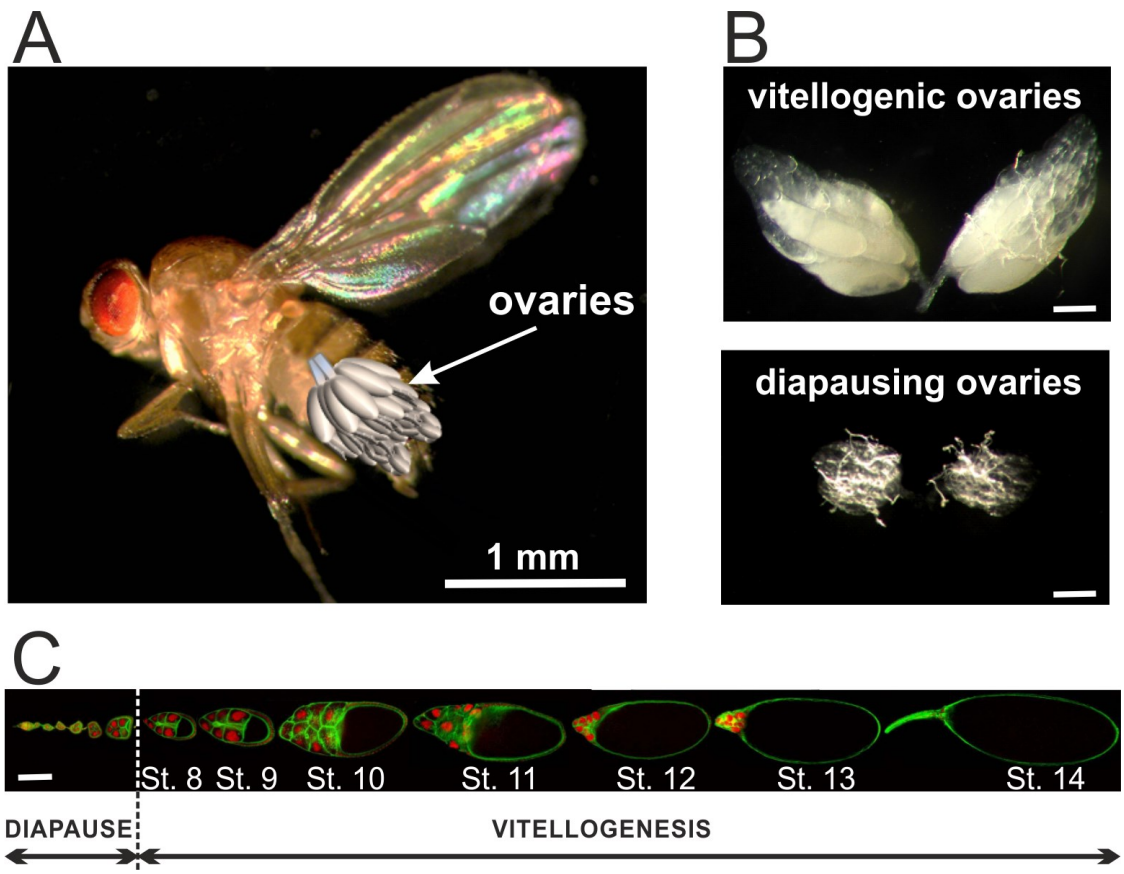

Figure 2. Adult reproductive diapause in the fruit fly Drosophila melanogaster. (A) The anatomical location of the ovaries in a *D. melanogaster* female inside the abdomen. (B) Representative images of vitellogenic (top) and diapausing ovaries (bottom). Scale bars = 0.2 mm. (C) Confocal cross-sections show the 14 morphological stages (St. 1-14) of egg chamber development. The transition to the vitellogenic stages is marked by the accumulation of yolk proteins from stage 8. During mid oogenesis (St. 9-10), the egg chamber continues to elongate, and the size of the oocyte greatly increases as a consequence of the continuous yolk uptake until it occupies the whole egg chamber during the late stages (St. 13-14). The confocal image is adapted from Cavaliere et al. 2008.

The laboratory strain (*Canton-S*) used by Saunders and his colleagues was reported to exhibit a clear photoperiodic diapause response: females reared in short days (less than 14 hours of light per day) and at low temperatures (10 or 12°C) enter a reproductive diapause, while those maintained in long days (16 hours of light per day) at the same temperature undergo ovarian development. However, diapause in this species is "shallow" (Saunders et al. 1989; Saunders 1990; Emerson et al. 2009a), since it can be terminated rapidly after shifting the flies to favorable conditions. If diapausing flies are exposed to higher temperatures (18 or 25°C) or long days (18 hours of light per day), independently from the conditions they have experienced before, reproductive development is immediately initiated and normal activity is resumed (Saunders et al. 1989; Tatar et al.

2001). Thus, *D. melanogaster* diapause apparently carries characteristics of both quiescence and diapause (Tatar et al. 2001). Considering the fragility of this reproductive arrest, many studies turned to use other insects to further dissect the molecular features of the diapause program. However, metabolite accumulation during dormancy highlights that, though shallow, diapause in this organism has similar features to that of more robustly-diapausing arthropods (Kubrak et al. 2014; Kučerová et al. 2016; Zonato et al. 2017). In addition, the large repertoire of genetic tools and successfully established molecular techniques in *D. melanogaster* makes this species an appealing model organism to study dormancy.

Diapausing flies are characterized by reduced food intake, increased stores of carbohydrates and lipids, activated immune genes, altered expression of genes related to insulin- and glucagon-like signaling, low mortality and overall a greatly extended lifespan (Kubrak et al. 2014; Schiesari et al. 2016). Diapause-associated traits, such as mortality, fecundity, stress resistance, lipid content, and egg-to-adult viability have been found to vary across the latitudinal gradient in natural populations of *Drosophila melanogaster* in North America (Schmidt et al. 2005a, b). Interestingly, diapause incidence has also been reported to change predictably with the latitude in this continent (Schmidt et al. 2005a).

1.3. Hormonal control of diapause

While the environmental signals regulating diapause have been known for a long time, the molecular bases of this phenomenon are still unclear and remain to be further investigated (Allen 2007). It is unidentified how the diapause-triggering environmental message (short photoperiod and low temperature) is translated into hormonal signals in the brain, leading to the initiation of the diapause program. Neurons in the *Pars intercerebralis* (*PI*) and *Pars lateralis* (*PL*) in the dorsal protocerebrum are believed to be involved in the transduction pathway for the environmental stimuli. These play a prominent role in the regulation of insect development, growth, metabolism, and reproduction via the growth factors and neuropeptides they release, that target key neuroendocrine glands (Shiga & Numata 2007). The ring-gland is the major hormonal center of *Drosophila melanogaster* and consists of two endocrine glands, the prothoracic gland and the *corpora allata*, and one neurohemal organ, the *corpora cardiaca* (reviewed in Dubrovsky 2009). These organs are densely innervated by brain neurosecretory cells, and play an essential role in the regulation

of insect growth via the hormones they produce and release in the hemolymph (Richard et al. 1998; 2001). Ecdysone, the prohormone of the major insect molting hormone, is synthesized in the prothoracic gland. It is assumed that ecdysone synthesis requires initial activation by the neuropeptide prothoracicotropic hormone (Huang et al. 2008). This peptide is produced by neurosecretory cells (PG neurons) in the lateral protocerebrum region of the brain. Once released into the hemolymph, ecdysone is converted by P450 monooxygenase to an active form, 20-hydroxyecdysone, and acts on target tissues via steroid receptor system (Petryk et al. 2003). Ecdysone plays vital roles in coordinating developmental transitions, for example larval molting and metamorphosis (Truman & Riddiford 2002; Dubrovsky 2005). After metamorphosis, the function of the prothoracic gland in the females is taken by the ovarian follicles and/or nurse cells of the females (Buszczak et al. 1999). During vitellogenesis, the process of yolk protein (vitellogenin) synthesis, transport, and uptake into the oocyte, significant ecdysone production takes place. The yolk protein coding genes are expressed in the fat body and ovarian follicle cells of the females, where yolk protein synthesis occurs (Brownes & Nöthiger 1981). These proteins are subsequently transported to the oocytes where they are stored and utilized for embryogenesis. It has been reported that ecdysone can activate *yolk protein* genes, thus enhancing the synthesis of vitellogenins (Brownes & Nöthiger 1981). The reproductive arrest during *D. melanogaster* diapause is characterized by suspended yolk deposition in the oocytes (Saunders et al. 1989; 1990).

Importantly, the action of ecdysone is directed by another key insect hormone, the lipid-like juvenile hormone (JH), which is synthesized and released from the *corpus allatum*. The presence of JH, ecdysone and 20-hydroxyecdysone induce larval molting by the production of a new larval cuticle, process critical to prevent metamorphosis (larva-to-pupa transition). JH is a key factor in many developmental processes, such as ovarian growth, diapause, cuticle pigmentation and metamorphosis (Saunders et al. 1990; Riddiford 1994; Dubrovsky 2005). The involvement of JH has also been reported in direct and indirect regulation of ecdysone biosynthesis in the prothoracic gland (Marchal et al. 2010).

In holometabolous insects, characterized by complete metamorphosis, the larva-to-larva molts require high JH concentration, and JH is still present until the early part of the final instar. However, in the final part of the last larval stage, when metamorphic molt takes place, there is a drop in its production (Baker et al. 1987). The main important insect

hormones, juvenile hormone, prothoracicotropic hormone and ecdysone, and their interaction during insect development, are critical to determine insect growth (Nijhout & Williams 1974; Rountree & Bollenbacher 1986).

JH and ecdysone are involved in the endocrine regulation of adult reproductive diapause, where the ovarian development is arrested at previtellogenic stages (Hodkova 1976; Saunders et al. 1990). For example, JH is an important regulator of dormancy in the linden bug *Pyrrhocoris apterus* (Hodkova 1976). In this species, JH has been shown to stimulate synthesis of yolk proteins in the fat bodies (organs analogous to vertebrate liver) and in the ovarian follicle cells. JH supports the uptake of yolk proteins by developing ovaries during the reproductive phase, while in diapause-destined individuals this JH action is disrupted leading to arrested ovarian development (Socha et al. 1991). In *Drosophila*, levels of both juvenile hormone and ecdysone are reduced during dormancy, and yolk deposition in the oocytes is suspended (Saunders et al. 1989; 1990). Similarly to *P. apterus*, JH promotes the early synthesis of yolk proteins by the fat bodies and the ovarian follicle cells. Accumulation of yolk proteins was also observed in the hemolymph of diapausing flies; however, due to the absence of stimulatory JH effect, their level was very low in the ovaries (Saunders et al. 1990). Topical application of JH in flies resumed yolk deposition in the ovaries, initiating the reproductive phase (Saunders et al. 1990). The northern house mosquito, *Culex pipiens*, enters adult reproductive diapause, which is also regulated by suppressed *corpus allatum* function (Readio et al. 1999).

It is worth noting that hormonal control of dormancy is also crucial in the case of embryonic, larval and pupal diapause (reviewed in Schiesari et al. 2011). *Bombyx mori* exhibits a maternally controlled embryonic diapause, determined by environmental factors, like photoperiod and temperature, experienced by the mother during the egg and larval stages (Hasegawa 1951). However, in this animal the effect of both light and temperature is reversed: eggs subjected to long photoperiods and high temperatures develop to adults that lay diapausing eggs due to the actions of the 24-amino acid peptide amide diapause hormone (DH). DH is secreted by the suboesophageal ganglion (SOG) and transduced from the mother to the embryo to induce dormancy (Hasegawa 1951). When the SOG is surgically removed from pupae, the emerging females fail to produce diapausing eggs. In contrast, females producing non-diapausing eggs gain the ability to become diapause-producers by

SOG transplantation from diapausing egg females (Hasegawa 1951; Fukuda 1951). The termination of diapause requires the actions of ecdysone, whose production promotes development by activated extracellular signal-regulated kinase (ERK) signaling in the yolk cells (Fujiwara et al. 2006).

In the southwestern corn borer, *Diatraea grandiosella*, diapause is induced in the final larval stage. Interestingly, the onset of the dormant state is marked by different integumental profile changes of the larvae: while non-diapausing larvae are spotted, the diapause-destined ones are immaculate (Chippendale & Yin 1974). In the induction and maintenance of diapause JH plays a key role, however, in contrast to the previous examples where diapause was characterized by a failure of JH production, its effects seem to be different in this species. Topical application of a juvenile hormone mimic to spotted diapausing larvae made them switch their development program and enter dormancy (Chippendale & Yin 1974).

Diapause-fated mature larvae of the fleshfly, *Boettcherisca peregrina*, enter the dormant state at the pupal stage. There are remarkable differences in the ecdysone profile of diapause- and non-diapause-destined individuals (Atsuko et al. 1988). While in non-diapausing insects, two large ecdysone peaks were detectable after pupariation, in flies programmed for diapause only one peak was present when larval-pupal transformation occurred, and afterwards the hormone levels remained undetectably low (Atsuko et al. 1988).

All of the aforementioned examples clearly demonstrate that insect hormones are key regulators of diapause, by determining the developmental program to be followed during insect life. However, another signaling pathway, insulin-like signaling, has also been implicated in diapause regulation in many species (Kimura et al. 1997; Sim & Denlinger 2008; Kubrak et al. 2014; Schiesari et al. 2016). A recent study by our laboratory (Schiesari et al. 2016) and another earlier report (Kubrak et al. 2014) demonstrated that insulin-like signaling mediates the overwintering response in *Drosophila melanogaster*. However, regulation of ovarian development by this signaling pathway is not limited to *Drosophila.* Insulin-like signaling is also involved in the control of adult reproductive diapause in the mosquito *Culex pipiens* (Sim & Denlinger 2013) and determines dauer formation (a diapause-like alternative developmental stage) in the nematode *Caenorhabditis elegans* (Kimura et al. 1997).

1.4. Insulin-like signaling in the regulation of dormancy

1.4.1. Components of the insulin signaling pathway

Insulin-like growth factors and insulin-like peptides (ILPs) are produced in various cell types and tissues at different developmental stages. After their release into the hemolymph circulation, ILPs can reach their target tissues and exert their biological functions. They are not only crucial regulators of development, growth and metabolic homeostasis but also of reproduction, stress resistance and lifespan (Tatar et al. 2001; Rulifson et al. 2002; Tatar 2003; Broughton et al. 2005; Broughton et al. 2010; Enell 2010). In *Drosophila*, similarly to many other species, impairment of insulin-like signaling is associated with extended longevity, increased stress resistance, and reduced reproduction, a set of phenotypes quite similar to what is seen in diapausing animals (Tatar et al. 2003). This signaling pathway has been identified as a major regulator of diapause through its effects on metabolic suppression, fat hypertrophy, and growth control (Puig et al. 2003; McElwee et al. 2006; Hahn & Denlinger 2007; Kubrak et al. 2014; Schiesari et al. 2016).

In *Drosophila*, eight ILPs (DILP1-8) have been identified that are encoded by different genes (Broeck 2001; Brogiolo et al. 2001; Slaidina et al. 2009; Colombani et al. 2012; Garelli et al. 2012; Okamoto et al. 2013). Four of these (DILP1, 2, 3 and 5) are expressed in two clusters of neurosecretory cells in the *Pars intercerebralis* region of the brain, known as insulin producing cells (IPCs), a subpopulation of median neurosecretory cells (MNCs) (Slaidina et al. 2009; Broughton et al. 2008). (For detailed description, localization and function of the individual DILPs, see chapter *1.6.2. Drosophila insulin-like peptides.*)

Binding of different DILPs to their receptors initiates a phosphorylation cascade including the enzymatic modification of numerous proteins (*Figure 3*). In the first step, due to the bound DILP to the receptor, the insulin receptor substrate protein called CHICO gets phosphorylated within the cell. Once CHICO is activated upon phosphorylation, it binds and activates downstream targets like phosphatidylinositol 3-kinase (PI3K). Activated PI3K phosphorylates phosphatidylinositol-4,5-bisphosphate (PIP2), converting it to phosphatidyl-inositol-3,4,5-trisphosphate (PIP3) (Britton et al. 2002) which, in turn, leads to the activation of two intracellular signaling proteins, AKT (also known as Protein Kinase B, PKB) and 3-phophoinositide-dependent protein kinase-1 (PDK-1) (Taniguchi et al. 2006; Teleman 2010; Antonova et al. 2012). Once activated, AKT phosphorylates the FoxO (Forkhead box O)

transcription factors. FOXOs play a crucial role in several cellular functions including transcription and cell-cycle progression (Kops et al. 1999; Alvarez et al. 2001), apoptosis (Brunet et al. 1999; Dijkers et al. 2000), and their role has been implicated also in the modulation of metabolic genes (Guo et al. 1999; Ayala et al. 1999; Hall et al. 2000; Schmoll et al. 2000; Nadal et al. 2002). The identified FOXO in Drosophila shows homology to its counterparts in Caenorhabiditis (Daf-16) and mammals (FoxO1, FoxO3, FoxO4 and FoxO6) (Kramer et al. 2003).

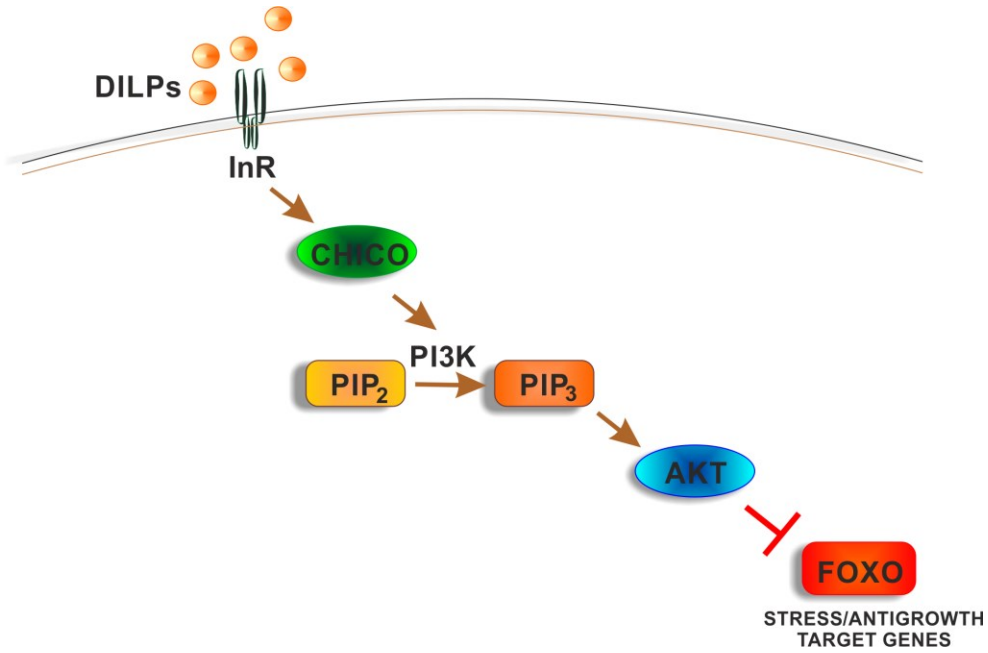

Figure 3. The canonical insulin-like signaling pathway in insects. The insulin-like proteins (DILPs) bind and activate the insulin receptor (InR) in the extracellular surface of the target cells. InR activates its receptor substrate (CHICO) that, in turn, activates its downstream target phosphatidylinositol 3-kinase (PI3K). Activated PI3K phosphorylates phosphatidylinositol-4,5-bisphosphate (PIP2) and thereby generates phosphatidylinositol-3,4,5-trisphosphate (PIP3). The PI3K cascade leads to the activation of AKT protein, which is bound to the plasma membrane. Once active, AKT enters the cytoplasm and inhibits the nuclear translocation of the transcription factor FoxO (Forkhead box-O). Thus, the FOXO-induced antigrowth program is prevented.

FOXO is normally activated by suppression of insulin-like signaling. In the absence of growth factors, FOXO translocates to the nucleus and upregulates a series of target genes, inducing an antigrowth program including cell cycle arrest, stress resistance, or apoptosis (Tran et al. 2003; Accili & Arden 2004). On the contrary, activated insulin signaling leads to AKT-mediated FOXO phosphorylation, resulting in the cytoplasmic localization and inactivation of FOXO via the ubiquitin-proteasome pathway (Huang & Tindall 2011).

1.4.2. Connections between insulin-like signaling and diapause

Insulin-like signaling has been implicated as a potential regulator cascade of diapause, due to its effects on many fitness-related traits that are determining a diapause-like physiological state. Indeed, it is known that this signaling pathway plays an important role in the regulation of fecundity, metabolism, stress resistance and longevity (Broughton et al. 2005; Giannakou & Partridge 2007; Broughton et al. 2010). In insects, an increasing number of evidence suggests that disruption of various components of the insulin-like signaling pathway correlates with the induction of diapause (Allen 2007; Sim & Denlinger 2008; Hahn & Denlinger 2011; MacRae 2010; Schiesari et al. 2011; Kubrak et al. 2014; Schiesari et al. 2016).

In *Drosophila*, a study of the PI3K encoding gene (*Dp110*) revealed the first link between insulin-like signaling and natural variation of reproductive diapause (Williams et al. 2006). It was reported that genetic manipulation of PI3K leads to significant changes in diapause incidence: its downregulation results in elevated diapause levels, while its upregulation has the opposite effect on dormancy (Williams et al. 2006). Indeed, shutting down certain components of the insulin-like signaling pathway results in flies with decreased body size, elevated lipid levels (Böhni et al. 1999) and increased diapause levels (Kubrak et al. 2014; Schiesari et al. 2016). Insulin receptor substrate *chico* hypomorph mutants are only half size of normal flies due to the reduction observed in cell size and cell number; they exhibit highly elevated lipid levels (Böhni et al. 1999) and are characterized by increased diapause incidence (Schiesari et al. 2016). Genetic ablation or reduced excitability of IPCs results in greatly elevated dormancy levels (Schiesari et al. 2016). By contrast, overexpression of *dilp2* and *dilp5* in the IPCs causes a marked reduction in diapause levels, similarly to that observed by the hyperexcitation of IPCs (Schiesari et al. 2016). The single mutations *dilp2*$^{-/-}$ and *dilp5*$^{-/-}$ (complete loss of the peptides) modestly promote diapause induction, while the triple mutant *dilp2,3,5*$^{-/-}$ and the *dilp1-5*$^{-/-}$ mutant (lacking *dilp1, -2, -3, -4* and *-5* genes) induce about 100% diapause (Kubrak et al. 2014; Schiesari et al. 2016).

Interestingly, IPC projections from the brain reach the important neuroendocrine glands (Rulifson et al. 2002). In *D. melanogaster* ecdysone release from the prothoracic gland is not only regulated by prothoracicotropic hormone but is also under the modulatory effect of insulin-like proteins (Layalle et al. 2008). Diapause is associated with JH shutdown

in many species (Saunders et al. 1990; Readio et al. 1999; Tu et al. 2005). Drosophila insulin receptor (InR) is present in the JH-producing *corpora allata* (Belgacem & Martin 2006), as well as in the nurse cells and oocytes (Garofalo & Rosen 1988), and insulin-like signaling in the germ cells is known to regulate ovarian development (LeFever & Drummond-Barbosa 2005). Mutation in many components of insulin-like signaling pathway leads to altered JH synthesis in *D. melanogaster* (Tatar et al. 2001; Tu et al. 2005). Females heteroallelic for InR mutations are dwarf, sterile, and their juvenile hormone biosynthesis is strongly reduced (Tatar et al. 2001). Exogenous application of the JH analog was found to induce dwarf females to initiate vitellogenesis (Tatar et al. 2001).

Interestingly, in homozygous *chico*^{1} mutant females, JH concentration and ecdysteroid levels released by the ovaries were approximately the same as in wild-type females (Richard et al. 2005), suggesting that the sterility observed in insulin-like signaling mutants is not always coupled to altered levels of these key hormones. Wild-type females did not undergo vitellogenesis when ovaries of *chico*^{1} mutants were transplanted into their body, indicating that CHICO is crucial for ovarian maturation, despite enough JH and ecdysteroids are present (Richard et al. 2005).

In summary, the developmental switch between reproductive phase and dormancy seems to be coordinated by complex hormonal events, including JH and ecdysone signaling pathways as well as insulin-like signaling (*Figure 4*). When conditions are favorable for normal development, the reproductive phase is initiated, and DILP release from the brain IPCs is promoted. Active insulin-like signaling induces JH secretion in the *corpus allatum*, which signals in the fat bodies and in the ovarian follicle cells to induce yolk protein synthesis, and thereby ovarian maturation (Saunders et al. 1990; Riddiford 1994; Dubrovsky 2005). Also, JH stimulates the ovaries to produce ecdysone that, in turn, promotes the uptake of the yolk proteins by the ovaries during vitellogenesis (Tu et al. 2005). Under diapause-inducing conditions, insulin-like signaling is downregulated, JH secretion in the *corpus allatum* is blocked (Saunders et al. 1990; Readio et al. 1999; Tu et al. 2005), and the ovarian synthesis of ecdysone is impaired.

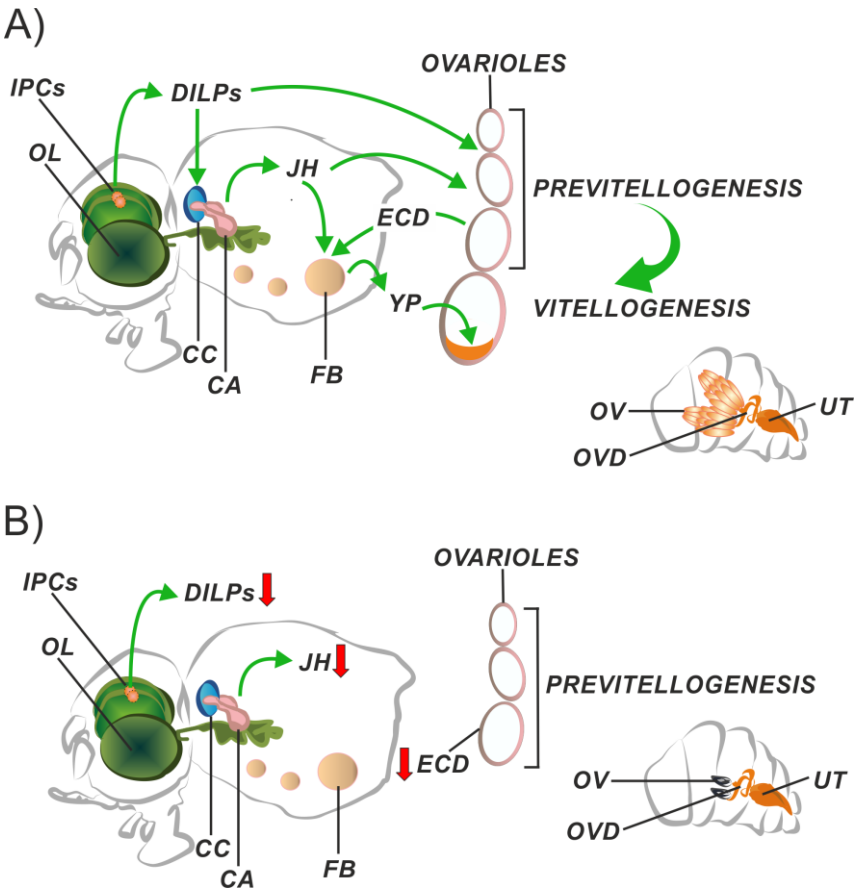

Figure 4. Endocrine signaling regulating the developmental switch from reproductive phase (A) to adult dormancy (B) in Drosophila melanogaster. (A) In the reproductive phase, insulin-like proteins (DILPs) are released from the IPCs, located in the dorsal brain. Insulin signaling (IIS) induces JH secretion in the *corpora allata* (CA) to secrete juvenile hormone (JH). Due to DILP signals in the ovaries, growth of egg chamber is induced and vitellogenesis is promoted. JH signals to fat bodies (FB) and the ovarian follicle cells to stimulate yolk protein (YP) synthesis, thereby inducing ovarian maturation. Additionally, JH stimulates the ovaries to synthesize ecdysone (ECD) that promotes the uptake of the YPs by the ovaries during vitellogenesis. (B) During diapause IIS is downregulated, JH production in the CA is abrogated, and the ovarian synthesis of ECD is impaired. *Corpora cardiaca* (CC), optic lobe (OL), ovary (OV), oviduct (OVD), uterus (UT). The figure is modified from Schiesari et al. 2011.

1.4.3. Factors that regulate IPC activity

Albeit we know a lot about structure, functional role and regulation of the IPCs and the different DILPs, our knowledge is still insufficient to reveal under what conditions IPCs are activated and how their activity is controlled. Many receptors have already been identified in these cells (*Figure 5*). For instance, they express the metabotropic receptors for the inhibitory neurotransmitter γ-aminobutyric acid, GABA. It was shown that $GABA_B$ receptors in IPCs inhibit DILP release (Enell et al. 2010). The inhibitory effect of the GABAergic neurons on the IPCs is exerted by the signal of a leptin-like protein, unpaired 2

(Upd2), secreted by the fat body and functioning as a nutrient-specific regulatory signal (Rajan & Perrimon 2012). It communicates the fed state to the IPCs by sensing fat and sugars, thereby remotely controlling DILP accumulation and affecting systemic growth and metabolism. Upon elevated lipid and carbohydrate levels in the hemolymph, Upd2 activates JAK/STAT (Janus kinase/signal transducers and activators of transcription) signaling in the GABAergic neurons that project onto the IPCs, thereby blocking GABA release (Rajan & Perrimon 2012). This inhibition relieves the IPCs from repression, resulting in DILP release.

DILP6 may serve as another signaling molecule from the fat bodies to IPCs. It is produced in the adult fat bodies, and its mRNA is positively modulated by dFOXO (Bai et al. 2012). Fat body-specific overexpression of *dilp6* leads to extended lifespan, elevated stress resistance, reduced fecundity, as well as lower *dilp2* and *dilp5* mRNA expression in the brain and decreased DILP2 release (Bai et al. 2012).

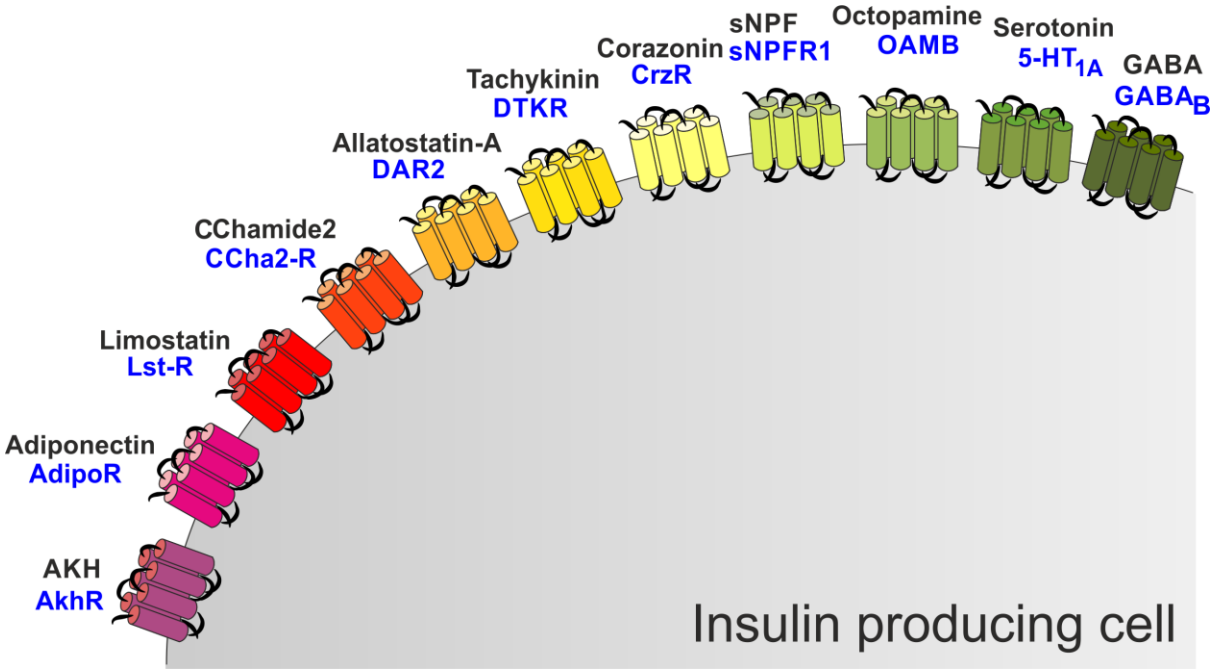

Figure 5. Neuropeptides, neurotransmitters, and peptide hormones acting on insulin producing cells in Drosophila melanogaster. Known and potential receptors located in the IPCs. GABA: γ-aminobutyric acid; sNPF: short neuropeptide F; AKH: adipokinetic hormone.

Another key regulator of the IPCs is the biogenic amine serotonin (5-HT). IPCs express the serotonin receptor 5-HT_{1A}, and processes of serotonergic neurons can be found in the proximity of the IPC branches (Luo et al. 2012). Knockdown of this receptor results in increased heat and cold sensitivity, decreased resistance to starvation, elevated hemolymph

glucose, body trehalose and body glycogen levels (Luo et al. 2012; 2014). In addition, 5-HT_{1A} knockdown leads to increases of *dilp2* and *-5* mRNA levels, as well as elevated DILP2 immunosignals in the IPCs (Luo et al. 2012). Furthermore, it was shown that IPCs express the octopamine receptor OAMB (Crocker et al. 2010; Luo et al. 2014). Knockdown of OAMB by targeted RNAi results in increased resistance to oxidative stress and elevated *dilp3* transcript levels in the brain (Luo et al. 2014).

The receptor for adiponectin (dAdipoR) was also identified in the IPCs (Kwak et al. 2013). Targeted RNAi against the IPC-specific dAdipoR leads to increased triglyceride level in the whole body, elevated sugar level in the hemolymph, and a reduction of circulating DILP2 in the hemolymph due to the accumulation of this peptide in the IPCs (Kwak et al. 2013).

Another neuropeptide, Drosophila tachykinin (DTK), also has receptors on the IPCs (Birse et al. 2011). Targeted knockdown of DTK receptor (DTKR) in the IPCs causes extended lifespan, elevated *dilp2* and *-3* transcript levels in fed flies, and increased *dilp2* in starved flies (Birse et al. 2011). Interestingly, there is a superposition between IPC dendrites and DTK-expressing varicosities in the *Pars intercerebralis* of the adult brain (Birse et al. 2011).

It has been shown that 6-8 bilaterally symmetric neurons in the *Pars lateralis*, called dorsal-lateral peptidergic neurons (DLPs), have axon terminations in the proximity of the IPCs (Kapan et al. 2012). They express the neuropeptides corazonin (Crz) and short neuropeptide F (sNPF), and their role has been implicated in the regulation of IPC activity (Kapan et al. 2012). IPCs express sNPFR1, and indirect data suggests also the existence of corazonin receptor (CrzR) on these cells (Lee et al. 2008; Kapan et al. 2012; Carlsson et al. 2013). Knockdown of either sNPF or Crz in the DLPs leads to extended lifespan upon starvation, as well as elevated glucose and trehalose levels in the hemolymph (Kapan et al. 2012). Knockdown of CrzR on IPCs results in increased starvation resistance (Kapan et al. 2012).

The neuropeptide allatostatin-A (Ast-A) also seems to influence IPC activity via its receptor, DAR2, expressed on the IPCs (Hentze et al. 2015). There is a superposition between Ast-A expressing neurons and IPCs in the dorsal brain and in the tritocerebrum. IPC-specific knockdown of DAR2 results in increased starvation resistance and decreased *dilp2* levels (Hentze et al. 2015). Ast-A signaling has also been suggested to function as part of a nutrient sensing mechanism, playing an important role in the modulation of feeding decision according to the internal nutrient state, thereby it shapes metabolic programs

(Hentze et al. 2015).

IPCs have recently been shown to express receptors for the polypeptide limostatin (Lst), which inhibits insulin production and release (Alfa et al. 2015). Limostatin deficient flies exhibit reduced lifespan, significant obesity and elevated levels of *dilp2, -3* and *-5* mRNA and circulating DILP2 (Alfa et al. 2015).

Another modulator of IPC activity is the peptide hormone CCHamide2, functioning as a nutrient-dependent regulator of insulin-like peptides through its receptor (CCHa2-R) present on the IPCs (Sano et al. 2015). It is highly expressed in the enteroendocrine cells of the midgut and induces *dilp5* expression in the brain. CCHa2-R mutants have growth effects and are characterized by developmental delay during the larval stages (Sano et al. 2015).

Finally, a possible direct functional connection has been suggested between IPCs and adipokinetic hormone (AKH) producing cells in the *corpora cardiaca* (Rulifson et al. 2002; Buch et al. 2008), most probably via AKH receptor (AKHR) expressed on the IPCs (Kim et al. 2015). The ablation of AKH-positive cells results in increased *dilp3* mRNA level, while ablation of IPCs leads to increased *akh* transcript level (Buch et al. 2008).

1.5. Links between circadian and seasonal timing systems

A central question in chronobiology is whether there is a possible connection between the circadian clock and the seasonal timing system. Although many studies in different insects provide evidence that certain clock genes are linked to seasonal responses like diapause (Pavelka et al. 2003; Goto et al. 2006; Tauber et al. 2007; Ikeno et al. 2011a, b; Meuti et al. 2015), the exact mechanism by which they regulate this seasonal response remains unclear. A big challenge in the field is to determine whether individual circadian clock genes affect photoperiodism independently from their role in the circadian network (gene pleiotropy), or they alter the circadian clock mechanism as a module, which in turn controls the photoperiodic diapause response (modular pleiotropy) (Emerson et al. 2009b). This relationship has been interpreted in various ways by different investigators and many contradictory reports emerged, finding no supporting evidence for the existence of a possible link between the two clock machineries.

Circadian molecular oscillations taking place at the core of the circadian clocks are generated by an evolutionary conserved, transcriptional-translational feedback system

(reviewed in Hardin 2005). In brief, in the central clock of *Drosophila melanogaster*, the heterodimer formed by CYCLE (CYC) and CLOCK (CLK) is the positive element that directly activates the transcription of the negative factors *period* (*per*), *timeless* (*tim*). The PER/TIM heterodimer negatively regulates the activity of the CYC/CLK complex, thereby shutting down their own transcription. Entrainment to light is regulated by the photoreceptor CRYPTOCHROME (CRY), which resets the circadian clock by promoting light-induced degradation of TIM (reviewed in Peschel & Helfrich-Förster 2011). The neuropeptide pigment dispersing factor (PDF) acts as a principal circadian neurotransmitter, playing an important role in the coordination of pacemaker interactions and behavioral rhythms (Renn et al. 1999). The best studied circadian behavior in *Drosophila* is the locomotor activity: wild-type flies show peaks of activity at the beginning and the end of the day and, more importantly, are able to anticipate the light-dark and dark-light transitions (Peschel & Helfrich-Förster 2011).

Drosophila melanogaster per null mutants were still able to distinguish between long and short photoperiods, therefore this gene does not seem to be causally involved in photoperiodic time measurement (Saunders et al. 1989). However, these mutants were characterized by a shorter critical photoperiod (approximately by 2 hours) compared to wild-type flies (Saunders et al. 1989). Another clock gene, *tim*, has also been investigated in this insect in relation to diapause induction (Tauber et al. 2007; Sandrelli et al. 2007). The sequence of *tim* contains two open reading frames, resulting in two different TIMELESS isoforms. While the long isoform protein consists of 1421 amino acids (L-TIM_{1421}), the short one contains 1398 amino acids (S-TIM_{1398}) (Rosato et al. 1997). The *ls-tim* allele generates both long L-TIM_{1421} and short S-TIM_{1398} products, while in the case of *s-tim*, deletion of the G nucleotide at position 294 interrupts the upstream open reading frame with a stop codon, therefore only S-TIM_{1398} can be generated from the downstream open reading frame (Rosato et al. 1997) (*Figure 6*).

It has been reported that L-TIM is more stable than S-TIM, and importantly, flies bearing *ls-tim* allele exhibit consistently higher diapause levels in every photoperiod (Tauber et al. 2007; Sandrelli et al. 2007). There is a latitudinal gradient of *ls-tim* frequency, with higher incidence of *ls-tim* in southern Europe. It was suggested that *ls-tim* allele is derived from the *s-tim*, arose in southern Italy about 10,000 years ago, and it has recently spread in all directions due to directional selection (Tauber et al. 2007). A latitudinal cline in *ls-tim*

frequencies was found also in Eastern USA, highlighting a twofold increase in the level of *ls-tim* in the north compared to the south (Pegoraro et al. 2017). Since in this continent the incidence of reproductive dormancy shows a strong latitudinal cline (Schmidt et al. 2005a), the higher frequency of the diapause-promoting *ls-tim* variant in the northern areas is likely contributing to this pattern.

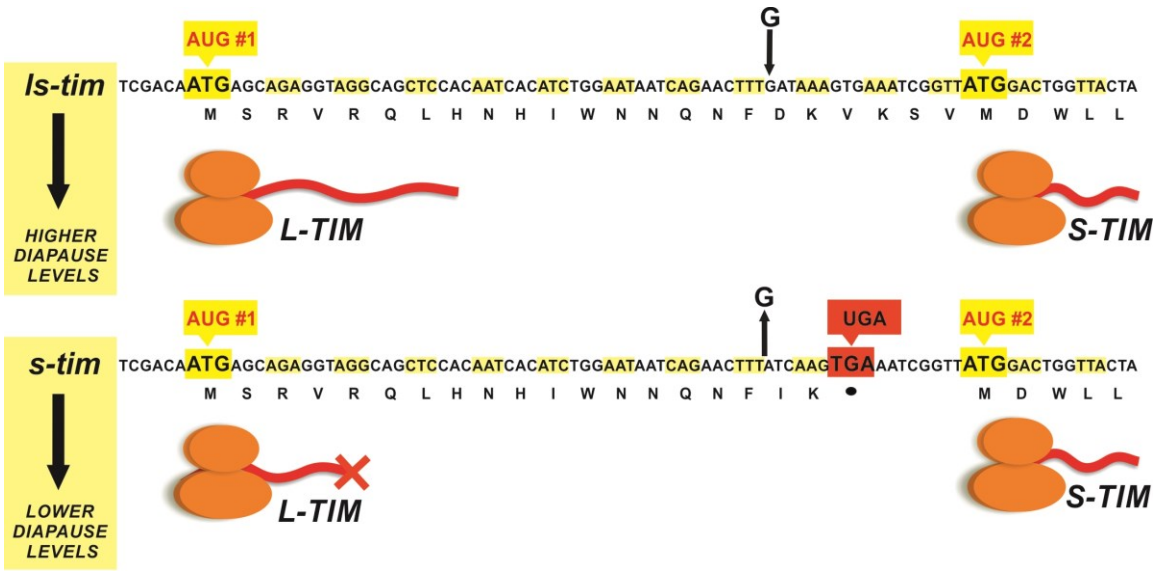

Figure 6. Natural polymorphisms in the timeless clock gene influence diapause incidence in Drosophila melanogaster. The *timeless* (*tim*) gene has two allelic forms: *s-tim* (short) and *ls-tim* (long and short). From the newly derived *ls-tim* allele both full-length L-TIM$_{1421}$ and short S-TIM$_{1398}$ proteins are translated from the two alternative start codons (AUG #1 and #2, respectively). In the case of *s-tim* allele, deletion of a G nucleotide (indicated by an arrow) leads to a creation of a stop codon (UGA) that interrupts the upstream reading frame. Thus, only the short S-TIM$_{1398}$ variant can be translated. This polymorphism affects the incidence of reproductive diapause in the flies: females bearing the *ls-tim* allele are more likely to enter diapause in every photoperiod compared to insects having the *s-tim* variant. The figure is modified after Tauber et al. 2007.

In the drosophilid fly *Chymomyza costata,* a non-photoperiodic diapausing mutant (*npd*) was identified, shown to be insensitive to diapause-inducing action of photoperiod (Riihimaa et al. 1988). Surprisingly, the mutation has been linked to the *tim* locus (Pavelka et al. 2003). While *tim* mRNA showed cycling oscillation in the head of wild-type insects, *tim* transcripts were not even detectable in *npd* mutants (Pavelka et al. 2003). The flesh fly, *Sarcophaga bullata*, enters pupal diapause at low temperature and short days. However, an identified variant fails to enter dormancy even under diapause-inducing conditions and loses also circadian rhythmicity of adult eclosion. The loss of both responses can be

explained by highly elevated *per* and *tim* mRNA levels found in this variant (Goto et al. 2006).

In the bean bug, *Riptortus pedestris*, RNAi directed against key clock genes disrupted the photoperiodic diapause response. Ovarian development was induced following *per* and *cry* shutdown, even when bugs experienced diapause-enhancing short days, whereas targeted RNAi against *cyc* repressed ovarian development during diapause-promoting long days (Ikeno et al. 2011a, b). In the Northern house mosquito, *Culex pipiens*, circadian clock genes have been implicated in the initiation of adult reproductive diapause (Meuti et al. 2015). Targeted RNAi against *period*, *timeless* and *cryptochrome2* resulted in reduced diapause levels even under diapause-triggering short day conditions. However, shutdown of *pigment dispersing factor* had the opposite effect, since females entered diapause even under long days (Meuti et al. 2015).

The aforementioned examples show that considerable work has been undertaken in an effort to dissect the role of the circadian clock in the regulation of diapause. However, we are still far away from completely understanding the possible interactions between the two timing systems.

1.6. Neuropeptides as signaling molecules

Neuropeptides are extracellular messengers, which can be considered as chemical communication signals between the cells of an organism. They mediate almost all physiological processes during an insect's life through a huge variety of peptide actions: they regulate physiological and behavioral processes including development, growth, reproduction, feeding, metabolic events, longevity, homeostasis and behavior, as well as learning and memory, olfaction and locomotion (Gäde & Goldsworthy 2003; Nässel & Winther 2010). The brain neurosecretory cells send axonal projections to the *corpora cardiaca* and/or *corpora allata*, regulating the activity of these neurohemal organs through their neuropeptides (Rulifson et al. 2002).

Neuropeptides can function as important modulators of heart contraction (Veenstra 1989), regulators of food intake and body size (Lee et al. 2004), or, as previously mentioned for PDF, act as output factors and neuromodulators of biological rhythms (Helfrich-Förster

1998; Renn et al. 1999). They exert their physiological functions by interacting with specific signal-transducing membrane receptors, initiating intracellular responses (Zupanc 1996).

The majority of the *Drosophila* neuropeptides act on G protein-coupled receptors (GPCRs), which are seven-transmembrane domain receptors, and belong to either of two classes: rhodopsin-like (Family A; Type I) and secretin class (Family B; Type II) (Brody & Cravchik 2000; Hewes & Taghert 2001). Approximately 45 G-protein-coupled peptide receptors are known in *D. melanogaster* and for many of these the corresponding ligands have already been identified and characterized. However, there are still gaps in our knowledge and further investigations need to be done in order to unravel the structure, distribution and function of numerous neuropeptides in this species (Nässel & Winther 2010). Many peptidergic neurons can be individually identified, while others have their cell bodies in identifiable clusters. Commonly insect neuropeptides are produced in small number of neurons/neurosecretory cells (Nässel & Winther 2010).

A milestone was achieved in the field of insect neuropeptide receptor research with the publication of the fruit fly genome (Adams et al. 2000). The availability of these data opened the opportunity to predict receptors based on genomic data and the identification of genes encoding neuropeptide precursors (Brody & Cravchik 2000; Hewes & Taghert 2001; Broeck 2001; Hauser et al. 2006). In addition, techniques like live imaging of calcium or cyclic AMP in identified neurons have been successfully employed to identify receptor localization (Shafer et al. 2008; Wang et al. 2010).

1.6.1. Neuropeptides in the regulation of insect diapause

One of the key questions in the field of diapause research is how the dormancy-triggering environmental signals (shortened photoperiod and decreasing temperature) are perceived, transmitted and interpreted in the brain, and how they are converted into hormonal signals resulting in diapause phenotype. *PI* and *PL* neurons are thought to be involved in the transduction pathway through which environmental stimuli are conveyed in the brain and initiate diapause response. These regions of the protocerebrum are best known for the neurosecretory cells that control development and regulate other cells via their growth factors and neuropeptides (Shiga & Numata 2007). They target endocrine

glands, which play an essential role in the regulation of insect growth and development (Richard et al. 1998; Richard et al. 2001).

Insulin-like peptides are crucial neuropeptides in the regulation of diapause in *Drosophila melanogaster* (Kubrak et al. 2014; Schiesari et al. 2016). However, our knowledge is still limited to fully understand the link between dormancy as a seasonal response and insulin-like signaling. *Figure 7* shows a simple model depicting the role of insulin-like signaling in the initiation of diapause.

There are several neuropeptides that can be candidates for messaging the "time of the year" information to the IPCs, thereby possibly playing a role in the transmission of the environmental information towards these neurosecretory cells. If we suppose that the information about the season is sensed by circadian clock neurons, we have to consider that *PI* neurons (including IPCs) do not express the circadian clock components, therefore they should get direct or indirect time information from the clock (Jaramillo et al. 2004; Cavanaugh et al. 2014; Barber et al. 2016).

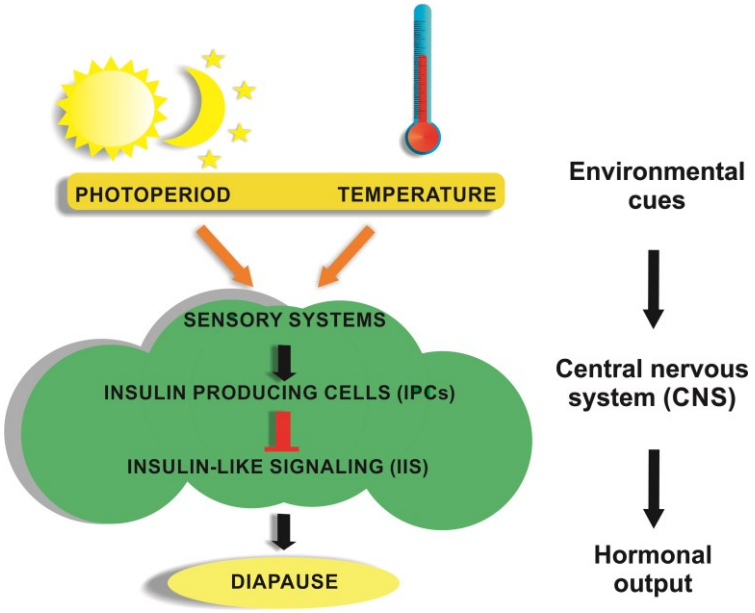

Figure 7. Schematic of a putative model for the role of insulin-like signaling in diapause induction. Photo- and thermoperiodic environmental cues are integrated in the *PI* of the *Drosophila* brain, where insulin producing cells are located, possibly via different sensory systems. Upon exposure to decreasing temperature and shortening days, the insulin-like signaling is downregulated, leading to physiological and hormonal changes which bring about arrested ovarian development.

For instance, the small ventrolateral neurons (s-LN$_v$s), a neuron cluster hosting the circadian clock in *Drosophila*, send axonal projections towards the dorsolateral

protocerebrum, in the vicinity of the insulin producing cells (Helfrich-Förster 1997). However, it has not been demonstrated yet whether there is a direct connection between these cells. The set of s-LN_vs consists of 5 cells per brain hemisphere, and their somata is located close to the accessory medulla (Helfrich-Förster 1997). Among them, four neurons share the same neuropeptide composition, co-expressing the neuropeptide pigment dispersing factor (PDF), short Neuropeptide F (sNPF), as well as the circadian photoreceptor CRYPTOCHROME (CRY) (Helfrich-Förster 1997; Johard et al. 2009). The 5th s-LN_v does not produce PDF but the neuropeptide ion transport peptide, and furthermore choline acetyl-transferase (Cha) and CRY (Johard et al. 2009). An additional set of PDF-producing neurons in the tritocerebrum (PDF-Tri) send projections close to the IPCs. Their cell bodies are located in the tritocerebrum and they extend arborizations to the *PI* and *PL* regions of the brain (Helfrich-Förster 1997). Interestingly, these neurons were reported to undergo apoptosis in the beginning of adulthood, thus after adult days 1-2 they are reported as no longer detectable (Helfrich-Förster 1997; Renn et al. 1999).

The set of dorsal-lateral peptidergic neurons, DLPs, can also be considered as possible candidates for the transmission of the environmental signals to the IPCs. They are located in the *Pars lateralis,* and were reported to have axonal terminations in the proximity of the IPCs (Kapan et al. 2012). They are also called “corazonin neurons”, since they express the neuropeptide corazonin (Crz), along with short neuropeptide F (Kapan et al. 2012). The receptor for sNPF (sNPFR1) is expressed on the IPCs (Lee et al. 2008; Kapan et al. 2012; Carlsson et al. 2013) and indirect data suggest the presence of corazonin receptor (CrzR) on these cells (Kapan et al. 2012). Thus, both sNPF and Crz can directly target the IPCs.

Importantly, PDF, sNPF, and Crz have already been suggested as diapause-modulating neuropeptides in insects (Huybrechts et al. 2004; Choi et al. 2005; Hamanaka et al. 2005; Ikeno et al. 2014; Meuti et al. 2015). The following paragraphs are dedicated to a more detailed introduction to the aforementioned neuropeptides, focusing especially on the characterization of different DILPs, PDF, sNPF, and Crz.

1.6.2. Drosophila insulin-like peptides

In *Drosophila melanogaster*, four of the eight identified insulin-like peptides (DILP1, 2, 3 and 5) are expressed in a set of median neurosecretory cells in the brain, located in the

PI and called insulin producing cells (IPCs) (Broughton et al. 2008; Slaidina et al. 2009; Liu et al. 2016). It was originally thought that DILP1 expression in the IPCs is restricted to stages prior to adulthood (Rulifson et al. 2002). However, recent study revealed that *dilp1*/DILP1 expression remains high in adults for many weeks during non-feeding stages and diapause (Liu et al. 2016).

Besides the IPCs in the brain, DILP2 shows a broad expression in the embryonic mesoderm, in the larval imaginal discs and in the salivary glands, as well as in some glial cells in the CNS (Rulifson et al. 2002). DILP2 expression has also been identified in four sets of brain neurons, which were classified based on their anatomical position in the brain: one posterior, one dorsal group, and two lateral groups (Cong et al. 2015).

Similarly to DILP2, DILP3 is not only present in the IPCs, but is also abundantly expressed in muscle cells of the adult midgut (Brogiolo et al. 2001; Rulifson et al. 2002).

As for DILP4, it shows high expression in the larval midgut, while its adult expression is not known (Brogiolo et al. 2001; Grönke & Partridge 2010).

Besides the IPCs, DILP5 is present in principal cells of the renal tubules and in adulthood also in follicle cells of the ovaries (Ikeya et al. 2002; Veenstra et al. 2008; Söderberg et al. 2011).

DILP6 is predominantly expressed in the adipose cells of the fat body, but it is present also in larval salivary glands and heart (Okamoto et al. 2009; Slaidina et al. 2009). DILP7 is detectable in specific neurons that innervate the female reproductive tract (Yang et al. 2008). DILP8 is expressed in imaginal discs of larvae (Colombani et al. 2012; Garelli et al. 2012) but also in the ovaries of adult females (Chintapalli et al. 2007). *Table 1* summarizes the localization of different DILPs in larval and adult stages.

Interestingly, direct manipulation of the individual DILPs revealed some redundancy and compensation among them. For instance, a compensatory increase in the level of *dilp3* and *5* mRNA was observed upon *dilp2* knockdown (Broughton et al. 2008).

Until 2015, there was only one identified *Drosophila* insulin receptor (dInR), which belongs to the receptor tyrosine kinase (RTK) family (Fernandez et al. 1995; Ruan et al. 1995; Brogiolo et al. 2001; Grönke et al. 2010). It shows structural similarities to the vertebrate insulin receptor, with a marked extension of the COOH-terminal β-chain domain (Böhni et al. 1999). Recently, another insulin receptor (Leucine-rich repeat-containing G

protein-coupled receptor 3, Lgr3) was discovered which acts as a direct receptor for the relaxin-like DILP8 (Colombani et al. 2015).

Table 1. The expression of different DILPs in adult and larval stages (after Nässel et al. 2013)

DILPs	***Location***	
	Larvae	***Adult***
DILP1	IPCs	IPCs (in diapausing flies)
DILP2	IPCs Imaginal discs Salivary glands Glial cells of CNS	IPCs Some posterior, dorsal and lateral neurons
DILP3	IPCs	IPCs Muscle cells of midgut
DILP4	Anterior midgut	–
DILP5	IPCs Principal cells in renal tubules	IPCs Follicle cells of ovary Principal cells in renal tubules
DILP6	Adipose cells Salivary glands Heart Glial cells of CNS	–
DILP7	Abdominal neuromeres	Abdominal neuromeres
DILP8	Imaginal discs	Ovary

IPCs have been proposed to be functionally analogous to pancreatic islet B cells (Rulifson et al. 2002). Interestingly, flies lacking IPCs share certain phenotypic features with diabetes mellitus (Rulifson et al. 2002). Their ablation results in developmental delay, growth retardation, reduced fecundity, extension of lifespan, elevated carbohydrate levels, as well as increased resistance to oxidative stress and starvation (Rulifson et al. 2002; Broughton et al. 2005). IPC ablated larvae attain a mean length only 60% of normal size, and adult flies are significantly smaller compared to controls, due to a reduction not only in the size but also in the number of cells (Rulifson et al. 2002). DILP2 overexpression alone was sufficient to increase organismal size by increasing cell size and cell number (Brogiolo et al. 2001). InR plays a crucial role in the development of the central nervous system and regulates both body- and organ size (Fernandez et al. 1995). *InR* knockout flies were found to die in early larval stages, while heteroallelic, hypomorphic mutants for this gene are characterized by developmental delay, adult dwarfism, extended lifespan, elevated

triglyceride levels and aberrant JH synthesis (Fernandez et al. 1995; Chen et al. 1996; Tatar et al. 2001; Clancy et al. 2001; Brogiolo et al. 2011). Interestingly, an extended lifespan was observed also in flies lacking the insulin receptor substrate CHICO (Clancy et al. 2001). Insulin signals appear to be regulators of JH synthesis: it was found that suppression of insulin-like signaling correlates with low JH production (Spielman 1974; Flatt et al. 2005; Tu et al. 2005).

IPCs seem to play a role in sleep regulation, most probably via the octopamine receptor (OAMB) expressed by these cells (Crocker et al. 2010; Cong et al. 2015): in fact, the loss of DILPs (except for DILP4) and dInR leads to significantly decreased total sleep amount (Cong et al. 2015). In addition, IPCs are involved in the regulation of locomotor activity in flies (Belgacem & Martin 2006), and apparently play a role in modulating the sensitivity of the circadian clock to oxidative stress (Zheng et al. 2007). Interestingly, it has recently been discovered that IPCs are functionally connected to the circadian clock network via DN1 clock that were found to have synaptic connections to these neurosecretory cells (Barber et al. 2016).

1.6.3. Pigment dispersing factor

Pigment-dispersing factor (PDF) is an 18-amino acid neuropeptide. Homberg et al. first suggested the involvement of this peptide in the regulation of insect circadian clock (Homberg et al. 1991). Subsequent study reported that in *Drosophila melanogaster*, some PER neurons are also immunostained with the antiserum against the crustacean pigment dispersing hormone (PDH), and the entire arborization pattern of these clock cells has been revealed (Helfrich-Förster 1997). Both the small and large subsets of the ventrolateral neurons (s-LN_vs and l-LN_vs, respectively) express PDF along with other clock genes (Helfrich-Förster & Homberg 1993; Helfrich-Förster 1997; Renn et al. 1999).

Figure 8 shows the main PDF-producing neurons in a young adult fly brain and provides also some detailed information about the number and the arborization pattern of these neurons. The s-LN_vs are the major circadian pacemaker neurons (Rieger et al. 2006). They send projections into the dorsal protocerebrum, in the vicinity of other circadian pacemaker clock neurons groups (DN1s and DN2s). The l-LN_vs project onto the surface of

the medulla (M) where their fibers create a widespread network. Furthermore, they also project contra-laterally in the posterior optic tract (Helfrich-Förster 1997).

A

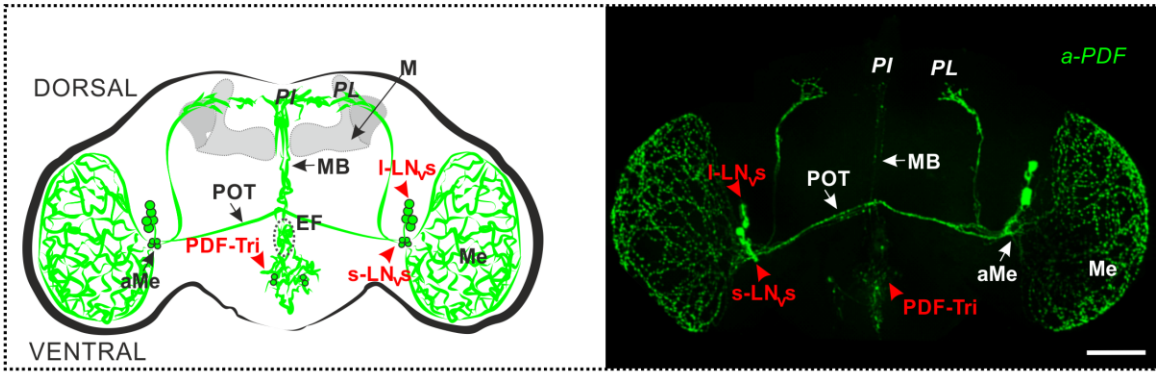

B

Cluster	*Number of cells*	*Location of the somata*	*Area of arborization*
s-LN$_v$s	4*	**L:** close to larval optic neuropil **P+A:** lateral protocerebrum close to the accessory medulla	**L:** dorsolateral brain lobes/ larval optic lobe neuropil **P+A:** dorsofrontally to the calyx of the mushroom body/accessory medulla
l-LN$_v$s	4-6*	**P+A:** lateral protocerebrum, slightly anterior and dorsal to the s-LN$_v$s	**P+A:** ipsi- and contralateral medulla cortex, dorsolateral protocerebrum/ accessory medulla, serpentine layer of medulla
PDF-Tri neurons	2-4	**P+A:** anterior-ventral in the trito-cerebrum	**P+A:** ventrally and laterally in the esophageal foramen, median bundle, *Pars intercerebralis*, and *lateralis*

Figure 8. Pigment dispersing factor-immunoreactive neurons in the fly brain. (A) *Left:* Schematic figure depicting the PDF$^+$ cells and their arborization pattern in the adult brain (highlighted in red arrowheads and text). l-LN$_v$s: large ventrolateral neurons; s-LN$_v$s: small ventrolateral neurons; PDF-Tri: PDF tritocerebrum neurons; *PI: Pars intercerebralis*; *PL: Pars lateralis*; M: mushroom bodies (in gray); ML: median bundle; POT: posterior optic tract; aMe: accessory medulla; Me: medulla; EF: esophageal foramen. *Right:* Representative confocal image showing the PDF$^+$ neurons in the brain using *anti-PDF* antibody (green). Scale bar = 100 µM (B) Table providing information about the pigment dispersing factor-expressing neurons in the brain. L: larvae; P: pupae; A: adult; * number of cells per brain hemisphere. The table is modified after Helfrich-Förster 1997.

Apart from the ventrolateral neurons, an additional PDF expressing neuron cluster is located in the tritocerebrum in the brain (henceforth PDF-Tri neurons), described as a developmentally-transient population of PDF-containing cells, which first can be detected during mid-pupal development (Helfrich-Förster 1997). Their projections form a network surrounding the ventral and lateral part of the esophageal foramen (EF). Their fibers grow

dorsally into the median bundle (MB), reaching also the *Pars intercerebralis* (*PI*) region (*Figure 8*). Some fibers grow laterally in the *Pars lateralis* (*PL*) creating connections with the fibers of s-LN_vs (Helfrich Förster 1997). However, these cells were reported to undergo apoptosis in young flies, within adult day 1-2 (Helfrich-Förster 1997; Renn et al. 1999). Instead, they are suggested to have an eclosion-related role in the fly (Helfrich-Förster 1997). Besides its expression in the brain, PDF is produced also in neurons located in the eighth abdominal neuromere of the ventral ganglion (PDFAb neurons), innervating the larval and adult intestine (Helfrich-Förster 1997). Importantly, PDF-Tri and PDF-Ab neurons are not considered to be circadian clock cells, and they do not express oscillating circadian clock proteins (Renn et al. 1999; Park et al. 2000; Gatto & Broadie 2011).

In 2005, three research groups simultaneously identified the receptor for PDF using different approaches (Hyun et al. 2005; Lear et al. 2005; Mertens et al. 2005, for review see also Helfrich-Förster 2005). The PDF receptor (PDFR, also called han) is a G-protein coupled seven-transmembrane receptor, encoded by *CG13758*. To determine its expression pattern in the brain, different antibodies were generated. Mertens and his colleagues produced an antiserum against the final 20 amino acids of the predicted C terminus (Mertens et al. 2005). Hyun and his colleagues generated an antibody against the peptide sequence of the N terminus of PDFR (Hyun et al. 2005). However, these antibodies reported different results. In one of the studies (Mertens et al. 2005), the receptor seemed to be present in a subset of clock neurons (DN1 and DN3 groups) and non-clock neurons in the lateral and dorsal protocerebrum, as well as in the subesophageal ganglion. However, the other study reported a different expression pattern: the receptor was found in the l-LN_vs, in seven DN1 neurons, in one DN3 neuron and in one LN_d neuron (dorsal lateral neuron) (Hyun et al. 2005). Since subsequent studies assessed that the two existing antisera fail to provide genetically verifiable data about the expression pattern of PDFR, they aimed to further dissect the question where exactly PDFR is present (Shafer et al. 2008; Im & Taghert 2010).

In vitro data suggest that PDF principally signals through cyclic adenosine monophosphate (cAMP) and only weakly through calcium (Ca^{2+}) (Hyun et al. 2005; Mertens et al. 2005). It has also been demonstrated that it signals through the adenylate cyclase isoform AC3 (Duvall & Taghert 2012). Fluorescence resonance energy transfer (FRET)-based genetically encoded cAMP sensors were employed to measure PDF receptivity of clock neurons (Shafer et al. 2008). These measurements are based on the real-time monitoring of

cAMP concentration changes upon PDF application. Increased cyclic nucleotide levels were detected in almost all groups of clock neurons as a response to PDF application to freshly dissected fly brains, suggesting that they express PDFR (Shafer et al. 2008). Among all the clock neurons, only the large LN_vs were not found to be sensitive to PDF (Shafer et al. 2008).

For a long time, approaches using different *pdfr*-GAL4 lines also encountered difficulties, since PDFR expression reconstituted by the existing lines could only partially rescue the behavioral defects of *pdfr* mutants (*pdfr5304* and *pdfr3369*, Hyun et al. 2005). Thus, they did not give a reliable picture about the expression pattern of the receptor. However, Im and Taghert described a ~70 kB PDFR transgene which does rescue the entire PDFR circadian behavioral defects (Im & Taghert 2010). The transgene was highly expressed in three LN_ds, six DN1s, the 5th s-LN_vs, while lower expression level was found in the four s-LN_vs and their projection, in two l-LN_vs, approximately four DN1s, DN2s, and DN3s, as well as in neuronal projections with the dorsal brain neuropil. In addition, it was present in non-clock cells as well: in the anterior and posterior surfaces of central brain and subesophageal ganglion (Im & Taghert 2010).

PDF is the principal circadian neurotransmitter in *Drosophila melanogaster* (Renn et al. 1999). Experiments using *Pdf* null mutant (Pdf^{01}) flies and selective ablation of PDF containing neurons indeed revealed the regulatory role of this peptide in the circadian network. While these mutated flies were largely entrained to light-dark cycles, the majority of them showed arrhythmicity under constant darkness (Renn et al. 1999). In case they remained rhythmic in DD, they displayed a shorter free-running period compared to wild-type flies. Furthermore, locomotor activity records of Pdf^{01} mutants and PDF cell-ablated flies revealed that they lack lights-on anticipatory activity and display advanced evening activity peak in LD cycles (Renn et al. 1999). All these observations indicate the importance of PDF-expressing LN_vs in the morning activity of the flies, and the maintenance of robust 24 h free-running rhythms (Renn et al. 1999).

Recent studies using *in vivo* imaging have revealed that the different circadian pacemaker neuron clusters exhibit group-specific daily changes in their intracellular Ca^{2+} level (Liang et al. 2016; Liang et al. 2017). PDF was found to set the correct phase of the DN3 Ca^{2+} waves, and along with light inputs, its role has been implicated in the regulation of Ca^{2+} activity phase of the LN_d neurons (Liang et al. 2017). PDF was reported to suppress basal Ca^{2+} levels over hours, thereby delaying the onset of the calcium waves in the

aforementioned cell groups. In addition, PDF signaling helps to terminate the peak of the Ca^{2+} rhythm in the s-LN_vs through a negative feedback (Liang et al. 2017).

PDF immunoreactivity in the termini of s-LN_vs dorsal projections shows circadian changes, reaching a maximum in the early morning (Park et al. 2000; Fernández et al. 2008). This observation strongly suggests rhythmic PDF release in this brain area (Park et al. 2000), providing therefore a candidate mechanism through which PDF may convey time of the day information from core pacemaker clock cells to downstream targets. In addition, in the s-LN_vs a daily change in PDF sensitivity was detected, which persisted even in constant darkness (Klose et al. 2016). Interestingly, their responsiveness to PDF was the greatest in the early daytime, when the availability of PDF ligand in the dorsal brain is also predicted to reach its maximum (Klose et al. 2016).

An increasing number of evidence suggests the involvement of PDF in diapause regulation in several insect species, but apparently it plays different roles (Hamanaka et al. 2005; Shiga & Numata 2009; Meuti et al. 2015). In the blow fly *Protophormia terraenovae*, ablation of the cell bodies of PDF producing cells, equivalent to s-LN_vs in *Drosophila*, has been found to eliminate photoperiodism, indicating that circadian clock neurons play a role in the photoperiodic clock mechanism (Shiga & Numata 2009). The regulatory role of PDF in diapause was suggested also in the mosquito *Culex pipiens* (Meuti et al. 2015). Upon *Pdf* knockdown, females which were reared under diapause-averting long day conditions entered a diapause-like state (Meuti et al. 2015). In the bean bug *Riptortus pedestris,* ablation of PDF-positive neurons stimulated ovarian development in bugs reared under diapause-inducing conditions (Ikeno et al. 2014). However, the question about how PDF mediates its effect on dormancy remains still unanswered and requires further investigation. It is also possible that PDF somehow plays a role in the regulation of crucial insect hormones, ecdysone and juvenile hormone, whose synthesis is disrupted during overwintering (Denlinger 1985; Richard et al. 2001; Denlinger 2002; Allen 2007). Interestingly, it has recently been demonstrated that PDF stimulates ecdysone biosynthesis in the silkworm *Bombyx mori* (Iga et al. 2014).

Besides its role in circadian timekeeping and its putative involvement in overwintering responses, PDF was claimed to be involved in many other diverse physiological processes. For instance, it was found to modulate male sex pheromone expression and mating behavior: targeted expression of membrane tethered-PDF in

oenocytes (cells responsible for the synthesis and expression of cuticular pheromones) results in increased sex pheromone biosynthesis (Krupp et al. 2013). These cells express the *pdfr* gene and the phase of their peripheral clock is modulated by PDF (Krupp et al. 2013). Moreover, PDF is apparently a regulator of sleep (Donlea et al. 2009).

It was reported that PDF released by the PDFAb neurons is able to remotely control the activity of distant tissues (Talsma et al. 2012). PDFR was found in ureter muscles, through which PDF regulates renal function by inducing ureter contractions (Talsma et al. 2012). These findings suggest that PDF, possibly functioning as a circulating neurohormone, can also reach distant targets which are not directly innervated, thus do not receive direct synaptic input from PDF-expressing neurons. Albeit not shown in flies, PDF has been found in the hemolymph of locusts (Persson et al. 2001).

1.6.4. short neuropeptide F

The neuropeptide sNPF is an orthologue of mammalian neuropeptide Y (NPY), which is produced in the mammalian hypothalamus and controls food consumption (Gehlert 1999). In *Drosophila melanogaster*, four sNPF peptides (sNPF-1-4) are generated from the same sNPF precursor by different enzymatic modifications (Lee et al. 2004). The *snpf* transcript and sNPF protein are expressed during all developmental stages. The localization of the peptide was observed both in the central and peripheral nervous system (Lee et al. 2004; Nässel et al. 2008). In larvae, sNPF is expressed in about 600 Kenyon cells (KC) per larval hemisphere and approximately 200 cell bodies in the CNS (Nässel et al. 2008). In the adult brain, strong sNPF signal is present in the medulla and in approximately 4000 KC of the mushroom bodies (Lee et al. 2004). In addition, it is expressed in two 6-8 bilaterally symmetric neurons in the *Pars lateralis* (dorsal lateral peptidergic neurons, DLPs) (Kapan et al. 2013), in processes in neuropil of the subesophageal ganglion, and in a set of the median neurons in the *Pars intercerebralis* (Nässel et al. 2008). Intriguingly, sNPF is produced also in few clock neurons: in the small ventrolateral neurons and in a subset of dorsal lateral neurons (Johard et al. 2009). It has been reported that *snpf* mRNA is one of the most strongly cycling transcripts in the s-LN$_v$s (Kula-Eversole et al. 2010).

Interestingly, some of the sNPF-producing neurons co-express also other neuropeptides, for instance, the s-LN$_v$s clock cells express PDF, the DN neurons produce

Cha, and the DLPs express Crz (Johard et al. 2009; Kapan et al. 2012). In addition, five pairs of large protocerebral neurosecretory cells in two clusters (ipc-1 and ipc-2a) co-express short neuropeptide F, tachykinin, and ion transport peptide (Kahsai et al. 2010a).

In *Drosophila melanogaster*, the four sNPFs act on a single G-protein coupled receptor (sNPFR1, *CG7395*) (Garczynski et al. 2002; Mertens et al. 2002). There is apparently no colocalization between sNPFR1 and sNPF-expressing neurons in the CNS (Carlsson et al. 2013). IPCs have been reported to express sNPFR, through which sNPF positively regulates insulin-like signaling in larvae (Lee et al. 2008). Indeed, a later study by Kapan and his colleagues confirmed the expression of the receptor on larval and adult IPCs (Kapan et al. 2012). However, according to a subsequent report only the adult IPCs express sNPFR1 (Carlsson et al. 2013). The receptor was found also in olfactory sensory neurons (Root et al. 2011; Carlsson et al. 2013), as well as in the large ventrolateral clock neurons (Kula-Eversole et al. 2010).

Apparently, sNPF has different effects on feeding and non-feeding circuits: an excitatory nature of the peptide was described in neurons involved in feeding, while its opposite role has been found in non-feeding pathways (Shang et al. 2013). In BG2-c6 neuronal cell line, sNPF treatment results in increased levels of cAMP in a dose-dependent manner, suggesting that the stimulatory G protein alpha-subunit is a key subunit of sNPFR1 (Hong et al. 2012; Chen et al. 2013). Correspondingly, sNPF was reported to have an excitatory effect on the olfactory sensory neurons (Root et al. 2011) as well as in the insulin producing cells, where the co-application of sNPF and octopamine led to remarkable increases of cAMP (Shang et al. 2013). By contrast, *in vivo* data from live optical imaging showed that sNPF application to larval motor neurons results in a slight decrease in cAMP levels, suggesting that the sNPF effect is inhibitory and sNPFR1 acts via G_o signaling (Vecsey et al. 2013). Similarly, in the large ventrolateral neurons, sNPF reduced the large cAMP responses evoked by the wake-promoting dopamine (Shang et al. 2013). It has recently been demonstrated that sNPF also signals by suppressing basal Ca^{2+} levels in circadian clock neurons (Liang et al. 2017).

Considering that the peptide is detectable during all developmental stages and is expressed in many neuron types, it comes as no surprise that it fulfills multiple functions. In *D. melanogaster,* sNPF promotes food intake and increases body size (Lee et al. 2004); it regulates growth by modulating the expression of insulin-like peptides in the IPCs (Lee et al.

2008). Namely, it was found in larvae that sNPF regulates positively systemic insulin signaling via its receptor, sNPFR1, through extracellular-regulated kinase (ERK) signaling (*Figure 9*). It promotes the transcription of *dilps* through ERK activation: the secreted DILPs inhibit the nuclear translocation of the transcription factor FOXO; therefore, FOXO remains in the cytoplasm and its antigrowth program is prevented (Lee et al. 2008). The body size of sNPF hypomorphic mutant (*sNPF*^{c00448}) is significantly smaller than that of the wild-type, and it has defects in food finding behavior (Lee et al. 2004; Root et al. 2011). In line with this, overexpression of sNPF in the nervous system results in increased body size (Lee et al. 2004). It was furthermore shown that this neuropeptide is involved in starvation-dependent food search behavior in the odorant receptor neurons (Root et al. 2011) and it modulates bitter sensitivity during starvation (Inagaki et al. 2014).

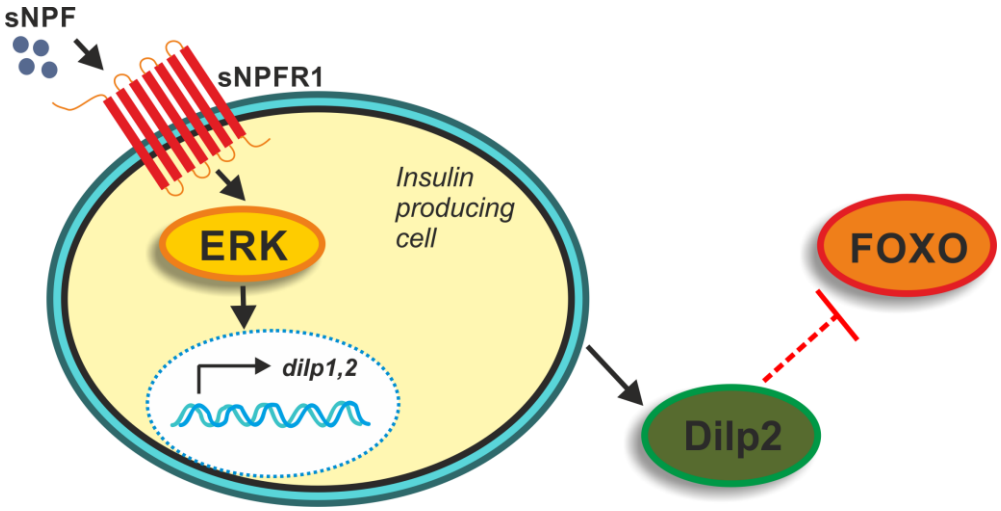

Figure 9. Activation of dilp transcripts by sNPF signaling regulates growth. sNPF, acting on its receptor (sNPFR1) on the IPCs, turns on the transcription of *Dilps* via ERK signaling. The secreted growth-promoting Dilps activate insulin-like signaling in target tissues, thereby the antigrowth events induced by FOXO are prevented. The figure is modified after Lee et al. 2008.

Interestingly, sNPF is also known as a sleep promoting inhibitory modulator, since it enhances nighttime sleep via the s-LN$_v$-to-l-LN$_v$ circuit (Shang et al. 2013). In locusts, it stimulates ovarian growth and increases vitellogenin levels (Schoofs et al. 2001), while in Colorado potato beetles it functions as a potential diapause regulator (Huybrechts et al. 2004). sNPF is also involved in the regulation of osmotic and metabolic stress (Kahsai et al. 2010a), as well as in the modulation of locomotion (Kahsai et al. 2010b). In addition, the role

of sNPF has been implicated in the regulation of lifespan: flies with diminished sNPF levels in DLPs display extended lifespan upon starvation, while overexpression of this peptide in the same neuron subset leads to reduced survival (Kapan et al. 2012).

Similarly to the neuropeptide PDF, sNPF has also been identified as a key factor in regulating the phase of Ca^{2+} rhythms generated in specific clock cells (Liang et al. 2017). This peptide was found to set the phase of spontaneous calcium waves in the DN1 clock neurons by suppressing their Ca^{2+} activity (Liang et al. 2017). In addition, sNPF produced by s-LN_vs, was also implicated in the regulation of prothoracicotropic hormone-producing neurosecretory cells (PG neurons) by serving as a timing signal between the core pacemaker cells and the PG neurons (Selcho et al. 2017). The received timing information is conveyed to the prothoracic gland and modulates its peripheral clock. Thus, sNPF provides an important link between the central and peripheral clock systems (Selcho et al. 2017).

1.6.5. Corazonin

Corazonin is a highly conserved amidated undecapeptide that functions as a neurohormone in the central nervous system of insects and crustaceans. It affects diverse physiological functions in a species-specific manner (Boerjan et al. 2010). This neuropeptide is thought to be the mammalian homolog of gonadotropin-releasing hormone (Cazzamali et al. 2002), which is directly regulated by stress hormones (Li et al. 2004). Corazonin was first identified from the *corpora cardiaca* of the cockroach *Periplaneta americana* based on its potent cardioacceleratory effect (Veenstra 1989).

As for the expression of Crz, from late embryonal stage until the larval stages the peptide is consistently detectable in three different neuronal groups: dorsal-lateral peptidergic neurons (DLPs), dorso-medial Crz neurons and Crz neurons in the ventral nerve cord. However, in the adult central nervous system of *Drosophila* only the DLPs are present, while the other two Crz cell groups are no longer detectable (Choi et al. 2005). Interestingly, in adult male flies Crz is expressed also in a cluster of four abdominal ganglion neurons (Lee et al. 2008). Crz-producing neurons have been shown to co-express membrane receptors for the diuretic hormones 31 and 44, suggesting the role of these peptides in the modulation of corazonergic neuronal activities (Johnson et al. 2005).

Drosophila Crz receptor (CrzR) is a member of G-protein coupled receptor family and shows structural homology to the mammalian Gonadotropin releasing hormone receptor (Cazzamali et al. 2002). Physiological roles of the CrzR *(CrzR; CG10698)* have not yet been extensively investigated; however it was reported to be involved in ethanol-related behavior and ethanol metabolism (Sha et al. 2014). The insulin producing cells have already been claimed to express CrzR, since IPC-specific knockdown of the *CrzR* gene leads to increased starvation resistance (Kapan et al. 2012). According to a recent report, knockdown of CrzR in peripheral tissues alters *dilp* transcript levels (Kubrak et al. 2016).

In the locusts *Locusta migratoria* and *Shistocerca gregaria,* Crz was identified as a dark-color inducing neuropeptide (dark-pigmentotropin), since it activates cuticle pigmentation during the gregarious phase (Tawfik et al. 1999). In *Drosophila*, the role of Crz has been implicated in the modulation of trehalose metabolism and triglyceride levels (Lee et al. 2008; Zhao et al. 2010; Kapan et al. 2012), in the regulation of resistance to oxidative stress and starvation (Kapan et al. 2012), as well as in the initiation of ecdysis (Kim et al. 2004). In addition, it has been proposed to function as a regulator of alcohol sedation sensitivity (McClure & Heberlein 2013). Corazonin may also be associated with biological clock functions as a putative target of pacemaker neurons, as it was suggested in the hawkmoth *Manduca sexta* (Wise et al. 2002) as well as in *Drosophila* (Choi et al. 2005). Interestingly, Crz-immunoreactive neurons were suggested to regulate photoperiod-controlled pupal diapause in *M. sexta* (Shiga et al. 2003).

2. AIMS OF THE PROJECT

The aim of the project was to investigate the putative role(s) of neuropeptides in the regulation of adult reproductive diapause in *D. melanogaster*. Since insulin-like signaling is known to be critical in determining insect dormancy, we decided to primarily focus our attention on neuron clusters that may signal to the insulin producing cells (IPCs) based on the existence of their axonal projections in the dorsal-dorsolateral fly brain (*Figure 10*).

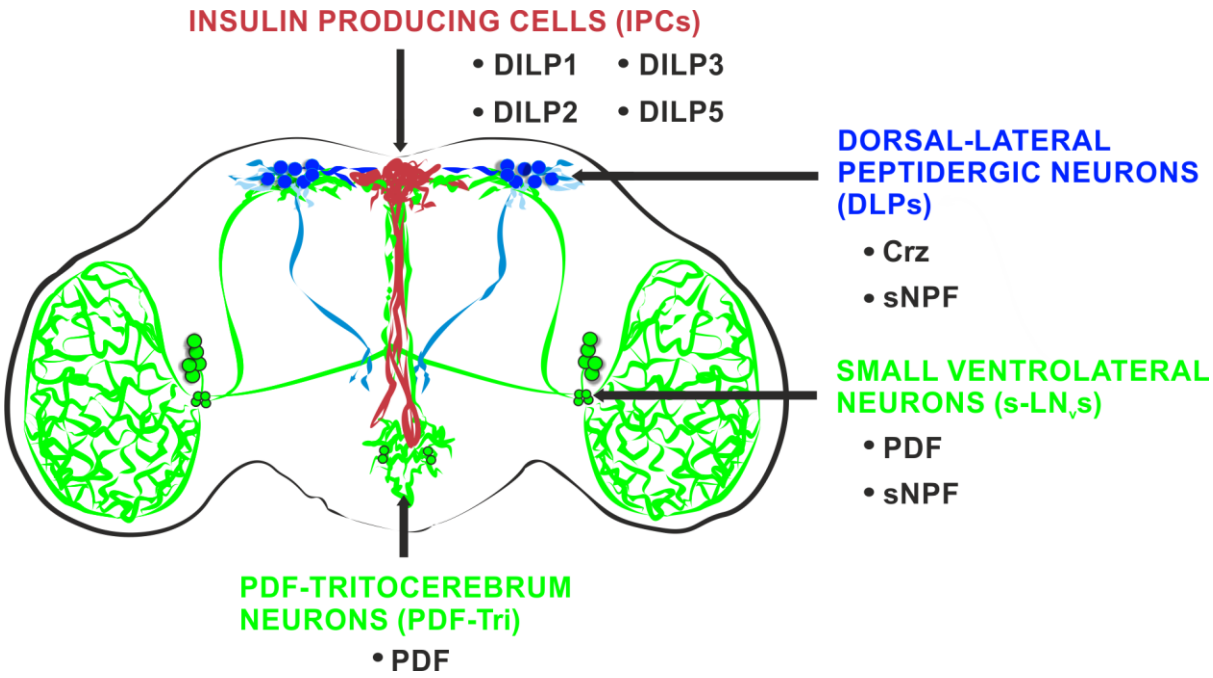

Figure 10. Putative neuronal network. The small ventrolateral neurons (s-LN_vs), the dorsal-lateral peptidergic neurons (DLPs), and the PDF tritocerebrum neurons (PDF-Tri) send neuronal projections in the vicinity of the insulin producing cells (IPCs) in the dorsal fly brain. The connection, if any, among these neurons can be facilitated by their neuropeptides. DILP1, -2, -3, -5: Insulin-like peptide 1, 2, 3, 5; PDF: pigment dispersing factor; sNPF: short neuropeptide F; Crz: corazonin.

We studied the role of the circadian neurotransmitter pigment dispersing factor (PDF), expressed in two different neuron clusters that can potentially contact the IPCs: the small ventrolateral neurons (s-LN_vs) and few neurons in the tritocerebrum (PDF-Tri). The s-LN_vs co-express PDF and short neuropeptide F (sNPF) (Helfrich-Förster 1997; Johard et al. 2009), and are known as the dominant pacemaker neurons of the circadian clock network (Rieger et al. 2006). Their axonal projections reach the dorsal brain area, where they are suggested to rhythmically release PDF (Fernández et al. 2008). In addition, we investigated the role of (a) PDF-Tri neurons that were found to project to the *PI* region (Helfrich-Förster

1997) and (b) of another small set of sNPF-expressing neurons, defined as dorsal-lateral peptidergic neurons (DLPs), which have axon terminations in the proximity of the IPCs. They co-express sNPF and the neuropeptide corazonin (Crz) (Kapan et al. 2012).

Using specific antibodies against the neuropeptides of interest, we characterized their localization and expression pattern in the fly brain, paying particular attention to their arborizations close to the IPCs. In addition, we aimed to unravel the possible existence of anatomical connections among the candidate neurons. To this end, live optical imaging was performed in the IPCs using genetically encoded sensors for cyclic AMP and calcium. Neuronal connections were further studied by GFP Reconstitution Across Synaptic Partners approach.

Finally, we attempted to improve our diapause experimental protocol by testing the effect of more natural-like light-dark profiles on the diapause response of the flies, to better mimic the natural daily fluctuation of light intensity and composition.

3. MATERIALS AND METHODS

3.1. Rearing conditions

All the fly stocks used for this study were maintained at 23°C, 70% relative humidity, in 12-hour light/12-hour dark cycles (LD 12:12) unless otherwise stated, in plastic vials containing standard cornmeal food (72.0 g/l corn flour, 79.3 g/l sugar, 8.5 g/l agar, 50.0 g/l dried yeast powder, 0.27% Methyl parahydroxybenzoate in ethanol, 0.3% propionic alcohol).

3.2. Fly stocks

Most of the described strains were obtained from stock centers as Bloomington Drosophila Stock Center (BDSC) or Vienna Drosophila RNAi Center (VDRC). In these cases, stock numbers are also indicated. The following lines were used in this study:

- *Hu-S* and *Hu-LS*: Strains originated from an isofemale line obtained from a natural population of Houten (Holland, 52.02° N; 5.16° E), collected in 2004. Using PCR genotyping, by classical genetic crossing methods, these lines were made homozygous either for the *s-tim* or *ls-tim* variant (Tauber et al. 2007; Sandrelli et al. 2007). (From Charalambos P. Kyriacou).
- *WTALA-S* and *WTALA-LS:* Northern Italian isofemale lines, collected in 2004. *WTALA-S* line (bearing *s-tim*) was originated from Postal (46.61° N; 11.19° E), while *WTALA-LS* (carrying *ls-tim*) was derived from Foresta (46.67° N; 11.12° E). Both lines, together with several others sampled in the same area, were used to establish the natural wild-type strain *WT-ALA* (Wild Type ALto Adige) (Tauber et al. 2007; Sandrelli et al. 2007).
- w^{1118}*; s-tim* and w^{1118}*; ls-tim:* Loss-of-function white mutant commonly used as a genetic background in transgenic manipulations. The flies have white eyes phenotype. w^{1118}*; s-tim* comes from Charlotte Förster, while w^{1118}; *ls-tim* was ordered from BDSC (*#5905*).
- *Canton-S*: Canton Special, standard laboratory wild-type *Drosophila melanogaster* strain. (BDSC *#1*).
- *Oregon-R:* Wild-type laboratory stock of *Drosophila melanogaster*. It was used as a control for han^{5304} mutant. (BDSC *#2376*).

- *Crz_1*-Gal4 (*w[1118]; P{w[+mC]=Crz-GAL4.391}3M*): Expresses the Gal4 in the dorsal-lateral peptidergic neurons (DLPs). (BDSC *#51976*).
- *Crz_2*-Gal4 (*w[1118]; P{w[+mC]=Crz-GAL4.391}4M*): Expresses the Gal4 in the DLPs. (BDSC *#51977*).
- *dilp2(p)*-Gal4: Expresses the Gal4 in the IPCs from early larval life (2nd instar) under the temporal control of *dilp2* gene promoter (Rulifson et al. 2002). The insertion is on the 2nd chromosome. (From Eric J. Rulifson).
- *$Elav^{C155}$*-Gal4 (*P{w[+mW.hs]=GawB}elav[C155]*): The line is used as a pan-neuronal driver; the Gal4 is expressed in all tissues of the embryonic nervous system beginning at stage 12. (BDSC *#458*).
- *gal1118:* GAL4 enhancer trap line, described as essentially restricted to the PDF-expressing LN_vs, with weaker expression in other clock cells as well as in a few non-clock cells (Blanchardon et al. 2001). (From Ezio Rosato).
- *Insp3*-Gal4: Expresses the Gal4 in IPCs from post-larval stages under temporal control of *dilp3* gene promoter (Buch et al. 2008). The insertion is on the 3rd chromosome. (From Michael J. Pankratz).
- *Pdf-Gal4* (*y[1] w[*]; P{w[+mC]=Pdf-GAL4.P2.4}2*)*: Gal4* transgene insertion under the control of *Pdf* promoter. Gal4 expression is driven only in the PDF-positive LN_vs and in PDF-Tri neurons (Renn et al. 1999; Park et al. 2000). (BDSC *#6900*).
- *R6*-Gal4: The line was generated from a male recombination experiment described by Hewes et al. (2000). The line was backcrossed to *yw^{67c23}* for 14 generations. It expresses the Gal4 almost exclusively in the s-LN_vs and very little (if at all) in the l-LN_vs. (From Charlotte Förster).
- *UAS-Epac1camps* (*w[1118]; P{w[+mC]=UAS-Epac1-camps}50A*): Genetically encoded intracellular cAMP FRET sensor (Shafer et al. 2008). (From Charlotte Förster).
- *UAS-GCamp3.0* (*w[1118]; P{y[+t7.7] w[+mC]=UAS-GCaMP3.T}attP40*): A GFP-based calcium sensor for imaging calcium dynamics (Tian et al. 2009). (From Charlotte Förster).
- *UAS-hid* (*P{w[+mC]=UAS-hid.Z}2/CyO*)*:* Expresses the apoptotic gene *head involution defective* (*hid*) to genetically ablate cells (Zhou et al. 1997). (From Charlotte Förster).
- UAS-*2xsNPF:* Expression of two copies of *sNPF* transgene, inserted on the 2nd and 3rd chromosomes (Lee et al. 2004). (From Kweon Yu).

- UAS-*CD8-GFP* (*y[1] w[*]; P{w[+mC]=UAS-mCD8::GFP.L}LL5, P{UAS-mCD8::GFP.L}2*): P-element insertion carrying the *gfp* gene under the control of UAS sequences. It expresses a membrane-bound form of GFP, helping to visualize Gal4-expressing cells. (BDSC *#5137*).
- *UAS-Crz-RNAi*$_1$: Targeted RNAi against *corazonin* (*crz*). The insertion is on the 2nd chromosome. (VDRC *KK106876*).
- *UAS-Crz-RNAi*$_2$*:* Targeted RNAi against *corazonin* (*crz*). The insertion is on the 2nd chromosome. (VDRC *GD30670*).
- UAS-*kir2.1* (*w*; P{UAS-Hsap\KCNJ2.EGFP}7*)*:* The line is used to silence neurons by reducing membrane excitability through the expression of the inward rectifying K^+ channel Kir2.1 (Baines et al. 2001). It had already been successful to silence clock neurons (Nitabach et al. 2002; Depetris-Chauvin et al. 2011). (From Charlotte Förster).
- UAS-*OrkΔ-C* (*y[1] w[*]; P{w[+mC]=UAS-Ork1.Delta-C}2*): Expression of a potassium channel that functions as neuronal silencer by reducing membrane excitability, thereby lowering neuropeptide release from target neurons (Nitabach et al. 2002). It had previously been effectively used to silence clock neurons (Nitabach et al. 2002). (From Michael B. O'Connor).
- UAS-*Na$^+$ChBac* (*y[1] w[*]; P{w[+mC]=UAS-NaChBac}2*): Expression of a bacterial sodium channel to hypersensitize neurons by enhancing their membrane excitability, thereby provoking increased release of their neuropeptides (Nitabach et al. 2006). The line had been successfully adopted to increase the electrical excitability of Drosophila clock neurons (Nitabach et al. 2006). (From Michael B. O'Connor).
- *UAS-Pdf:* Expression of *Pdf* transgene, inserted on the 2nd chromosome (Renn et al. 1999). (From Charlotte Förster).
- UAS-*sNPFR1-DN*: Expression of a dominant negative form of sNPF receptor (Lee et al. 2008). (From Kweon Yu).
- w;*Pdf*-LexA,LexAop-*CD4::GFP^{11}/CyO*;UAS-*CD4::GFP$^{1-10}$/TM6b*: Recombinant line for GRASP analysis (Feinberg et al. 2008), expressing a fragment of the GFP (GFP^{11}) in the PDF^+ neurons, and containing also the complementary fragment (GFP^{1-10}) in a UAS construct. (From François Rouyer).
- lexAop-*CD8-GFP-2ACD8-GFP*;UAS-*mLexA-VP16-NFAT,*lexAop-*CD2-GFP/TM6b:* Transgenic

flies for CaLexA system to label active neurons in the brain (Masuyama et al. 2012). A truncated version of Nuclear factor of activated T-cells (NFAT) is fused to the DNA binding domain derived from the bacterial repressor LexA, and to the VP16 activation domain. Upon increasing Ca^{2+} concentration, the LexA-VP16-NFAT chimeric transcription factor shuttles to the nucleus and promotes the expression of the *gfp* reporter gene under the control of LexA operator (LexAop). (From Ezio Rosato).

- *han*^{5304} mutant: The flies bear a large C-terminal deletion of PDF receptor (han), a mutation that generates a behavioral phenocopy to the *Pdf*^{01} peptide mutant. (Hyun et al. 2005). (From Charlotte Förster).
- *Hu-S Pdf*^{01}and *Hu-LS Pdf*^{01}*:* The mutant *Pdf*^{01} was isolated by EMS screening, and carries a nucleotide substitution resulting in a premature STOP codon (Y21STOP) (Renn et al. 1999). The line has been "houtenized", by putting the flies in the natural genetic background of Houten (*Hu-S* and *Hu-LS*) by repetitive backcrossing through 8 generations. (From Charalambos P. Kyriacou).

In order to use a control in which the specific transgene (GAL4 or UAS) was in the same condition of heterozygosis as in the experimental line, we have crossed all the parental lines to the *w*^{1118} strain (generic genotype *w*^{1118}*;P-element/+*).

Moreover, heterozygous controls were generated according to the *timeless* allele of the UAS and GAL4 strains used in the experiments. For this purpose, *w*^{1118}*; s-tim* and *w*^{1118}; *ls-tim* lines were adopted that express either *s-* or *ls-timeless* isoform in their genome. For experiments with *han* mutant, *Oregon-R* was used as control.

3.3. Binary expression systems

The GAL4-UAS (Brand & Perrimon 1993) and LexA-lexAop systems (Lai & Lee 2006) are the most powerful binary systems for precise manipulation of gene expression in *D. melanogaster* (*Figure 11*). These techniques consist of two independent components initially separated into two distinct transgenic lines. In the GAL4-UAS system, the first component is the yeast transcriptional activator GAL4, which is expressed under the control of a cell- or tissue-specific promoter. The second element is the upstream activating sequence (UAS), an enhancer to which GAL4 specifically binds to activate gene transcription. The target gene is

transcriptionally silent, unless flies carrying it are crossed to those of an activator line containing the GAL4. In the progeny of this cross the transgene will be expressed in the same spatial and temporal patterns as the specific driver (Brand & Perrimon 1993).

In the LexA-LexAop system, the lexA DNA binding domain of *E. coli* is fused to a transactivator domain, which binds to and activates the LexA operator (*LexAop*), thereby turning on the expression of the LexAop-linked transgene (Lai & Lee 2006).

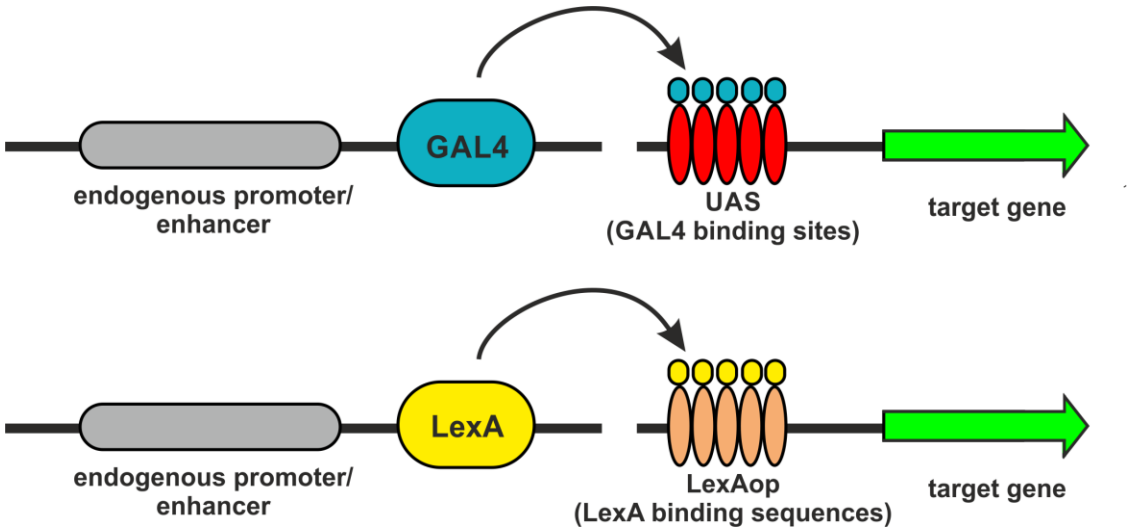

***Figure 11. Binary expression systems in Drosophila melanogaster*.** In the UAS-GAL4 system (upper panel), the yeast GAL4 transcription factor is expressed in a tissue-specific pattern in the driver line. In the responder line, the expression of the target gene is under the control of UAS (upstream activation sequence)-sites, to which GAL4 can bind. When the parental lines containing the UAS-GAL4 elements are crossed, in the progeny GAL4 binds to UAS and turns on the expression of UAS-target gene. In the LexA-LexAop system (lower panel), the *E. coli*-derived transcriptional activator LexA binds to the LexA operator (LexAop), thereby inducing the expression of the transgene downstream of LexAop.

3.4. Polymerase chain reaction for *timeless* genotyping

All the *Drosophila melanogaster* lines used in this project have been genotyped by polymerase chain reaction (PCR) in order to identify the allele of the *timeless* (*s-tim* or *ls-tim*) gene and to ensure the genetic homogeneity, for the *timeless* locus, between the experimental flies and their corresponding controls.

3.4.1. Extraction of genomic DNA

The genomic DNA was extracted from individual adult females. 10 flies were tested. A single fly was homogenized in 50 µl of extraction buffer (Tris HCl pH = 8.2 10 mM, EDTA 2 mM, NaCl 25 mM); after addition of 1 µl of Proteinase K (10 mg/ml) samples were incubated at 37°C for 45 min, followed by 3 min at 100°C to inactivate the enzyme. Finally, samples were centrifuged for 3 min at maximum speed, and the supernatant was stored at -20°C until processing.

3.4.2. PCR parameters

The *timeless* region containing the polymorphic site was amplified using a reverse primer and two different forward primers, which allow selective amplification of the different *tim* alleles (Tauber et al. 2007). The size of the amplified product is 689 bp. As an internal control for PCR efficiency, another *timeless* region has also been amplified. The size of this control fragment is 488 bp. Sequence and positions of primers are detailed in *Table 2*.

Table 2. Parameters of primers used for timeless genotyping PCR.

Primer	Sequence	Length	Position
GA (forward) specific for ls-tim	*5'-TGGAATAATCAGAACTTT**GA**-3'*	*20 nt*	*311-330*
AT (forward) specific for s-tim	*5'-TGGAATAATCAGAACTTT**AT**-3'*	*20 nt*	*311-330*
TIM-3' (reverse)	*5'-AGATTCCACAAGATCGTGTT-3'*	*20 nt*	*923-942*
C5 (forward) control primer	*5'-CATTCATTCCAAGCAGTATC-3'*	*20 nt*	*2438-2457*
C3 (reverse) control primer	*5'-TATTCATGAACTTGTGAATC-3'*	*20 nt*	*2786-2805*

The reaction products were analyzed in 1.5% agarose electrophoresis gel to determine the genotype of the individual samples. *Appendix Table 1* shows the *timeless* genotype of each line used in our diapause experiments.

3.5. Diapause assay

All the fly stocks and crosses used for diapause assay were maintained at 23°C in LD 12:12 cycles during their entire development. Newly eclosed flies (collected within 5 hours

after eclosion) were placed in new culture tubes, and immediately exposed to diapause-inducing conditions, i.e. at 12°C in LD 8:16 or LD 15:9 (rectangular LD cycles) for 11 days (PROTOCOL 1).

After 11 days, flies were killed in absolute ethanol and were immediately analyzed in PBS 1x (137 mM NaCl, 2.7 mM KCl, 10 mM sodium phosphate dibasic, 2 mM potassium phosphate monobasic, pH=7.4). The ovaries of females were dissected under 40x zoom with LeicaMZ6 stereomicroscope, and diapause levels were scored. Each female was considered being in diapause in the complete absence of vitellogenic oocytes in its gonads, when yolk deposition is not yet visible (Saunders et al. 1989; *see Figure 2*). Diapause levels were later presented as the proportion of diapausing females among all the dissected individuals. At least 5 replicates of n>60 flies were dissected for each genotypes, unless stated otherwise.

Importantly, the rearing conditions have been changed for some diapause experiments to test a new protocol (PROTOCOL 2), in which flies were exposed to 18°C and LD 8:16 during their development. In some cases, diapause levels were also scored after 30 days. These special conditions will be mentioned separately when describing the individual experiments. *Appendix Table 2* provides a numerical summary of all diapause data presented in this study.

3.6. Immunocytochemistry

For immunocytochemistry (ICC), female flies were collected at ZT1 (Zeitgeber time 1 h, 1 h after light-on), and immediately fixed in 4% paraformaldehyde (PFA) diluted in PBS, by incubating the samples on a rotating wheel at room temperature (RT) for 100 min. After 3 washes in PBS, fly brains were dissected in ice-cold PBS using LeicaMZ6 stereomicroscope. Brains were fixed in PFA 4% for 40 min at RT and then washed 6 times in 0.3% PBST (0.3% Triton X-100 in PBS 1x). Next, a permeabilization step with detergents was performed in 1% PBST (1% Triton X-100 in PBS 1x) for 10 min, followed by an overnight blocking step in 1% bovine serum albumin (BSA) in 0.3% PBST at 4°C. Afterwards, the brains were incubated in primary antibody solution (diluted in 0.1% BSA, 0.3% PBST) on a shaker for 3 days at 4°C. After 6 washes in 1% BSA in 0.3% PBST at RT, another blocking step was performed in 1% BSA in 0.3% PBST at 4°C, followed by hybridization with the secondary antibody (diluted in 0.1% BSA, 0.3% PBST) overnight at 4°C. Samples were again washed 6 times in PBS and then

mounted onto microscope slides using Vectashield mounting medium (Vector Laboratories, Inc.). Samples were stored at -20°C until microscopic evaluation. Brains have been visualized using either a semi-confocal microscope (Nikon Eclipse 80i equipped with a QiCAM Fast Camera using the Image ProPlus software) or confocal microscope (ZEISS LSM700 running ZEN Lite software; objectives EC Plan-Neofluar 20x/0.50 M27, Plan-Apochromat 40x/1.3 Oil Ph3 M27 or Plan-Apochromat 63x/1.40 Oil Ph3 M27). For each brain, individual images were taken at different depths in order to create z-series. The size of each section, with either one of the microscope used, was approximately 1 µm ± 0.2. *Table 3* and *Table 4* provide information about the primary and secondary antibodies used in this study.

Table 3. Basic information about the primary antibodies used in this study

Detected neuropeptide	Origin	Working concentration	Provenience
PDF	*mouse*	*1:5000*	*Hybridoma Bank*
DILP2	*rabbit*	*1:2000*	*Jan A. Veenstra (University of Bordeaux)*
Crz	*rabbit*	*1:1000*	*Jan A. Veenstra (University of Bordeaux)*
sNPF	*rabbit*	*1:2000*	*Jan A. Veenstra (University of Bordeaux)*
GFP	*mouse*	*1:500*	*Thermo Fisher Scientific*

Table 4. Basic information about the secondary antibodies used in this study

Name	IgG detected	Origin	Working concentration	Provenience
Alexa Fluor 488	*mouse*	*goat*	*1:250*	*Invitrogen*
Cy3	*rabbit*	*goat*	*1:500*	*Jackson ImmunoResearch*

For quantification of the immunocytochemical signals, Fiji software was used. Staining index has been calculated using different methods. In the experiments where intensity was measured in the cell bodies (for example, in the l-LN_vs and IPCs), the individual cells were outlined manually. The backgrounds were selected adjacent to the cells of interest, and the staining index was calculated as (S-B)/B, where S = fluorescent signal of the specific cell, and B = background. When quantifying PDF-Tri signals in the tritocerebrum, two different methods were tested, both of them provided identical results. In the first method, a circular

shape of the same size was placed on the images directly under the posterior optic tract and intensity values were measured inside the circle. Backgrounds were selected near the circle, and the same formula was used as mentioned above. In the alternative method, photos were magnified in order to track the border line of the fluorescent signal, and intensity was measured inside the outlined area. Three areas adjacent to the region of interest were selected and averaged to create an average background (B_{avg}). Pixel intensity (($S-B_{avg}$)/B_{avg}) multiplied by area was used to create a staining index. Similar approach was used to quantify DILP axon, PDF intensity staining along the IPC axon and cell bodies, as well as to quantify PDF in the axonal termini of s-LN_vs.

3.7. GFP Reconstitution Across Synaptic Partners (GRASP)

GFP Reconstitution Across Synaptic Partners (GRASP) is a system that allows identifying synapse formation between specific neurons in living nervous systems (Feinberg et al. 2008). Two complementary fragments of GFP (a long GFP^{1-10} and a shorter GFP^{11}) are expressed on the extracellular membranes of different neurons. The functional GFP reporter is reconstituted and fluorescence appears at the points of contact when synapses are formed between the two cells. In the present work, a possible synaptic contact between PDF-positive neurons and insulin producing cells was investigated by GRASP analysis. GFP^{11} was expressed in the membrane of the PDF^{+} neurons, while GFP^{1-10} was encoded in the IPCs, using genetically engineered transgenic flies. Fly brains were analyzed in immunocytochemistry, and images were acquired with a ZEISS LSM700 confocal microscope using ZEN Lite software.

3.8. Live optical imaging in the insulin producing cells

Live optical imaging is a sensitive method to measure concentration changes of the second messenger cyclic adenosine monophosphate (cAMP) and Ca^{2+} in living fly brains. The function of the genetically encoded cAMP sensors are based on the cAMP-binding properties of EPAC (exchange protein directly activated by cAMP) - a molecule mediating non-protein kinase A (PKA)-dependent cAMP signaling (de Rooij et al. 1998). In the Epac-based sensor used in this study (Shafer et al. 2008), a cyan fluorescent protein (CFP) and a

yellow fluorescent protein (YFP) flank a truncated Epac1, containing only the cAMP-binding domain. When not bound to cAMP, the Epac-based sensor supports fluorescence resonance energy transfer (FRET) from CFP to YFP. The binding of cAMP forces the CFP and YFP domains to move apart, leading to a reduction in FRET levels when cAMP levels rise (*Figure 12A*).

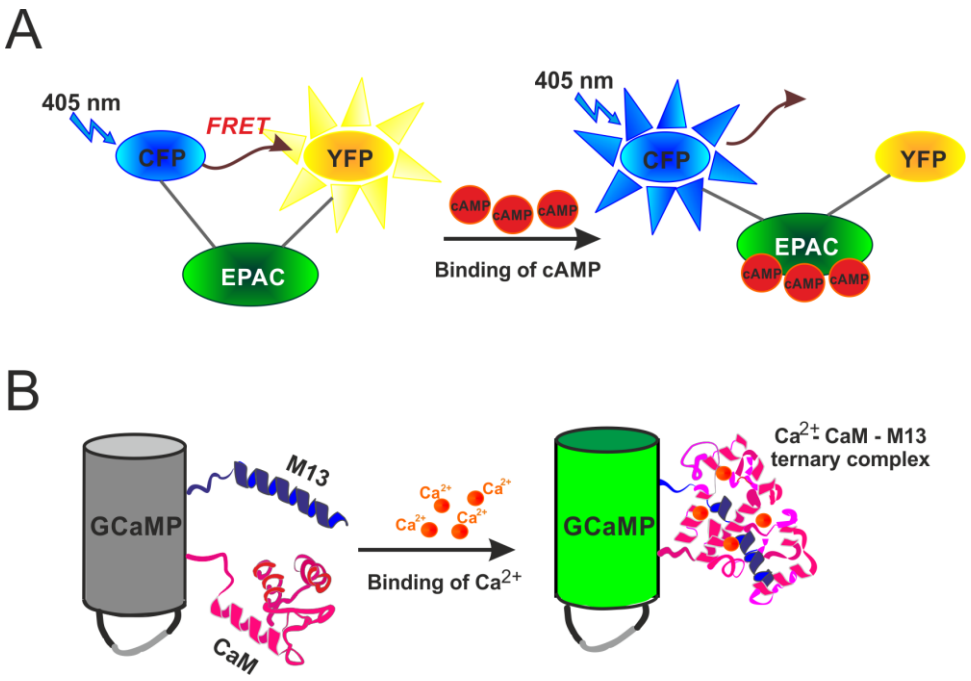

Figure 12. A schematic figure of the genetically encoded sensors. (A) Basic design of an EPAC-based cAMP FRET sensor. The cAMP-binding protein EPAC is flanked by a cyan and yellow fluorescent protein (CFP and YFP, respectively). In the absence of cAMP, the excitation of CFP leads to enhanced resonance energy transfer (FRET) from CFP to YFP. As soon as cAMP is bound, it forces the CFP and YFP domains to move apart leading to a reduction in FRET levels which is proportional to the cAMP concentration. (B) Schematic representation of GCaMP calcium sensor. The sensor consists of a circularly permutated GFP, calmodulin (CaM) and M13 peptide. When not bound to Ca^{2+}, the GFP is present in a poorly fluorescent state. Upon Ca^{2+} binding, intramolecular CaM-M13 interaction is induced, leading to the formation of a ternary complex which brings back GFP to its native functional structure with high fluorescence intensity. Figure (B) is modified after Lindenburg & Merkx 2014.

To real-time monitor Ca^{2+} concentration changes, a genetically encoded calcium indicator, GCaMP3 was adopted (Nakai et al. 2001). The sensor is based on circularly permutated green fluorescent protein (cpGFP), the calcium-binding protein calmodulin (CaM), and the Ca^{2+}/CaM-binding M13 domain of myosin light chain kinase (*Figure 12B*). When not bound to Ca^{2+}, cpGFP exists in a poorly fluorescent state. When Ca^{2+} concentration increases, CaM undergoes a conformational change and the created CaM-Ca^{2+}

complex binds the M13 domain, restoring cpGFP to its native functional structure (Nakai et al. 2001).

For the experiments, neuropeptides (see more details in *Table 5*) were dissolved in 50% acetonitrile in 10^{-2} M concentration, and then samples were lyophilized and stored at -20°C until time of testing. For cAMP imaging, the cAMP sensor UAS-*Epac1camps* (Shafer et al. 2008) was expressed under the control of the *dilp2(p)*-Gal4 driver line in wild-type and PDF receptor null mutant (*han*) background (Hyun et al. 2005). Female flies, maintained at 25°C, were anesthetized on ice and brains were freshly dissected in cold hemolymph-like saline (HL3; Stewart et al. 1994) and mounted at the bottom of a plastic cap of a Petri dish (35x10 mm, Becton Dickenson Labware, New Jersey) in HL3 with the dorsal surface up. Brains were allowed to recover from dissection 15 minutes prior to imaging. Live imaging was conducted by using an epifluorescent imaging setup (VisiChrome High Speed Polychromator System, ZEISS Axioskop2 FS plus, Visitron Systems GmbH) with a 40x dipping objective (ZEISS 40x/1.0 DIC VIS-IR).

Table 5. Neuropeptides used for live optical imaging

Neuropeptide	***Sequence***	***Provenience***
Pigment dispersing factor (PDF)	*NSELINSLLSLPKNMNDAa*	*Iris Biotech GmbH*
short Neuropeptide F-1 (sNPF-1)	*AQRSPSLRLRFa*	
Adipokinetic hormone (AKH)	*pQLTFSPDWa*	*gift from Christian Wegener (University of Würzburg, Germany)*
Allatostatin-C (Ast-C)	*pEVRYRQCYFNPISCF*	*gift from Paul H. Taghert (Washington University in St. Louis)*
Tachykinin 4 (DTK-4)	*APVNSFVGMRa*	
dFMRFamide 4	*SDNFMRFa*	

IPCs were brought into focus and regions of interest (ROIs) were defined on single cell bodies using the Visiview Sotfware (version 2.1.1, Visitron Systems, Puchheim, Germany). Time-lapse frames were imaged with 0.2 Hz by exciting the CFP fluorophore of the cAMP sensor with a violet light (405 nm). CFP and YFP emissions were separately detected with a CCD-camera (Photometrics, CoolSNAP HQ, Visitron Systems GmbH) for 1000 s using a beam splitter. After measuring baseline FRETs for ~100 s, substances were bath-

applied drop-wise using a pipette. Peptides used in this study were applied in a final concentration of 10 µM in 0.1% DMSO in HL3 (45 µl 10^{-4}M neuropeptide solution was added to 405 µl HL3). The water-soluble forskolin derivate NKH477 (Sigma Aldrich) served as positive control in a concentration of 10 µM, while HL3 with 0.1% DMSO was used as negative control. In the case of tetrodotoxin (TTX) treatments, brains were incubated for 15 min in 2 µM TTX in HL3 prior to imaging and substances were co-applied together with 2 µM TTX. Intensity data for CFP and YFP emissions of all ROIs were transported to Excel software, and Inverse Fluorescence Resonance Energy Transfer (iFRET) was calculated over time according to the following equation: iFRET = CFP/(YFP-CFP*0.357) (Shafer et al. 2008). Thereby, raw CFP and YFP emission data were background corrected; in addition, YFP data were further corrected by subtracting the CFP spillover into the YFP signal, which was determined as 0.357 (35.7% of the CFP signal). Next, iFRET traces of individual neurons were normalized to baseline and were averaged for each treatment. Finally, maximum iFRET changes were calculated for individual neurons within time intervals of 100-200 s and 100-1000 s to quantify and contrast response amplitudes of each treatment.

For Ca^{2+} imaging, brains expressed the UAS-*GCamp3.0* sensor in the insulin producing cells (*dilp2(p)*-Gal4) (Nakai et al. 2001). The preparation of the brain samples was the same as in the case of cAMP imaging, and the same microscope was used with a modified setup, measuring GFP fluorescence without a beam splitter. The cholinergic agonist carbamylcholine (1 mM CCh) was used to generate rapid Ca^{2+} increases (Nakai et al. 2001). After subtraction of background fluorescence, changes in fluorescence intensity were calculated for each ROI as $\Delta(F/F_0) = [(F_n - F_0)/F_0] \times 100$ with F_n as fluorescence intensity at time point *n* and F_0 as the baseline fluorescence calculated prior to the application of the different substances to the brain. The microscope settings were kept the same in the case of the different experimental conditions.

Appendix Figure 1, *2*, and *3* show the single neuron traces recorded during both calcium and cAMP imaging.

3.9. CaLexA system

CaLexA (calcium-dependent nuclear import of LexA) is a novel activity reporter system for defining active neurons (Masuyama et al. 2012) (*Figure 13*). The technique is

based on the calcium-responsive transcription factor NFAT (nuclear factor of activated T cells), which is fused to the VP16 transcriptional activator and LexA DNA-binding domain, forming the synthetic transcription factor LexA-VP16-NFAT. Upon increasing Ca^{2+} concentration in the active neurons, LexA-VP16-NFAT shuttles to the nucleus and turns on the expression of *gfp*.

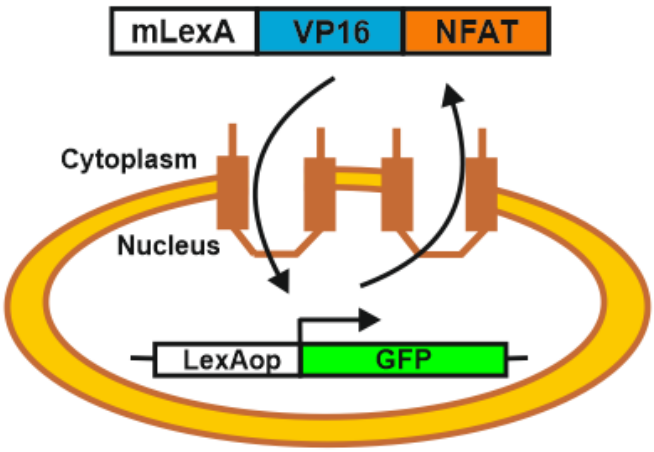

Figure 13. The schematic illustration of the CaLexA system. The method is based on the Ca^{2+}-dependent nuclear localization of the NFAT Ca^{2+}-responsive transcription factor. A truncated version of NFAT is fused to DNA binding domain derived from the bacterial repressor LexA, and to the VP16 activation domain. Upon Ca^{2+} accumulation, the LexA-VP16-NFAT chimeric transcription factor goes to the nucleus and induces the expression of the *gfp* reporter gene under the control of LexA operator (LexAop). The figure is modified after Masuyama et al. 2012.

3.10. Generation of natural-like light-dark profiles

To investigate the effect of photoperiod on diapause induction, late autumnal and summer days were simulated in the laboratory relying on real dataset registered in Northern Italy (Treviso 45.67° N; 12.23° E, Vanin et al. 2012). The experimental setup takes into account the intensity changes of natural sunlight throughout the day, and in addition, better mimics outdoor light conditions in term of spectral composition. The overwintering response of four *Drosophila* natural populations was studied: *Hu-S*, *Hu-LS*, *WTALA-S* and *WTALA-LS* (See *Materials and Methods, page 41; Figure 14A*).

To generate natural-like light profiles accordingly to outdoor conditions, a custom-built programmable simulator (constructed by Dr. Stefano Bastianello, Euritmi S.A.S,

Selvazzano Dentro, Italy) was employed, which dictated the selected light regimes in an incubator (SANYO ELECTRIC MLR-351 versatile environmental test chamber). The adopted

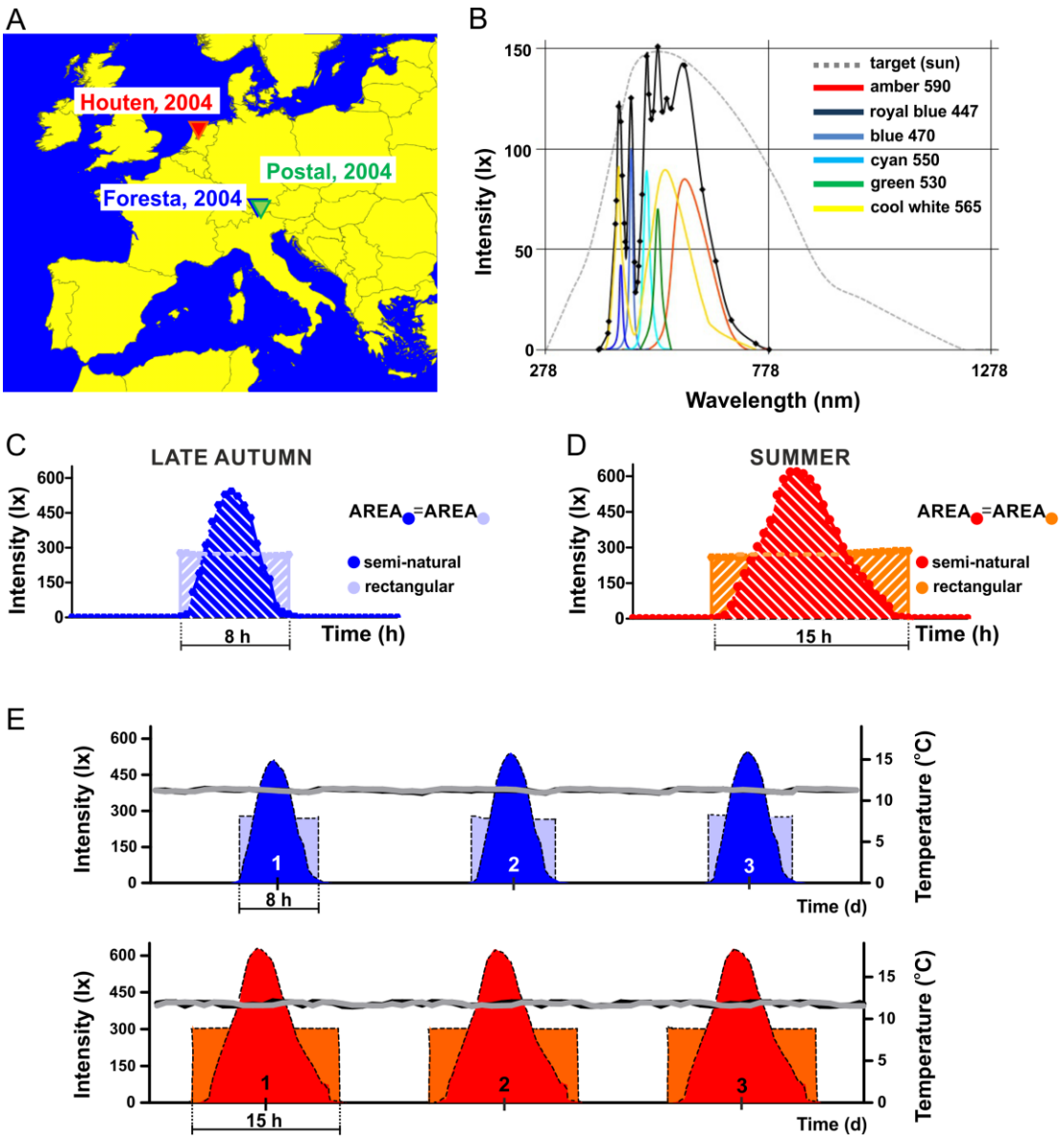

Figure 14. Simulated profiles to mimic light conditions of consecutive late autumnal and summer days. (A) The origin of the *D. melanogaster* field lines used in this study: Houten (Holland), Postal (Italy; designated as *WTALA-S*), and Foresta (Italy; designated as *WTALA-LS*). (B) Color composition of the generated light profiles. Various selected LED sources are employed to approximate as much as possible the target profile of the Sun (gray dotted line). The different color components and their wavelength are listed on the right. The sum of the contribution of all the individual colors is marked by black continuous line. (C, D) A representative late autumnal and summer day, and a corresponding rectangular short (LD 8:16) and long (LD 9:15) day. The integral of the semi-natural and rectangular profiles are equal in the case of both late autumnal and summer conditions. (E) Three representative days of the simulated late autumnal (upper panel) and summer profiles (lower panel). Gray and black curves indicate the recorded temperature data during rectangular and semi-natural light settings, respectively.

device combines outputs of six groups of LEDs with different emission spectra (*Figure 14B*), and produces sophisticated light profiles with progressively changing light intensity over the day (described also in Vanin et al. 2012; Green et al. 2015a, b). Sunset and sunrise data were obtained from the online database of the Naval Observatory (USNO) Astronomy Application Department (http://aa.usno.navy.mil/faq/docs/RST_defs.php; 'Rise, Set, and Twilight Definitions').

To mimic late autumnal days, light conditions of a late November day were simulated, adopting a day length of ~9 h (8 h 59 m, 30th of November 2014). Considering that fruit flies have been shown to favor shaded conditions in nature (Rieger et al. 2007), ~510 lux maximum light intensity was selected, a value close to what has been recorded by the Trikinetics environmental sensor when placed in a shaded place outdoors (Vanin et al. 2012). To ensure that individuals under the rectangular LD cycles (used as controls) are subjected to equal amounts of light, the integral of the continuous light curve was calculated, yielding 290 lux constant light intensity to be used during the 8 hours of photophase of rectangular cycles (*Figure 14C, E).*

In the case of summer days, a photoperiod of 15 h was employed for the rectangular profile, keeping 290 lux constant light intensity. Considering that on the longest summer day in Treviso the photoperiod is ~15.5 h (15 h, 42 m, 21st of June 2015), and that areas determined by the light profiles must be the same between rectangular and semi-natural conditions, 620 lux was adopted as maximum light intensity to mimic a real summer. All experiments were carried out at 12^{o}C, and both the temperature and light data were continuously monitored (*Figure 14D, E*).

3.11. Statistics

Data were analyzed with R software (version 3.0.1, www.r-project.org). In the case of normally distributed data (Shapiro-Wilk normality test, $p>0.05$), statistical significance was tested by a pairwise t-test, while not normally distributed data were analyzed by Wilcoxon test. In the case of multiple comparisons, raw p-values were further adjusted by Bonferroni correction, and these corrected p-values served as significance levels. For diapause assays, all data were transformed to arcsine value, prior to be statistically analyzed, and then one-way or two-way ANOVA with post-hoc Tukey's HSD tests were applied.

4. RESULTS

4.1. Genetic manipulations of PDF$^+$ neurons alter diapause levels

In order to test whether PDF$^+$ neurons in the brain are involved in the regulation of diapause, these cells were genetically manipulated by using *Pdf*-Gal4 driver line that allows target gene expression in the PDF-producing neurons (Renn et al. 1999; Park et al. 2000). To this end, two different approaches were used: (1) *"gain of function"*, by increasing membrane excitability and thereby enhancing the release of neuropeptides, or overexpressing target neuropeptides; (2) *"loss of function"*, by reducing membrane excitability and thereby silencing target neurons and reducing the release of their neuropeptides, or genetically ablate target cells.

First of all, the neurons were hypersensitized by the overexpression of a bacterial depolarization-activated sodium channel (Nitabach et al. 2006), and the diapause response of the flies was analyzed. Since this manipulation enhances the membrane excitability of PDF$^+$ cells (Nitabach et al. 2006), the neurons are believed to be more prompt to release their synthesized neuropeptides, including PDF, sNPF, and possibly other additional neurotransmitters. Interestingly, the hypersensitization resulted in significantly reduced diapause levels in the experimental flies (*Pdf>Na$^+$ChBac* 8.3 ± 5.1%, ***p<0.001) compared to both controls (+>*Na$^+$ChBac* 51.2 ± 6.5% and *Pdf*>+ 37.3 ± 1.6%) (*Figure 15A*).

Next, we overexpressed the circadian neurotransmitter PDF in the same subset of cells using UAS-*Pdf* transgenic line. The overexpression led to significantly reduced diapause levels in the experimental flies (*Pdf>Pdf* 16.0 ± 5.4%, ***p<0.001) compared to control females (+>*Pdf* 68.2 ± 5.5% and *Pdf*>+ 37.3 ± 3.9%) (*Figure 15A*). Then, we wondered whether the other neuropeptide, sNPF, could have a modulatory effect on diapause levels. Since sNPF is widely expressed in the fly brain (Lee et al. 2004; Nässel et al. 2008), we first overexpressed it with the pan-neuronal driver *elav^{C155}*-Gal4 and checked the effect of its broad overexpression on the diapause response of flies. To efficiently perform this manipulation, UAS-*2xsNPF* transgenic flies that carry two copies of the *snpf* transgene were used (described by Lee et al. 2004). We found that the pan-neuronal overexpression of sNPF induced a significant reduction in diapause levels in the experimental flies (*elav>2xsNPF* 6.6 ± 3.2%, ***p<0.001) compared to both controls (*elav*>+ 67.5 ± 6.6% and +>*2xsNPF* 43.8 ± 1.4%) (*Figure 15B*). Considering that both *elav^{C155}*-Gal4 and UAS-*2xsNPF* flies carry the *ls-timeless* allele (*Appendix Table1*), known to favor diapause (Tauber et al. 2007), the

observed diapause-antagonist effect of sNPF seems even more potent in this background. In order to check whether sNPF produced by the ventrolateral neurons influences diapause, we narrowed the peptide overexpression specifically in the PDF^{+} neurons. We detected a highly significant decrease in diapause levels in the experimental flies (*Pdf>2xsNPF* 4.3 ± 1.7%, ***p<0.001) compared to the controls (*Pdf*>+ 59.8 ± 2.7% and +>*2xsNPF* 29.8 ± 4.6%) (*Figure 15C*). Thus, the abundant expression of sNPF only in the PDF-expressing neurons apparently phenocopies the effect caused by the pan-neuronal overexpression of the peptide.

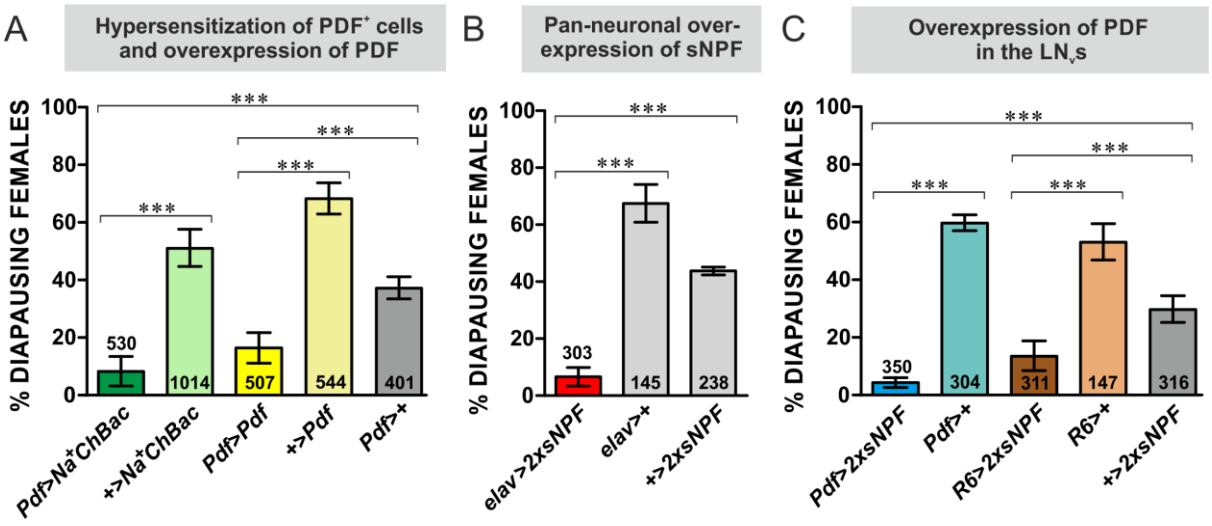

Figure 15. Enhanced activity of PDF-producing neurons reduces diapause levels. (A) Hypersensitization of PDF^{+} cells by the expression of a bacterial sodium channel (*Pdf>Na^{+}ChBac*) and overexpression of PDF (*Pdf>Pdf*) both result in a significant reduction of diapause levels. (B) Pan-neuronal overexpression of sNPF (*elav>2xsNPF*) leads to a significant decrease in the proportion of diapausing females. (C) Overexpression of sNPF in the PDF-producing neurons (*Pdf>2xsNPF*) and in the small ventrolateral neurons (*R6-Gal4>2xsNPF*) triggers females to come out of diapause. Numbers within bars refer to the number of dissected females considered in the diapause assays. Data are presented as mean ± SD. ANOVA on arcsine transformations, followed by post-hoc Tukey HSD test. ***p<0.001, n.s. not significant.

Similar results were obtained when sNPF was overexpressed only in the small ventrolateral neurons, as we observed significantly reduced diapause levels (*R6>2xsNPF* 13.5 ± 5.1%, ***p<0.001) when compared to control females sharing the same *timeless* backgrounds (*R6*>+ 52.7 ± 6.2% and +>*2xsNPF* 29.8 ± 4.6%) (*Figure 15C*). Therefore, sNPF produced by these neurons is apparently involved in the negative regulation of diapause by promoting ovarian growth. To test how diapause levels are influenced upon inhibition of neuropeptide release from the PDF-producing neurons, we dampened their neuronal

excitability by expressing two different potassium channels (UAS-*kir2.1* and UAS-*OrkΔ-C*, respectively) under the control of *Pdf*-Gal4 driver. The neuronal overexpression of these channels leads to increased potassium efflux and membrane hyperpolarization, thereby preventing the firing of action potentials (Nitabach et al. 2002). PDF$^+$ cell-specific expression of *kir2.1* induced a slight increase in the percentage of diapausing females; however it was not statistically different from the control females (*Figure 16A*). Flies expressing the *OrkΔ-C* transgene showed a significantly greater tendency to enter diapause (*Pdf*>UAS-*Ork* 55.7 ± 10.9%) compared to both controls (*Pdf*>+ 31.8 ± 4.7%, **p<0.001, and +>*Ork* 19.4 ± 5.9%, ***p<0.001) (*Figure 16B*).

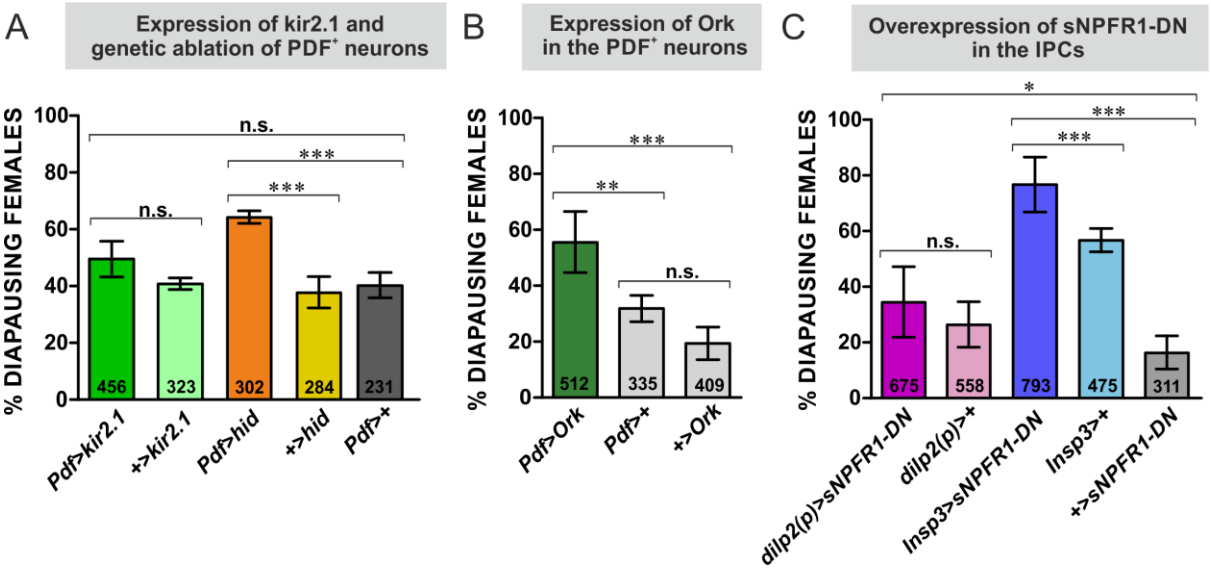

Figure 16. Inhibited neuronal activity of PDF$^+$ cells and impairment of sNPF signaling in the IPCs increase diapause levels. (A) Expression of the potassium channel *kir2.1* (*Pdf>kir2.1*) induces a small, but not statistically significant increase in diapause levels. Genetic ablation of PDF-producing neurons (*Pdf>hid*) provokes a higher proportion of females to enter reproductive diapause in comparison with the controls (C) Overexpression of a dominant negative form of *sNPFR1* (UAS-*sNPFR1-DN*) in the insulin producing cells under the control of an early and a late IPC driver (*dilp2(p)*-Gal4 and *Insp3*-Gal4, respectively). The experimental flies show higher diapause levels compared to the controls (in the case of *dilp2(p)*-Gal4 driver statistically significant increase only compared to one of the controls). Numbers within bars refer to the number of dissected females considered in the diapause assays. Data are presented as mean ± SD. ANOVA on arcsine transformations, followed by post-hoc Tukey HSD test. ***p<0.001, **p<0.01, *p<0.05, n.s. not significant.

Next, we asked whether diapause levels are altered when PDF$^+$ neurons are genetically ablated. To induce cell death in these neuron clusters, the pro-apoptotic protein hid (head involution defective) was overexpressed with the help of UAS-*hid* transgenic line, which has already been shown to efficiently ablate circadian neurons (Stoleru et al. 2004).

We found that this manipulation provokes a larger proportion of females to undergo diapause (*Pdf>hid* 65.5 ± 2.3%, ***p<0.001) compared to the controls (+>*hid* 38.6 ± 5.6% and *Pdf*>+ 40.3 ± 4.4%) (*Figure 16A*).

Based on these results, PDF-expressing neurons seem to be involved in the regulation of the overwintering behavior in *Drosophila*, since influencing their activity alters diapause levels. Their actions are most probably mediated by the neuropeptides PDF and sNPF they produce.

4.2. sNPFR1 signaling in the IPCs modulates dormancy

It is known that sNPF receptor (sNPFR1) is expressed on the insulin producing cells (Lee et al. 2008; Kapan et al. 2012; Carlsson et al. 2013), through which sNPF regulates growth by turning on the transcription of different *dilps* (Lee et al. 2008). To investigate whether sNPFR1 signaling in the IPCs influences the diapause response of the flies, a dominant negative form of the sNPFR1 (UAS-*sNPFR1-DN*, described in Lee et al. 2008) was expressed under the control of two different drivers specific for the IPCs. The first driver, *dilp2(p)*-Gal4 (*p* refers to *precocious*), starts the expression from early larval life (2nd instar), while *Insp3*-Gal4 drives gene expression from post larval phases (Rulifson et al. 2002; Buch et al. 2008).

Flies expressing *sNPFR1-DN* showed different diapause phenotypes depending on the IPC driver used. Expression of the transgene from the early larval stages did not seem to largely affect the proportion of diapausing females (*Figure 16C*). Although the mutant females exhibited significantly higher incidence of diapause compared to the UAS control (*dilp2(p)>sNPFR1-DN* 34.6 ± 12.7% compared to +>*sNPFR1-DN* 16.4 ± 6.0%, *p<0.05), no difference was found compared to the Gal4 control. However, in the case of the later-expressed driver, a significantly higher proportion of the experimental flies underwent diapause (*Insp3*>*sNPFR1-DN* 77.1 ± 9.9%) compared to both controls (*Insp3*>+ 57.1 ± 4.2%, ***p<0.001 and +>*sNPFR1-DN* 16.4 ± 6.0, ***p<0.001).

These results suggest that impaired sNPF signaling in the IPCs is likely to affect diapause levels. However, the effect is more dominant in the case of the later-expressed driver (*Insp3*-Gal4). Since both drivers are specific for the 14 IPCs in the brain (Rulifson et al. 2002; Buch et al. 2008), the disparity between the two results may be caused by the

quantitative differences between *dilp2(p)*- and *Insp3*-Gal4 regarding the strength of transgene expression.

Our earlier data suggest that sNPF from the ventrolateral neurons modulates diapause levels (*Figure 15C*); however it is not yet known whether sNPF from these cells exerts its effect by acting on the IPCs. Moreover, one should consider that many sNPF-expressing cells are present in the brain that can potentially target the IPCs. For instance, the dorsal-lateral peptidergic neurons in the *Pars lateralis* have already been suggested to influence IPC activity via their neuropeptides (Kapan et al. 2012).

4.3. DLPs seem not to be involved in the regulation of diapause

The dorsal-lateral peptidergic neurons (DLPs) are 6-8 bilaterally symmetric neurons that have axon terminations in the proximity of the insulin producing cells (Kapan et al. 2012). They co-express the neuropeptides Crz and sNPF that modulate IPC activity by acting on their receptors, located on the insulin producing cells (Kapan et al. 2012). Interestingly, DLPs were found to affect survival, stress resistance and circulating carbohydrate and lipid levels (Kapan et al. 2012; Kubrak et al. 2016). Since diapause is associated with increased survival and stress resistance, as well as altered metabolism, the question arises whether DLPs are involved in the regulation of this seasonal response. To address this issue, two DLP-specific *Crz*-Gal4 driver lines (designated as Crz_1-Gal4 and Crz_2-Gal4) were used in which the inserted P-element is located at different chromosomes (Chr 2 and Chr 3, respectively).

First, the Gal4 expression pattern of these two transgenic lines was tested by expressing a membrane-bound form of green fluorescent protein (UAS-*CD8-GFP*). In the case of both drivers, we detected GFP in the DLPs (6-8 neurons in the *Pars lateralis*) and in their axonal projections in the *Pars intercerebralis* (*PI*), in the median bundle (MB) along the brain midline, as well as in the tritocerebral neuropil (*Figure 17A*). Another set of axons emerges from the DLPs runs in the posterior lateral tract (PLT).

To investigate whether DLPs and their neuropeptides regulate the overwintering behavior in flies, we hypersensitized these neurons by overexpressing Na^+ChBac. Although the experimental flies exhibited significantly lower diapause levels compared to the UAS control ($Crz_1>Na^+ChBac$ 26.8 ± 6.7% compared to $+>Na^+ChBac$ 65.4 ± 6.7%, ***p<0.001), there was no detectable difference compared to the Gal4 control (*Figure 17B*).

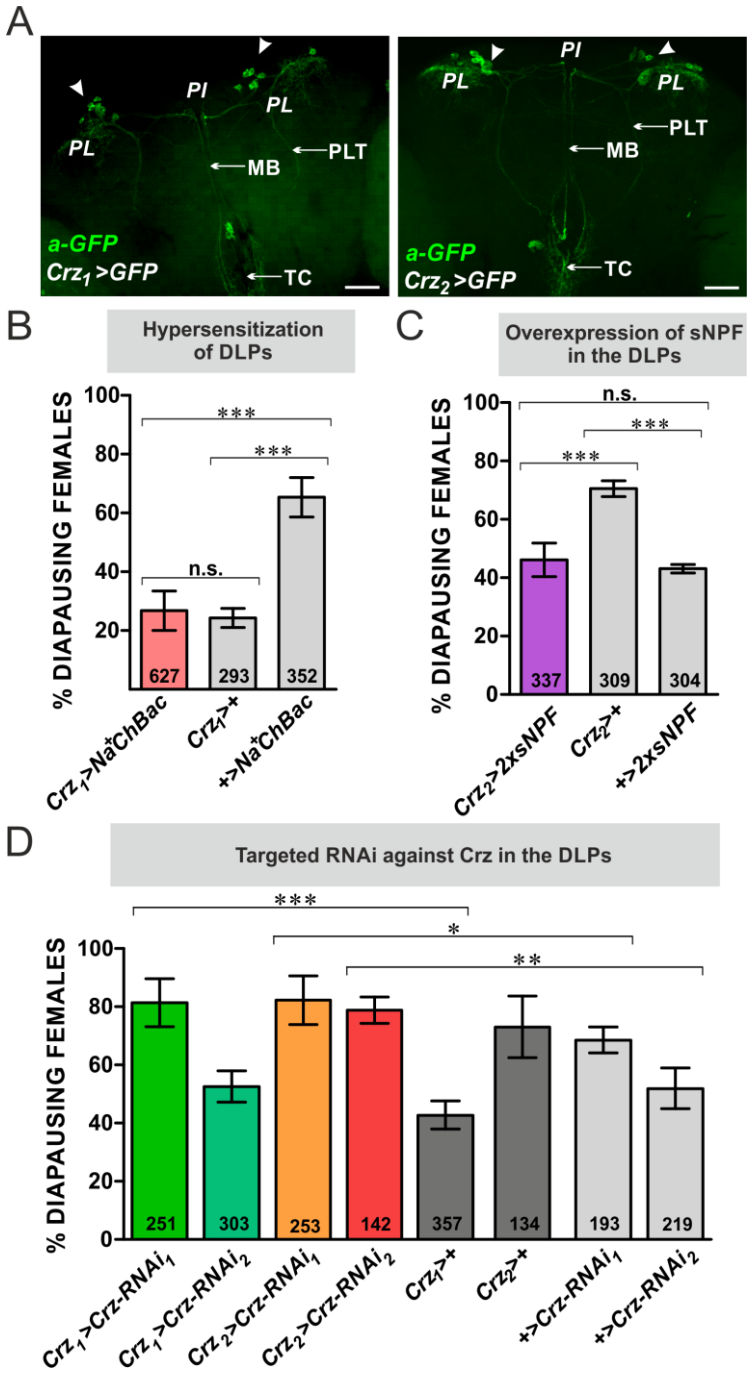

Figure 17. Genetic manipulation of the dorsal-lateral peptidergic neurons has no effect on diapause behavior. (A) Representative confocal images (z-stack) showing the expression of a membrane-bound GFP under the control of two different *Crz*-Gal4 drivers (Crz_1-Gal4 and Crz_2-Gal4). GFP expression was detected by *anti-GFP* antibody. White arrowheads indicate the location of DLPs in each brain hemisphere in the *Pars lateralis* (*PL*). They have axons running across the median bundle (MB) to the tritocerebrum (TC) and in the posterior lateral tract (PLT). Scale bar = 40 µM. (B) Overexpression of a bacterial sodium channel in the DLPs (Crz_1>Na^+*ChBac*) does not alter diapause levels (no difference from the Gal4 control). (C) Overexpression of sNPF does not influence the diapause response of the flies (no difference from the UAS control). (D) Targeted knockdown of *Crz* in the DLPs does not have a major effect on diapause levels. Only significant differences are indicated. Numbers within bars refer to the number of dissected females considered in the diapause assays. Data are presented as mean ± SD. ANOVA on arcsine transformations, followed by post-hoc Tukey HSD test. ***p<0.001, **p<0.01, *p<0.05, n.s. not significant.

Next, we overexpressed sNPF in the DLPs to check its possible effect on reproductive diapause. We found that this genetic manipulation induced approximately half of the females (Crz$_2$>*2xsNPF* 46.1 ± 5.8%) to enter diapause, which was a significant reduction compared to the percentage of diapausing females in the case of the GAL4 control (*Crz$_2$*>+ 70.5 ± 2.7%, ***p<0.001) (*Figure 17C*). However no difference was detected compared to the UAS control. This finding suggests that, even though DLP processes extend into the proximity of the IPCs, sNPF signaling from these cells does not alter diapause levels.

To further investigate the possible involvement of Crz signaling in the regulation of diapause, *Crz* expression was downregulated by RNAi-mediated knockdown. Two different UAS-*Crz-RNAi* lines (designated as UAS-*Crz-RNAi$_1$* and UAS-*Crz-RNAi$_2$*) were used to perform the experiments with the aforementioned two *Crz*-Gal4 drivers, creating four different combinations of crosses (*Crz$_1$*-Gal4>UAS-*Crz-RNAi$_1$*, *Crz$_1$*-Gal4>UAS-*Crz-RNAi$_2$*, *Crz$_2$*-Gal4>UAS-*Crz-RNAi$_1$*, *Crz$_2$*-Gal4>UAS-*Crz-RNAi$_2$*). In the case of the *Crz$_1$*-Gal4 driver, the proportion of diapause exhibited by the experimental flies was very different depending on the expressed RNAi construct (*Crz$_1$*>*Crz-RNAi$_1$* 81.4 ± 2.7% and *Crz$_1$*>*Crz-RNAi$_2$* 52.6 ± 5.4%) (*Figure 17D*). Importantly, only in one case there was a statistically significant difference between experimental flies and controls, when higher percentage of *Crz$_1$*>*Crz-RNAi$_1$* females were found to enter the diapause compared to their Gal4 control (*Crz$_1$*>+ 42.8 ± 4.8%, ***p<0.001). DLP-specific expression of UAS-*Crz-RNAi$_1$* with *Crz$_2$*-Gal4 driver induced diapause in the majority of the females (83.3 ± 8.5%), and even if the percentage of the dormant flies was significantly higher compared to the UAS control (+>*Crz-RNAi$_1$* 68.6 ± 4.4%), no difference from the Gal4 control was observed (*Figure 17D*). In the case of the second RNAi construct, the experimental flies and the Gal4 control entered the dormant state at very similar percentages, but the UAS control exhibited significantly lower diapause levels (+>*Crz-RNAi$_2$* 52.0 ± 7.0%, **p<0.01). These data suggest that the downregulation of *Crz* does not affect the diapause response. Nevertheless, it has to be pointed out that the gene knockdown for the *Crz-RNAi$_1$* construct with a *Crz*-gal4 driver led to a reduction of 62% of *Crz* levels (McClure & Heberlein 2013).

Altogether, these data suggest that DLPs are likely not involved in the regulation of reproductive diapause in *Drosophila*. When their neuronal activity was genetically manipulated through the altered expression of their neuropeptides, diapause behavior did not show marked changes. Even though in some cases there were differences compared to

one of the two controls, any of the experiments produced consistent and convincing results with significant differences from both controls.

4.4. PDF-Tri neurons survive in the cold

Our results based on diapause assays suggest the involvement of the neuropeptide PDF in the regulation of diapause. However, it remains to be investigated whether PDF can exert its effect acting on the IPCs. As known from previous reports, two clusters of PDF-producing neurons, the small ventrolateral neurons and PDF-Tri cells, send axonal projections to the dorsal fly brain (Helfrich-Förster 1997; Park et al. 2000). Thus, PDF from these cells can possibly target areas close to the *Pars intercerebralis* where IPCs are located. Importantly, PDF is believed to function as a neurohormone, therefore it can reach also distant tissues not directly innervated (Persson et al. 2001; Talsma et al. 2012; Krupp et al. 2013).

To investigate the relationship between insulin producing cells and PDF^+ neurons, the expression pattern of both PDF and IPCs were studied by double-staining fly brains with antibodies against PDF and DILP2. Moreover, to test the effect of temperature on the projection pattern and production of these neuropeptides, experiments were performed at three different temperatures in the wild-type *Canton-S* laboratory strain and in *Hu-S* field line. As for the experimental protocol, flies were reared at 23°C in LD 12:12 and newly eclosed flies (6 h post eclosion) were placed at 12°C, 18°C or 23°C in short days (LD 8:16).

We found that PDF-Tri neurons, that have been reported to undergo apoptosis in the very beginning of adult life (Helfrich-Förster 1997; Renn et al. 1999), surprisingly survived in the cold (both at 12°C and 18°C) even in nearly two-week-old flies (*Figure 18A*). PDF immunoreactivity in these cells were found to exhibit significant temperature-dependent changes both in *Hu-S* (Kruskal-Wallis test $H(2) = 15.885$, ***$p<0.001$) and *Canton-S* (Kruskal-Wallis test $H(2) = 19.346$, ***$p<0.001$) lines (*Figure 18A* and *B*). In *Hu-S*, the signal was significantly lower at higher temperature (23°C 0.41 ± 0.07) compared to that measured both at 18°C (0.71 ± 0.05, **$p<0.01$) and 12°C (1.00 ± 0.13, ***$p<0.001$) (*Figure 18B, left panel*). There was a small decrease at 18°C compared to 12°C but it was not statistically significant.

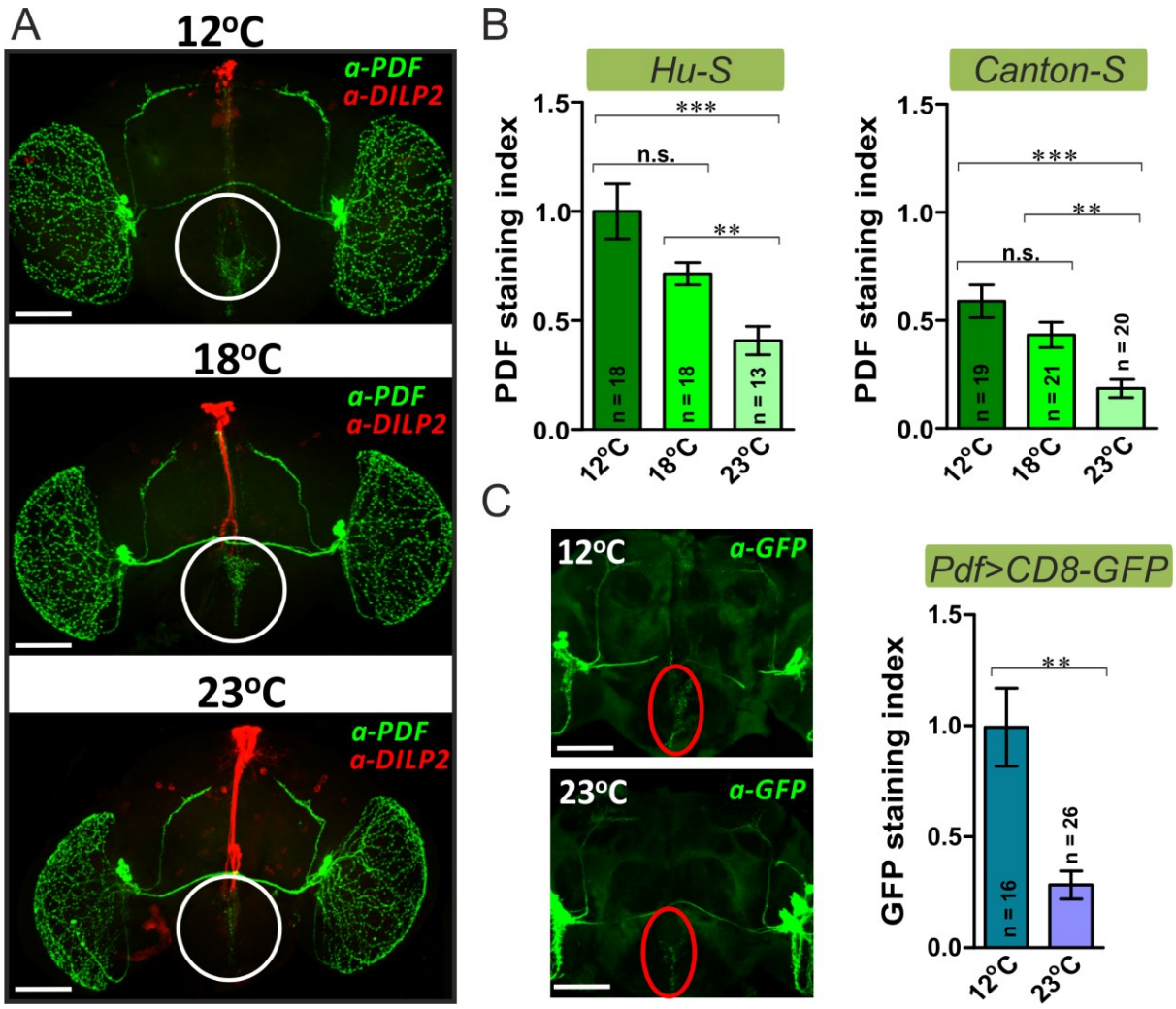

Figure 18. PDF-Tri neurons survive at cold temperatures even in two-week-old flies. (A) Representative confocal images (Z-stack) of *Hu-S* fly brains double-stained with *anti*-PDF (in green) and *anti*-DILP2 (in red) antibodies at different temperatures (12°C, 18°C, and 23°C). White circles show the area in which PDF-Tri neurons are located. PDF-Tri cells and their arborizations can be seen both at 12°C and 18°C. Scale bars = 100 µM. (B) Quantification of PDF signal in the tritocerebrum in *Hu-S* and *Canton-S* strains highlights temperature-dependent differences, with significantly higher PDF-Tri at low temperatures (both at 12°C and 18°C). n = number of dissected brains. (C) *Pdf*-Gal4-driven GFP expression (*Pdf>CD8-GFP*) in the PDF$^+$ cells confirms the persistence of PDF-Tri at low temperature. *Left:* representative images of brains showing the tritocerebrum area with the PDF-Tri structure (red circle). Scale bars = 100 µM. *Right:* Quantification of GFP signal reveals significantly higher GFP levels at 12°C. Data are normalized to the mean GFP level measured at 12°C. n = number of dissected brains. Data are presented as mean ± SEM. Non-parametric Kruskal-Wallis test followed by pairwise comparisons using Wilcoxon's rank sum test. ***p<0.001, **p<0.01, n.s. not significant.

In the case of *Canton-S*, PDF levels were generally lower compared to those in *Hu-S*, however the temperature-dependent change in the level of PDF-Tri was very similar (*Figure 18B, right panel*). At 23°C the signal was strongly reduced (0.19 ± 0.04), corroborating the results of earlier studies that reported the apoptosis of this structure at room temperature (Helfrich-Förster 1997; Renn et al. 1999). Significantly higher PDF immunostaining was found

both at 18°C (0.43 ± 0.06, **p<0.01) and 12°C (0.59 ± 0.08, ***p<0.001). Similarly to *Hu-S*, a small decrease at 18°C compared to 12°C was observed, however it was not statistically significant.

To further confirm the persistence of these neurons in the cold, a membrane-bound form of GFP was expressed under the control of *Pdf*-Gal4 driver, and GFP immunostaining in the tritocerebrum was quantified. While at 12°C PDF neurons were still detectable in the tritocerebrum, GFP signal was reduced by ~70% at room temperature (**p<0.01), supporting the hypothesis of a temperature-dependent persistence of these cells in adulthood (*Figure 18C*).

Regarding the projection pattern of PDF-Tri neurons, their branches reach the *Pars intercerebralis* containing the richest group of neurosecretory cells, including the IPCs. Based on our confocal images, their axonal projections are very close to the insulin producing cells, and PDF signal is apparently present along the whole axonal projection of the IPCs (*Figure 18A, 12°C and 18°C*). It is not yet known whether the presence of these cells and their neuronal projections in the cold is merely due to a slowed down apoptosis or rather to other mechanisms contributing in keeping them alive to fulfill a role at low temperatures. In any case, the presence of these neurons and their arborizations in the brain in the cold implies that their neuronal connections, either directly through synapses or indirectly, could still influence unidentified biological processes.

To further investigate temperature-dependent PDF changes, we quantified PDF staining in the large ventrolateral neurons (l-LN_vs), the largest PDF-producing neurons in the brain. We observed significant differences at the three different temperatures in the case of both *Hu-S* (Kruskal-Wallis test H(2) = 7.077, *p<0.05) and *Canton-S* (Kruskal-Wallis test H(2) = 9.059, *p<0.05) strains (*Figure 19A*). In *Hu-S* flies, there was a gradual increase in the PDF staining in these cells with the increasing temperature (12°C 1.00 ± 0.07; 18°C 1.11 ± 0.08 and 23°C 1.24 ± 0.08), statistically significant between 12°C and 23°C (*p<0.05) (*Figure 19A, upper panel*). Very similar temperature-dependent PDF changes were found in *Canton-S* females (12°C 1.00 ± 0.06; 18°C 1.33 ± 0.09 and 23°C 1.35 ± 0.08), highlighting a statistically significant, approximately 35% increase at 23°C compared to 12°C (**p<0.01) (*Figure 19A, lower panel*).

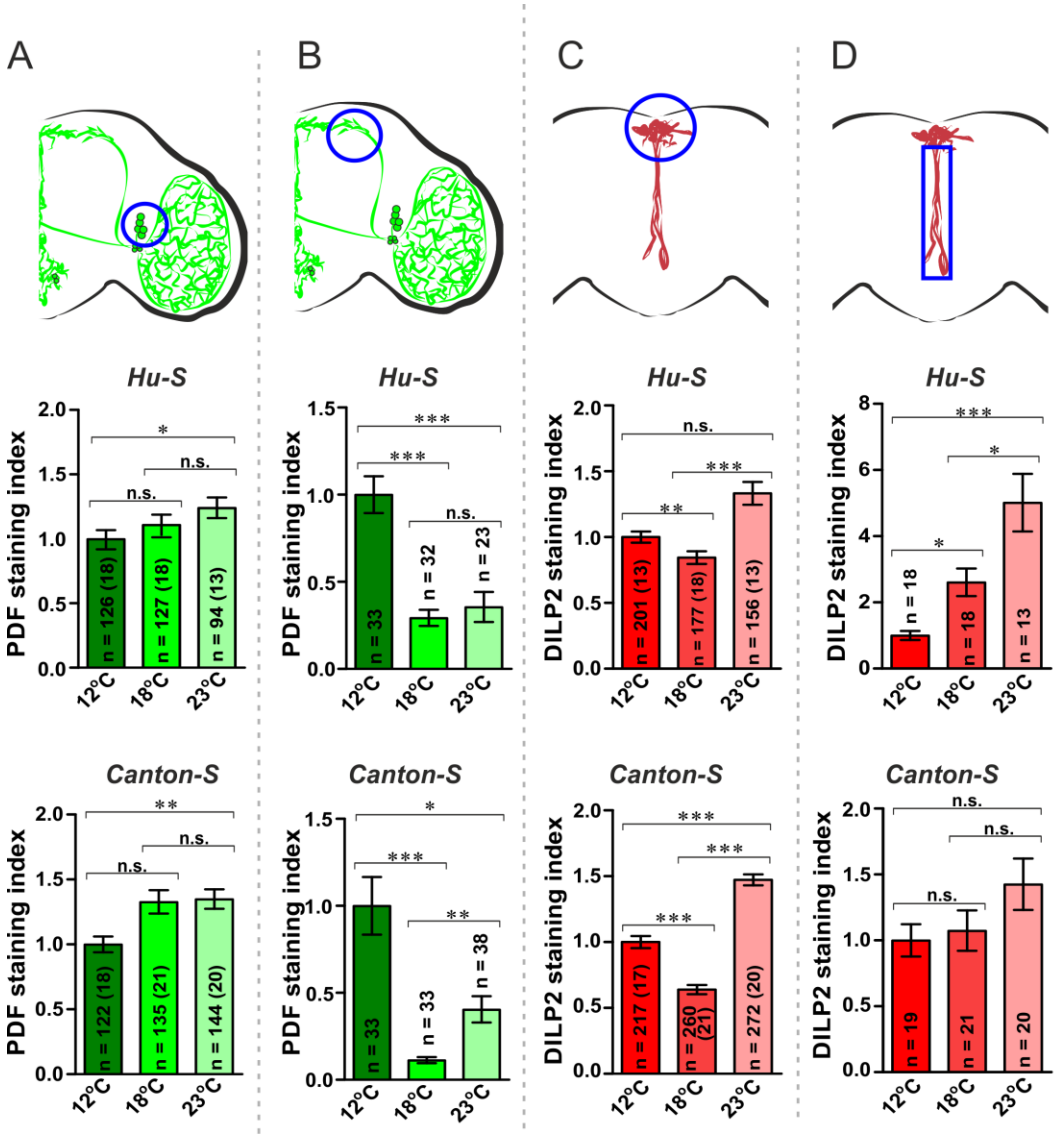

***Figure 19. Levels of PDF and DILP2 in the fly brain* are influenced by temperature.** Schematic figures at the top show the area of quantification. The effect of 12°C, 18°C, and 23°C was tested in *Hu-S* and *Canton-S* strains. Flies were dissected after 11 days at ZT1. (A) Quantification of PDF staining in the l-LN$_v$s reveals significantly higher peptide levels at 23°C compared to those at 12°C in both *Hu-S* and *Canton-S* lines. (B) Quantification of PDF staining in the axon termini of s-LN$_v$s in the dorsal fly brain shows significant increase at 12°C compared to higher temperatures. (C) Quantification of DILP2 signal in the cell bodies of IPCs highlights temperature-dependent differences in both genotypes. The lowest level was detected at 18°C, while both at 12°C and 23°C a significant increase was found. (D) DILP2 immunostaining in the IPC axonal projection shows a significant rise with the increasing temperature in *Hu-S* strain, while no statistically different changes are found in *Canton-S*. Data are normalized to the mean value measured at 12°C in the case of each graph, and are presented as mean ± SEM. Non-parametric Kruskal-Wallis test followed by Bonferroni-corrected Wilcoxon pairwise comparisons. ***p<0.001, **p<0.01, *p<0.05; n.s. not significant.

Next, we focused our attention on the small ventrolateral neurons (s-LN$_v$s) that send axonal projections towards the dorsal brain. PDF immunostaining has been found to display rhythmic changes in the dorsal termini of these cells, suggesting rhythmic PDF release with

the highest rate in 1 to 3 h after light-on (Park et al. 2000; Fernández et al. 2008). Hence, samples were harvested at ZT1 (Zeitgeber Time 1) to ensure maximum PDF levels in the dorsal fly brain. We found temperature-dependent differences in the level of PDF staining in the dorsal brain in the case of both genotypes (*Hu-S*, Kruskal-Wallis test H(2) = 28.421, ***p<0.001; *Canton-S*, Kruskal-Wallis test H(2) = 24.517, ***p<0.001) (*Figure 19B*).

In *Hu-S* flies, upon temperature increase, a marked reduction in the PDF immunostaining was found either at 18°C and 23°C (a drop of ~71% and ~66%, respectively), both significantly lower compared to PDF levels at 12°C (***p<0.001). However, no differences between 18°C and 23°C were observed (18°C 0.29 ± 0.05 compared to 23°C 0.35 ± 0.09, n.s.). Similarly to *Hu-S*, *Canton-S* individuals had significantly higher signal at low temperature and showed a significant reduction at 18°C (a drop of ~88%, ***p<0.001) and 23°C (a reduction of ~60%, *p<0.05). In addition, the staining at 23°C was significantly increased compared to that at 18°C (23°C 0.41 ± 0.08 compared to 18°C 0.11 ± 0.02, **p<0.01). Altogether these data possibly suggest that at low temperature more PDF is released in the dorsal brain, which might target neurosecretory cells in the protocerebrum. However, relying only on PDF staining levels it is very hard to draw reliable conclusions on neuropeptide release. It is not clear whether significantly higher staining in the cell bodies indicates low neuropeptide release, or on the contrary, suggests a higher release as a consequence of a continuous peptide resupply from the cell bodies. In addition, a possible internal peptide degradation or loss of activity can further complicate the functional interpretation of the data.

Next, we investigated DILP2 expression in the brain by using *anti*-DILP2 antibody. First, DILP2 immunostaining was quantified in the cell bodies of IPCs. Significant temperature-dependent differences were found in the staining in both *Hu-S* (Kruskal-Wallis test H(2) = 22.826, ***p<0.001) and *Canton-S* flies (H(2) = 188.34, ***p<0.001), with no strong differences in staining pattern between genotypes (*Figure 19C*). Interestingly, in the case of both lines, the lowest DILP2 expression was detected at 18°C. Compared to this value, the immunostaining in *Hu-S* was significantly higher both at 12°C and 23°C (increases of ~18% and ~58%, respectively). Similarly to *Hu-S*, significantly higher staining levels were found in *Canton-S* flies both at 12°C and 23°C (rises of ~56% and ~130%, respectively) compared to that at 18°C. These unexpected changes in the level of DILP2 may be explained by the fact that in diapausing flies at low temperature *dilp* transcripts were found to be

paradoxically upregulated (Kubrak et al. 2014; Schiesari et al. 2016). Therefore, it is possible that these accumulated transcripts are also translated, but the peptides are retained in the cells rather than released into the hemolymph.

Finally, we quantified DILP2 immunostaining in the IPC axonal projection. In the case of *Hu-S* flies, marked temperature-dependent changes were found (Kruskal-Wallis test H(2) = 20.945, ***p<0.001), highlighting significantly higher levels with the rising temperature (*Figure 19D, top panel*). Compared to 12^{o}C, a more than two-fold increase was observed at 18^{o}C (*p<0.05), while a five-fold rise was detected at 23^{o}C (***p<0.001). The observed increase at 23^{o}C can be due to the fact that IPCs are known to be crucial regulators of growth and metabolism, processes favored at higher temperatures. On the contrary, downregulation of insulin-like signaling is observed at low temperature in diapausing females, correlating with the lower staining intensity found in the axonal projection.

Interestingly, in *Canton-S* females DILP2 staining did not show statistically significant changes at the three different temperatures (Kruskal-Wallis test H(2) = 0.237, n.s.) (*Figure 19D, lower panel*). However, when comparing the immunostaining between 12^{o}C and 23^{o}C, the p-value was close to the threshold of statistical significance (12^{o}C 1.00 ± 0.12 compared to 23^{o}C 1.43 ± 0.20, p = 0.10), suggesting a trend similar to that observed in *Hu-S* females. It is unclear why DILP2 immunostaining in the axonal projection is more influenced by temperature in *Hu-S* flies. However, it worth noting that downregulation of insulin-like signaling can also be downstream of DILP peptide level, since high production of DILPs does not definitely mean highly activated insulin-like signaling. For instance, similarly to mammals, different insulin-binding proteins were identified in *Drosophila*, which can largely influence the binding of DILPs to their receptor, thereby modulating insulin-like signaling (Arquier et al. 2008; Honegger et al. 2008; Okamoto et al. 2013).

4.5. Genetic manipulations of *gal1118*-expressing neurons affect diapause

Since PDF-expressing neurons in the tritocerebrum unexpectedly survive in the cold, they are likely present and functioning also in flies in the wild that experience the advent of winter and are about to enter the dormant state. Therefore, the question can arise whether these cells could be involved in the regulation of overwintering behavior. However, the

investigation of their possible role faces difficulties at the point when PDF-Tri-specific genetic manipulations should be performed. To our knowledge, there are no driver lines available to drive gene expression exclusively in the PDF-Tri cluster (Charlotte Förster and Mareike Selcho, Biozentrum, Würzburg, personal communication). Therefore, we decided to try another approach by looking for a driver line that is specific for the ventrolateral neurons but does not drive transgene expression in PDF-Tri cells. Blanchardon et al. (2001) described a P-Gal4 enhancer trap line, *gal1118*, expressed in the LN_vs but not in the PDF-Tri neurons (Blanchardon et al. 2001). To corroborate this result, we tracked the expression of a membrane-bound GFP under the control of *gal1118* (*w;UAS-GFP;gal1118*) in flies developed at 18^{o}C in LD 8:16 and subsequently placed at 12^{o}C for 11 days, maintaining the same short photoperiod (*Figure 20A*).

Similarly to Blanchardon and his colleagues, we found *gal1118*-expression in the l-LN_vs, in the s-LN_vs and some other small-sized neurons closed to the s-LN_vs, in the LN_ds clock neurons in the dorsal-lateral brain, several cells in the medulla (gme) and *Pars intercerebralis* (gpi), few cells located near the mushroom body calyces (gmbc), as well as in neurons in the dorsal fly brain (gd) possibly including the two DN2 clock neurons. Importantly, no *gal1118* expression was found in the tritocerebrum (*Figure 20A*).

Next, *gal1118*-positive cells were hypersensitized by expressing *Na^{+}ChBac*. This manipulation induced a drop to ~9% of diapause in the experimental flies (*gal1118>Na^{+}ChBac* 9.1 ± 6.3%), while both controls exhibited ~45% of diapause (*gal1118*>+ 45.1 ± 12.1%, ***p<0.001 and +>*Na^{+}ChBac* 44.6 ± 8.2%, ***p<0.001) (*Figure 20B*). A similar result was obtained by overexpressing the same sodium channel under the control of *Pdf*-Gal4 (*Figure 15A*). The overexpression of PDF in these cells resulted in ~20% of diapause (*gal1118>Pdf* 19.7 ± 8.2%), a significant reduction compared to both controls, in which diapause percentages ranged between 41 and 45% (+>*Pdf* 41.6 ± 7.5%, *p<0.05 and *gal1118*>+ 45.1 ± 12.1%) (*Figure 20B*). These results indicate that PDF is a diapause-antagonist peptide, corroborating the data obtained by the overexpression of this peptide under the control of *Pdf*-Gal4 driver (*Figure 15A*).

However, expression of the potassium channel Ork in the *gal1118*-positive cells did not alter diapause levels; no significant difference was found between the experimental flies and UAS control (*Figure 20B*). This result is different from that obtained by using *Pdf*-Gal4 driver, which led to significantly higher diapause levels in the experimental flies upon UAS-

Ork expression (*Figure 16B*). Although this difference between the two drivers can suggest a possible involvement of PDF-Tri in diapause regulation, we cannot exclude the possibility that the observed contrast is due to the effect(s) of other *gal1118*-expressing neurons in the brain.

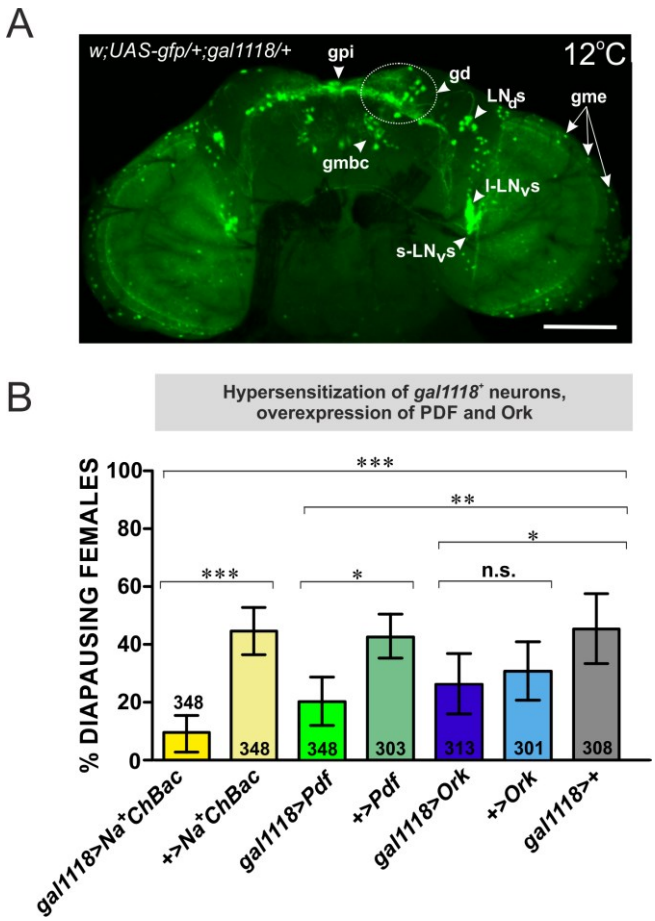

Figure 20. Genetic manipulation in the gal1118-expressing neurons leads to altered diapause levels. (A) Representative confocal image showing the expression of *gal1118* in the brain of a 11-day-old homozygous *w*;UAS-*gfp;gal1118* adult female at 12°C. The most important cells expressing *gal1118* are indicated by white arrow or arrowhead. GFP was expressed in the small and large ventrolateral neurons (s-LN_vs and l-LN_vs), in the dorsal lateral neurons (LN_ds); several cells in the *Pars intercerebralis* (gpi), cells in the dorsal fly brain (gd, located in the area inside the white circle; possibly involving the two DN2 clock neurons), few cells near the mushroom body calyces (gmbc), *gal1118*-expressing cells in the medulla (gme). Abbreviations were used after Blanchardon et al. 2001. No *gal1118*-expression was observed in the tritocerebrum. Scale bar = 100 µM. (B) Overexpression of a bacterial sodium channel in the *gal1118*-expressing neurons (*gal1118>Na$^+$ChBac*) results in a significant reduction in the proportion of diapausing females compared to both controls (***p<0.001). Overexpression of PDF in the *gal1118*$^+$ neurons (*gal1118>Pdf*) leads to significantly lower diapause levels compared to both Gal4 and UAS controls (**p<0.01 and *p<0.05, respectively). Inhibiting the release of neuropeptides from the *gal1118* expressing neurons through the expression of a potassium channel (*gal1118>Ork*) does not alter diapause levels (no statistically significant difference compared to the UAS control). Numbers in each column indicate the number of dissected females. One-way ANOVA after arcsine transformation, followed by post-hoc Tukey HSD test. ***p<0.001, **p<0.01, *p<0.05, n.s. not significant.

4.6. Effects of different diapause-inducing conditions on *Pdf* null flies

Since we found that overexpression of the neuropeptide pigment dispersing factor in the PDF^{+} neurons causes a significant reduction in the percentage of diapausing females (*Figure 15A, 20B*), the question arises as what happens to diapause levels in the absence of PDF? To address this question, *Pdf*^{01} flies were tested in diapause assays in two different genetic backgrounds, *Hu-S* and *Hu-LS* (*Pdf*^{01} *Hu-S* and *Pdf*^{01} *Hu-LS*, respectively). *Hu* lines are Dutch *D. melanogaster* field lines originated from Houten (see *Materials and Methods, page 41*), known to express different isoforms of the *timeless* clock gene (*s-* and *ls-timeless*, respectively). As it has been previously reported, *ls-timeless* enhances the incidence of diapause in every photoperiod compared to flies bearing the *s-timeless* variant (Tauber et al. 2007). Therefore, investigating diapause response in these different backgrounds allows us to see whether *Pdf* null flies exhibit altered diapause levels depending on the *timeless* allele they carry in their genome.

In line with previous results (Tauber et al. 2007), our data confirm that *timeless* has a significant effect on the incidence of reproductive diapause (***p<0.001), highlighting increased diapause levels in females bearing the *ls-timeless* variant (*Hu-S* 6.6 ± 3.0% compared to *Hu-LS* 34.8 ± 3.6%, ***p<0.001) (*Figure 21A*). This effect was not diminished in the absence of PDF, since mutant flies in the two different *timeless* backgrounds also showed a marked difference in their diapause response (*Hu-S Pdf*^{01} 14.2 ± 3.6% compared to *Hu-LS Pdf*^{01} 38.3 ± 6.1%, ***p<0.001), similar to that observed in the case of wild-type females. When focusing on the effect of *Pdf*^{01} mutation on reproductive dormancy, we found that mutant females in *s-timeless* background exhibited a small, but statistically significant increase in diapause levels (14.2 ± 3.6%, **p<0.01) compared to *Hu-S* control (6.6 ± 3.6%). This result corroborates the finding that overexpression of PDF in the PDF-producing neurons leads to lower diapause levels (*Figure 15A, 20B*). However, when comparing the proportion of dormant females in the mutant in *ls-timeless* background to their corresponding control, only a slight but not statistically significant increase was detected.

Then, since PDF-Tri neurons were found to survive much longer in the cold, we decided to modify our diapause experimental protocol and test diapause levels in females

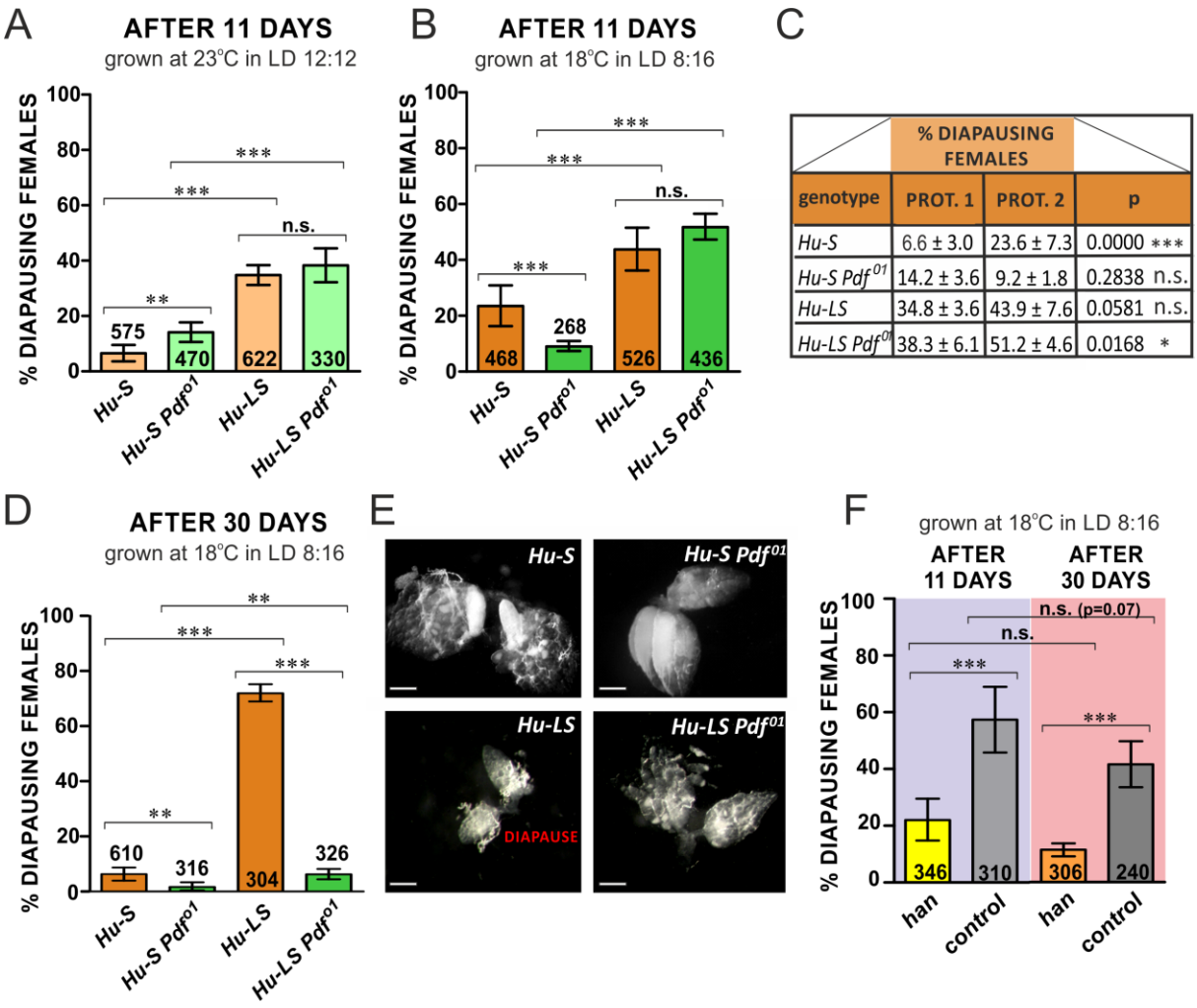

Figure 21. Diapause in Pdf^{01} and PdfR^{0} mutant flies - testing a new experimental protocol. (A) Diapause levels in PDF null mutant females in *s-* and *ls-timeless* backgrounds (*Hu-S Pdf*^{01} and *Hu-LS Pdf*^{01}, respectively). Flies were grown at 23°C in LD 12:12 before being exposed to diapause inducing conditions (PROTOCOL 1). After 11 days, *Pdf*^{01} females in *s-timeless* backgrounds showed a small, but significant increase compared to the control (**p<0.01), while no difference was observed between the mutant and its control in *ls-timeless* females. Independently from the mutation in *Pdf*, individuals bearing *ls-timeless* isoform exhibited consistently higher diapause levels (***p<0.001). (B) Testing *Pdf*^{01} females using a new experimental protocol by growing flies at 18°C in LD 8:16 during their development before diapause induction (PROTOCOL 2). The effect of PDF in *s-timeless* females changed, since controls showed significantly higher diapause levels compared to the mutant (***p<0.001), while no PDF-effect is seen in *ls-timeless* females. (C) The table shows the incidence of diapause in the *Pdf*^{01} mutants and their corresponding controls in the two different experimental protocols (PROT. 1 and PROT. 2), highlighting significant differences between the diapause response of the flies. (D) Diapause levels after one month, using PROTOCOL 2. *Pdf*^{01} flies have significantly reduced diapause levels compared to their corresponding controls both in *s-* and *ls-timeless* backgrounds (**p<0.01 and ***p<0.001, respectively). (E) Representative images of ovaries after 1 month. *Hu-S* and *Hu-S Pdf*^{01} females had very developed ovaries with stages 12, 13 and 14. *Hu-LS Pdf*^{01} had less developed ovaries mainly with stages 8-9, while the majority of *Hu-LS* females were in diapause. Scale bar = 0.2 mm. (F) PDFR null mutant (*han*) flies show significantly decreased diapause levels (***p<0.001) both after 11 and 30 days. Numbers within bars refer to the number of dissected females considered in the diapause assays. Data are presented as mean ± SD. ANOVA on arcsine transformations, followed by post-hoc Tukey HSD test. ***p<0.001, **p<0.01, *p<0.05, n.s. not significant.

which were exposed to a lower temperature prior to diapause induction. Thus, instead of leaving them to develop at 23°C in LD 12:12, they were grown at 18°C under a short photoperiod (LD 8:16). The previous experiments were therefore repeated using this new diapause protocol (PROTOCOL 2) in order to test its possible effect on diapause levels. Surprisingly, *Pdf*^{01} mutants in *s-timeless* background exhibited significantly lower diapause levels (*Hu-S Pdf*^{01} 9.2 ± 1.8%, ***p<0.001) compared to their control (*Hu-S* 23.6 ± 7.3%) (*Figure 21B*). In the case of *Hu-LS Pdf*^{01}, only a slight, not statistically significant increase was observed compared to the controls (*Figure 21B*). In addition*, ls-timeless* females exhibited significantly higher diapause levels compared to their *s-timeless* counterpart (***p<0.001). In the case of the wild-type lines, *Hu-S* females showed 23.6 ± 7.3% of diapause, while the corresponding *ls-timeless* females 43.9 ± 7.6% (***p<0.001) (*Figure 21B*). As for the PDF null mutants, in the *s-timeless* background less than 10% of the females entered diapause (9.2 ± 1.8%), while a significantly higher proportion of flies was in diapause in the *ls-timeless* background (43.9 ± 7.6%, ***p<0.001) (*Figure 21B*). When comparing diapause levels obtained with the two protocols, ANOVA revealed significant genotype ($F_{(3,48)}$ = 138.569, ***p<0.001) and protocol ($F_{(1,48)}$ = 39.436, ***p<0.001) effects, as well as genotype x protocol interaction ($F_{(3,48)}$ = 17.912, ***p<0.001) (*Figure 21C*). Interestingly, using PROTOCOL 2 that better approximates the outdoor conditions experienced by flies in the wild before going to the dormant state, there was a general increase in diapause levels (*Figure 21C*). Only *Hu-S Pdf*^{01} females showed very similar diapause levels in the two different conditions (p = 0.283, n.s.), while the other lines exhibit statistically significant or nearly significant (in the case of *Hu-LS* p = 0.0581) increase (*Figure 21C*).

To examine how diapause incidence changes over time, flies from the same crosses were left in diapause inducing conditions also for 30 days. Interestingly, we found that also after such a long time the *timeless s-ls* effect was still present, since females in *ls* background showed consistently higher diapause levels (*Figure 21D*). In the case of *Pdf*^{01} mutant in *s-timeless* background, only few females were found in the dormant state after a month (*Hu-S Pdf*^{01} 1.8 ± 1.5%), while in the control group there was a small, but statistically significant increase in the proportion of diapausing individuals (6.4 ± 2.4%, **p<0.01). Intriguingly, in the case of *ls-timeless* background, the majority of the females in the control group remained in diapause also after one month (*Hu-LS* 72.1 ± 3.1%), while in *Pdf*^{01} flies there was a drastic decrease in diapause levels (*Hu-LS Pdf*^{01} 6.3 ± 1.8%, ***p<0.001) (*Figure 21D, E*).

These results suggest that PDF might have a role in keeping flies, carrying *ls-timeless,* in diapause for long time. However, it is not clear how this PDF effect is mediated, and why changes in diapause levels are modulated only after 30 days in *ls-timeless* background.

When the results after one month were compared to those obtained after 11 days using PROTOCOL 2, ANOVA revealed significant genotype ($F_{(3,42)}$ = 206.811, ***p<0.001) and time ($F_{(1,42)}$ = 91.936, ***p<0.001) effects, as well as genotype x time interaction ($F_{(3,42)}$ = 93.892, ***p<0.001). We found that except for *Hu-LS*, all the other lines showed statistically significant reduction in diapause levels, which in the case of *Hu-S* was approximately 17% (from 23.6 ± 7.3% to 6.4 ± 2.4%, ***p<0.001), in the case of *Hu-S* Pdf^{01} ~7% (from 9.2 ± 1.8% to 1.8 ± 1.5%, ***p<0.001) and in *Hu-LS* Pdf^{01} it was about 46% (from 51.9 ± 4.6% to 6.3 ± 1.9%, ***p<0.001) (*Figure 21B, D*). However, *Hu-LS* females showed a significant increase of ~28% in the percentage of diapausing females after 30 days (from 43.9 ± 7.6% to 72.1 ± 3.1%, ***p<0.001) (*Figure 21B, D*).

Next, we investigated diapause response in PDF receptor null mutant (*han*) flies (described in Hyun et al. 2005) using PROTOCOL 2, both after 11 and 30 days. After 11 days, *han* mutant females showed significantly lower diapause levels compared to their corresponding control (*han* 22.2 ± 7.3% compared to 57.4 ± 11.6%, ***p<0.001) (*Figure 21F*). Very similar results were obtained after one month, highlighting significantly lower proportion of diapausing females in the mutant (*han* 11.4 ± 2.3% compared to 41.7 ± 8.2%, ***p<0.001) (*Figure 21F*). 2-way ANOVA revealed significant genotype ($F_{(1,15)}$ = 81.1788, ***p<0.001) and time ($F_{(1,15)}$ = 13.6594, **p<0.01) effects, but no genotype x time interaction ($F_{(1,15)}$ = 0.0559, p = 0.816, n.s.).

To sum up, through these experiments several different issues have been addressed including the action of PDF on the incidence of reproductive diapause, the importance of the environmental parameters experienced by flies during development, and last but not least, how diapause levels change over time. Using the new diapause protocol (PROTOCOL 2), flies are subjected to a lower temperature and a short photoperiod through all their development. This modification apparently induces a higher proportion of females to enter diapause. Pdf^{01} flies were found to behave differently depending on the conditions they were subjected to before diapause induction. This altered behavior is further complicated by the fact that PDF seems to have different effects depending on the *timeless* allele present in the genome. In PROTOCOL 1, in the absence of PDF a higher proportion of females entered

dormancy in the *s-timeless* genetic background compared to the control, while no differences were observed in females carrying the *ls-timeless* variant. With the new experimental settings (PROTOCOL 2), we found the opposite, as higher diapause levels were exhibited by *Hu-S* flies compared to Pdf^{01} females. Similar patterns were seen also after 30 days, however *Hu-S* flies showed a general reduction of diapause levels after this period of time. In the case of *ls-timeless* background, PDF did not influence diapause after 11 days, but did so after 30 days, causing a dramatic difference between control and *Hu-LS* Pdf^{01} *females*: while the majority of *Hu-LS* flies were still in diapause, the mutants underwent reproductive development. Therefore, after one month the effect of PDF tended to be the same in both genetic backgrounds, enhancing diapause levels. In line with these data, in the absence of PDF receptor females displayed significantly decreased diapause levels, both after 11 and 30 days.

4.7. PDF expression in two differently diapausing field lines

To further investigate the involvement of PDF in diapause, we studied its expression profile in the differently diapausing field lines, *Hu-S* and *Hu-LS*. As it was shown in our previous experiments (*Figure 21A, B, D*) and earlier studies (Tauber et al. 2007), *ls-timeless* enhances diapause incidence in every photoperiod. When flies were exposed to a lower temperature and short photoperiod from the beginning of their development (18°C in LD 8:16, PROTOCOL 2), the diapause rate was ~24% in *Hu-S* and ~52% in *Hu-LS* (*Figure 21B*). We analyzed PDF expression in these two natural populations, reared at 18°C in LD 8:16, and subsequently placed either at 12°C or 23°C for a period of 11 or 30 days.

First, PDF immunostaining was quantified in the cell bodies of the large ventrolateral neurons (l-LN_vs). At higher temperature, staining levels were found consistently higher in all the conditions tested (*Figure 22A*). This result is in accordance with data obtained using PROTOCOL 1, that reported significantly higher PDF levels in these cells at 23°C compared to those at 12°C both in *Hu-S* and *Canton-S* flies (*Figure 19A*). Interestingly, after 30 days in *Hu-S* flies, PDF intensity increased at both temperatures compared to that after 11 days (*Figure 22A, B*). More specifically, its level after 30 days rose by ~38% (from 1.000 ± 0.039 to 1.381 ± 0.084, ***$p<0.001$) at 12°C, while at 23°C an increase of ~50% was measured (from 1.318 ± 0.084 to 2.082 ± 0.110, ***$p<0.001$) compared to that after 11 days. However, no change

over time was found in the case of *Hu-LS* females (at 12°C from 0.952 ± 0.026 to 0.861 ± 0.034, n.s.; at 23°C from 1.179 ± 0.042 to 1.108 ± 0.056; n.s.) (*Figure 22A, B*). When comparing PDF levels in *Hu-S* and *Hu-LS* flies, they differed only after 30 days, being significantly elevated in *Hu-S* flies (***p<0.001) (*Figure 22A, right panel*).

When studying the intensity of PDF immunostaining in the axonal termini of s-LN_vs, no difference was observed between *Hu-S* and *Hu-LS* lines after 11 days in the cold (1.000 ± 0.124 and 1.074 ± 0.079, respectively, n.s.) (*Figure 22B, left panel*). However, there was a significant drop of ~70% in the staining level in *Hu-LS* flies compared to that at 23°C (from 3.442 ± 0.266 to 1.074 ± 0.079) (*Figure 22B, left panel*). After 30 days, in *Hu-LS* females the staining showed a small but statistically significant decrease of ~30% compared to that in *Hu-S* (1.326 ± 0.159 compared to 0.876 ± 0.132, *p<0.05) (*Figure 22B, right panel*). Interestingly, a conspicuous change in PDF immunostaining was measured in *Hu-S* flies: while in the cold PDF level did not change significantly over time, at 23°C a 2.5-fold increase was detected compared to that after 30 days (1.149 ± 0.120 compared to 3.331 ± 0.432, ***p<0.001) (*Figure 22B, table*). Thus, it became similar to that observed in *Hu-LS* flies after 30 days at the same temperature (3.309 ± 0.297, n.s.) (*Figure 22B, right panel*). It is worth noting that in *Hu-S* flies there was a dramatic increase in PDF staining in this brain area after 11 days at cold temperatures (both at 12 and 18°C) when PROTOCOL 1 was used (*Figure 19B*). This marked temperature-dependent difference was completely abolished in this line when flies were developed at 18°C in LD 8:16 (PROTOCOL 2), since irrespective of temperature PDF immunostaining was found to be equal in the dorsal fly brain (*Figure 22B, left panel*).

When quantifying PDF staining in the tritocerebrum area, a higher signal was present in the *Hu-LS* line after 11 days in the cold compared to that in *Hu-S*, but it was statistically not significant (1.000 ± 0.115 compared to 1.309 ± 0.144, n.s.) (*Figure 23A, left panel*). At 23°C, PDF staining was reduced in both strains; however in *Hu-S* flies only a decrease of ~22% was observed, not significantly different from that measured in the cold. In the case of *Hu-LS*, its level largely decreased by ~50% compared to that at 12°C (from 1.309 ± 0.144 to 0.667 ± 0.106, ***p<0.001) (*Figure 23A, left panel*).

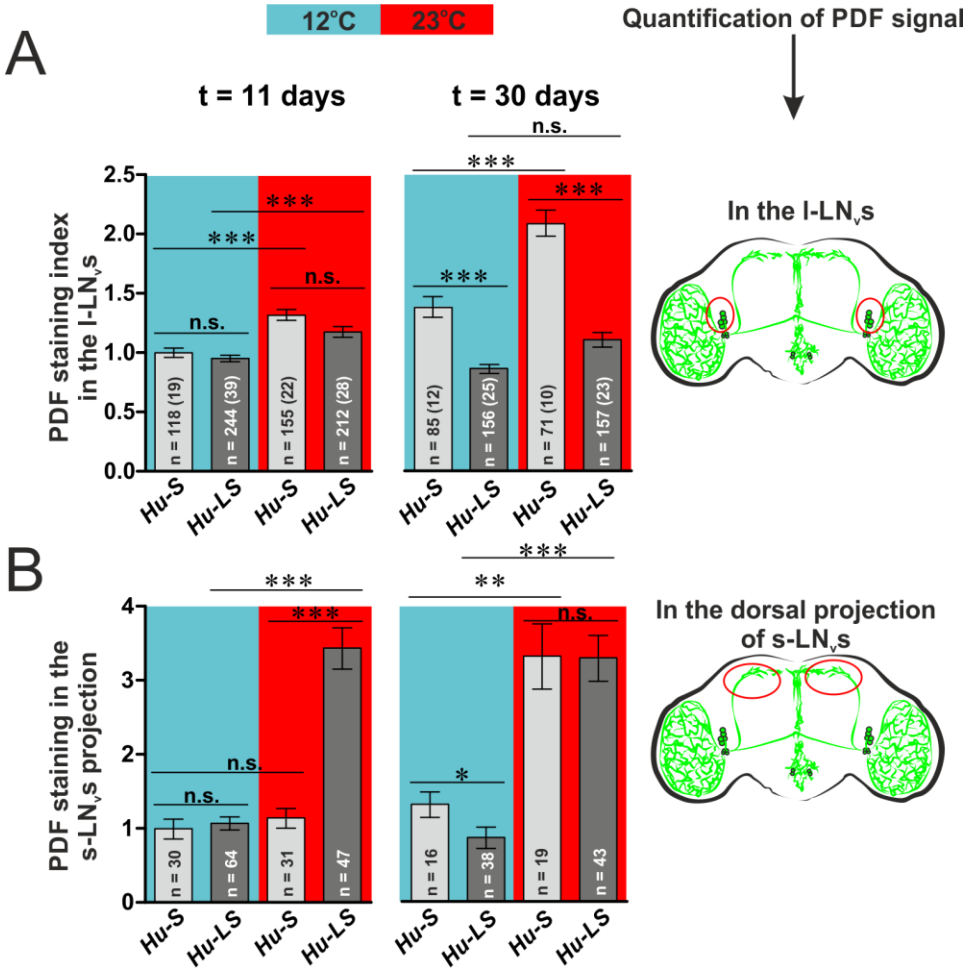

Strain	11 days	30 days	p	
Hu-S	1.000 ± 0.124	1.326 ± 0.159	0.2602	n.s.
Hu-LS	1.074 ± 0.079	0.876 ± 0.132	0.2090	n.s.
Hu-S	1.149 ± 0.120	3.331 ± 0.432	0.0000	***
Hu-LS	3.442 ± 0.266	3.309 ± 0.297	0.8345	n.s.

Figure 22. PDF expression profile in the ventrolateral neurons of Hu-S and Hu-LS field lines. Experiments were performed at 12°C and 23°C both after 11 and 30 days. The blue areas refer to cold temperature, while results from 23°C are shown in red. The left panels display the data after 11 days, while graphs on the right side demonstrate results after 30 days. Red areas in the schematic images indicate the region in which the quantification was performed. (A) *Left:* PDF intensity in the large ventrolateral neurons highlights temperature-dependent differences, with higher staining at 23°C compared to 12°C. *Right:* After 30 days in *Hu-S* flies, PDF levels were significantly elevated at both temperatures. n = number of neurons (in parentheses: n of brains). Data are normalized to average PDF staining at 12°C after 11 days in *Hu-S*. (B) *Left:* After 11 days, PDF staining in the projection of the s-LNvs in the dorsal fly brain revealed a significant difference between *Hu-S* and *Hu-LS* flies at 23°C, while no difference was observed in the cold. *Right:* After 30 days, signal levels were significantly lower at 12°C than at 23°C. In the cold, *Hu-S* flies had significantly higher staining than *Hu-LS*. n = number of hemispheres. Data are normalized to average PDF staining at 12°C after 11 days in *Hu-S*. The bottom table shows the time-dependent changes in the signal level in the s-LNvs projection in the two lines, along with the results of the statistical analyses. The color code corresponds to the two different temperatures (blue: 12°C; red: 23°C). Data are presented as mean ± SEM. Kruskal-Wallis test followed by Bonferroni-corrected Wilcoxon pairwise-comparisons. ***p<0.001, **p<0.01, *p<0.05, n.s. not significant.

It is important to note that during our previous experiments when PROTOCOL 1 was used (development at 23°C in LD 12:12), larger differences were detected between 12°C and 23°C (*Figure 18B*). In the case of *Hu-S* females, there was a decrease of ~60% (*Figure 18B, left panel*), while the drop in the signal level at 23°C was not even significant when PROTOCOL 2 was applied. This may suggest that subjecting flies to a lower temperature and short photoperiod through their development leads to higher PDF expression in the tritocerebrum cells and their projections.

After 30 days, there was a general reduction in the staining at both temperatures (*Figure 23A, right panel*). Though, *Hu-LS* individuals had consistently higher levels of PDF-Tri compared to those in *Hu-S.* More specifically, the intensity of PDF immunostaining was more than two-fold in the cold (0.715 ± 0.094 compared to 0.332 ± 0.101, *p<0.05), and even if at 23°C the signal was very low in both lines, still remained significantly higher in the *Hu-LS* strain (0.111 ± 0.028 compared to 0.016 ± 0.007, **p<0.01) (*Figure 23A, right panel*).

PDF-Tri neurons send projections dorsally into the median bundle, extending their branches also in the *Pars intercerebralis* of the protocerebrum. Thus, we aimed at analyzing PDF staining along the axonal projection of the IPCs. After 11 days in the cold, in *Hu-LS* females, the staining was twice as intense as that in *Hu-S* (0.601 ± 0.064 compared to 0.305 ± 0.062, *p<0.05), and even if the signal seemed reduced at 23°C in both lines, the difference between *Hu-LS* and *Hu-S* remained robust (0.421 ± 0.093 compared to 0.057 ± 0.079, **p<0.01) (*Figure 23B, left panel*). Surprisingly, in *Hu-LS* females the staining levels did not differ between the two temperatures, suggesting that PDF signal is constantly high near the axonal projection of the IPCs in this line (*Figure 23B, left panel*). When measuring PDF immunostaining in this brain area after 30 days, there was an overall decrease in the signal at both temperatures in both genotypes compared to data measured after 11 days (*Figure 23B, right panel*). At 12°C, PDF staining was higher in *Hu-LS* flies than that in *Hu-S*; however this difference was not statistically significant (0.222 ± 0.058 compared to 0.087 ± 0.034, n.s.). At 23°C, the signals seem to be reduced, however this reduction was statistically significant only in *Hu-LS* flies compared to that at 12°C (0.222 ± 0.058 compared to 0.085 ± 0.060, ***p<0.001) (*Figure 23B, right panel*).

Finally, we quantified PDF near the cell bodies of the IPCs. The pattern of staining was very similar to that observed along the axonal projection of IPCs (*Figure 23B*). After 11 days in the cold, there was a significant difference between *Hu-S* and *Hu-LS* flies, with higher

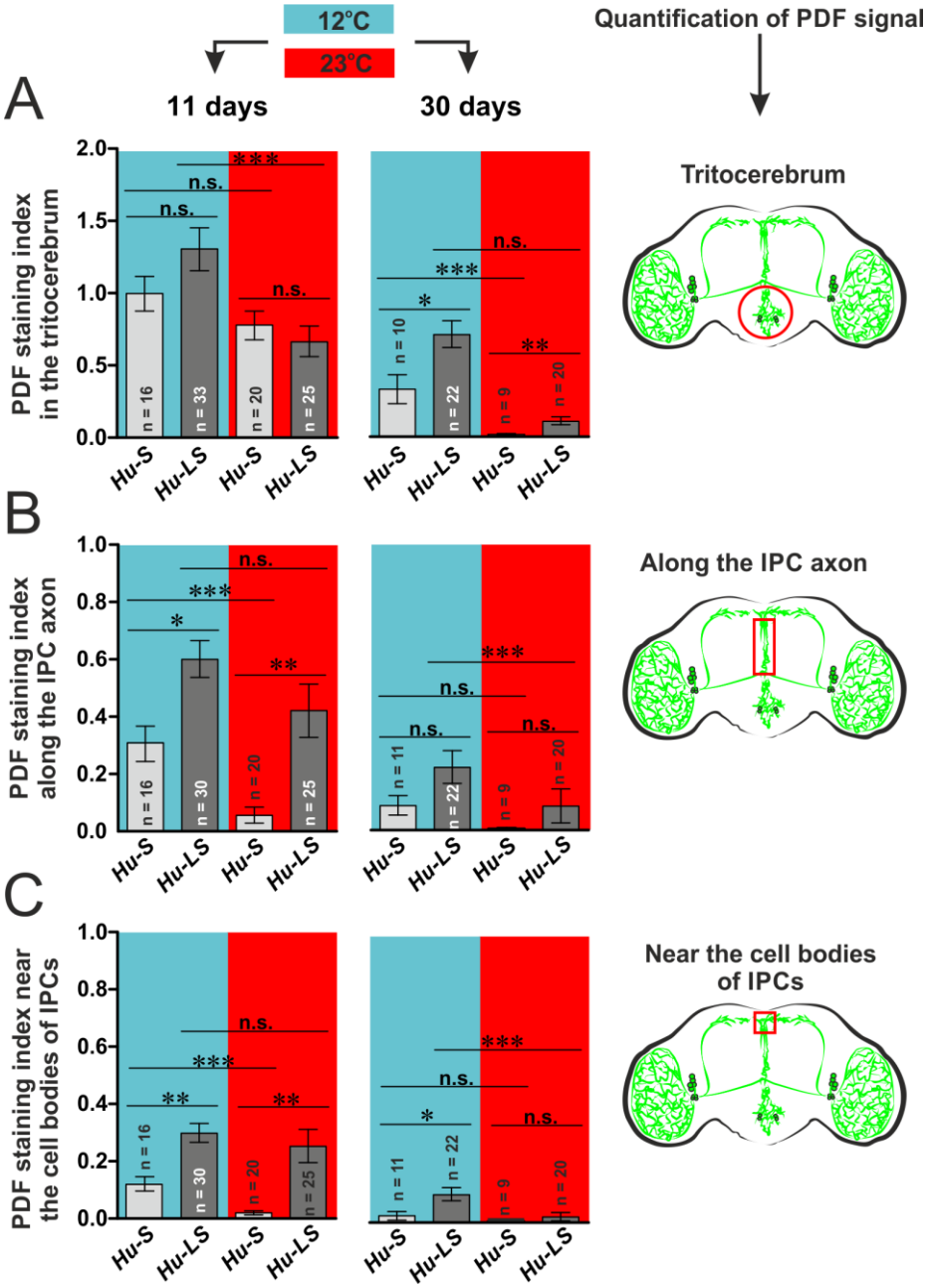

Figure 23. Expression pattern of PDF-Tri in two differently diapausing field lines. Experiments were performed at 12°C (blue areas) and 23°C (red areas) both after 11 and 30 days. The left panels show the results after 11 days, while graphs on the right display the results after 30 days. Red areas in the schematic images indicate the region in which the quantification was performed. (A) *Left:* There was a slight increase in PDF intensity in the cold in *Hu-LS* compared to *Hu-S* (n.s.). At the higher temperature the signal was reduced, but the reduction was statistically significant only in the *Hu-LS* strain. *Right:* After 30 days, there was a general reduction in all the signals; however *Hu-LS* flies had consistently higher levels of immunostaining. (B) *Left:* After 11 days, PDF staining along the IPC axonal projection was significantly higher in *Hu-LS* at both temperatures. *Right:* After 30 days, the overall reduction of signal levels was observed. *Hu-LS* flies had more PDF in the cold; however this difference was not statistically significant. (C) *Left:* After 11 days, there was significantly higher PDF staining in the vicinity of DILP cells in *Hu-LS* flies at both temperatures. *Right:* After 30 days, signals were strongly reduced in all the conditions. Though, in the cold *Hu-LS* flies had significantly higher staining than *Hu-S* females. n = number of brains. Data are normalized to average PDF staining in the tritocerebrum at 12°C after 11 days in the *Hu-S* line, and are presented as mean ± SEM. Kruskal-Wallis test followed by Bonferroni-corrected Wilcoxon pairwise-comparisons. ***p<0.001, **p<0.01, *p<0.05, n.s. not significant.

PDF levels in the *ls*-line (0.300 ± 0.033 compared to 0.121 ± 0.025, **p<0.01) (*Figure 23C, left panel*). Similar tendency was found at 23°C, with significantly stronger PDF immunostaining in *Hu-LS* females (0.254 ± 0.058 compared to 0.020 ± 0.007, **p<0.01). Interestingly, in the case of *Hu-LS*, PDF staining around the IPCs was as high as it was at 23°C (*Figure 23C, left panel*). When looking at PDF levels after 30 days, a general reduction can be observed. However, *Hu-LS* flies still had higher immunostaining in the cold compared to *Hu-S* females (0.099 ± 0.023 compared to 0.023 ± 0.015, *p<0.05) (*Figure 23C, right panel*).

Figure 24A summarizes the changes that occur in the PDF-Tri and their arborizations in the tritocerebrum (TRITO), along the IPC axonal projection (AXON) and near the cell bodies of the IPCs (CELL) in both strains, considering also the two different time intervals (11 and 30 days).

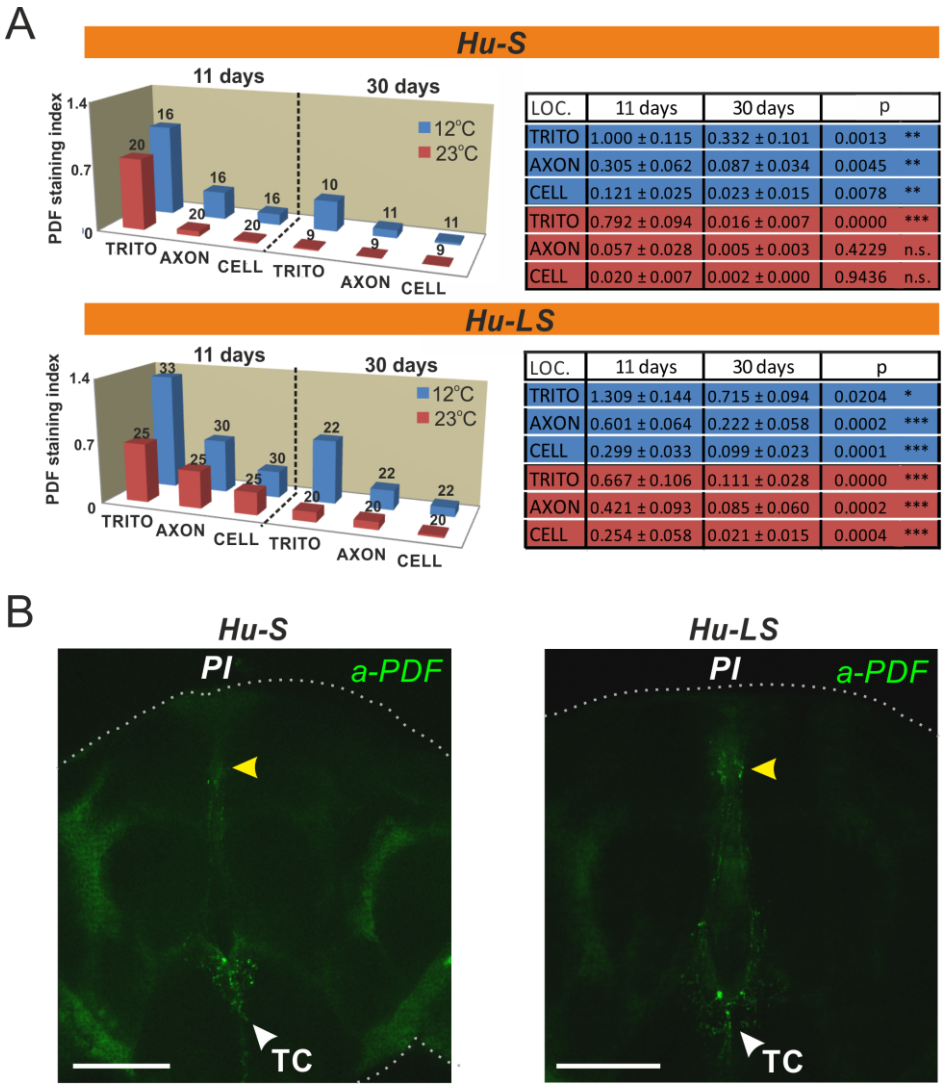

Figure 24. Temperature- and time-dependent changes in the PDF-Tri arborization. (See next page for legend.)

(A) The panel on the top refers to *Hu-S* flies, while the bottom panel to *Hu-LS* flies. The left side of each graph shows the detected levels of PDF staining after 11 days, while the right side represents those after 30 days. TRITO, AXON, and CELL texts refer to the location (LOC.) of the PDF signal measured (in the TRITOcerebrum, along the AXONal projection of the IPCs, and around the CELL bodies of the IPCs, respectively). Numbers represent number of brains. The tables next to each graph show the comparison between the signals in the different areas at both temperatures and time intervals, highlighting also the Bonferroni-corrected p-values. Blue color refers to data obtained at 12^{o}C, while red represents results from 23^{o}C. The graphs show the mean values. In the tables data are presented as mean ± SEM. Kruskal-Wallis test followed by Bonferroni-corrected Wilcoxon pairwise-comparisons. ***p<0.001, **p<0.01, *p<0.05, n.s. not significant. (B) Representative confocal images depicting the PDF staining in *Hu-S* (left) and *Hu-LS* (right) brains after 11 days at 12^{o}C (single optic sections). White arrowheads indicate the tritocerebrum (TC), where PDF seems to be more abundantly expressed in the *Hu-LS* line. Yellow arrowheads indicate PDF staining in the *Pars intercerebralis* (*PI*) region, where the cell bodies of the IPCs are located. Brains are outlined by dashed lines. PDF signal is stronger in the *Hu-LS* strain. Scale bar = 50 μm.

Apparently *Hu-S* flies have less PDF signal in the cold compared to that detected in *Hu-LS* individuals. The latter not only express more PDF after 11 days, but do so also after 30 days. Though, all the signals seem to be strongly reduced after this period of time. *Figure 24B* shows representative images of fly brains after 11 days in the cold (12^{o}C), highlighting more abundant PDF staining both in the tritocerebral area (TC) and in the *Pars intercerbralis* (*PI*) region in the *Hu-LS* line.

4.8. IPCs are connected to PDF-expressing neurons in the cold

Based on our confocal images, PDF-Tri neurons seem to have their arborization in the near proximity of the insulin producing cells and their axonal bundles; we then wondered whether there is a synaptic connection between these cells. To investigate this question, we used synaptic-targeted GFP reconstitution across synaptic partners (GRASP) technique (Feinberg et al. 2008). The method is based on the expression of two complementary fragments of the GFP on the cell membrane of different neurons. If the processes of these neurons are within synaptic distance, a functional GFP signal can be reconstituted at the cell-cell contact site, emitting green fluorescence (*See Materials and Methods, page 49*). A study by Cavanaugh et al. (2014) has already addressed the question whether possible synaptic connections exist between *PI* cells and PDF^{+} neurons; however their experiments were performed at room temperature, where PDF-Tri neurons undergo apoptosis in young adults. Indeed, in their analysis they focused on PDF-producing clock cells and their connections to *PI* cells. They never observed GRASP signal between *PI* cells and PDF-

expressing neurons, therefore concluded that s-LN$_v$s do not directly contact *PI* cells (Cavanaugh et al. 2014).

We adopted an IPC-specific driver line (*dilp2(p)*-Gal4) to express the larger fragment of GFP (GFP$^{1-10}$) in the IPCs, while the complementary fragment of the protein (GFP^{11}) was expressed in the PDF$^+$ neurons. Newly eclosed flies, developed at 18^{o}C in short days (PROTOCOL 2), were placed either at 12^{o}C or 23^{o}C in LD 8:16 for 11 days before brain dissections. We detected no GRASP signal in the majority of the brains (75%) at 23^{o}C (*Figure 25B*), while in the cold the signal was present in almost every brain, reflecting the reconstitution of GFP fluorescence at points of contact between the IPCs and PDF$^+$ cells (*Figure 25C, D*).

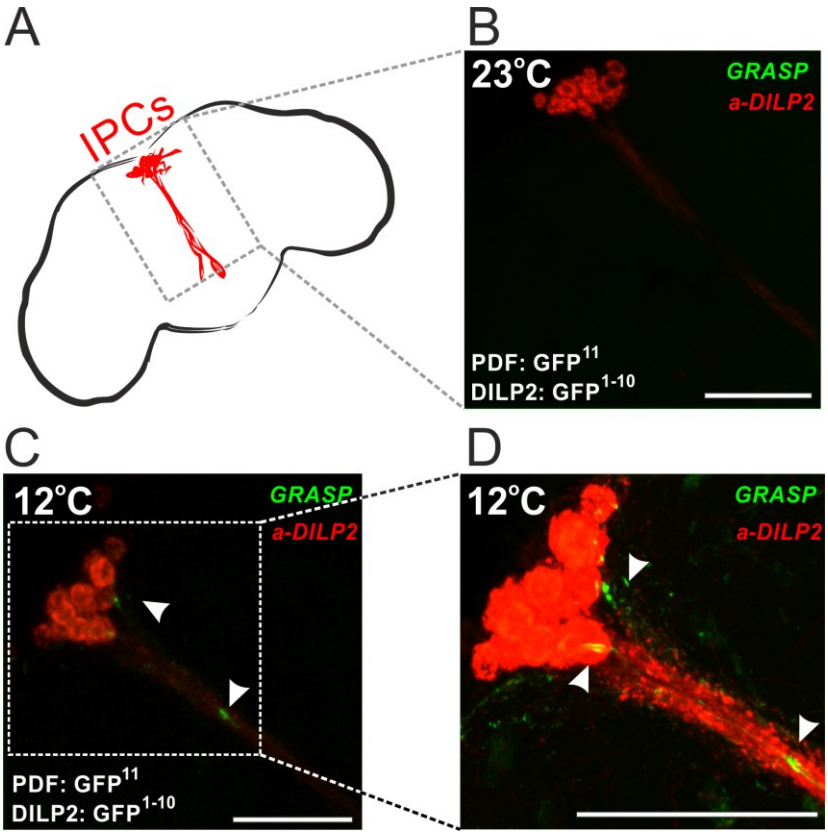

Figure 25. IPCs are functionally connected to PDF-positive neurons in the cold. (A) Schematic figure of the fly brain showing the set of insulin producing cells and their axonal projections. Area indicated by dashed rectangle is shown in the confocal photos B and C. (B) No GRASP signal was detected between PDF$^+$ neurons and IPCs at 23^{o}C (*w;Pdf-LexA,LexAop-CD4::GFP11/dilp2(p)-Gal4;UAS-CD4::GFP1-10/+*). Representative confocal image (Z-stack). (C) GRASP signal (indicated by white arrowheads) appears at the points of contact between the IPCs and PDF$^+$ neurons in the vicinity of the insulin producing cell bodies and along their axonal projection. Representative confocal image (Z-stack). (D) A close-up of the area outlined with the dashed rectangle in figure C showing the *PI* region with the IPCs. GRASP signal is present close to the cell bodies and along the DILP axon (marked by white arrowheads). IPCs are stained with *anti*-DILP2 antibody. Scale bar = 50 µM.

GFP fluorescence was observed near the cell bodies of insulin producing cells in the *PI*, and in some brains also in the proximity of the IPC axonal projection in the median bundle (*Figure 25C, D*). These data suggest that IPCs are connected to PDF^{+} neurons in the cold, and therefore get synaptic contact from these cells. The temperature-dependent existence of the signal suggests that the contact is likely to exist between the IPCs and PDF-Tri neurons.

4.9. IPCs are activated by cold temperature

In order to study how IPCs respond to long-term cold treatment, the CaLexA neuronal tracing method was used, which had already been successful in defining active neurons in the brain (Masuyama et al. 2012). High intracellular Ca^{2+} levels trigger the nuclear translocation of a modified NFAT transcriptional factor, leading to the expression of GFP reporter gene only in active neurons (*See Materials and Methods, page 52*). Flies were developed at 18°C in LD 8:16 cycles (PROTOCOL 2) prior to being placed at either 12°C or 23°C for 11 days, maintaining the same photoperiod. Exposure to 12°C induced significantly higher accumulation of activity-dependent GFP in the IPCs and along their axonal projection compared to that in samples at 23°C (12°C 1.00 ± 0.61 compared to 23°C 0.14 ± 0.04, ***$p<0.001$) (*Figure 26*).

This result shows that IPCs respond to chronic cold exposure. Since insulin-like signaling is known to be downregulated during diapause at low temperature (Kimura et al. 1997; Allen et al. 2007; Sim & Denlinger 2008; Kubrak et al. 2014; Schiesari et al. 2016), this result is unexpected. However, it has recently been published that DILP1/*dilp1,* believed to be expressed only before adulthood*,* is surprisingly detectable for many weeks in diapausing flies, highlighting the possibility that these cells might be active to produce this peptide for a certain reason (Liu et al. 2016). Another explanation for their activation would rely on some surprising recent findings that documented the paradoxical upregulation of *dilp2,-3,-5* in diapausing flies (Kubrak et al. 2014; Schiesari et al. 2016). This indicates the existence of active biological processes in these cells even under this limited condition.

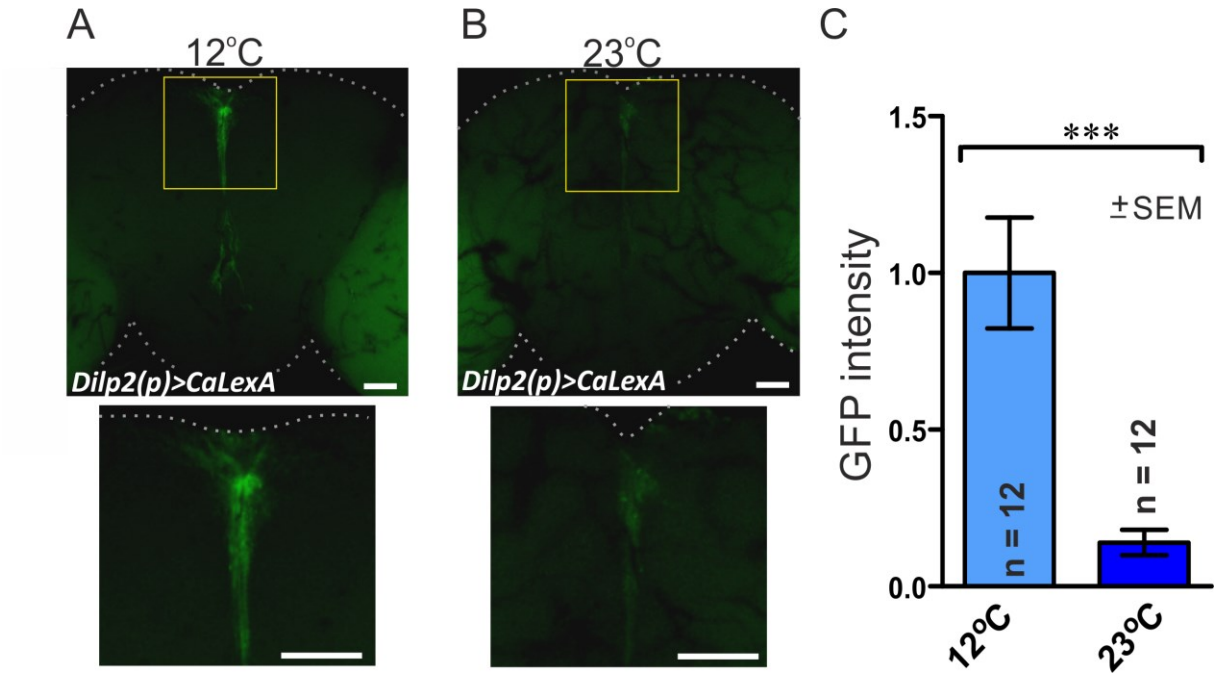

Figure 26. IPCs get activated by low temperature. CaLexA-based immunocytochemistry of adult IPCs after exposing flies (developed at 18°C in LD 8:16) either to 12°C (A) or 23°C (B) in LD 8:16 for 11 days. Flies express an activity reporter system in the IPCs (*w;lexAop-CD8-GFP-2ACD8-GFP/dilp2(p)-Gal4;UAS-mLexA-VP16-NFAT,lexAop-CD2-GFP/TM6b,* or briefly *Dilp2(p)>CaLexA)*, based on the calcium-responsive transcription factor NFAT and its Ca^{2+}-dependent transport to the nucleus. Upon high Ca^{2+} concentration it locates to the nucleus and turns on the transcription of *gfp*, thus GFP levels positively correlate with Ca^{2+} levels (A) Representative confocal Z-projection stack of a fly brain at 12°C. Strong GFP signal can be observed in the cell bodies of IPCs and along their axonal projection (upper image), reflecting high IPC activity. The area highlighted in yellow is shown in higher magnification in the bottom image. (B) Representative confocal image of a brain at 23°C. Very faint signal is present in the IPCs and along their projection. The bottom image is a close-up of the brain region marked in yellow in the upper image. Whole brain is outlined in white in figure A and B, and scale bars indicate 50 µM. (C) Quantification of GFP signal at the two different temperatures highlights higher GFP levels at 12°C (***p<0.001, Mann-Whitney test) than at 12°C. Data are normalized to average GFP intensity at 12°C. n = number of brains.

4.10. IPCs respond to bath-applied PDF and sNPF

Since our diapause assays suggested a modulatory action of both PDF and sNPF on diapause, we decided to further investigate the effects of both neuropeptides on the IPCs, using genetically encoded cAMP- and Ca-sensors. They are fluorescent protein-based sensors, enabling real-time monitoring of second messenger concentration changes in the living brain (*See Materials and Methods, page 49*). Considering that PDF was found to signal primarily via cAMP and not by Ca^{2+} (Hyun et al. 2005; Mertens et al. 2005; Duvall & Taghert 2012), we started our experiments focusing on the cAMP measurements. Therefore, the cAMP sensor UAS-*Epac1camps(50A)* was expressed under the control of *dilp2(p)*-Gal4 driver

to ensure IPC-specific expression (Shafer et al. 2008). First, synthetic PDF was bath-applied to freshly dissected fly brains, meanwhile concentration changes in cAMP have been continuously recorded in the sensor-expressing neurons. A similar experimental design had previously been successfully adopted to demonstrate the presence of PDF receptors on clock neurons (Shafer et al. 2008). The IPCs reacted with a slow increase of ~9% in intracellular cAMP upon 10^{-5} M PDF application ($PDF_{(100\text{-}1000\ s)}$ 8.7 ± 1.9%, ***p<0.001) (*Figure 27A*).

This PDF-mediated cAMP rise appeared due to direct activation of the IPCs, since a similar increase of ~10% was also observed after blocking neuronal conduction by the sodium channel blocker tetrodotoxin (TTX) ($PDF+TTX_{(100\text{-}1000\ s)}$ 10.3 ± 2.1, p***p<0.001) (*Figure 27A*). When focusing on short-term responses (from the application point of the peptide at 100 s until 200 s) (*Figure 27B*), no significant changes were found between the negative control ($HL3_{(100\text{-}200\ s)}$ 0.53 ± 0.81%) and PDF applications with and without TTX ($PDF_{(100\text{-}200\ s)}$ 1.21 ± 0.53% and $PDF+TTX_{(100\text{-}200\ s)}$ -0.17 ± 0.77%, n.s.).

When synthetic sNPF was bath-applied to cAMP-sensor expressing brains, a similar effect was observed, highlighting a slow but significant cAMP increase in the insulin producing cells compared to the negative control ($sNPF_{(100\text{-}1000\ s)}$ 8.1 ± 1.3% compared to $HL3_{(100\text{-}1000\ s)}$ -3.1 ± 2.4%, ***p<0.001) (*Figure 28A*). A comparable change was detected when sNPF was applied in the presence of TTX, reflecting a direct activation of IPCs by sNPF (*Figure 28A*). These data can be explained by the presence of sNPFR1 on the IPCs, as already demonstrated in previous studies (Lee et al. 2008; Kapan et al. 2012; Carlsson et al. 2013). However, similarly to PDF, the short-term responses to sNPF were not found to be significantly different from the negative control ($sNPF_{(100\text{-}200\ s)}$ 2.2 ± 0.5% and $sNPF+TTX_{(100\text{-}200\ s)}$ 2.5 ± 0.8% compared to $HL3_{(100\text{-}200\ s)}$ 0.5 ± 0.8%, n.s.) (*Figure 28B*).

Surprisingly, when sNPF and PDF were co-applied to the brains, a rapid and long-lasting cAMP increase of ~15% was recorded in the insulin producing cells ($sNPF+PDF_{(100\text{-}1000\ s)}$ 14.8 ± 2.8% compared to $HL3_{(100\text{-}1000\ s)}$ -3.1 ± 2.4%, ***p<0.001) (*Figure 29A*). Since our statistical analysis is based on the calculation of the maximum inverse FRET changes for each individual neuron between 100-1000 s, it fails to show any marked changes after the application point in the case where such changes end up smaller than the largest point reached. Thus, in this time interval the effect of the co-application does not seem to be

different from that of sNPF and PDF single applications (sNPF$_{(100\text{-}1000\ s)}$ 8.1 ± 1.3% and PDF$_{(100\text{-}1000\ s)}$ 8.7 ± 1.9%, n.s.).

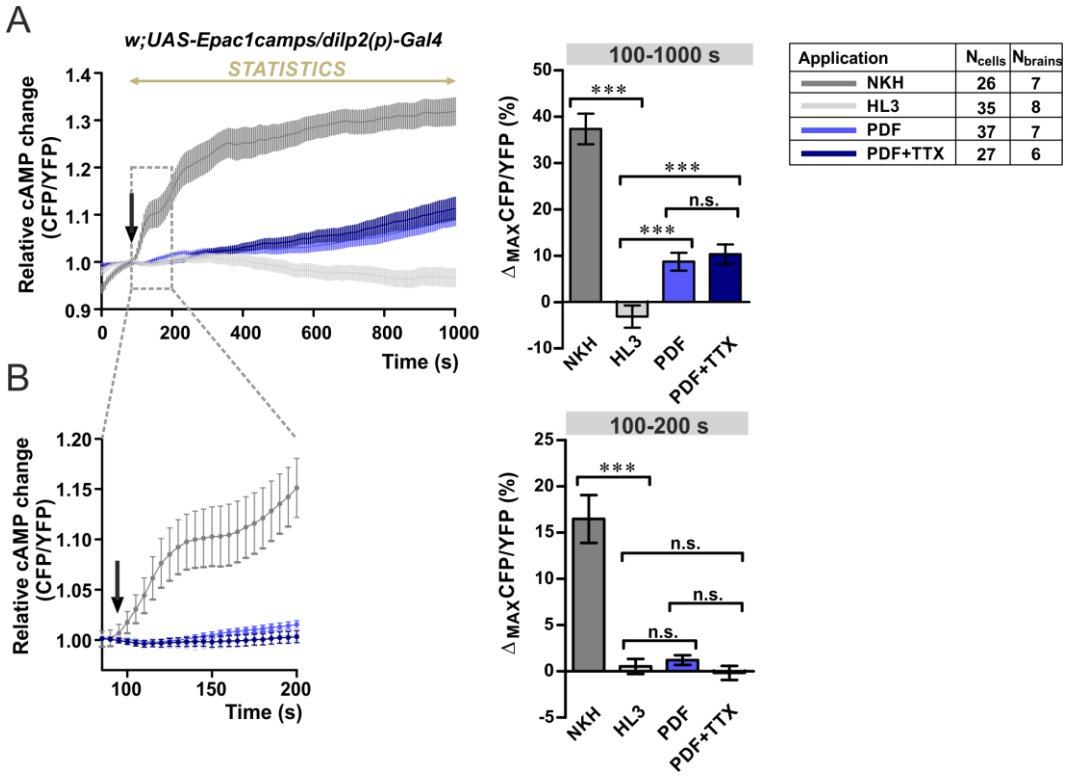

Figure 27. Bath-applied PDF evokes cAMP increases in the IPCs. *Ex vivo* live-cAMP imaging of insulin producing cells (A) *Left:* Average inverse FRET traces (CFP/YFP) in IPCs reflecting intracellular changes in cAMP levels. Substances were bath-applied to freshly dissected fly brains at 100 s (indicated by a black arrow). Application of 10^{-5} M adenylate cyclase activator NKH477 (designated as NKH) induced a robust increase in cAMP, indicating that the general procedure was working. As a negative control, hemolymph-like saline (HL3) was applied. 10^{-5} M synthetic PDF peptide led to an increase in cAMP level, indicating a functional connection between PDF expressing cells and IPCs. To test whether this connection was direct or mediated by interneurons, brains were incubated in 2µM TTX for ~15 min prior to imaging and 10 µM PDF were then co-applied together with 2µM TTX. The IPCs responded with similarly increasing levels in cAMP, indicating a direct connection between PDF^{+} cells and IPCs. Data are presented as mean ± SEM. *Middle:* Maximum inverse FRET changes were quantified for each individual neuron and averaged for each pharmacological treatment from 100 s until 1000 s. Statistical comparison revealed significant increases in cAMP levels compared to the negative control (HL3) for NKH, PDF as well as PDF+TTX. Error bars represent SEM and letters indicate statistical significances. *Right:* Table shows the color code of the different treatments and the number of neurons (N_{cells}) in the dissected brains (N_{brain}) considered in this analysis. (B) *Left:* Graph shows a close-up of the immediate changes in cAMP levels occurring from the application point until 200 s. No significant changes can be observed when PDF or PDF+TTX were applied. Data are shown as mean ± SEM. *Right:* Maximum inverse FRET changes in the case of each neuron from 100-200 s. Kruskal-Wallis test followed by Bonferroni-corrected Wilcoxon pairwise-comparisons. ***p<0.001, n.s. not significant.

However, when looking at the cAMP changes over time, the co-application of sNPF+PDF induced an immediate increase in cAMP levels (*Figure 29A, left panel, red curve*),

which was absent when only sNPF or PDF was applied to the brains (*Figure 29A, left panel, yellow and blue curves, respectively*).

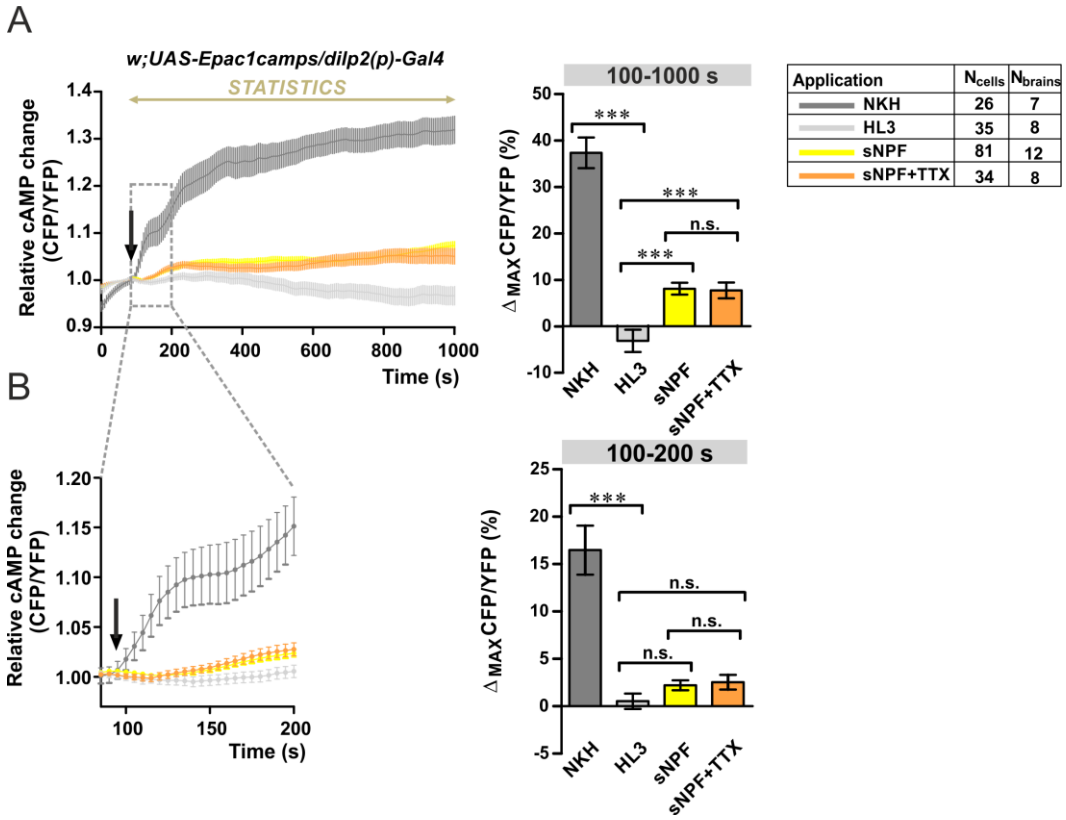

Figure 28. Bath-applied sNPF induces cAMP increases in the IPCs. (A) *Left:* Average inverse FRET traces (CFP/YFP) of IPCs reflecting intracellular changes in cAMP levels. The application point of the different substances is indicated by a black arrow (at ~100 s). The adenylate cyclase activator NKH (10^{-5} M) was used as positive control, while hemolymph-like saline (HL3) was applied as negative control. Synthetic sNPF peptide induces an increase in cAMP, which persists also in the presence of 2µM TTX, suggesting that the response is direct and not mediated by interneurons. Data are presented as mean ± SEM. *Middle:* Maximum inverse FRET changes quantified for each individual neuron and averaged for each pharmacological treatment from 100 s until 1000 s. Statistical comparison revealed significant increases in cAMP levels compared to the HL3 for NKH, sNPF, as well as sNPF+TTX. Data are presented as mean ± SEM. *Right:* The table shows the color code of the different treatments and the number of neurons (N_{cells}) in the dissected brains (N_{brain}) considered in this analysis. (B) *Left:* Graph shows a high magnification view of the immediate cAMP level changes occurring from the application point until 200 s. No significant changes compared to the negative control can be observed when sNPF or sNPF+TTX were applied. Data are shown as mean ± SEM. *Right:* Maximum inverse FRET changes for each neuron from 100-200 s. Kruskal-Wallis test followed by Bonferroni-corrected Wilcoxon pairwise-comparisons. ***p<0.001, n.s. not significant.

To better examine cAMP responses occurring right after the application of the two peptides, the immediate changes from 100-200 s were also calculated. A rapid increase of ~8% was found (sNPF+PDF$_{(100\text{-}200\ s)}$ 8.1 ± 2.0%), significantly higher than those observed after

the single peptide applications ($sNPF_{(100\text{-}200\ s)}$ 2.2 ± 0.5% and $PDF_{(100\text{-}200\ s)}$ 1.2 ± 0.5%, **p<0.01) (*Figure 29B*).

Importantly, as when co-applying the two peptides, the number of peptide molecules were doubled in the solution (2 x 10^{-5} M), we checked how cAMP responses change when concentration of the single peptides is halved in the co-application. Thus, the measurements were repeated in 10^{-5} M final concentration (designated as $sNPF_{1/2}$+$PDF_{1/2}$), which resulted in a significant increase of ~6% in cAMP levels compared to the negative control ($sNPF_{1/2}$+$PDF_{1/2(100\text{-}200\ s)}$ 5.5 ± 2.0 % compared to $HL3_{(100\text{-}200\ s)}$ -3.1 ± 2.4%, *p<0.05).

However, when looking at the cAMP changes from 100 s to 1000 s (*Figure 29A, left panel, pink curve*), cAMP concentration seems to increase at the beginning of the application point until ~400s, while after this rise a slow reduction can be observed. Focusing on the short-term responses induced by the $sNPF_{1/2}$+$PDF_{1/2}$ co-application, a significant rise of ~5% was found in the cAMP levels ($sNPF_{1/2}$+$PDF_{1/2(100\text{-}200\ s)}$ 4.6 ± 0.6%), which was significantly higher than the increase of ~1% due to single PDF application ($PDF_{(100\text{-}200s)}$ 1.2 ± 0.5%, **p<0.01) (*Figure 29B*). Although not found statistically significant, it is higher than the ~2% increase recorded due to sNPF application (2.1 ± 0.5%). Therefore, it seems that the co-application induced an immediate increase in cAMP levels, which was not detectable in the case of the single neuropeptide applications. When comparing sNPF+PDF co-application to $sNPF_{1/2}$+$PDF_{1/2}$ (14.8 ± 2.8% compared to 5.5 ± 2.0%), the latter apparently evoked lower cAMP increases; however the difference between them was not found to be statistically significant (*Figure 29B*).

There is another important issue that needs to be considered in analyzing the action of sNPF+PDF on the IPC. Although averaging cAMP changes in the individual neurons resulted in a strong excitatory effect (*Figure 29, left panels, red curve*), it appears to be much more complex when analyzed at single neuron level. *Figure 29C* shows the recorded cAMP changes in two different brains. In the first brain (*left panel*), five different IPCs were selected and all of them responded with an increase in cAMP level due to the co-application. However, in another brain (*right panel*), six IPCs were selected among which one responded positively, two were refractory, while three showed a large reduction of cAMP levels. These findings can be due to the heterogeneity of the individual IPCs, as already documented in earlier studies (Jaramillo et al. 2004; Söderberg et al. 2012; Barber et al. 2016). They do not

only differ in neuropeptide composition (Jaramillo et al. 2004; Söderberg et al. 2012), but also show marked differences in their electrophysiological parameters (Barber et al. 2016).

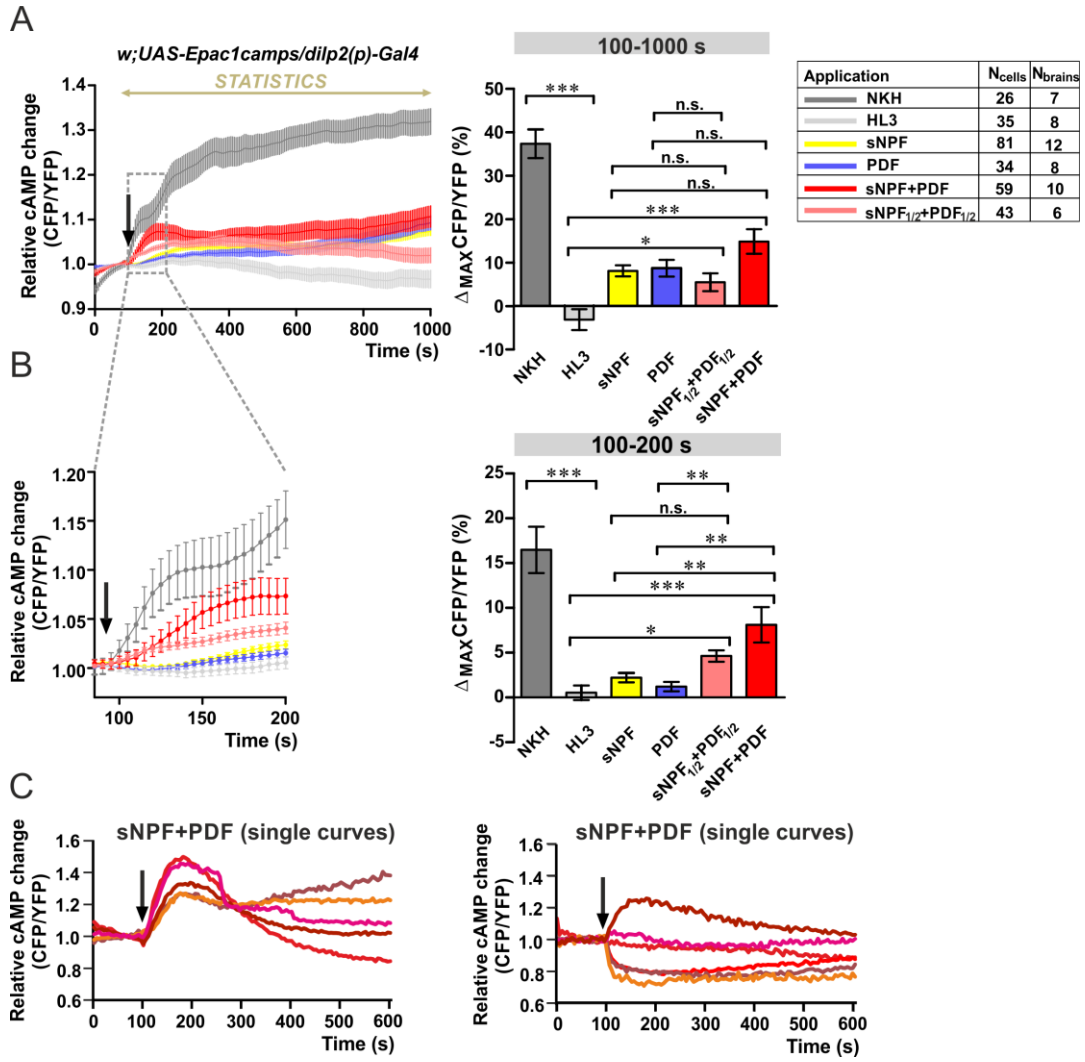

Figure 29. Co-application of sNPF and PDF evokes large cAMP increases in the IPCs. (A) *Left:* Average inverse FRET traces (CFP/YFP) of IPCs reflecting intracellular changes in cAMP levels. The application point of the different substances is shown by a black arrow (at ~100 s). The adenylate cyclase activator NKH (10^{-5} M) was used as positive control, while hemolymph-like saline (HL3) was applied as negative control. Synthetic sNPF peptide induces an increase in cAMP, which persists also in the presence of 2µM TTX, suggesting that the response is direct and not mediated by interneurons. Data are presented as mean ± SEM. *Middle:* Maximum inverse FRET changes quantified for each individual neuron and averaged for each treatment from 100 s until 1000 s. Statistical comparison revealed significant differences in cAMP levels between the different applications, indicated in the graph. Data are shown as mean ± SEM. *Right:* Table indicates the color code of the different treatments and the number of neurons (N_{cells}) in the dissected brains (N_{brain}) considered in this analysis. (B) *Left:* Graph shows a close-up of the immediate changes in cAMP levels from the application point until 200 s. Error bars represent SEM and letters indicate statistical significances. *Right:* Maximum inverse FRET changes for each neuron from 100-200 s. (C) Representative single-neuron traces in two different brains. *Left:* 5 selected IPCs responded to co-applied sNPF+PDF with large cAMP changes. *Right:* Among the selected 6 IPCs 3 responded negatively, two did not seem to be altered by the application, while one responded with a large cAMP increase. Kruskal-Wallis test followed by Bonferroni-corrected Wilcoxon pairwise-comparisons. ***p<0.001, **p<0.01, *p<0.05, n.s. not significant.

Therefore, it is possible that individual IPCs express different receptors, and react differently to certain neuropeptides.

To check whether the sNPF+PDF-induced large cAMP changes are due to direct activation of the IPCs, the co-application was performed also in the presence of TTX (*Figure 30A*). It has already been described that both single sNPF and PDF treatments appeared to generate direct cAMP responses (*Figure 28A, orange curve, and Figure 27A, dark blue curve, respectively*), since they were not blocked when brains were incubated with TTX. When sNPF+PDF was co-applied in the presence of TTX, an increase of ~13% was induced in the level of cAMP which was significantly higher than the negative control (sNPF+PDF+TTX$_{(100\text{-}1000\ s)}$ 13.2 ± 2.2% compared to HL3$_{(100\text{-}1000\ s)}$ -3.1 ± 2.4%, ***p<0.001) (*Figure 30A*). Although this response was not statistically significant from the single sNPF+TTX and PDF+TTX applications during the time interval of 100-1000 s (sNPF+TTX$_{(100\text{-}1000\ s)}$ 7.7 ± 1.7% and PDF+TTX$_{(100\text{-}1000\ s)}$ 10.3 ± 2.1%, n.s.), when looking at cAMP changes between 300-600 s, the sNPF+PDF+TTX curve (magenta) runs above the sNPF+TTX (orange) and PDF+TTX (dark blue) curves (sNPF+PDF+TTX$_{(300\text{-}600\ s)}$ 9.8 ± 1.4% compared to sNPF+TTX$_{(300\text{-}600\ s)}$ 5.5 ± 1.2%, *p<0.05, while compared to PDF+TTX$_{(300\text{-}600\ s)}$ 5.2 ± 1.5%, p = 0.08, a trend close to significance) (*Figure 30A*). When comparing the effect of sNPF+PDF co-application on cAMP levels in the presence or absence of TTX, no difference was observed when the time period of 100-1000 s was analyzed (sNPF+PDF$_{(100\text{-}1000\ s)}$ 14.8 ± 2.8% compared to sNPF+PDF+TTX$_{(100\text{-}1000\ s)}$ 13.2 ± 2.2%, n.s.) (*Figure 30B*). However, when looking at the curve that indicates the relative cAMP changes over time, a difference appears compared to the co-application without TTX (*Figure 30B, magenta and red curves*): the immediate large increase in cAMP levels seems to be strongly decreased by half (from ~8% to ~4%) in the presence of TTX. Though, this reduction did not seem to be statistically significant when analyzed between 100-200 s (sNPF+PDF$_{(100\text{-}200\ s)}$ 8.1 ± 2.0% compared to sNPF+PDF+ TTX$_{(100\text{-}200\ s)}$ 4.1 ± 0.6%, p = 0.10, n.s.).

To sum up, these results highlight the interesting possibility of a synergistic interaction between the circadian neuropeptide PDF and the growth-promoting peptide sNPF, which may have a special contact with each other in regulating the activity of insulin producing cells. The cAMP responses induced by the sNPF+PDF co-application seem to be, at least partially, due to direct activation of the insulin producing cells.

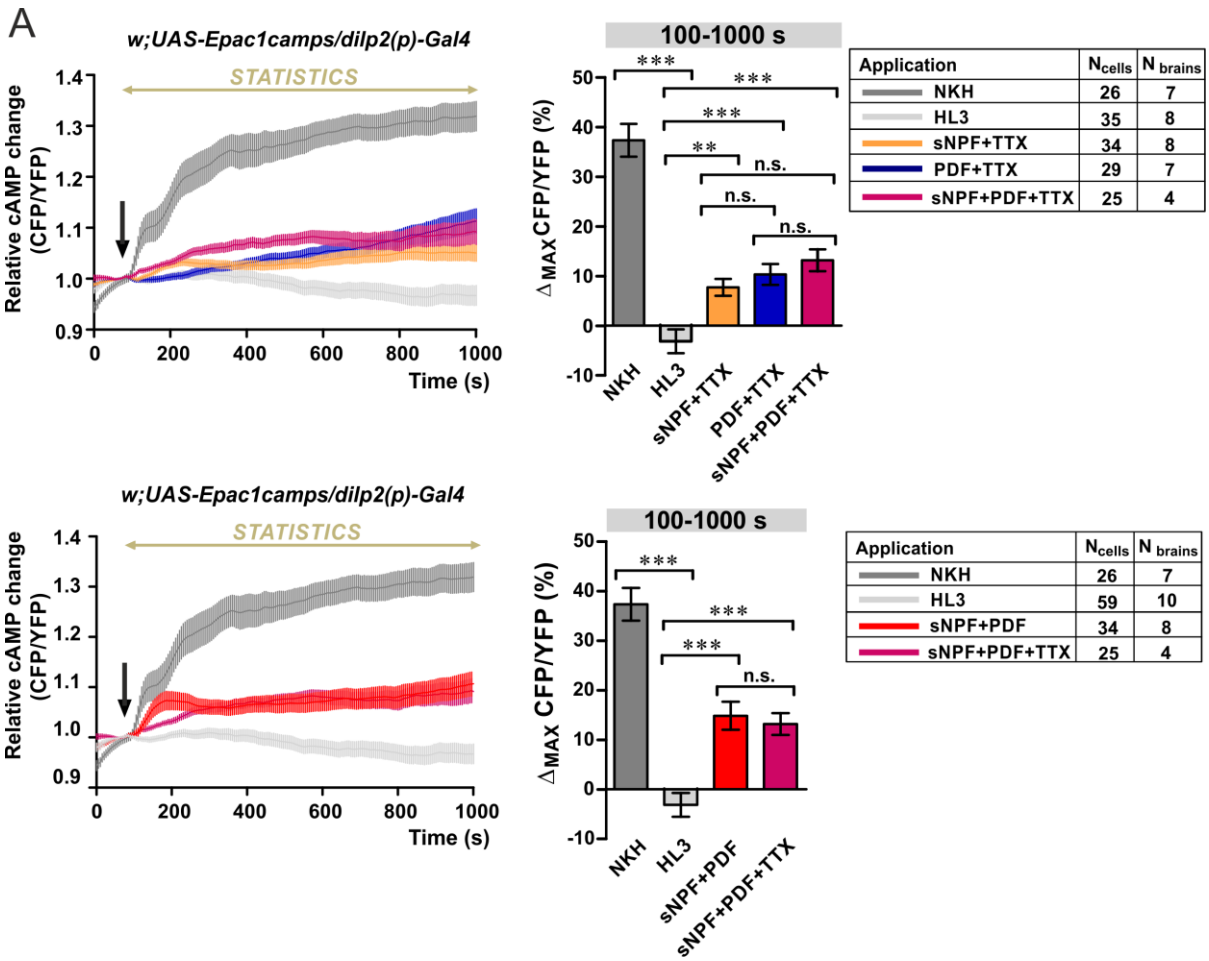

Figure 30. The sNPF+PDF-induced large cAMP increase is, at least partially, due to direct activation of the IPCs. (A) *Left:* Average inverse FRET traces (CFP/YFP) of IPCs reflecting intracellular cAMP changes. Synthetic sNPF and PDF peptides induce an increase in the level of cAMP in the presence of 2µM TTX, suggesting that these responses are not mediated by interneurons. Similar effect was observed in the case of sNPF+PDF+TTX co-application. Between ~300-600 s the co-applied peptides induced larger cAMP increases (magenta curve) compared to the single PDF and sNPF applications in the presence of TTX (orange and dark blue curves, respectively). *Middle:* Maximum inverse FRET changes quantified for each individual neuron and averaged for each treatment from 100 s until 1000 s. Statistical comparison showed significant increases in cAMP levels compared to the HL3 for NKH, sNPF+TTX, PDF+TTX, as well as sNPF+PDF+TTX. *Right:* Table shows the color code of the different treatments and the number of neurons (N_{cells}) in the dissected brains (N_{brain}) considered in this analysis. (B) *Left:* Average inverse FRET traces (CFP/YFP) of IPCs reflecting intracellular changes in cAMP levels. Co-application of sNPF+PDF leads to increased cAMP levels also in the presence of TTX, however the initial large cAMP increase seems to be reduced (n.s.). Data are shown as mean ± SEM. *Middle:* Maximum inverse FRET changes counted for each neuron from 100-1000 s. *Right:* Table showing the number of neurons and brains considered in the analysis. The application point of the different substances is indicated by a black arrow. As a positive control, adenylate cyclase activator NKH (10^{-5} M) was used, while hemolymph-like saline (HL3) served as negative control. Error bars indicate SEM and letters show statistical significances. Kruskal-Wallis test followed by Bonferroni-corrected Wilcoxon pairwise-comparisons. ***p<0.001, **p<0.01, n.s. not significant.

To test whether the large cAMP increases induced by the co-application of sNPF and PDF are specific for these two neuropeptides, and the widely-expressed sNPF peptide

requires the circadian neuropeptide as a signaling partner to exert a synergistic effect on the insulin-producing cells, we co-applied sNPF with other *Drosophila* neuropeptides. The effect of four different peptides, the FMRFamide SDNFMRFa, adipokinetic hormone (AKH), Drosophila tachykinin (DTK), and allatostatin-C (Ast-C) was tested.

Among these four peptides, AKH and DTK have already been identified as possible regulators of IPC activity (Rulifson et al. 2002; Buch et al. 2008; Kim et al. 2015; Birse et al. 2011). While the former functions as a circulating peptide hormone, playing a crucial role in lipid and carbohydrate metabolism (Gäde & Auerswald 2003), the latter was found to fulfill various functions in the nervous system, including the modulation of olfactory and locomotor behavior (Winther et al. 2006). FMRFamides (Phe-Met-Arg-Phe-NH_2) are believed to have a hormonal function, though our knowledge about their role is still very limited and so far no function has been identified for them in the brain (Schneider et al. 1993; Nässel 1993). As for Ast-C, very little is known about its actions, although it was shown to decrease heart rate in *Drosophila* (Price et al. 2002).

When sNPF was co-applied with SDNFMRFa, AKH or DTK, cAMP levels were significantly reduced compared to the sNPF+PDF co-application (sNPF+$PDF_{(100\text{-}1000\ s)}$ 14.8 ± 2.8% compared to sNPF+$SDNFMRFa_{(100\text{-}1000\ s)}$ -3.6 ± 3.6%, *p<0.05; compared to sNPF+ $AKH_{(100\text{-}1000\ s)}$ -2.5 ± 1.6%, **p<0.01, compared to sNPF+$DTK_{(100\text{-}1000\ s)}$ 0.2 ± 3.1%, *p<0.05) (*Figure 31A*). It is not known whether IPCs are directly or indirectly affected by SDNFMRFa, however it seems that the sNPF-induced cAMP responses disappeared in the presence of SDNFMRFa, suggesting its inhibitory effect on the IPCs. As for AKH, a possible functional connection has already been documented between IPCs and AKH-producing cells in the *corpora cardiaca* (Rulifson et al. 2002; Buch et al. 2008). The genetic ablation of IPC results in increased level of *akh* transcript, while ablation of AKH-expressing cells alters *dilp3* mRNA level (Buch et al. 2008). This connection is likely to be regulated through AKH receptor (AKHR), expressed on the IPCs (Kim et al. 2015). As for the third peptide, DTK, based on our imaging the excitatory effect of sNPF was no longer observed when co-applying it with DTK, suggesting the possible negative effect of this peptide on cAMP levels in the IPCs. Surprisingly, there was an immediate inhibitory effect directly after the application point of sNPF+DTK, which becomes more evident when short-term cAMP responses are considered (*Figure 31B*). Interestingly, IPC dendrites and DTK-expressing varicosities overlap in the *PI*

region of the adult brain, and the receptor for DTK has been reported to be expressed on the IPCs through which DTK regulates lifespan and *dilp* transcript levels (Birse et al. 2011).

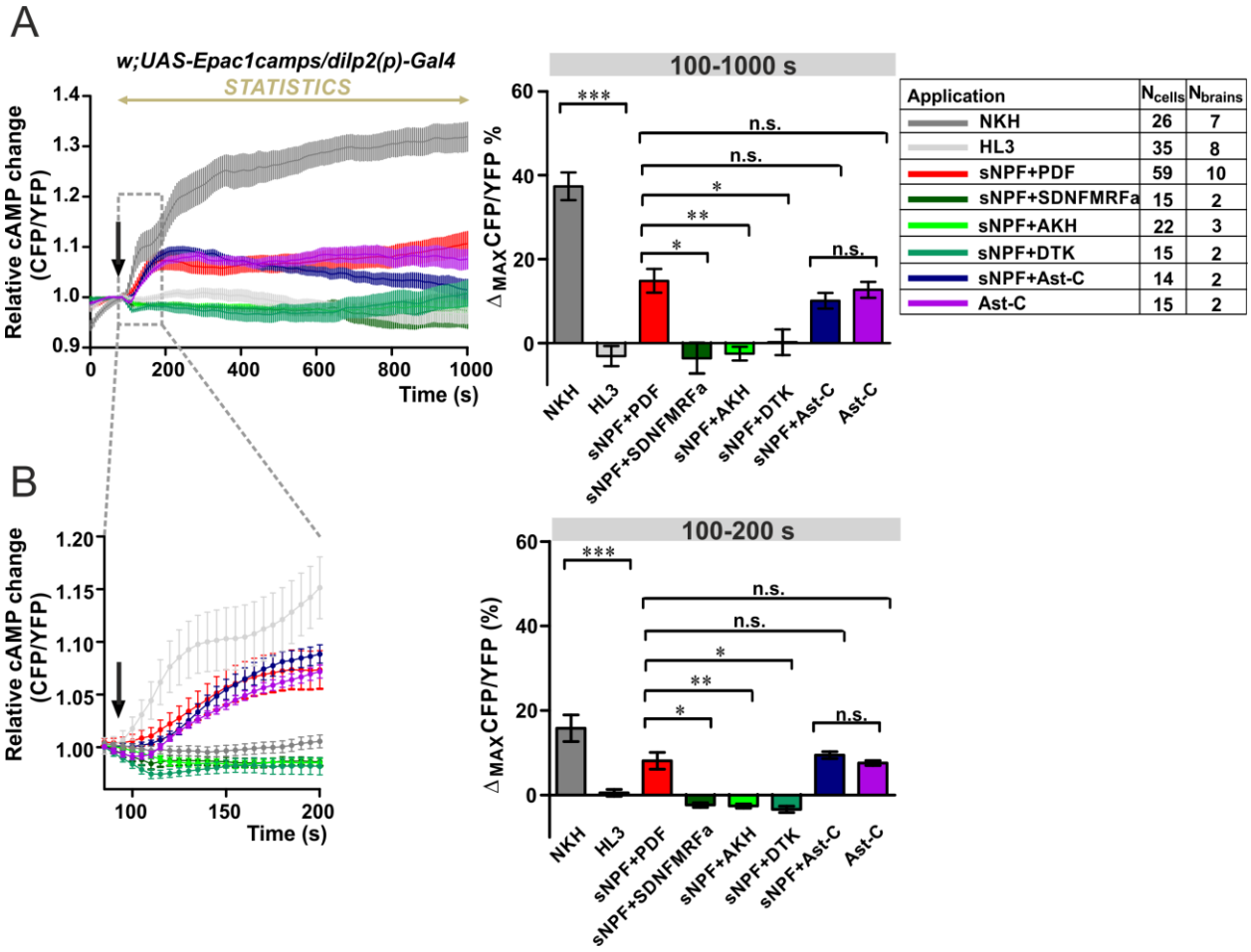

Figure 31. Co-application of sNPF with other random Drosophila peptides suggests that sNPF and PDF may have a unique interaction. (A) *Left:* Average inverse FRET traces (CFP/YFP) of IPCs reflecting intracellular cAMP changes. 10^{-5} M synthetic sNPF was co-applied with PDF, SDNFMRFa, AKH (adipokinetic hormone), DTK (Drosophila tachykinin), Ast-C (Allatostatin-C) /10^{-5}M for each/ or 10^{-5} M Ast-C was added alone. The application point of the different substances is indicated by a black arrow. As a positive control, 10^{-5} M adenylate cyclase activator NKH was used, while hemolymph-like saline (HL3) was applied as negative control. *Middle:* Maximum inverse FRET changes quantified for each individual neuron and averaged for each treatment from 100 s until 1000 s. Statistical comparison revealed that co-application of sNPF with SDNFMRFa, AKH, and DTK resulted in a significant decrease of cAMP levels compared to the sNPF+PDF co-application. sNPF+Ast-C led to a significant increase in the level of cAMP, however similar change was observed in the case of Ast-C application alone. *Right*: Table shows the color code of the different treatments and the number of neurons (N_{cells}) in the dissected brains (N_{brain}) considered in this analysis. (B) *Left:* High magnification view of the immediate cAMP level changes occurring from the application point until 200 s. Compared to the sNPF+PDF co-application, SDNFMRFa, AKH and DTK lead to a significant reduction of cAMP levels when applied together with sNPF, while neither co-applied nor single Ast-C applications show difference. *Right:* Maximum inverse FRET changes calculated for each neuron from 100-200 s. Data are shown as mean ± SEM. Kruskal-Wallis test followed by Bonferroni-corrected Wilcoxon pairwise-comparisons. ***p<0.001, **p<0.01, *p<0.05, n.s. not significant.

When sNPF was co-applied with Ast-C, a statistically significant increase in intracellular cAMP levels was induced, similarly to that observed in the case of sNPF+PDF co-application (Ast-$C_{(100\text{-}1000\ s)}$ 10.1 ± 1.9% compared to sNPF+$PDF_{(100\text{-}1000\ s)}$ 14.8 ± 2.8%, n.s.) (*Figure 31A, dark blue curve compared to the red*). This increase was an immediate and rapid change, with a trend similar to that registered due to sNPF+PDF co-application in short term (sNPF+Ast-$C_{(100\text{-}200s)}$ 9.4 ± 0.8% compared to sNPF+$PDF_{(100\text{-}200\ s)}$ 8.1 ± 2.0%, n.s.) (*Figure 31B*). To test whether Ast-C alone affects IPCs by altering cAMP concentration in these cells, it was applied separately to the fly brains. Surprisingly, Ast-C evoked a large cAMP increase of ~13% in the IPCs, which was as large as the rise generated by sNPF+Ast-C and sNPF+PDF co-applications regarding both long- and short-term responses (Ast-$C_{(100\text{-}1000\ s)}$ 12.7 ± 1.9%; Ast-$C_{(100\text{-}200\ s)}$ 7.6 ± 0.6%) (*Figure 31A* and *B*). Therefore, we conclude that Ast-C peptide alone is responsible for the rapid cAMP response that appeared upon sNPF+Ast-C co-application. To our knowledge, no data is available regarding Ast-C receptor distribution in *Drosophila*, and no connection has been revealed between IPCs and Ast-C. Although allatostatin-A (Ast-A) was found to influence IPC activity via its receptor, DAR2, expressed on the IPCs (Hentze et al. 2015), this peptide is very different from Ast-C in terms of consensus amino acid sequence and distribution (Nässel & Winther 2010).

To check whether PDF- and sNPF-evoked cAMP responses are regulated by PDF receptor (han) (Hyun et al. 2005), the cAMP sensor UAS-*Epac1camps(50A)* was expressed in PDFR null mutant background (*han;dilp2(p)*-Gal4;UAS-*Epac1camps(50A)*). We found that application of PDF no longer resulted in an increase in intracellular cAMP levels compared to the negative control HL3, and surprisingly neither did sNPF ($PDF_{(100\text{-}1000\ s)}$ 2.5 ± 2.7% and sNPF $_{(100\text{-}1000\ s)}$ 0.3 ± 1.9% compared to $HL3_{(100\text{-}1000\ s)}$ 2.3 ± 2.6, n.s.) (*Figure 32A*). The rapid increase in cAMP levels, induced by sNPF+PDF directly after the application point in the wild-type background (*Figure 29A, B*), was completely diminished in this mutant (sNPF+$PDF_{(100\text{-}200\ s)}$ 1.8 ± 1.0% compared to $HL3_{(100\text{-}200\ s)}$ 1.9 ± 0.9%) (*Figure 32B*), and so was the late cAMP increase (sNPF+$PDF_{(100\text{-}1000\ s)}$ -1.0 ± 3.2% compared to $HL3_{(100\text{-}1000\ s)}$ 2.3 ± 2.6%) (*Figure 32A*). To sum up, apart from the large difference between the positive and negative controls, no statistically significant changes were found in the case of any application compared to the negative control (*Figure 32A, B*). These results indicate that the cAMP responses in the IPCs due to PDF and sNPF applications are apparently mediated by PDFR, expressed on the insulin producing cells.

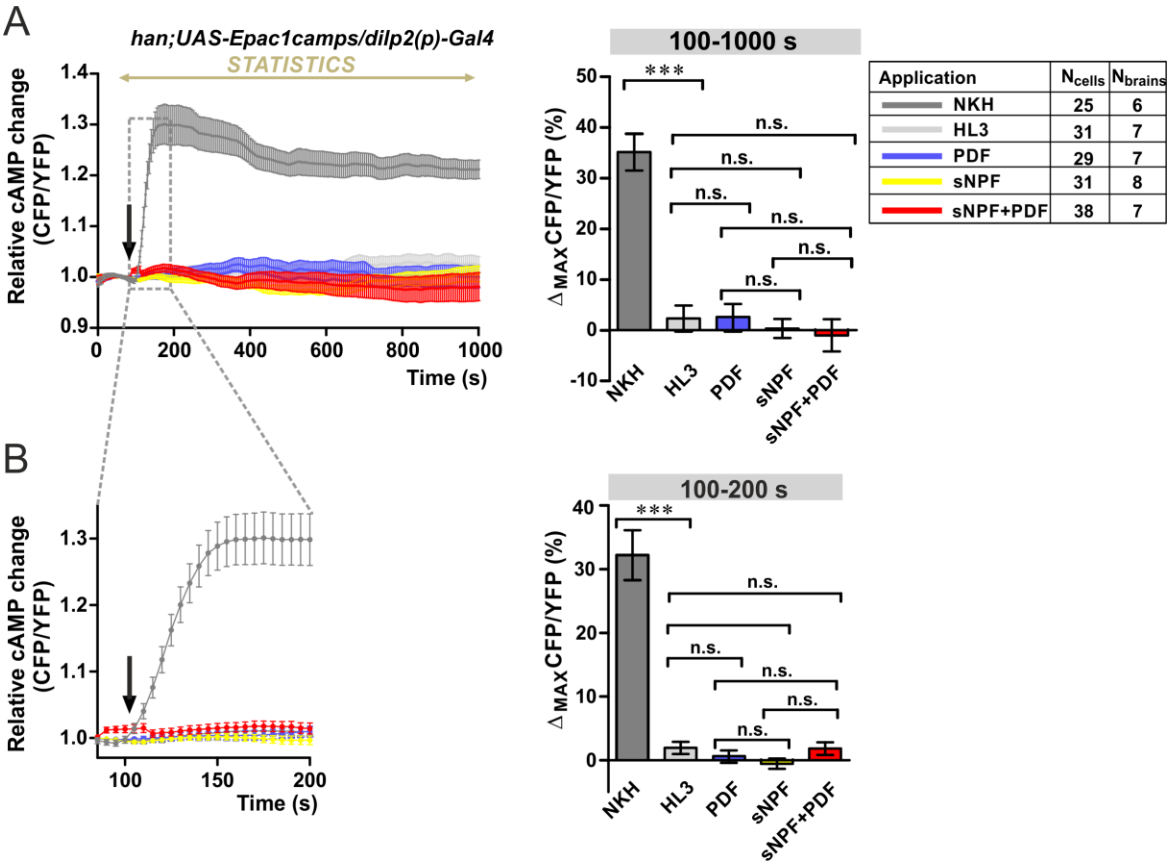

Figure 32. The effects of both PDF and sNPF are abolished in PDFR null mutant (han) flies. (A) *Left:* Average inverse FRET traces (CFP/YFP) of IPCs reflecting intracellular cAMP changes. Application of synthetic PDF (10^{-5} M) and sNPF (10^{-5} M) did not alter cAMP levels, and neither did the co-application of the two peptides. The application point of the different substances is indicated by a black arrow. As a positive control, 10^{-5} M adenylate cyclase activator NKH was used, while hemolymph-like saline (HL3) was applied as negative control. *Middle:* Maximum inverse FRET changes quantified for each individual neuron and averaged for each treatment from 100 s until 1000 s. *Right*: Table shows the color code of the different treatments and the number of neurons (N_{cells}) in the dissected brains (N_{brain}) considered in this analysis. (B) *Left:* A close-up of the immediate cAMP level changes occurring from the application point until 200 s. Compared to the negative control HL3, none of the neuropeptide applications altered significantly cAMP levels. *Right:* Maximum inverse FRET changes in the case of each neuron from 100-200 s. Data are shown as mean ± SEM. Kruskal-Wallis test followed by Bonferroni-corrected Wilcoxon pairwise-comparisons. ***p<0.001, n.s. not significant.

Finally, we also performed calcium imaging in the IPCs to register possible changes of this second messenger. Even though earlier studies suggest that PDF primarily signals through cAMP and not by calcium (Hyun et al. 2005; Mertens et al. 2005; Duvall & Taghert 2012), we aimed at checking whether in the IPCs there could be another signaling pathway involved. Furthermore, we tested the possible effect of sNPF on intracellular Ca^{2+} levels. To do so, a genetically encoded calcium sensor was expressed specifically in the insulin producing cells under the control of *dilp2(p)*-Gal4 (*dilp2(p)*-Gal4>UAS-*GCamp3.0*) (Tian et al.

2009). First, PDF was added to freshly dissected fly brains and Ca^{2+} levels were continuously recorded.

In line with previous reports, we found that the application of PDF did not alter Ca^{2+} levels in the insulin producing cells, since no differences were observed from the negative control ($PDF_{(100\text{-}200\ s)}$ -10.6 ± 1.9% compared to $HL3_{(100\text{-}200\ s)}$ -9.1 ± 1.7%, n.s.) (*Figure 33*). However, sNPF induced a small but significant increase in Ca^{2+} concentration ($sNPF_{(100\text{-}200\ s)}$ 3.4 % ± 2.8%, *p<0.05), which was still detectable when neuronal conductivity was blocked by TTX, suggesting that this response is not mediated by interneurons but is due to the direct activation of the IPCs ($sNPF+TTX_{(100\text{-}200\ s)}$ 5.4 ± 3.5%, *p<0.05) (*Figure 33*).

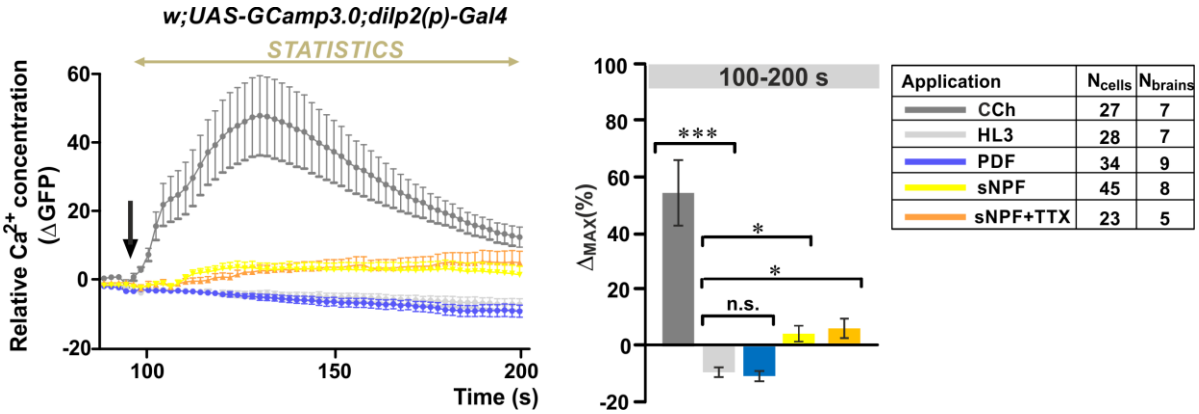

Figure 33. The neuropeptide sNPF induces a small increase in the intracellular Ca^{2+} level, while PDF has no effect. (A) *Left:* Average changes in GFP fluorescence of IPCs reflecting intracellular changes in Ca^{2+} levels. Substances were bath-applied to freshly dissected fly brains at ~100 s (indicated by a black arrow). The cholinergic agonist carbamylcholine (1 mM CCh) was used as positive control, which induced a robust increase in Ca^{2+}, indicating that the general procedure was working. As a negative control, hemolymph-like saline (HL3) was applied. Application of 10^{-5} M synthetic PDF peptide did not alter Ca^{2+} levels, while 10^{-5} M sNPF induced a small but significant increase in Ca^{2+} levels. This calcium response seems to be due to direct activation of the IPCs, since it was not blocked in the presence of the sodium channel blocker TTX (2µM). *Middle:* Maximum Ca^{2+} changes (%) for each individual neuron were calculated and averaged for each pharmacological treatment from 100 s until 200 s. Statistical comparison revealed significant increases in Ca^{2+} levels compared to the negative control (HL3) for CCh, sNPF and sNPF+TTX, while PDF had no effect. Data are presented as mean ± SEM. *Right:* Table shows the color code of the different treatments and the number of neurons (N_{cells}) in the dissected brains (N_{brain}) considered in this analysis. Kruskal-Wallis test followed by Bonferroni-corrected Wilcoxon pairwise-comparisons. ***p<0.001, *p<0.05, n.s. not significant.

4.11. A tight spatial relationship between PDF and sNPF processes in proximity of the IPCs and their axonal projection

After having seen that the co-application of sNPF and PDF evoked large cAMP increases in the insulin producing cells (*Figure 29A, B*), we investigated where these two neuropeptides might potentially contact each other in the brain. It is well known that the small ventrolateral neurons co-express PDF and sNPF (Johard et al. 2009). However, strong sNPF expression was reported also in the tritocerebral area (Nässel et al. 2008). Since PDF-Tri cells are also located in this brain region, we aimed at studying whether the tritocerebrum could also be a possible connection point of these peptides. For this purpose, adult brains were double-stained with antibodies against PDF and sNPF, and expression pattern of these two peptides was studied at low temperature (12^{O}C) after 11 days.

As it has already been reported, sNPF is widely expressed in the brain (Lee et al. 2004; Nässel et al. 2008). We found abundant expression in the tritocerebrum area (TC) as well as in the Kenyon cells of the mushroom bodies (MB), cells in the *Pars intercerbralis* (*PI*), and two sNPF fibers (F) from the *PI* towards the TC acrossing the median bundle (M) (*Figure 34B, C, D left panels*). High magnification confocal images revealed a tight spatial relation between sNPF fibers (F) and PDF-Tri branches that run to the *PI*, therefore this area can be a possible region were these two peptide might interact to regulate IPC activity (*Figure 34C, D*). Interestingly, PDF and sNPF processes in the tritocerebrum (*Figure 34E*) and the median bundle (*Figure 34F*) might also represent functional contacts between the two peptides.

However, it is noteworthy that the *PI* region contains the richest group of neurosecretory cells, among which many have a projection pattern similar to that of IPCs. For instance, *kurs58*-Gal4^{+} neurosecretory cells (entirely complementary cells to IPCs) in the *PI* have axonal projections acrossing the median bundle, reaching the tritocerebrum area (Cavanaugh et al. 2014). The DLP neurons, located in the *Pars lateralis*, also send axonal projections running into the median bundle towards the tritocerebrum (*Figure 17A*, Kapan et al. 2012). Therefore, the fact that sNPF and PDF signals were found close to each other in the *PI* region, in the median bundle, and in the tritocerebrum area points only to the possibility of their physical interaction. Further investigations need to be done to better understand this issue using additional approaches.

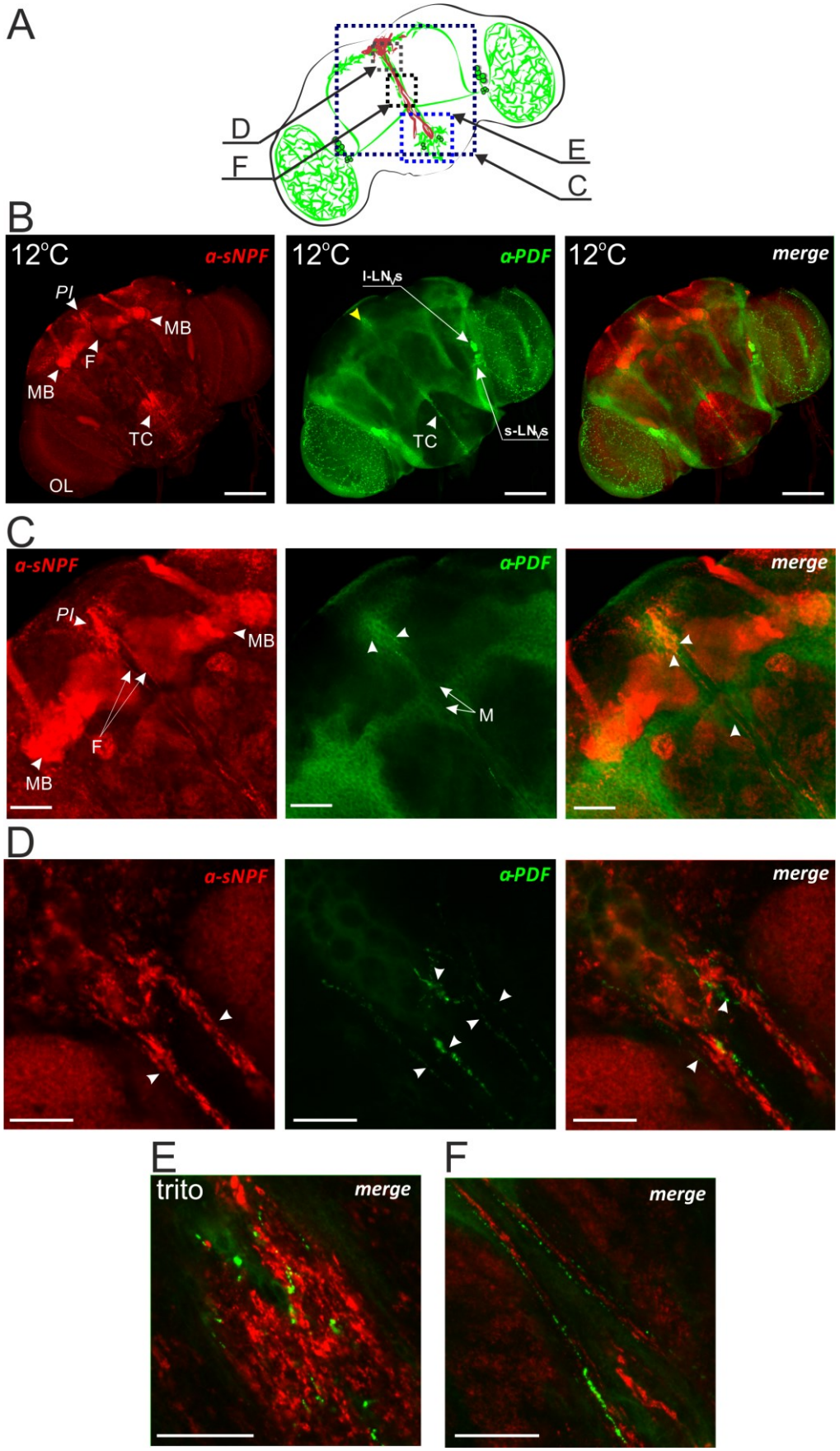

Figure 34. PDF-Tri processes in the PI, along the median bundle, and in the tritocerebrum are located very close to sNPF axon branches (See next page for legend.)

(A) Schematic figure indicating the location of IPCs (in red) and PDF^+ neurons (in green) in the adult fly brain. Dotted rectangles show the brain areas presented in the subsequent confocal images. (B) *Left:* Representative confocal image (single optic section) of the sNPF-expressing neurons (red). *PI* indicates the sNPF-expressing cells in the *Pars intercerebralis*. Two robust sNPF fibers (F) are running down from the *PI* to the tritocerebrum area (or *vice versa*). The tritocerebrum (TC) and mushroom bodies (MB) are strongly stained. OL = optic lobe. *Middle:* PDF-expressing cells (green) in the brain (single optic section). Processes of PDF-Tri neurons are still present in the cold in the TC, and their projections are visible also in the *PI* area (indicated by yellow arrowhead). s-LN_vs and l-LN_vs: small- and large ventrolateral neurons, respectively. *Right:* Merge of the red and green channels. Scale bar = 100 μM. (C) Higher magnification of the *PI* area and mushroom bodies (MB) (single optic section). *Left:* sNPF fibers (F) along the median bundle and in the *PI* region are intensively stained. *Middle:* Faint PDF staining in the *PI* region (indicated by white arrowheads) and in the median bundle (M). *Right:* Merge of the two channels showing the vicinity of PDF and sNPF fibers in the median bundle and in the *PI* region (indicated by white arrowheads). Scale bar = 50 μM (D). Magnified view of the *PI* (Z-stack of 3 single layers). *Left:* Parallel sNPF fibers running towards/from the *PI* (marked by white arrowheads). *Middle:* PDF staining showing the processes of PDF-Tri neurons in the *PI* (white arrowheads). *Right:* Merge of sNPF and PDF channels showing the tight spatial relations between axon branches of sNPF- and PDF-producing neurons in the protocerebrum (indicated by white arrowheads). Scale bar = 20 μM. (E) Higher magnification of the tritocerebral area indicating the vicinity of PDF and sNPF processes in this brain region (single optic section). Scale bar = 20 μM. (F) Magnified view of the sNPF and PDF-Tri fibers in the median bundle shows their tight spatial localization. Scale bar = 20 μM. Flies were reared at 18°C in LD 8:16 prior to being placed at 12°C for 11 days.

4.12. Simulation of natural-like light-dark profiles induces photoperiodic diapause in the flies

In the laboratory, experimental animals are kept in an artificial environment that can be considered only a very rough approximation of the outdoor conditions. Most commonly constant temperature and simple light on/off cycles are adopted to keep flies in the lab. Knowing that the circadian clock in flies has been found to exhibit unexpected changes in the wild compared to what is seen in the lab (Vanin et al. 2012; Menegazzi et al. 2013), it would be crucial to adopt more natural-like conditions similar to those experienced by flies in nature.

It is generally thought that, the temperature effect takes precedence over photoperiodic effect in the regulation of fruit fly's diapause response (Saunders et al. 1989; Saunders 1990; Emerson et al. 2009a). However, to further dissect this issue, we set up an experiment to study diapause under generated semi-natural photoperiods (*See in details in Materials and Methods, page 53*). Briefly, these profiles simulate light conditions of short, late autumnal days and summer days, with continuously changing light intensity throughout the days, considering also natural light composition. The corresponding control flies were kept under the commonly used rectangular profiles (LD 8:16 and LD 15:9, respectively).

Importantly, the overall amount of light received by flies was the same when using semi-natural and rectangular profiles.

The diapause response of four different *Drosophila melanogaster* field lines (*Hu-S*, *Hu-LS*, *WTALA-S*, and *WTALA-LS*) was tested using the new light profiles during the 11 days of diapause induction. Flies were developed at 23^{o}C in LD 12:12 prior to being placed under diapause-promoting conditions (PROTOCOL 1). We found that subjecting flies to semi-natural late autumnal days induced a higher proportion of females to enter the dormant state compared to the corresponding control flies kept in rectangular LD 8:16 cycles (*Figure 35A*). ANOVA revealed significant effect for light profile ($F_{(1,140)}$ = 31.7262, ***p<0.001), highlighting that using the new protocol the flies entered diapause at consistently higher percentages. We additionally found a significant *timeless*-influence on the incidence of diapause (ANOVA $F_{(1,140)}$ = 168.6957, ***p<0.001), confirming significantly higher levels of dormancy in the case of *Hu-LS* and *WTALA-LS* females, both carry the *ls-timeless* isoform. The effect of *timeless* was present independently from the type of the light profile used (no significant *timeless* x light profile interaction was found; $F_{(1,140)}$ = 0.9907, p = 0.3213, n.s.). This result is in line with our previous data that reported significant *timeless*-effect on diapause levels (*Figure 21A, B*), and corroborates the results obtained by Tauber et al. (2007).

Interestingly, flies exposed to semi-natural summer days were more rapid to exit from diapause compared to females kept in long rectangular LD cycles (*Figure 35B*). ANOVA showed significant effect for light profile ($F_{(1,120)}$ = 62.7602, ***p<0.001), meaning that all the lines kept in more natural-like summer days exhibited persistently lower diapause percentages compared to their control. A significant modulatory effect for *timeless* was also observed ($F_{(1,120)}$ = 155.7563, ***p<0.001), since a higher percentage of flies entered diapause in *ls-timeless* background. The diapause-promoting effect of *ls-timeless* was independent from the adopted light profile (no significant *timeless* x light profile interaction was revealed; $F_{(1,120)}$ = 1.3004, p = 0.2564, n.s.).

Intriguingly, when comparing rectangular conditions between summer and late autumnal days, ANOVA did not show significant effect for season on the diapause levels ($F_{(1,126)}$ = 0.1277, n.s.). Indeed, approximately the same percentage of females entered diapause in the two different seasons, suggesting that *Drosophila melanogaster* does not exhibit a photoperiodic diapause when exposed to these simplified light conditions.

However, when semi-natural profiles were used to better mimic natural environment, a significant season effect was revealed by ANOVA ($F_{(1,138)}$ = 81.294, ***p<0.001), suggesting

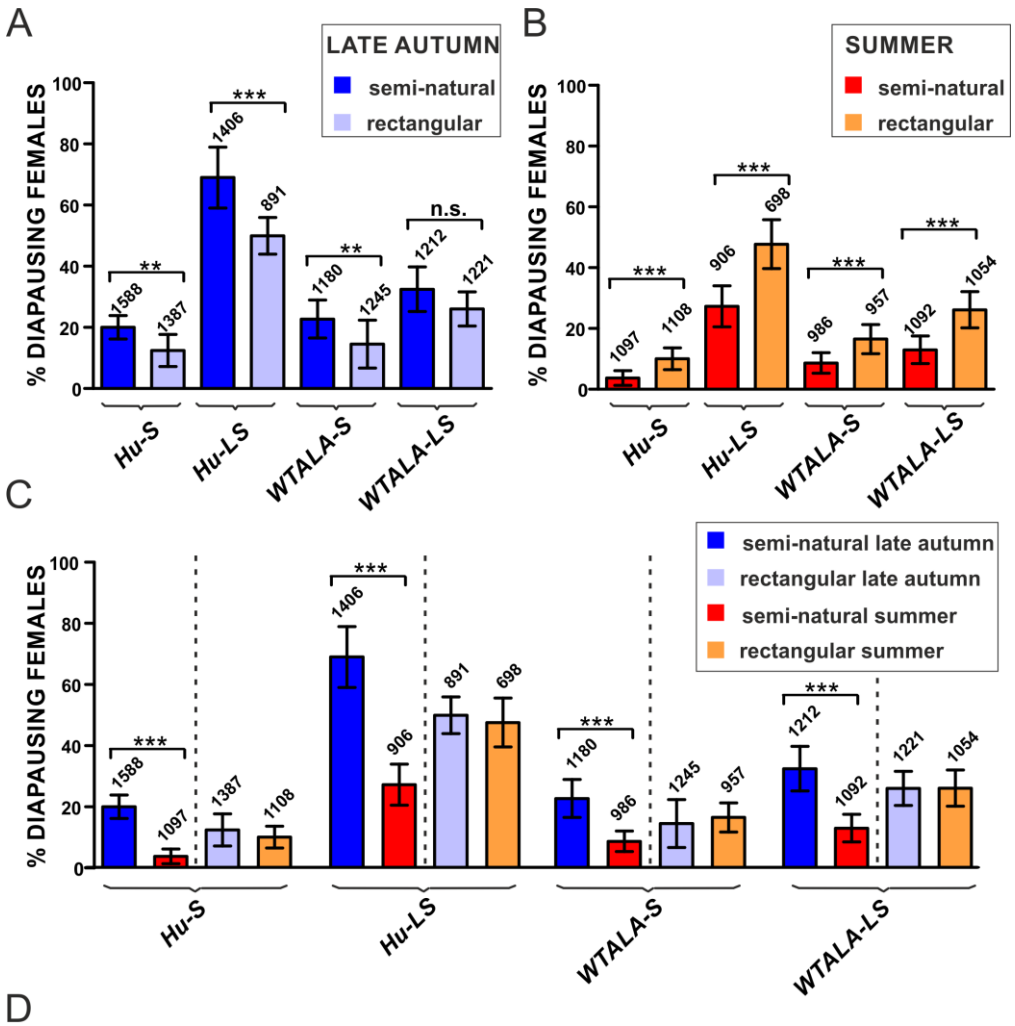

Protocol		Genotype			
		Hu-S	*Hu-LS*	*WTALA-S*	*WTALA-LS*
semi-natural	*late autumn*	20.1 ± 3.8	69.0 ± 9.8	22.7 ± 6.2	32.5 ± 7.3
	summer	3.7 ± 2.4	27.3 ± 6.8	8.7 ± 3.4	13.0 ± 4.5
retangular	*late autumn*	12.5 ± 5.3	50.0 ± 6.0	14.6 ± 7.8	26.1 ± 5.1
	summer	10.1 ± 3.6	47.7 ± 8.0	16.5 ± 4.8	26.2 ± 6.0

Figure 35. Semi-natural light profiles largely affect the incidence of diapause in Drosophila field lines. (A) Simulation of consecutive late autumnal days induced a higher proportion of females to enter diapause (dark blue bars) compared to controls kept in short rectangular LD cycles (LD 8:16; light blue bars). (B) Generation of summer light conditions promoted diapause response in a significantly smaller proportion of females (red bars) compared to controls subjected to long rectangular LD cycles (LD 15:9; orange bars). (C) Photoperiodic diapause appeared when semi-natural light profiles were used, highlighting significantly higher levels of diapause during late autumnal days. When flies were exposed to rectangular LD cycles, diapause levels did not differ when long and short days were compared. (D) Summary of diapause results. The table presents the mean of diapause incidence ± SD (%) under the different conditions. In graphs (A), (B), (C), numbers above each column indicate the number of dissected females, and data are shown as mean ± SD. ANOVA after arcsine transformation, followed by post-hoc Tukey HSD test. ***p<0.001, **p<0.01, *p<0.05, n.s. not significant.

that using more sophisticated light profiles photoperiodism appears, and a significantly higher proportion of flies enters dormancy during late autumnal days than in summer days.

5. DISCUSSION

5.1. PDF$^+$ neurons modulate the diapause response of the flies

Neuroanatomical studies revealed the involvement of PDF-positive neurons in the regulation of photoperiodic diapause in several insect species (Shiga & Numata 2009; Yasuyama et al. 2015; Meuti et al. 2015). In the brain, the ventrolateral neurons express the circadian clock-associated gene *Pdf*, and have been found to be crucial for the generation of circadian rhythms (Renn et al. 1999). These cells send axonal projections to the dorsal brain, near the *Pars lateralis* and *Pars intercerebralis* regions, which play a crucial role in the regulation of hormonal processes that determine diapause. Even though the center of the endocrine system for dormancy control is believed to be in the *PI*, the neurosecretory cells located in this brain area do not own a circadian clock, therefore they are thought to receive timing information from other cells to control diapause response (Jaramillo et al. 2004; Foltenyi et al. 2007; Allada & Chung 2010; Cavanaugh et al. 2014; Barber et al. 2016). In *Drosophila melanogaster*, insulin producing cells in the *PI* have been identified as key regulators of dormancy (Kubrak et al. 2014; Schiesari et al. 2016), however it is unclear how their activity is regulated to exert their effect on this seasonal response. A synaptic connection between IPCs and DN1 clock cells has recently been reported, suggesting that these neurons in the *PI* get timing information from the DN1 neurons (Barber et al. 2016). Since the ventrolateral neurons were found to have a synaptic connection to the DN1 clock cells (Cavanaugh et al. 2014), the timing information towards the IPCs can originate from the main pacemaker neurons in an indirect way. Here we show that genetic manipulation of PDF-producing neurons in *Drosophila melanogaster* influences the diapause response of the flies. Moreover, this modulation is probably exerted via their neuropeptides, pigment dispersing factor (PDF) and short neuropeptide F (sNPF) (for summary, see *Table 6*).

Accumulating evidence suggests the involvement of PDF in the regulation of diapause in several species, however it apparently plays different roles. Here we found that, using the diapause protocol after Saunders et al. 1989, overexpression of PDF in the PDF$^+$ neurons enhances ovarian development in the flies, leading to significantly reduced diapause levels. In the blow fly, *Protophormia terraenovae*, ablation of PDF-immunoreactive neurons (PDF-ir), equivalent to the LN_vs in *Drosophila melanogaster*, disrupts not only the circadian activity rhythms but also the photoperiodic diapause response, highlighting the

involvement of these cells in the regulation of dormancy (Shiga & Numata 2009). Moreover, *PI* neurons of the blow fly were found to receive synaptic contacts from PDF-immunoreactive fibers (Yasuyama et al. 2015). In the northern house mosquito, *Culex pipiens,* targeted RNAi against *Pdf* resulted in females that, under diapause-averting conditions, accumulated greater lipid stores and were not able to develop their ovaries (Meuti et al. 2015). In the bean bug, *Riptortus pedestris*, targeted *Pdf-RNAi* did not affect diapause response (Ikeno et al. 2014). Interestingly, in the silk worm *Bombyx mori*, a novel function of PDF has recently been reported. It was found to stimulate the biosynthesis of the key insect hormone ecdysone in the prothoracic glands in a specific larval stage, thereby playing an important role in the timing of ecdysone production (Iga et al. 2014). It is possible that a similar regulation works also in other insects.

Another neuropeptide produced in the ventrolateral neurons, sNPF, was also found to affect diapause response (summarized in *Table 6*). Pan-neuronal overexpression of this peptide resulted in a marked reduction of diapause levels in the flies. Overexpression of sNPF specifically in the PDF^{+}-neurons was able to phenocopy this effect, suggesting that sNPF in these cells play a crucial role in diapause regulation. Accordingly, we found that disruption of sNPF signaling in the IPCs induced a higher proportion of females to enter the dormant state, further supporting the role of this signaling pathway in modulating diapause. Interestingly, this peptide has already been reported to affect ovarian development and dormancy in other organisms. In locusts, sNPF was documented to have a gonadotropic action, stimulating ovarian growth (Cerstiaens et al. 1999; Schoofs et al. 2001). In the red imported fire ant, *Solenopsis invicta,* sNPFR expression was found on the ovaries, suggesting that sNPF signaling may regulate processes at the oocyte pole (Lu & Pietrantonio 2011). Furthermore, sNPF was suggested to function as a potential diapause-regulating neuropeptide in the Colorado potato beetle, *Leptinotarsa decemlineata.* Analysis of the extract of head ganglia and retrocerebral complexes revealed that the sNPF-related peptides (Led-NPF-I and -II) were absent in the extract of diapausing animals, indicating their involvement in the regulation of adult diapause in this species (Huybrechts et al. 2004). In line with this finding, also other studies documented the growth-promoting effect of sNPF. For instance, sNPF was found to enhance the transcription of different *dilp* transcripts by acting on its receptor on the IPCs, thereby promoting growth (Lee et al. 2008).

Table 6. Summary of the effects of PDF and sNPF on diapause incidence

	Pdf-Gal4[(1)]	*R6*-Gal4[(2)]	*gal1118*[(3)]	*Elav*-Gal4[(4)]	*Insp3*-Gal4[(5)]	*Mutants*
Enhancing PDF-signaling						
UAS-*Pdf*	↓	-	↓	-		
Enhancing sNPF-signaling						
UAS-*2xsNPF*	↓	↓	-	↓		
Enhancing PDF and sNPF-signaling						
UAS-*Na$^+$ChBac*	↓	-	↓	-		
Reducing PDF signaling						
Pdf^0 mutant						↑↓*
PdfR mutant (*han*)						↓
Reducing sNPF signaling						
UAS-*sNPFR1-DN* (expression of a dominant negative receptor)					↑	
Reducing PDF- and sNPF-signaling						
UAS-hid (*ablation*)	↑	-	-	-		
UAS-Ork (*silencing*)	↑	-	**No effect**	-		

[(1)]Expressed in the s-LN$_v$s, l-LN$_v$s, PDF-Tri and PDF-Ab

[(2)]Expressed in the s-LN$_v$s

[(3)]Expressed in the s-LN$_v$s, l-LN$_v$s, some LN$_d$s, several cells in the *PI* and dorsal brain, few cells near the mushroom bodies and in the medulla

[(4)]Pan-neuronal distribution

[(5)]Expressed in the brain IPCs

↓↑ Changes in diapause levels using PROTOCOL 1. (development at 23°C in LD 12:12)

↓ Changes in diapause levels using PROTOCOL 2. (development at 18°C in LD 8:16)

* Depends on *tim* (*s*/*ls*) background and age

We found that hypersensitization of PDF$^+$ neurons by the overexpression of a bacterial sodium channel leads to significantly lower diapause levels, while genetic ablation of these cells results in the opposite phenotype (*Table 6*). When these cells were ablated in the clearly photoperiodic fly *P. terraenovae*, flies no longer discriminated photoperiod, and exhibited a diapause incidence of 48% in diapause-averting long days (LD 18:6), and 55% in dormancy-inducing short day conditions (LD 12:12) (Shiga and Numata 2009). Thus, the ablation apparently induced diapause response in flies which were not supposed to be diapausing. In contrast, ablation of the brain region containing PDF-medulla neurons in the bug *R. pedestris* induced ovarian development even under diapause-promoting short-days. Thus, our results seem to be more similar to those obtained in *P. terraenovae*, since in the flies the ablation provoked a higher proportion of females to enter diapause. However,

there appear to be marked species-specific differences in the role of these cells in modulating the photoperiodic response. Importantly, as found in *Drosophila melanogaster*, other neuropeptides and neurotransmitters can also colocalize in these cells (Johard et al. 2009); therefore with the genetic ablation not only PDF but also other factors are removed, thereby making the interpretation of the results even more difficult. In addition, one needs to consider that, with the ablation of the PDF-medulla (PDF-Me) neurons the key circadian clock center is erased, which can also affect the diapause response of the flies. Indeed, an increasing number of studies suggests the involvement of circadian clock genes in the regulation of diapause in several insects: *D. melanogaster* (Tauber et al. 2007; Sandrelli et al. 2007), *R. pedestris* (Ikeno et al. 2010, Ikeno et al. 2011a, Ikeno et al. 2011b, Ikeno et al. 2013), *C. pipiens* (Meuti et al. 2015), *C. costata* (Pavelka et al. 2003), as well as in *S. bullata* (Goto et al. 2006).

When studying the diapause response of *Pdf* null mutant (Pdf^{01}), two different strains were used, bearing either *s- or ls-tim* variant in their genome (*Hu-S* Pdf^{01} *and Hu-LS* Pdf^{01}*,* respectively). The reasoning behind this was to see whether the diapause-promoting effect of *ls-tim* (Tauber et al. 2007) can be somehow related to PDF. LS-TIM is believed to attenuate the photosensitivity of the circadian clock due to its weaker interaction with the circadian photoreceptor CRYPTOCHROME (CRY) (Tauber et al. 2007; Sandrelli et al. 2007). In the northern latitudes, where lengthening days often couple to very low temperatures, possessing an attenuated circadian photosensitivity can be advantageous, allowing flies to enter diapause more readily (Sandrelli et al. 2007).

After 11 days spent in diapause-inducing conditions, a slight but statistically significant increase was found in the percentage of diapausing females in the mutants (*Table 6*). This corroborates the data found in the case of the overexpression of PDF peptide in the PDF^{+} neurons. However, this change in the *Pdf* null mutant was only observed in *s-tim* background, whilst *Pdf* mutation did not alter diapause levels in flies bearing the *ls-tim* variant. Therefore, the effect of PDF is apparently different depending on the *tim* isoform. Our data suggests that *ls-tim* effect is irrespective of PDF: *ls-tim* flies showed consistently higher levels of diapause even when PDF was absent. A possible interaction between different *timeless* isoforms and PDF has not yet been investigated. However, it was found that *tim* mRNA cycling dampens in the clock neurons of Pdf^{01} mutants under DD (Peng et al. 2003), and the loss of PDF reduces TIM levels in PDF-negative clock neurons. A decrease of -

50% was found in the LN_ds and in DN1 neurons (Seluzicki et al. 2014). Another interesting issue to be considered is that *timeless* mRNA splicing has been shown to be under temperature modulation (Boothroyd et al. 2007; Montelli et al. 2015). The $tim^{unspliced}$ isoform, which is 33 amino acid shorter than the full-length $tim^{spliced}$ variant due to a premature STOP codon, is more prevalent under cold temperatures (Boothroyd et al. 2007). This spicing event may serve as a posttranscriptional mechanism involved in seasonal adaptation (Montelli et al. 2015). Different *tim* splicing variants show different levels of interactions with the circadian photoreceptor CRY. The unspliced *tim* form has a higher affinity for CRY, independently from its association with S-TIM or L-TIM (Montelli et al. 2015).

When testing a new diapause protocol by raising flies at a lower temperature and short days from the beginning of their development (18^{o}C, LD 8:16, PROTOCOL 2), we surprisingly found that in *s-tim* flies the effect of PDF turned out to be the opposite: in the absence of the peptide diapause levels were significantly lower compared to those in the control (*Table 6*). Nevertheless, the lack of PDF did not cause any observable change in the diapause response of *ls-tim* flies. In general, the new diapause protocol induced higher dormancy levels in the lines, most probably due to the different rearing conditions experienced by flies before adulthood. It suggests that maintaining flies at lower temperatures during their development induces a higher proportion of females to enter diapause, likely as a result of a better simulation of what is going on in nature approaching harsh seasons. Importantly, *timeless*-effect on diapause still remained significant, highlighting its robust influence.

As the reverse effect of PDF, observed in case of *Hu-S* flies when using PROTOCOL 2, was unexpected, flies were dissected also after 30 days to see how diapause levels change over time. After this period of time, the action of PDF seemed to be consistent with that observed after 11 days. Additionally, a more robust difference appeared in *ls-tim* background: the majority of *Hu-LS* females were still in diapause, when the corresponding control females were outside dormancy. This may suggest a possible role for PDF in keeping *ls-tim* flies in diapause for long time. In line with this, we found that in PDF receptor mutant (*han*) flies diapause levels are significantly lower compared to controls, both after 11 and 30 days.

Therefore, the question arises concerning how the same neuropeptide can mediate two paradoxical biological functions? Interestingly, PDF has already been suggested to act contradictorily in different parts of the brain. The period of the behavioral rhythms was found to be lengthened when increasing amount of PDF was present in the accessory medulla, whilst higher PDF levels in the dorsal part of the brain correlated with shorter periods (Wülbeck et al. 2008; Yoshii et al. 2009). Thus, it seems that PDF is able to both accelerate and slow down some target clocks. The authors reasoned that the PDF-evoked cAMP increases in PDF receptor expressing cells do not necessarily result in the same cellular responses. The clock cells may express different pools of enzymes, including kinases and phosphatases that might change the phosphorylation of the target proteins in different ways (Yoshii et al. 2009). In our case, considering the heterogeneity of the individual IPCs (Jaramillo et al. 2004; Söderberg et al. 2012; Barber et al. 2016), it is also possible that these kinds of differences exist among the 14 IPCs. Another important issue to be considered is that the l-LN_vs express the *dimmed* gene that results in C-terminally amidated PDF, while the s-LN_vs express non-amidated peptide (Park et al. 2008). The amidated PDF has been shown to be much more active and has a longer half-time compared to the non-amidated form (Park et al. 2008). The ratio between amidated and non-amidated neuropeptide might display temperature-dependent changes, and their relative proportion possibly acts modulating biological processes.

5.2. Temperature-dependent changes in PDF expression

To our knowledge, patterns of PDF at different temperatures have not yet been investigated in earlier studies. Since this project aims to unravel the role of this peptide in the overwintering behavior of the flies, its expression was examined under different thermal conditions. In the brain of *D. melanogaster*, apart from 16 PDF^+ ventrolateral clock neurons, PDF expression was reported also in 2-4 developmentally-transient neurons in the tritocerebrum, defined as PDF-Tri (Helfrich-Förster 1997). PDF-Tri branches form a network surrounding the ventral and lateral part of the esophageal foramen, and have dorsal projections into the median bundle reaching the *Pars intercerebralis*, where their processes apparently terminate. These cells were reported to undergo apoptosis in early adult life, therefore after adult day 1-2 they are no longer detectable (Helfrich-Förster 1997; Renn et

al. 1999). Those observations have been made in flies raised at about 23-25^{o}C. Co-expression of the apoptotic gene *reaper* (*rpr*) and the anti-apoptotic gene *p35* leads to a defect in the apoptotic program, resulting in the persistence of these neurons up to adult day 10 (Renn et al. 1999).

We surprisingly observed the persistence of PDF-Tri cells and their projections both at 12^{o}C and 18^{o}C during adult life. PDF-Tri immunostaining was strongly reduced or completely disappeared at higher temperature (23^{o}C), corroborating the findings of earlier studies that documented their disappearance in young adults (Helfrich-Förster 1997; Renn et al. 1999). Based on our confocal images, PDF-Tri projections in the median bundle and in the *PI* are located in the near proximity of insulin producing cells and their axonal projection. Interestingly, the prolonged persistence of PDF-Tri neurons was observed in the *Drosophila* model of fragile X syndrome (FXS), which is a heritable genetic disorder causing intellectual disability in humans (Gatto & Broadie 2011). It was found that *dfmr1* null mutant (characterized by the complete loss of *fragile X mental retardation* gene), are unable to initiate normal programmed cell death, resulting in the long-term persistence of PDF-Tri neurons (Gatto & Broadie 2011). It is generally thought that the disappearance of these neurons indicates their potential role only in a specific time interval. Even though not proved experimentally, they have been suggested to have an eclosion-related role (Helfrich-Förster 1997). However, we observed that in the cold these cells and their arborizations persist for long during adulthood, raising the possibility of their involvement in cold-related functions. According to our present knowledge, PDF-Tri cells do not function as clock neurons in the circadian circuit. They do not express the clock protein PER (Gatto & Broadie 2011), and the circadian rhythm of locomotor activity is not altered by their aberrant retention in flies (Renn et al. 1999).

As far as we can tell, there is no driver line available that could be used for targeted gene expression exclusively in the PDF-Tri neurons. Thus, a GAL4 enhancer trap, *gal1118* was adopted which primarily targets the PDF-expressing neurons but not the PDF-Tri cells (Blanchardon et al. 2001). However, *gal1118* is not only expressed in the ventrolateral clock neurons but also in the lateral dorsal clock neurons (LN_dS), the medulla, the *PI*, a few cells located near the mushroom body, as well as in neurons in the dorsal fly brain including a subgroup of DN1 and possibly DN2 clock neurons. The hypersensitization of *gal1118*-expressing cells resulted in significantly reduced diapause levels, thereby producing a

phenotype similar to that observed in the case of hypersensitization of *Pdf*-Gal4-expressing cells (*Table 6*). Significantly reduced diapause levels were also found when *gal1118*-specific overexpression of PDF was tested, corroborating the result obtained by *Pdf*-Gal4-driven overexpression of the same transgene (*Table 6*). These data further confirm the diapause-antagonist effect of PDF under this experimental condition. Interestingly, expression of the hyperpolarizing K-channel Ork provided different results depending on whether it was regulated by *Pdf*-Gal4 or *gal1118* driver: while under the control of *Pdf-Gal4* it led to higher incidence of diapause, it did not cause an observable difference from the control group when *gal1118* driver was used (for summary, see *Table 6*). Thus, the unchanged diapause levels could be explained as a resultant of two opposing effects: (1) a diapause-promoting influence caused by the inhibited PDF release from the LN_vs, and (2) the diapause-reducing effect of PDF released from the tritocerebrum cells. However, as mentioned before, we have to consider that the expression pattern of *Pdf*-Gal4 and *gal1118* does not only differ in the tritocerebrum region, but also in some other brain areas (Blanchardon et al. 2001). It would be interesting to perform these manipulations also using the new diapause protocol (PROTOCOL 2), knowing that the effect of PDF on diapause seems to be different when flies are subjected to 18^{o}C and short days prior to being placed under diapause-inducing conditions. In addition, the longer persistence of PDF-Tri neurons in the cold and the fact that the more diapausing line *Hu-LS* is characterized by higher PDF-Tri immunostaining, would rather suggest a possible role for these cells to promote diapause. Further investigations will need to be done to dissect this issue.

We additionally observed that the temperature at which the flies develop prior to being exposed to 12^{o}C, apparently affects the abundance of PDF in the tritocerebrum. This hypothesis is based on the fact that, the reduction of PDF staining in *Hu-S* flies between 12^{o}C and 23^{o}C was ~60% when PROTOCOL 1 was used (development at 23^{o}C in LD 12:12), but only a drop of 22% under PROTOCOL 2 (development at 18^{o}C in LD 8:16). This suggests that developing flies at 18^{o}C probably led to stronger PDF expression in the tritocerebrum, which then at 23^{o}C could not disappear in 11 days. When comparing PDF-Tri patterns in the differently diapausing *Hu-S* and *Hu-LS* lines, the more-diapausing *Hu-LS* strain was found to have higher PDF levels in the tritocerebrum. Even though signal levels were largely reduced at warmer temperature (23^{o}C) in the *Hu-LS* line, in *Hu*-S flies the reduction was not even significant. Additionally, we found higher PDF immunoreactivity along the DILP axon and

near the somata of the IPCs in *Hu-LS* flies, and this difference between the two strains holds true also after 30 days. Surprisingly, *Hu-LS* females seem to have high level of PDF in this brain region also at room temperature. Therefore, it is difficult to tell whether the abundant PDF expression along the IPCs and their axonal projection can be related to diapause induction.

Apart from the large temperature-dependent changes in PDF-Tri, expression of PDF seems to be highly influenced by temperature also in other brain regions. We found that, irrespective of the experimental protocol used, PDF immunoreactivity was consistently higher in the somata of the large ventrolateral neurons at higher temperature, possibly indicating accumulation of PDF combined with little release from the terminals. Knowing that the l-LN$_v$s project tangentially in the distal medulla of the optic lobe and contra-laterally in the posterior optic tract (Helfrich-Förster 1997), PDF may be more abundant in these areas at 12^{o}C than at 23^{o}C. However, relying only on immunocytochemical data it is difficult to conclude about neuropeptide release. In addition, we do not know whether PDF from the l-LN$_v$s can influence IPC activity, although based on their anatomical location and their projection pattern, s-LN$_v$s or PDF-Tri seem more suited for this role. However, the l-LN$_v$s and s-LN$_v$s are closely located, and believed to communicate with each other via their arborizations. The small cells are known to express functional PDF autoreceptors (Shafer et al. 2008), thereby can regulate the amount of the secreted and/or released PDF peptide. Indeed, it was found that PDF released from the large cells activates PDF receptor on the s-LN$_v$s (Schlichting et al. 2016). Using a genetically encoded cAMP sensor, the PDF-induced cAMP response of the s-LN$_v$s was found to be dependent on the peptide concentration (Shafer et al. 2008). Thus, it is probable that the higher PDF immunostaining, found in the somata of the large cells at 23^{o}C in our experiments, is sensed also by the s-LN$_v$s and might affect their function.

PDF immunostaining in the axon termini of s-LN$_v$s in the dorsal protocerebrum is known to display rhythmic changes during the day, strongly suggesting rhythmic PDF release (Park et al. 2000; Fernández et al. 2008). Since the staining reaches a maximum in the early hours after light-on (Park et al. 2000), our samples were harvested at ZT1 time point (1 hour after light-on). Interestingly, in this brain region the results highlighted large protocol-dependent differences. Under the old protocol, PDF levels were significantly higher at 12^{o}C than at 23^{o}C. This might suggest enhanced PDF release in the dorsal brain under these

experimental conditions. In *Hu-S* flies, tested in both conditions, this marked difference was completely abolished when the new experimental protocol was used. Since only the rearing temperature and photoperiod are different between the two protocols, these parameters are likely to be responsible for this effect. It is difficult to understand whether the lack of this abundant PDF signal at 12^{o}C can be related to the increased diapause levels observed in *Hu-S* females when the diapause protocol was changed. In the higher-diapause line *Hu-LS*, PDF immunostaining in this brain area was found to be equal to that in *Hu-S* flies. However, this level is strongly reduced compared to that in *Hu-LS* at 23^{o}C. This finding suggests that from the s-LN$_v$s projection there may be less PDF signal released in the cold than at 23^{o}C. When studying PDF expression in this brain region after 30 days, the biggest change observed was the disappearance of the marked difference between *Hu-S* and *Hu-LS* flies at 23^{o}C, since in *Hu-S* flies PDF immunostaining intensity increased compared to that detected after 11 days.

The overall results obtained in *Hu-S* flies under the two different experimental protocols (PROTOCOL 1 and 2), we can conclude that diapause increased when the flies were developed at 18^{o}C (from 7% to 24%). Marked changes have been observed in PDF immunostaining in the different brain areas due to the switch between the protocols. While in the l-LN$_v$s no significant differences have been found (for both, the staining was higher at 23^{o}C than at 12^{o}C), indirect data suggest that PDF is more abundant in the tritocerebrum when flies are reared at 18^{o}C. In addition, while in the dorsal fly brain, the projection from s-LN$_v$s was significantly more stained at cold temperature compared to that 23^{o}C, this difference was no longer present when the new experimental protocol was used. When comparing the two differently diapausing *Hu-S* and *Hu-LS* strains, significantly higher PDF signals were found in the *LS*-line in the tritocerebrum, along the DILP axon and near the somata of the IPCs, highlighting a possible role for these cells in keeping flies in diapause. However, this issue will need to be further confirmed by studying other lines.

5.3. Temperature-dependent changes in the IPCs

Adopting the CaLexA system to label active neurons in the nervous system, we found that IPCs got activated by cold temperature. At 12^{o}C, higher level of activity-dependent GFP accumulation was detected in the somata of the IPCs and along their axonal projection in

every brain sample tested. In contrast, in females at room temperature, only very weak GFP expression was observed in the IPCs. This result was unexpected, since insulin-like signaling is known to be downregulated when flies enter diapause at low temperature (Kimura et al. 1997; Allen et al. 2007; Sim & Denlinger 2008; Kubrak et al. 2014; Schiesari et al. 2016). Therefore, it is unlikely that these cells are active because of the production of growth-promoting DILPs. Interestingly, these neurosecretory cells have been reported to be directly innervated by cold-sensing neurons (Li & Gong 2015). A temperature shift from 25^{o}C to 18^{o}C was found to trigger their activation, through which they promote the transcription of insulin-like peptide genes (*dilp2*, *dilp3*, *dilp5*) as well as the secretion of DILP2 protein. This mechanism is thought to be responsible for the larger body size reached by flies at lower temperatures (Li & Gong 2015). However, the activation of the IPCs at 12^{o}C is more probably due to different biological processes occurring in these cells when flies are exposed to cold. For a long time it was believed that expression of *dilp2*, *-3*, and *-5* but not *dilp1* is detected in the adult IPCs (Rulifson et al. 2002; Broughton et al. 2005). However, a recent study revealed the unexpected, long-lasting expression of DILP1 during non-feeding stages and reproductive dormancy (Liu et al. 2016). Though its role in ovarian development is not yet known.

Another explanation for the activation of the IPC at 12^{o}C can be related to the paradoxical upregulation of *dilp2, -3* and *-5* transcripts, observed in diapausing flies (Kubrak et al. 2014; Schiesari et al. 2016). Thus, it is possible that the upregulated *dilp* transcripts are also translated into peptides, however for some reason, the produced DILPs are either retained in the cell bodies, or after being released into the hemolymph their activity is inhibited by being bound to different proteins (Arquier et al. 2008; Honegger et al. 2008; Okamoto et al. 2013). Similarly to mammals, there are insulin binding proteins also in *Drosophila* (Arquier et al. 2008; Honegger et al. 2008). For instance, the protein Imaginal morphogenesis protein-Late 2 (Imp-L2) functions as an inhibitory cofactor of DILPs, since it is able to bind to DILP2 and DILP5, thereby modifying the insuling-like signaling pathway by repressing the binding of these peptides to their receptor (Arquier et al. 2008; Honegger et al. 2008). Another functional insulin binding protein, called secreted decoy of InR (SDR), was also identified in *Drosophila* that binds to different insulin-like peptides and alters insulin-like signaling during development (Okamoto et al. 2013).

When temperature-dependent DILP2 changes were studied in the cell bodies of the IPCs in flies developed at 23°C, DILP2 intensity was the highest at 23°C, while lowest at 18°C. Surprisingly, DILP2 levels were higher at 12°C compared to those at 18°C. This can be related to the fact that, as mentioned above, *dilp* genes in the IPCs (including *dilp2*) were found to be contradictorily upregulated during diapause (Kubrak et al. 2014; Schiesari et al. 2016). This upregulation is difficult to explain, it could be due to a possible communication between the ovary and IPCs via an unknown factor, that can signal to the IPCs when ovarian growth is limited, inducing a mechanism for the activation of *dilp* transcription. If we suppose that this enhanced *dilp2* transcription is followed by DILP translation, it can cause the increased DILP2 levels observed at 12°C. When DILP2 immunostaining was analyzed in the axonal projection, the two studied lines provided different results: while the staining in *Hu-S* flies displayed a temperature-dependent increase, in *Canton-S* flies there were no significant changes at the three different temperatures. This can also suggest that downregulation of insulin-like signaling is downstream of DILPs ligand in the insulin-like signaling cascade. As previously mentioned, different insulin binding proteins can regulate the amount of DILPs that potentially target the insulin receptor, thereby modifying the insulin signaling cascade. Their actions could explain why DILP2 immunostaining did not exhibit marked changes in the IPC axon in *Canton-S* flies at different temperatures. Their importance is shown by the fact that overexpression of *Imp-L2* in neuroendocrine cells induces ~100% of the females to enter diapause by inhibiting DILPs in the hemolymph (Schiesari et al. 2016). In addition, increased levels of Imp-L2 were reported to bring about up-regulated *dilp2*, *-3* and -5 transcripts (Alic et al. 2011), similar to that observed in diapausing females (Kubrak et al. 2014; Schiesari et al. 2016).

5.4. Neuronal connection between PDF-positive neurons and IPCs

Being key regulators of essential biological processes like development, growth, metabolic homeostasis, reproduction, and stress resistance, IPCs are known to express many receptors for different peptide hormones, neuropeptides and neurotransmitters (Lee et al. 2008; Enell et al. 2010; Crocker et al. 2010; Birse et al. 2011; Bai et al. 2012; Kapan et al. 2012; Luo et al. 2012; Rajan & Perrimon 2012; Kwak et al. 2013; Luo et al. 2014; Hentze et al. 2015; Alfa et al. 2015; Sano et al. 2015). However, PDFR expression has not yet been

suggested on these neurosecretory cells. Interestingly, earlier study by Lear et al. (2005) reported prominent *pdfr* expression in the *Pars intercerebralis* region using fluorescent *in situ* hybridization, although the potentially PDF-responsive cells were not specified in this brain area. However, later on the reliability of the available PDFR antibodies has been questioned, giving rise to the development of other methods to further dissect the issue where exactly PDFR is expressed (Shafer et al. 2008). For instance, live optical imaging based on the expression of genetically encoded sensors has been successfully introduced to study receptivity of neurons to different neuropeptides. Using this system, Shafer et al. (2008) detected large and long-lasting cAMP increases in many clock neuron groups due to bath-applied PDF, suggesting the expression of PDFR on these cells. Here we show that synthetic PDF peptide evokes cAMP increases in the insulin producing cells, and these responses are not mediated by interneurons, but are due to direct activation of the IPCs. Since the increases are absent in *han* background, they seem to be regulated by PDF receptor.

Apparently, the PDF-evoked cAMP responses in the IPCs are not as robust as those registered in different clock neurons (Shafer et al. 2008). However, a possible lower incidence of PDFR on these neurosecretory cells may explain this difference, and can greatly affect ligand efficacy. On the other hand, one needs to consider that there are 14 IPCs in the *PI*, and as it has recently been reported, individual IPCs show some heterogeneity (Jaramillo et al. 2004; Söderberg et al. 2012; Barber et al. 2016). Apart from their marked differences in their electrophysiological parameters (Barber et al., 2016), they also differ in their protein- and neuropeptide composition (Jaramillo et al. 2004; Söderberg et al. 2012). Therefore, it is possible that individual IPCs, at least partially, express different receptors.

The small ventrolateral neurons send axonal projections towards the dorsal brain, however their branches do not seem to reach the *PI* region (Cavanaugh et al. 2014). Cavanaugh et al. (2014) investigated possible synaptic connections between *PI* cells and PDF^+ neurons, using GFP reconstitution across synaptic partners (GRASP) approach (Feinberg et al. 2008). Expression of one half of the GFP in the PDF^+ neurons and the other half under in *PI* cells did not yield GFP-positive signals, therefore suggesting that s-LN_vs do not directly contact *PI* cells (Cavanaugh et al. 2014). However, our GRASP analysis revealed that, in the cold, IPCs in the *PI* are connected to PDF^+ neurons, and therefore get synaptic contact from these cells. The detected GRASP signal was temperature-dependent, and predominantly present at low temperature (12^oC); thus suggesting that the interaction

between IPCs and PDF^+ neurons comes from PDF-Tri. However, when discussing about PDF signaling, it is important to emphasize that PDF apparently can be released in a paracrine fashion to activate its receptor (Hyun et al. 2005; Lear et al. 2005; Mertens et al. 2005). Indeed, it has been reported that neuropeptide signaling does not necessarily rely on synaptic contacts. The released peptides can target also distant tissues through diffusion (Jan & Jan 1982; Talsma et al. 2012; Krupp et al. 2013) enabling regions to receive input from these cells even though they do not seem to be directly innervated. For instance, despite the lack of a direct synaptic connection between LN_vs and LN_d neurons, PDF secreted from s-LN_vs was found to activate PDFR in LN_d to prolong mating duration (Kim et al. 2013). Considering the hypothesis that PDF can be released in a paracrine manner from varicosities (Helfrich-Förster et al. 2007) and receptors may be localized outside synaptic regions, we can also suggest that IPCs can be activated by PDF released by nearby s-LN_vs axon termini.

Our imaging assays indicate a cAMP increase in the IPCs due to short neuropeptide-F application, similar to that recorded in the case of PDF. This response was detectable also in the presence of the sodium-channel blocker TTX, thus suggesting that IPCs are sNPF-responsive cells. In addition, sNPF application resulted in a small, but significant increase of Ca^{2+} levels in the insulin producing cells, which was also not blocked by TTX, indicating again a direct response. It has already been reported that the G-protein coupled receptor for sNPF (sNPFR1) is expressed on the insulin producing cells (Lee et al. 2008; Kapan et al. 2012; Carlsson et al. 2013). In larval IPCs, sNPF was found to positively regulate insulin-like signaling via sNPFR1 (Lee et al. 2008). Kapan et al. (2012) identified sNPFR1 also on the IPCs of adult flies (Kapan et al. 2012). However, a subsequent study reported that only the adult IPCs express sNPFR1, while during larval stages the receptor is not present on these cells (Carlsson et al. 2013). In any case, our live optical imaging was performed on adult females that expressed sNPFR1 on their IPCs.

Interestingly, sNPF is known for both its inhibitory and excitatory nature, documented in several studies. Indeed, sNPF apparently acts differently in feeding and non-feeding circuits. While in neurons involved in feeding, its excitatory action has been shown, the opposite effect was observed when sNPF was studied in relation to non-feeding pathways (Shang et al. 2013). Experiments in larval motor neurons suggest that sNPF receptor mediates native inhibitory signaling, acting via G_o signaling to reduce cAMP level

(Vecsey & Griffith 2014). A very recent study revealed that, similarly to PDF, sNPF signals also by suppressing basal Ca^{2+} levels in certain circadian clock clusters (Liang et al. 2017). On the contrary, this neuropeptide seems to have an excitatory effect on the olfactory sensory neurons (Root et al. 2011), and it was documented to significantly enhance cAMP responses of IPCs to the biogenic amine octopamine (Shang et al. 2013). sNPF treatment causes dose-dependent cAMP increases in BG2-c6 neuronal cell line, suggesting that the stimulatory G protein alpha-subunit is a key subunit of sNPFR1 (Hong et al. 2012; Chen et al. 2013).

As the aforementioned examples show, the opposing molecular and electrophysiological effects of sNPF are hard to understand. One possibility is that, sNPFR1 couples to more than one G-protein subtype. Increasing number of evidence suggests that the same GPCR can couple to different G-proteins, thereby being involved in high variety of mechanisms and pathways (Offermann et al. 1996; Conchon et al. 1997; Wu et al. 1997; Montrose-Rafizadeh et al. 1999; Kilts et al. 2000; Holst et al. 2001; Palanche et al. 2001; Skrzydelski et al. 2003). For instance, the glucagon receptor in human atrial membranes has been reported to couple to the stimulatory G_s protein as well as to the inhibitory $G_{i/o}$ (Kilts et al. 2000). The neurokinin-1 receptor (NK1R) exists in two high-affinity ligand-binding states: the lower of the two couples to $G_{q/11}$ (activation of phospholipase C), while the higher corresponds to coupling to G_s stimulatory G-protein (Holst et al. 2001). Interestingly, in the case of the neurokinin-2 receptor (NK2R) the opposite coupling was observed: upon low agonist concentration rapid calcium response happens ($G_{q/11}$ coupling), while high levels of neurokinin results in G_s-coupling (Palanche et al. 2001). Similar complexity may be applicable to sNPF receptor as well. Considering that sNPF processes in the insulin producing cells seem to be involved in the regulation of different biological processes (Lee et al. 2008; Shang et al. 2013), it is possible that multiple signaling pathways can be activated by a single sNPFR1, involving more than one G-protein subtype. Studying sNPF signaling in the IPCs is further complicated by the fact that there are large numbers of sNPF-producing neurons in the brain that can signal to the IPCs (Lee et al. 2004; Nässel et al. 2008; Kapan et al. 2012), and sNPF coming from different neuron groups can be responsible for the regulation of distinct processes. It is also important to emphasize that, when performing live optical imaging, the synthetic sNPF neuropeptide is externally added to the samples. Although it enables the detection of cAMP concentration changes, it cannot approximate fully what happens in a living brain under physiological conditions. For example, using this method it is

not clear how the insulin producing cells react to sNPF coming from different neurons, and whether changes in the sNPF concentration from the different sources could also influence the G-protein coupling of the receptor.

Surprisingly, co-application of sNPF and PDF neuropeptides brought about rapid and immediate cAMP responses in the insulin producing cells. These combined responses were greater than the sum of their separate activities, suggesting a possible synergistic action of PDF and sNPF on the IPCs. However, when co-applying the two peptides, the number of peptide molecules in the solution was the double of that of the single applications. Thus, concentration of the co-applied peptides was halved, ensuring that their total concentration is equal to that of the single applications. Under this condition, we observed that the two peptides evoke significant cAMP increase in the IPCs, which is detectable directly after the application point. Based on these results, sNPF and PDF apparently act co-operatively on these neurosecretory cells. Despite TTX suppression of action potentials in the rest of the brain, the sNPF+PDF co-application still evoked a significant, but less robust cAMP increase in the IPCs, indicating a partially direct response. Earlier studies have already provided clear evidence for synergy between different peptides. For example, a synergistic action between diuretic peptides from the migratory locust *Locusta migratoria* has been found. The peptides Locusta-DP (a CRF-related peptide) and locustakinin (an insect myokinin) act synergistically to stimulate Malpighian tubule fluid secretion (Coast 1995). In addition, the existence of synergistic interactions has been reported between the neuropeptides calcitonin gene-related peptide (CGRP) and vasoactive perivascular neuropeptide substance P (SP) in mediating endothelial cell growth (Villablanca et al. 1994).

According to our findings, the large cAMP increases induced by the co-application of PDF and sNPF are possibly specific to these two neuropeptides, however we cannot exclude the possibility that other neuropeptides, not tested in our imaging system, could have similar effect in co-application with sNPF. Nevertheless, in our hands, any of the four randomly selected *Drosophila* neuropeptides (AKH, DTK, Ast-C, and SDNFMRFa) had a similar interaction with sNPF as the circadian neurotransmitter PDF. Interestingly, we found that in PDFR null mutant flies the co-application of sNPF and PDF no longer resulted in an increase of cAMP concentration and, surprisingly, neither did sNPF application alone. Thus, it seems that the absence of PDFR influences also the effect of sNPF on the insulin producing cells. This result can be due to a possible cross-talk between PDFR and sNPFR1. Extensive

evidence accumulated over the last few years that highlight the existence of GPCR complexes (homo- or hetero-oligomeric complexes), raising the possibility of various cooperative effects between GPCRs (reviewed in O'Dowd & Lee 2002). Such GPCR-GPCR interrelations can be important for the fine-tuning of different cellular signaling profiles, providing an opportunity for their ligands to coordinate biological processes by acting in a synchronized manner (Rozenfeld & Devi 2010). In our case, the binding of one ligand (PDF) to its receptor can possibly modify the interaction of another ligand (for example sNPF) with its receptor in a positive way. Thus, due to this complex interaction the related signaling outcome is also modified/amplified, resulting in a large increase in cAMP concentration. For instance, it was shown that the dopamine receptor D2R and somatostatin receptor SSTR5 physically interact and form a heteromeric complex. The creation of the D2R-SSTR5 complex results in an increased functional activity, leading to the synergistic inhibition of cAMP (Rocheville et al. 2000). Such interrelations can also be valid for sNPFR1 and PDFR, however further investigations need to be done to study this possibility.

PDF and sNPF are co-expressed in the small LN_vs (Johard et al. 2009; Kula-Eversole et al. 2010). In addition, the analysis of sNPF-PDF double stained brains revealed the physical proximity of the two peptides in the tritocerebrum, in the median bundle, and in the *Pars intercerebralis* region. However, we have not yet understood whether these areas can be possible contact points for these two peptides involved in the modulation of IPC activities.

Interestingly, it has recently been found that sNPF (produced in the s-LN_vs and in a subset of dorsal lateral neurons) and PDF mediate critical interactions between pacemaker neuron groups by setting the phase of the endogenous Ca^{2+} rhythms, discovered in the different clock neuron clusters (Liang et al. 2017). PDF was found to be primarily involved in determining the phase of Ca^{2+} rhythms of LN_d and DN3 clusters, while sNPF sets that of DN1 (Liang et al. 2017). Thus, the two signaling pathways act dynamically to facilitate the right timing of pacemaker neuronal activities.

5.5. The dorsal-lateral peptidergic neurons seem not to be involved in the regulation of diapause

Their documented modulatory roles in diapause-related traits make the dorsal-lateral peptidergic neurons (DLPs) appealing candidates for diapause research. They are

located in the *Pars lateralis* of the protocerebrum, and co-express sNPF and corazonin (Kapan et al. 2012). Their axonal projections reach the area of the insulin producing cells, where their neuronal processes seem to be interacting with those of IPCs. These neurons are known to be involved in modulating the stress physiology of the flies (Kapan et al. 2012; Kubrak et al. 2016). Targeted RNAi against *Crz* in the DLPs has been reported to affect metabolism and resistance to starvation stress (Kapan et al. 2012). Knockdown of Crz receptor in starving flies results in increased circulating and stored carbohydrate levels, as well as leads to altered *dilp3, dilp5* transcript profiles (Kubrak et al. 2016).

Despite the role of these cells in the aforementioned biological processes, our experiments do not support their involvement in the regulation of diapause. Their hyperexcitation did not alter significantly the proportion of diapausing females compared to control individuals, and neither did the DLP-specific overexpression of sNPF and targeted corazonin knockdown in these cells. Even though in some experiments significant differences were found compared to either the UAS or Gal4 control, we were unable to detect robust differences compared to both controls. Therefore, corazonin apparently helps to cope with metabolic stress experienced during starvation, but does not function as a diapause-regulator neuropeptide.

Nevertheless, it is important to stress that in the case of all diapause assays performed to clarify the possible involvement of DLPs in the regulation of dormancy, flies were reared at 23^{o}C in LD 12:12 during their development, and were introduced to diapause-inducing conditions only at the adult stage (PROTOCOL 1). Therefore, we cannot exclude the possibility that the application of the new diapause protocol (PROTOCOL 2) would highlight a different role for DLPs.

5.6. Photoperiodism in *Drosophila melanogaster*

Most of the biological studies, including also chronobiological experiments, rely on simplified laboratory conditions with artificial day-light cycles and constant temperatures. These conditions can only be considered as a rough approximation of the complex natural habitat the flies encounter in nature. In their study of the circadian behavioral rhythms in the wild, Vanin et al. (2012) first pointed out some unexpected features of the fruit fly behavior compared to those observed under laboratory conditions. When kept in the

laboratory, *Drosophila melanogaster* displays a well-known bimodal activity profile with maximal activity concentrated in the morning and evening. Surprisingly, besides the morning and evening peaks, an additional afternoon peak also appears during outdoor conditions (Vanin et al. 2012). The discovery of the "afternoon siesta" was a big surprise for the scientific community, and it shaped our current knowledge about *Drosophila* circadian behavioral rhythm, emphasizing the importance of studying organisms in their natural environments. In a subsequent study by Menegazzi et al. (2013) the neuronal expression of the canonical clock proteins PERIOD and TIMELESS was tracked in nature. Interestingly, remarkable differences were found in the expression profile of these clock components in the wild compared to earlier findings of laboratory studies (Menegazzi et al. 2013).

Since the circadian clock system is apparently highly influenced by natural conditions (Vanin et al. 2012; Menegazzi et al. 2013; Montelli et al. 2015), seasonal responses like diapause can also be affected by more natural-like parameters. Thus, we improved our experimental protocol to study the plasticity of diapause behavior under semi-natural conditions. Most insects exhibit a photoperiodic diapause initiated by shortening day length (Tauber et al. 1986). The exit from the dormant state is provoked by lengthening days, perceived by the organism as an indicator of an approaching favorable season. In the laboratory, in most of the cases, natural light conditions are roughly mimicked by rectangular light-dark cycles. Despite of this very simplified light-on/off cycles, photoperiod-driven diapause remains robust in some Drosophilids, like in *D. littoralis*, *D. montana* and *D. ezoana* (Lankinen 1986; Salminen et al. 2015), therefore can be well studied under laboratory conditions. However, *Drosophila melanogaster* exhibits a "shallow" reproductive dormancy, which is regulated primarily by temperature and not by photoperiod (Saunders et al. 1989; Saunders 1990; Emerson et al. 2009a). The exit from this "shallow" diapause occurs immediately when flies are transferred to warm temperatures, regardless of the photoperiod (Saunders et al. 1989; Tatar et al. 2001). Therefore, overwintering in *D. melanogaster*, in part, shares features of both diapause and quiescence (Tatar et al. 2001).

Saunders et al. (1989) reported a clear photoperiodic diapause response in the wild-type *Canton-S* strain of *Drosophila melanogaster* (Saunders et al. 1989). Female flies exposed to short days at 12^{o}C entered reproductive diapause, while those maintained in long days underwent ovarian maturation at the same low temperature (Saunders et al. 1989). However, it is important to emphasize that *Canton-S* strain has been domesticated in

laboratory conditions for about 100 years (Bridges 1916), and the absence of key external stimuli in the environment of captive animals might affect behavioral phenotypes (Price 1999; Stanley & Kulathinal 2016). Therefore, photoperiodic diapause should be reasonably studied in natural fly populations, which have been sampled and introduced to the laboratory conditions more recently.

In a study by Tauber et al. (2007), natural populations of European *Drosophila melanogaster* were tested, and they were found to exhibit higher diapause levels when reared in short photoperiods (Tauber et al. 2007). However, Emerson and his colleagues reported that American *D. melanogaster* lines, maintained at 11^{o}C, entered the dormant state irrespectively of the photoperiod (Emerson et al. 2009a). The authors concluded that low temperature is the primary environmental cue that regulates the reproductive dormant state in this species (Emerson et al. 2009a).

Interestingly, a recent study adopted a more natural-like diapause protocol, in which both the rectangular LD cycles and temperature were gradually changed in order to mimic the shortening days of upcoming winters, and lengthening days of the approaching spring (Zonato et al. 2017). This winter/spring scenario was found to enhance the diapause response of females and generated more stable diapause phenotypes (Zonato et al. 2017). Although this protocol recognizes the necessity for changes in both photoperiod and temperature cycles, it adopts exclusively rectangular profiles for both parameters.

In general, many biological experiments are performed in different incubators that have their own lighting system, relying on fluorescent light tubes that generate the selected light regime. However, one needs to consider that the majority of input energy comes out as heat production, thus long photoperiods very often couple to higher temperatures, which creates difficulties to study clear photoperiodic effects. Many laboratories adopt different light boxes to keep the samples under the desired photoperiod. They often contain light-emitting diodes (LEDs) as light sources. However, heat generation occurs also within the LED apparatus as a consequence of the inefficiency of the light producing semiconductor operations. Therefore, when studying the effect of different photoperiods on diapause, we have to ensure that the observed phenotype is due to the photoperiod and not influenced by temperature cycles. Since in a relatively small, closed light box these temperature fluctuations are quite problematic to eliminate, our LED-containing light device is suspended from the top of an incubator and functions as a lamp. Therefore, the incidentally occurring

temperature cycles can be continuously corrected by the internal temperature-sensor of the incubator.

When planning our experiments, one of our aims was to gain more information about the nature of photoperiodic diapause in European *D. melanogaster* populations. To this end, a more natural-like late autumnal profile and a summer scenario were adopted, taking into consideration the continuous light intensity changes throughout the days. In the corresponding control experiments, rectangular LD cycles (LD 8:16 and LD 15:9, respectively) were generated. Importantly, we ensured that the flies were exposed to equal amounts of light when using semi-natural and rectangular profiles.

In our hands, all the four *D. melanogaster* lines failed to distinguish between long and short days when kept in rectangular LD cycles. However, we noticed that a higher proportion of flies entered diapause upon exposure to semi-natural late autumnal days, compared to individuals exposed to rectangular light regimes. In addition, we observed that flies in semi-natural summer days exhibited lower diapause levels compared to their corresponding controls, reared in rectangular LD 15:9 cycles. A strong photoperiodic effect was detected when comparing semi-natural autumnal and summer days, revealing the importance of using more natural-like protocols.

REFERENCES

Accili, D., & Arden, K. C. (2004). FoxOs at the crossroads of cellular metabolism, differentiation, and transformation. *Cell*, *117*(4), 421-426.

Adams, M. D., Celniker, S. E., Holt, R. A., Evans, C. A., Gocayne, J. D., Amanatides, P. G., ... & George, R. A. (2000). The genome sequence of *Drosophila melanogaster. Science*, 287(5461), 2185-2195.

Alfa, R. W., Park, S., Skelly, K. R., Poffenberger, G., Jain, N., Gu, X., … & Kim, S. K. (2015). Suppression of insulin production and secretion by a decretin hormone. *Cell Metabolism*, *21*(2), 323-333.

Alic, N., Hoddinott, M. P., Vinti, G., & Partridge, L. (2011). Lifespan extension by increased expression of the Drosophila homologue of the IGFBP7 tumour suppressor. *Aging Cell*, *10*(1), 137-147.

Allada, R., & Chung, B. Y. (2010). Circadian organization of behavior and physiology in Drosophila. *Annual Review of Physiology*, *72*, 605-624.

Allen, M. (2007). What makes a fly enter diapause? *Fly, 1*(6), 307-310.

Alvarez, B., Martínez-A, C., Burgering, B. M., & Carrera, A. C. (2001). Forkhead transcription factors contribute to execution of the mitotic programme in mammals. *Nature*, *413*(6857), 744-747.

Antonova, Y., Arik, A. J., Moore, W., Riehle, M. A., Brown, M. R. (2012). Insulin-like peptides: structure, signaling, and function, in *Insect Endocrinology*, ed Gilbert L. I., editor. (San Diego, CA: Academic Press), 63-92.

Arquier, N., Géminard, C., Bourouis, M., Jarretou, G., Honegger, B, Paix A, Léopold, P. (2008). Drosophila ALS regulates growth and metabolism through functional interaction with insulin-like peptides. *Cell Metabolism, 7*(4), 333-338.

Atsuko, M., Hiromu, K., & Tetsuya, O. (1988). Different profiles of ecdysone secretion and its metabolism between diapause-and nondiapause-destined cultures of the fleshfly, *Boettcherisca peregrina*. *Comparative Biochemistry and Physiology Part A: Physiology*, *91*(1), 157-164.

Ayala, J. E., Streeper, R. S., Desgrosellier, J. S., Durham, S. K., Suwanichkul, A., Svitek, C. A., … & O'Brien, R. M. (1999). Conservation of an insulin response unit between mouse and human glucose-6-phosphatase catalytic subunit gene promoters: transcription factor FKHR binds the insulin response sequence. *Diabetes*, *48*(9), 1885-9.

Bai, H., Kang, P., & Tatar, M. (2012). Drosophila insulin-like peptide-6 (dilp6) expression from fat body extends lifespan and represses secretion of Drosophila insulin-like peptide-2 from the brain. *Aging Cell*, *11*(6), 978-985.

Baines, R. A., Uhler, J. P., Thompson, A., Sweeney, S. T., & Bate, M. (2001). Altered electrical properties in Drosophila neurons developing without synaptic transmission. *Journal of Neuroscience*, *21*(5), 1523-1531.

Baker, F. C., Tsai, L. W., Reuter, C. C., & Schooley, D. A. (1987). *In vivo* fluctuation of JH, JH acid, and ecdysteroid titer, and JH esterase activity, during development of fifth stadium *Manduca sexta*. *Insect Biochemistry*, *17*(7), 989-996.

Barber, A. F., Erion, R., Holmes, T. C., & Sehgal, A. (2016). Circadian and feeding cues integrate to drive rhythms of physiology in Drosophila insulin-producing cells. *Genes & Development, 30*(23), 2596-2606.

Beckingham, K. M., Armstrong, J. D., Texada, M. J., Munjaal, R., & Baker, D. A. (2007). *Drosophila melanogaster* - the model organism of choice for the complex biology of multi-cellular organisms. *Gravitational and Space Research, 18*(2), 17-29.

Belgacem, Y. H., & Martin, J. R. (2006). Disruption of insulin pathways alters trehalose level and abolishes sexual dimorphism in locomotor activity in Drosophila. *Journal of Neurobiology*, *66*(1), 19-32.

Birse, R. T., Söderberg, J. A., Luo, J., Winther, A. M., & Nässel, D. R. (2011). Regulation of insulin-producing cells in the adult Drosophila brain via the tachykinin peptide receptor DTKR. *The Journal of Experimental Biology*, *214*(24), 4201-8.

Blanchardon, E., Grima, B., Klarsfeld, A., Chélot, E., Hardin, P. E., Préat, T., & Rouyer, F. (2001). Defining the role of Drosophila lateral neurons in the control of circadian rhythms in motor activity and eclosion by targeted genetic ablation and PERIOD protein overexpression. *European Journal of Neuroscience*, *13*(5), 871-888.

Boerjan, B., Verleyen, P., Huybrechts, J., Schoofs, L., & De Loof, A. (2010). In search for a common denominator for the diverse functions of arthropod corazonin: a role in the physiology of stress? *General and Comparative Endocrinology*, *166*(2), 222-33.

Böhni, R., Riesgo-Escovar, J., Oldham, S., Brogiolo, W., Stocker, H., Andruss, B. F., Beckingham, K., & Hafen, E. (1999). Autonomous control of cell and organ size by CHICO, a Drosophila homolog of vertebrate IRS1–4. *Cell*, *97*(7), 865-875.

Boothroyd, C. E., Wijnen, H., Naef, F., Saez, L., & Young, M. W. (2007). Integration of light and temperature in the regulation of circadian gene expression in Drosophila. *PLoS Genetics*, *3*(4), e54.

Bownes, M., & Nöthiger, R. (1981). Sex determining genes and vitellogenin synthesis in *Drosophila melanogaster*. *Molecular Genetics and Genomics*, *182*(2), 222-8.

Brand, A. H., & Perrimon, N. (1993). Targeted gene expression as a means of altering cell fates and generating dominant phenotypes. *Development*, *118*(2), 401-415.

Bridges, C. B. (1916). Non-disjunction as proof of the chromosome theory of heredity. *Genetics*, *1*(2), 107.

Britton, J. S., Lockwood, W. K., Li, L., Cohen, S. M., & Edgar, B. A. (2002). Drosophila's insulin/PI3-kinase pathway coordinates cellular metabolism with nutritional conditions. *Developmental Cell*, *2*(2), 239-249.

Brody, T., & Cravchik, A. (2000). *Drosophila melanogaster* G protein-coupled receptors. *The Journal of Cell Biology*, *150*(2), F83-F88.

Broeck, J. V. (2001). Neuropeptides and their precursors in the fruitfly, *Drosophila melanogaster*. *Peptides*, *22*(2), 241-254.

Brogiolo, W., Stocker, H., Ikeya, T., Rintelen, F., Fernandez, R., & Hafen, E. (2001). An evolutionarily conserved function of the Drosophila insulin receptor and insulin-like peptides in growth control. *Current Biology*,

11(4), 213-221.

Broughton, S. J., Piper, M. D. W., Ikeya, T., Bass, T. M., Jacobson, J., Driege, Y., … Partridge, L. (2005). Longer lifespan, altered metabolism, and stress resistance in Drosophila from ablation of cells making insulin-like ligands. *Proceedings of the National Academy of Sciences of the United States of America*, *102*(8), 3105-3110.

Broughton, S., Alic, N., Slack, C., Bass, T., Ikeya, T., Vinti, G., … & Partridge, L. (2008). Reduction of DILP2 in Drosophila triages a metabolic phenotype from lifespan revealing redundancy and compensation among DILPs. *PLoS One*, *3*(11), e3721.

Broughton, S. J., Slack, C., Alic, N., Metaxakis, A., Bass, T. M., & Driege, Y. & Partridge, L. (2010). DILP-producing median neurosecretory cells in the Drosophila brain mediate the response of lifespan to dietary restriction. *Aging Cell*, *9*(3), 336-346.

Brunet, A., Bonni, A., Zigmond, M. J., Lin, M. Z., Juo, P., Hu, L. S., … & Greenberg, M. E. (1999). Akt promotes cell survival by phosphorylating and inhibiting a Forkhead transcription factor. *Cell*, *96*(6), 857-868.

Buch, S., Melcher, C., Bauer, M., Katzenberger, J., & Pankratz, M. J. (2008). Opposing effects of dietary protein and sugar regulate a transcriptional target of Drosophila insulin-like peptide signaling. *Cell Metabolism*, *7*(4), 321-332.

Buszczak, M., Freeman, M. R., Carlson, J. R., Bender, M., Cooley, L., & Segraves, W. A. (1999). Ecdysone response genes govern egg chamber development during mid-oogenesis in Drosophila. *Development*, *126*(20), 4581-9.

Carlsson, M. A., Enell, L. E., & Nässel, D. R. (2013). Distribution of short neuropeptide F and its receptor in neuronal circuits related to feeding in larval Drosophila. *Cell and Tissue Research*, *353*(3), 511-523.

Cavaliere, V., Bernardi, F., Romani, P., Duchi, S., & Gargiulo, G. (2008). Building up the Drosophila eggshell: first of all the eggshell genes must be transcribed. *Developmental Dynamics*, *237*(8), 2061-2072.

Cavanaugh, D. J., Geratowski, J. D., Wooltorton, J. R., Spaethling, J. M., Hector, C. E., Zheng, X., ... & Sehgal, A. (2014). Identification of a circadian output circuit for rest: activity rhythms in Drosophila. *Cell*, *157*(3), 689-701.

Cazzamali, G., Saxild, N. P. ., & Grimmelikhuijzen, C. J. (2002). Molecular cloning and functional expression of a corazonin receptor. *Biochemical and Biophysical Research Communications*, *298*(1), 31-36.

Cerstiaensa, A. N. J. A., Benfekihb, L., Zouitenc, H., Verhaerta, P., De Loofa, A., & Schoofsa, L. (1999). Led-NPF-1 stimulates ovarian development in locusts. *Peptides*, *20*(1), 39-44.

Chen, C., Jack, J., & Garofalo, R. S. (1996). The Drosophila insulin receptor is required for normal growth. *Endocrinology*, *137*(3), 846-856.

Chen, W., Shi, W., Li, L., Zheng, Z., Li, T., Bai, W., & Zhao, Z. (2013). Regulation of sleep by the short neuropeptide F (sNPF) in *Drosophila melanogaster*. *Insect Biochemistry and Molecular Biology*, *43*(9), 809-819.

Chintapalli, V. R., Wang, J., & Dow, J. A. (2007). Using FlyAtlas to identify better *Drosophila melanogaster* models of human disease. *Nature Genetics*, *39*(6), 715-20.

Chippendale, G. M., & Yin, C. M. (1974). Juvenile hormone and the induction of larval polymorphism and diapause of the southwestern corn borer, *Diatraea grandiosella*. *Journal of Insect Physiology*, *20*(9), 1833-1847.

Choi, Y. J., Lee, G., Hall, J. C., & Park, J. H. (2005). Comparative analysis of Corazonin-encoding genes (Crz's) in Drosophila species and functional insights into Crz-expressing neurons. *Journal of Comparative Neurology*, *482*(4), 372-385.

Clancy, D. J., Gems, D., Harshman, L. G., Oldham, S., Stocker, H., Hafen, E., … & Partridge, L. (2001). Extension of life-span by loss of CHICO, a Drosophila insulin receptor substrate protein. *Science*, *292*(5514), 104-106.

Coast, G. M. (1995). Synergism between diuretic peptides controlling ion and fluid transport in insect malpighian tubules. *Regulatory Peptides*, *57*(3), 283-296.

Colombani, J., Andersen, D. S. & Léopold, P. (2012). Secreted peptide Dilp8 coordinates Drosophila tissue growth with developmental timing. *Science*, *336*(6081), 582–585.

Colombani, J., Andersen, D. S., Boulan, L., Boone, E., Romero, N., Virolle, V., … & Léopold, P. (2015). Drosophila Lgr3 couples organ growth with maturation and ensures developmental stability. *Current Biology*, *25*(20), 2723-2729.

Conchon, S., Barrault, M. B., Miserey, S., Corvol, P., & Clauser, E. (1997). The C-terminal third intracellular loop of the rat AT1A angiotensin receptor plays a key role in G protein coupling specificity and transduction of the mitogenic signal. *Journal of Biological Chemistry*, *272*(41), 25566-25572.

Cong, X., Wang, H., Liu, Z., He, C., An, C., & Zhao, Z. (2015). Regulation of sleep by Insulin-like peptide system in *Drosophila melanogaster*. *Sleep*, *38*(7), 1075-83.

Crocker, A., Shahidullah, M., Levitan, I. B., & Sehgal, A. (2010). Identification of a neural circuit that underlies the effects of octopamine on sleep:wake behavior. *Neuron*, *65*(5), 670-681.

de Rooij, J., Zwartkruis, F. J., Verheijen, M. H., Cool, R. H., Nijman, S. M., Wittinghofer, A., & Bos, J. L. (1998). Epac is a Rap1 guanine-nucleotide-exchange factor directly activated by cyclic AMP. *Nature*, *396*(6710), 474-477.

Denlinger, D. L. (1985). Hormonal control of diapause. In *Comprehensive Insect Physiology, Biochemistry and Pharmacology,* Pergamon Press, Oxford. p. 353-412.

Denlinger, D. L. (2002). Regulation of Diapause. *Annual Review of Entomology*, *47*, 93-122.

Depetris-Chauvin, A., Berni, J., Aranovich, E. J., Muraro, N. I., Beckwith, E. J., & Ceriani, M. F. (2011). Adult-specific electrical silencing of pacemaker neurons uncouples molecular clock from circadian outputs. *Current Biology*, *21*(21), 1783-1793.

Dijkers, P. F., Medema, R. H., Lammers, J. W. J., Koenderman, L., & Coffer, P. J. (2000). Expression of the pro-

apoptotic Bcl-2 family member Bim is regulated by the forkhead transcription factor FKHR-L1. *Current Biology*, *10*(19), 1201-1204.

Dolezel, D. (2015). Photoperiodic time measurement in insects. *Current Opinion in Insect Science*, *7*, 98-103.

Donlea, J. M., Ramanan, N., & Shaw, P. J. (2009). Use-dependent plasticity in clock neurons regulates sleep need in Drosophila. *Science*, *324*(5923), 105-108.

Dubrovsky, E. B. (2005). Hormonal cross talk in insect development. *Trends in Endocrinology and Metabolism*, *16*(1), 6-11.

Duvall, L. B., & Taghert, P. H. (2012). The circadian neuropeptide PDF signals preferentially through a specific adenylate cyclase isoform AC3 in M pacemakers of Drosophila. *PLoS Biology*, *10*(6), e1001337.

Gwinner, E. (1986). Circannual rhythms. Springer; Heidelberg, Germany

Emerson, K. J., Uyemura, A. M., McDaniel, K. L., Schmidt, P. S., Bradshaw, W. E., & Holzapfel, C. M. (2009a). Environmental control of ovarian dormancy in natural populations of *Drosophila melanogaster*. *Journal of Comparative Physiology A: Neuroethology, Sensory, Neural, and Behavioral Physiology*, *195*(9), 825-829.

Emerson, K. J., Bradshaw, W. E., & Holzapfel, C. M. (2009b). Complications of complexity: integrating environmental, genetic and hormonal control of insect diapause. *Trends in Genetics*, *25*(5), 217-225.

Enell, L. E., Kapan, N., Söderberg, J. A., Kahsai, L., & Nässel, D. R. (2010). Insulin signaling, lifespan and stress resistance are modulated by metabotropic GABA receptors on insulin producing cells in the brain of Drosophila. *PloS One*, *5*(12), e15780.

Feinberg, E. H., VanHoven, M. K., Bendesky, A., Wang, G., Fetter, R. D., Shen, K., & Bargmann, C. I. (2008). GFP Reconstitution Across Synaptic Partners (GRASP) defines cell contacts and synapses in living nervous systems. *Neuron*, *57*(3), 353-363.

Fernández, M. P., Berni, J., & Ceriani, M. F. (2008). Circadian remodeling of neuronal circuits involved in rhythmic behavior. PLoS Biology, *6*(3), e69.

Fernandez, R., Tabarini, D., Azpiazu, N., Frasch, M., & Schlessinger, J. (1995). The Drosophila insulin receptor homolog: a gene essential for embryonic development encodes two receptor isoforms with different signaling potential. *The EMBO Journal*, *14*(14), 3373-84.

Flatt, T., Tu, M. P., & Tatar, M. (2005). Hormonal pleiotropy and the juvenile hormone regulation of Drosophila development and life history. *Bioessays*, *27*(10), 999-1010.

Foltenyi, K., Greenspan, R. J., & Newport, J. W. (2007). Activation of EGFR and ERK by rhomboid signaling regulates the consolidation and maintenance of sleep in Drosophila. *Nature Neuroscience*, *10*(9), 1160-1167.

Fujiwara, Y., Tanaka, Y., Iwata, K. I, Rubio, R. O., Yaginuma, T., Yamashita, O., & Shiomi, K. (2006). ERK/MAPK regulates ecdysteroid and sorbitol metabolism for embryonic diapause termination in the silkworm,

Bombyx mori. *Journal of Insect Physiology*, *52*(6), 569-575.

Fukuda, S. (1951). The Production of the diapause eggs by transplanting the suboesophageal ganglion in the silkworm. *Proceedings of the Imperial Academy*, *27*(10), 672-677.

Gäde, G., & Auerswald, L. (2003). Mode of action of neuropeptides from the adipokinetic hormone family. *General and Comparative Endocrinology*, *132*(1), 10-20.

Gäde, G., & Goldsworthy, G. J. (2003). Insect peptide hormones: A selective review of their physiology and potential application for pest control. *Pest Management Science*, *59*(10), 1063-1075.

Garczynski, S. F., Brown, M. R., Shen, P., Murray, T. F., & Crim, J. W. (2002). Characterization of a functional neuropeptide F receptor from *Drosophila melanogaster*. *Peptides*, *23*(4), 773-780.

Garelli, A., Gontijo, A. M., Miguela, V., Caparros, E., & Dominguez, M. (2012). Imaginal discs secrete insulin-like peptide 8 to mediate plasticity of growth and maturation. *Science*, *336*(6081), 579-582.

Garofalo, R. S., & Rosen, O. M. (1988). Tissue localization of *Drosophila melanogaster* insulin receptor transcripts during development. *Molecular and Cellular Biology*, *8*(4), 1638-47.

Gatto, C. L., & Broadie, K. (2011). Fragile X mental retardation protein is required for programmed cell death and clearance of developmentally-transient peptidergic neurons. *Developmental Biology*, *356*(2), 291-307.

Gehlert, D. R. (1999). Role of hypothalamic neuropeptide Y in feeding and obesity. *Neuropeptides*, *33*(5), 329-338.

George, S. R., O'Dowd, B. F., & Lee, S. P. (2002). G-protein-coupled receptor oligomerization and its potential for drug discovery. *Nature Reviews Drug Discovery*, *1*(10), 808-820.

Giannakou, M. E., & Partridge, L. (2007). Role of insulin-like signalling in Drosophila lifespan. *Trends in Biochemical Sciences*, *32*(4), 180-188.

Goto, S. G., Han, B., & Denlinger, D. L. (2006). A nondiapausing variant of the flesh fly, *Sarcophaga bullata*, that shows arrhythmic adult eclosion and elevated expression of two circadian clock genes, *period* and *timeless*. *Journal of Insect Physiology*, *52*(11), 1213-1218.

Green, E. W., O'Callaghan, E. K., Hansen, C. N., Bastianello, S., Bhutani, S., Vanin, S., ... & Kyriacou, C. P. (2015a). Drosophila circadian rhythms in seminatural environments: Summer afternoon component is not an artifact and requires TrpA1 channels. *Proceedings of the National Academy of Sciences*, *112*(28), 8702-8707.

Green, E. W., O'Callaghan, E. K., Pegoraro, M., Armstrong, J. D., Costa, R., Kyriacou, C. P. (2015b) Genetic analysis of Drosophila circadian behavior in seminatural conditions. *Methods in Enzymology*, 551:121-33.

Grönke, S., Clarke, D. F., Broughton, S., Andrews, T. D., & Partridge, L. (2010). Molecular evolution and functional characterization of Drosophila insulin-like peptides. *PLoS Genetics*, *6*(2), e1000857.

Grönke, S., Partridge, L. (2010). The functions of insulin-like peptides in insects, in IGFs: Local repair and

survival factors throughout life span, eds Clemmons D. C., Robinson I. C. A. F., Christen Y., editors. (Dordrecht: Springer), 105-124.

Guo, S., Rena, G., Cichy, S., He, X., Cohen, P., & Unterman, T. (1999). Phosphorylation of serine 256 by protein kinase B disrupts transactivation by FKHR and mediates effects of insulin on insulin-like growth factor-binding protein-1 promoter activity through a conserved insulin response sequence. *Journal of Biological Chemistry*, *274*(24), 17184-17192.

Hahn, D. A., & Denlinger, D. L. (2007). Meeting the energetic demands of insect diapause: Nutrient storage and utilization. *Journal of Insect Physiology*, *53*(8), 760-773.

Hahn, D. A., & Denlinger, D. L. (2011). Energetics of insect diapause. *Annual Review of Entomology*, *56*(1), 103-121.

Hall, R. K., Yamasaki, T., Kucera, T., Waltner-Law, M., O'Brien, R., & Granner, D. K. (2000). Regulation of phosphoenolpyruvate carboxykinase and insulin-like growth factor-binding protein-1 gene expression by insulin. The role of winged helix/forkhead proteins. *Journal of Biological Chemistry*, *275*(39), 30169-30175.

Hamanaka, Y., Yasuyama, K., Numata, H., & Shiga, S. (2005). Synaptic connections between pigment-dispersing factor-immunoreactive neurons and neurons in the pars lateralis of the blow fly *Protophormia terraenovae*. *Journal of Comparative Neurology*, *491*(4), 390-399.

Hardin, P. E. (2005). The circadian timekeeping system of Drosophila. *Current Biology*, *15*(17), R714-22.

Hasegawa, K. (1951). Studies on the voltinism in the silkworm, *Bombyx mori* L., with special reference to the organs concerning determination of voltinism (a preliminary note). *Proceedings of the Japan Academy, 27*(10), 667-671.

Hauser, F., Cazzamali, G., Williamson, M., Blenau, W., & Grimmelikhuijzen, C. J. (2006). A review of neurohormone GPCRs present in the fruitfly *Drosophila melanogaster* and the honey bee *Apis mellifera*. *Progress in Neurobiology*, *80*(1), 1-19.

Helfrich-Förster, C. (1997). Development of pigment-dispersing hormone-immunoreactive neurons in the nervous system of *Drosophila melanogaster*. *Journal of Comparative Neurology*, *380*(3), 335-354.

Helfrich-Förster, C. (1998). Robust circadian rhythmicity of *Drosophila melanogaster* requires the presence of lateral neurons: A brain-behavioral study of disconnected mutants. *Journal of Comparative Physiology A*, *182*(4), 435-453.

Helfrich-Förster, C. (2005). Neurobiology of the fruit fly's circadian clock. *Genes, Brain, and Behavior*, *4*(2), 65-76.

Helfrich-Förster, C. (2005). PDF has found its receptor. *Neuron*, *48*(2), 161-163.

Helfrich-Förster, C., Shafer, O. T., Wülbeck, C., Grieshaber, E., Rieger, D., & Taghert, P. (2007). Development and morphology of the clock-gene-expressing lateral neurons of *Drosophila melanogaster*. *Journal of Comparative Neurology*, *500*(1), 47-70.

Helfrich-Förster, C., & Homberg, U. (1993). Pigment-dispersing hormone-immunoreactive neurons in the nervous system of wild-type *Drosophila melanogaster* and of several mutants with altered circadian rhythmicity. *Journal of Comparative Neurology*, *337*(2), 177-190.

Hentze, J. L., Carlsson, M. A., Kondo, S., Nässel, D. R., & Rewitz, K. F. (2015). The neuropeptide allatostatin A regulates metabolism and feeding decisions in Drosophila. *Scientific Reports*, *5*, 11680.

Hewes, R. S., Schaefer, A. M., & Taghert, P. H. (2000). The *cryptocephal* gene (ATF4) encodes multiple basic-leucine zipper proteins controlling molting and metamorphosis in Drosophila. *Genetics*, *155*(4), 1711-1723.

Hewes, R. S., & Taghert, P. H. (2001). Neuropeptides and neuropeptide receptors in the *Drosophila melanogaster* genome. *Genome Research*, *11*(6), 1126-1142.

Hodek, I. (1971). Induction of adult diapause in *Pyrrhocoris apterus* L. by short cold exposure. *Oecologia*, *6*(2), 109-117.

Hodková, M. (1976). Nervous inhibition of corpora allata by photoperiod in *Pyrrhocoris apterus*. *Nature*, *263*, 619-21.

Holst, B., Hastrup, H., Raffetseder, U., Martini, L., & Schwartz, T. W. (2001). Two active molecular phenotypes of the tachykinin NK1 receptor revealed by G-protein fusions and mutagenesis. *Journal of Biological Chemistry*, *276*(23), 19793-19799.

Homberg, U., Würden, S., Dircksen, H., & Rao, K. R. (1991). Comparative anatomy of pigment-dispersing hormone-immunoreactive neurons in the brain of orthopteroid insects. *Cell and Tissue Research*, *266*(2), 343-357.

Honegger, B., Galic, M., Köhler, K., Wittwer, F., Brogiolo, W., Hafen, E., & Stocker, H. (2008). Imp-L2, a putative homolog of vertebrate IGF-binding protein 7, counteracts insulin signaling in Drosophila and is essential for starvation resistance. *Journal of Biology*, *7*(3), 10.

Hong, S. H., Lee, K. S., Kwak, S. J., Kim, A. K., Bai, H., Jung, M. S., … & Yu, K. (2012). Minibrain/Dyrk1a regulates food intake through the Sir2-FOXO-sNPF/NPY pathway in Drosophila and mammals. *PLoS Genetics*, *8*(8), 1-15.

Huang, H., & Tindall, D. J. (2011). Regulation of FOXO protein stability via ubiquitination and proteasome degradation. *Biochimica et Biophysica Acta* (BBA)-*Molecular Cell Research*, *1813*(11), 1961-1964.

Huang, X., Warren, J. T., & Gilbert, L. I. (2008). New players in the regulation of ecdysone biosynthesis. *Journal of Genetics and Genomics*, *35*(1), 1-10.

Huybrechts, J., De Loof, A., & Schoofs, L. (2004). Diapausing Colorado potato beetles are devoid of short neuropeptide F I and II. *Biochemical and Biophysical Research Communications*, *317*(3), 909-916.

Hyun, S., Lee, Y., Hong, S. T., Bang, S., Paik, D., Kang, J., … & Bae, E. (2005). Drosophila GPCR Han is a receptor for the circadian clock neuropeptide PDF. *Neuron*, *48*(2), 267-78.

Iga, M., Nakaoka, T., Suzuki, Y., & Kataoka, H. (2014). Pigment dispersing factor regulates ecdysone

biosynthesis via bombyx neuropeptide G protein coupled receptor-B2 in the prothoracic glands of *Bombyx mori*. *PLoS One*, *9*(7), e103239.

Ikeno, T., Tanaka, S. I., Numata, H., & Goto, S. G. (2010). Photoperiodic diapause under the control of circadian clock genes in an insect. *BMC Biology*, *8*(1), 116.

Ikeno, T., Numata, H., & Goto, S. G. (2011a). Circadian clock genes *period* and *cycle* regulate photoperiodic diapause in the bean bug *Riptortus pedestris* males. *Journal of Insect Physiology*, *57*(7), 935-938.

Ikeno, T., Numata, H., & Goto, S. G. (2011b). Photoperiodic response requires mammalian-type cryptochrome in the bean bug *Riptortus pedestris*. *Biochemical and Biophysical Research Communications*, *410*(3), 394-397.

Ikeno, T., Ishikawa, K., Numata, H., Goto, S.G. (2013). Circadian clock gene, *Clock*, is involved in the photoperiodic response of the bean bug *Riptortus pedestris*. *Physiological entomology*, *38*(2), 157-162.

Ikeno, T., Numata, H., Goto, S. G., & Shiga, S. (2014). Involvement of the brain region containing pigment-dispersing factor-immunoreactive neurons in the photoperiodic response of the bean bug, *Riptortus pedestris*. *The Journal of Experimental Biology*, *217*(3), 453-62.

Ikeya, T., Galic, M., Belawat, P., Nairz, K., & Hafen, E. (2002). Nutrient-dependent expression of insulin-like peptides from neuroendocrine cells in the CNS contributes to growth regulation in Drosophila. *Current Biology*, *12*(15), 1293-1300.

Im, S. H., & Taghert, P. H. (2010). PDF receptor expression reveals direct interactions between circadian oscillators in Drosophila. *Journal of Comparative Neurology, 518*(11), 1925-1945.

Inagaki, H. K., Panse, K. M., & Anderson, D. J. (2014). Independent, reciprocal neuromodulatory control of sweet and bitter taste sensitivity during starvation in Drosophila. *Neuron*, *84*(4), 806-820.

Jan, L. Y., & Jan, Y. N. (1982). Peptidergic transmission in sympathetic ganglia of the frog. *The Journal of Physiology, 327*(1), 219-246.

Jaramillo, A. M., Zheng, X., Zhou, Y., Amado, D. A., Sheldon, A., Sehgal, A., & Levitan, I. B. (2004). Pattern of distribution and cycling of SLOB, Slowpoke channel binding protein, in Drosophila. *BMC Neuroscience*, *5*(3).

Johard, H. A., Yoishii, T., Dircksen, H., Cusumano, P., Rouyer, F., Helfrich-Förster, C., & Nässel, D. R. (2009). Peptidergic clock neurons in Drosophila: ion transport peptide and short neuropeptide F in subsets of dorsal and ventral lateral neurons. *Journal of Comparative Neurology*, *516*(1), 59-73.

Johnson, E. C., Shafer, O. T., Trigg, J. S., Park, J., Schooley, D. A., Dow, J. A., & Taghert, P. H. (2005). A novel diuretic hormone receptor in Drosophila: evidence for conservation of CGRP signaling. *The Journal of Experimental Biology*, *208*(7), 1239-46.

Kahsai, L., Kapan, N., Dircksen, H., Winther, Å. M. E., & Nässel, D. R. (2010a). Metabolic stress responses in Drosophila are modulated by brain neurosecretory cells that produce multiple neuropeptides. *PLoS One*, *5*(7), e11480.

Kahsai, L., Martin, J. R., & Winther, A. M. (2010b). Neuropeptides in the Drosophila central complex in modulation of locomotor behavior. *The Journal of Experimental Biology*, *213*(13), 2256-2265.

Kapan, N., Lushchak, V., Luo, J., & Nässel, D. R. (2012). Identified peptidergic neurons in the Drosophila brain regulate insulin-producing cells, stress responses and metabolism by coexpressed short neuropeptide F and corazonin. *Cellular and Molecular Life Sciences, 69*(23)*,* 4051-4066.

Kilts, J. D., Gerhardt, M. A., Richardson, M. D., Sreeram, G., Mackensen, G. B., Grocott, H. P., ... & Schwinn, D. A. (2000). β2-adrenergic and several other G protein-coupled receptors in human atrial membranes activate both Gs and Gi. *Circulation Research*, *87*(8), 705-709.

Kim, W. J., Jan, L. Y., & Jan, Y. N. (2013). A PDF/NPF neuropeptide signaling circuitry of male *Drosophila melanogaster* controls rival-induced prolonged mating. *Neuron*, *80*(5), 1190-1205.

Kim, J., & Neufeld, T. P. (2015). Dietary sugar promotes systemic TOR activation in Drosophila through AKH-dependent selective secretion of Dilp3. *Nature Communications*, *6*, 1-10.

Kim, Y. J., Spalovská-Valachová, I., Cho, K.-H., Zitnanova, I., Park, Y., Adams, M. E., & Zitnan, D. (2004). Corazonin receptor signaling in ecdysis initiation. *Proceedings of the National Academy of Sciences of the United States of America*, *101*(17), 6704-6709.

Kimura, K. D., Tissenbaum, H. A., Liu, Y., & Ruvkun, G. (1997). daf-2 , an insulin receptor–like gene that regulates longevity and diapause in *Caenorhabditis elegans*. *Science*, *277*(5328), 942-946.

Kops, G. J., de Ruiter, N. D., De Vries-Smits, A. M., Powell, D. R., Bos, J. L., & Boudewijn M. T. (1999). Direct control of the Forkhead transcription factor AFX by protein kinase B. *Nature*, *398*(6728), 630-634.

Kramer, J. M., Davidge, J. T., Lockyer, J. M., & Staveley, B. E. (2003). Expression of Drosophila FOXO regulates growth and can phenocopy starvation. *BMC Developmental Biology*, *3*(1), 5.

Kreitzman, L., & Foster, R. (2009). Seasons of Life: The biological rhythms that enable living things to thrive and survive. Yale University Press.

Krupp, J. J., Billeter, J. C., Wong, A., Choi, C., Nitabach, M. N., & Levine, J. D. (2013). Pigment-dispersing factor modulates pheromone production in clock cells that influence mating in Drosophila. *Neuron*, *79*(1), 54-68.

Kubrak, O. I., Kučerová, L., Theopold, U., & Nässel, D. R. (2014). The sleeping beauty: How reproductive diapause affects hormone signaling, metabolism, immune response and somatic maintenance in *Drosophila melanogaster*. *PLoS One*, *9*(11), e113051.

Kubrak, O. I., Lushchak, V., Zandawala, M., & Nässel, D. R. (2016). Systemic corazonin signalling modulates stress responses and metabolism in Drosophila. *Open Biology*, *6*(11), 160152.

Kučerová, L., Kubrak, O. I., Bengtsson, J. M., Strnad, H., Nylin, S., Theopold, U., & Nässel, D. R. (2016). Slowed aging during reproductive dormancy is reflected in genome-wide transcriptome changes in *Drosophila melanogaster*. *BMC Genomics*, *17*(1), 50.

Kula-Eversole, E., Nagoshi, E., Shang, Y., Rodriguez, J., Allada, R., & Rosbash, M. (2010). Surprising gene

expression patterns within and between PDF-containing circadian neurons in Drosophila. *Proceedings of the National Academy of Sciences of the United States of America*, *107*(30), 13497-502.

Kwak, S. J., Hong, S. H., Bajracharya, R., Yang, S. Y., Lee, K. S., & Yu, K. (2013). Drosophila adiponectin receptor in insulin producing cells regulates glucose and lipid metabolism by controlling insulin secretion. *PLoS One*, *8*(7), e68641.

LaFever, L., & Drummond-Barbosa, D. (2005). Direct control of germline stem cell division and cyst growth by neural insulin in Drosophila. *Science*, *309*(5737), 1071-1073.

Lai, S.-L., & Lee, T. (2006). Genetic mosaic with dual binary transcriptional systems in Drosophila. *Nature Neuroscience*, *9*(5), 703-709.

Lankinen, P. (1986). Geographical variation in circadian eclosion rhythm and photoperiodic adult diapause in *Drosophila littoralis*. *Journal of Comparative Physiology A*, *159*(1), 123-142.

Layalle, S., Arquier, N., & Léopold, P. (2008). The TOR pathway couples nutrition and developmental timing in Drosophila. *Developmental Cell*, *15*(4), 568-577.

Lear, B. C., Merrill, C. E., Lin, J. M., Schroeder, A., Zhang, L., & Allada, R. (2005). A G Protein-coupled receptor, groom-of-PDF, is required for PDF neuron action in circadian behavior. *Neuron*, *48*(2), 221-227.

Lee, K. S., Kwon, O. Y., Lee, J. H., Kwon, K., Min, K. J., Jung, S. A., … & Yu, K. (2008). Drosophila short neuropeptide F signalling regulates growth by ERK-mediated insulin signalling. *Nature Cell Biology*, *10*(4), 468-75.

Lee, K. S., You, K. H., Choo, J. K., Han, Y. M., & Yu, K. (2004). Drosophila short neuropeptide F regulates food intake and body size. *Journal of Biological Chemistry*, *279*(49), 50781-50789.

Li, Q., & Gong, Z. (2015). Cold-sensing regulates Drosophila growth through insulin-producing cells. *Nature Communications*, *6*:10083.

Li, X. F., Bowe, J. E., Mitchell, J. C., Brain, S. D., Lightman, S. L., & O'Byrne, K. T. (2004). Stress-induced suppression of the gonadotropin-releasing hormone pulse generator in the female rat: A novel neural action for calcitonin gene-related peptide. *Endocrinology*, *145*(4), 1556-1563.

Liang, X., Holy, T. E., & Taghert, P. H. (2016). Synchronous Drosophila circadian pacemakers display nonsynchronous Ca^{2+} rhythms *in vivo*. *Science*, *351*(6276), 976-981.

Liang, X., Holy, T. E., & Taghert, P. H. (2017). A series of suppressive signals within the Drosophila circadian neural circuit generates sequential daily outputs. *Neuron*. *94*(6):1173-1189

Lindenburg, L., & Merkx, M. (2014). Engineering genetically encoded FRET sensors. Sensors, *14*(7), 11691-11713.

Lissandron, V., Rossetto, M. G., Erbguth, K., Fiala, A., Daga, A., & Zaccolo, M. (2007). Transgenic fruit-flies expressing a FRET-based sensor for *in vivo* imaging of cAMP dynamics. *Cellular Signalling*, *19*(11), 2296-2303.

Liu, Y., Liao, S., Veenstra, J. A., & Nässel, D. R. (2016). Drosophila insulin-like peptide 1 (DILP1) is transiently expressed during non-feeding stages and reproductive dormancy. *Scientific Reports*, *6*, 26620.

Lu, H. L., & Pietrantonio, P. V. (2011). Immunolocalization of the short neuropeptide F receptor in queen brains and ovaries of the red imported fire ant (*Solenopsis invicta Buren*). *BMC neuroscience*, *12*(1), 57.

Luo, J., Becnel, J., Nichols, C. D., & Nässel, D. R. (2012). Insulin-producing cells in the brain of adult Drosophila are regulated by the serotonin 5-HT1A receptor. *Cellular and Molecular Life Sciences*, *69*(3), 471-84.

Luo, J., Lushchak, V., Goergen, P., Williams, M. J., & Nässel, D. R. (2014). Drosophila insulin-producing cells are differentially modulated by serotonin and octopamine receptors and affect social behavior. *PLoS One*, *9*(6), e99732

MacRae, T. H. (2010). Gene expression, metabolic regulation and stress tolerance during diapause. *Cellular and Molecular Life Sciences*, *67*(14), 2405-2424.

Marchal, E., Vandersmissen, H. P., Badisco, L., Van de Velde, S., Verlinden, H., Iga, M., … & Broeck, J. V. (2010). Control of ecdysteroidogenesis in prothoracic glands of insects: A review. *Peptides*, *31*(3), 506-519.

Masuyama, K., Zhang, Y., Rao, Y., & Wang, J. W. (2012). Mapping neural circuits with activity-dependent nuclear import of a transcription factor. *Journal of neurogenetics*, *26*(1), 89-102.

Fernández, M. P., Berni, J., & Ceriani, M. F. (2008). Circadian remodeling of neuronal circuits involved in rhythmic behavior. *PLoS Biology*, *6*(1), e69.

McClure, K. D., & Heberlein, U. (2013). A small group of neurosecretory cells expressing the transcriptional regulator apontic and the neuropeptide corazonin mediate ethanol sedation in Drosophila. *The Journal of Neuroscience : The Official Journal of the Society for Neuroscience*, *33*(9), 4044-54.

McElwee, J. J., Schuster, E., Blanc, E., Thornton, J., & Gems, D. (2006). Diapause-associated metabolic traits reiterated in long-lived daf-2 mutants in the nematode *Caenorhabditis elegans*. *Mechanisms of ageing and development, 127*(5), 458-472.

Menegazzi, P., Vanin, S., Yoshii, T., Rieger, D., Hermann, C., Dusik, V., … Costa, R. (2013). Drosophila clock neurons under natural conditions. *Journal of Biological Rhythms*, *28*(1), 3-14.

Mertens, I., Meeusen, T., Huybrechts, R., De Loof, A., & Schoofs, L. (2002). Characterization of the short neuropeptide F receptor from *Drosophila melanogaster*. *Biochemical and Biophysical Research Communications*, *297*(5), 1140-1148.

Mertens, I., Vandingenen, A., Johnson, E. C., Shafer, O. T., Li, W., Trigg, J. S., … Taghert, P. H. (2005). PDF receptor signaling in Drosophila contributes to both circadian and geotactic behaviors. *Neuron*, *48*(2), 213-219.

Meuti, M. E., Stone, M., Ikeno, T., & Denlinger, D. L. (2015). Functional circadian clock genes are essential for the overwintering diapause of the Northern house mosquito, *Culex pipiens*. *The Journal of Experimental Biology*, *218*(3), 412-22.

Montelli, S., Mazzotta, G., Vanin, S., Caccin, L., Corrà, S., De Pittà, C., ... & Costa, R. (2015). *period* and *timeless*

mRNA splicing profiles under natural conditions in *Drosophila melanogaster*. *Journal of Biological Rhythms*, *30*(3), 217-227.

Montrose-Rafizadeh, C., Avdonin, P., Garant, M. J., Rodgers, B. D., Kole, S., Yang, H., ... & Bernier, M. (1999). Pancreatic glucagon-like peptide-1 receptor couples to multiple G proteins and activates mitogen-activated protein kinase pathways in Chinese hamster ovary cells. *Endocrinology*, *140*(3), 1132-1140.

Nadal, A., Marrero, P. F., & Haro, D. (2002). Down-regulation of the mitochondrial 3-hydroxy-3-methylglutaryl-CoA synthase gene by insulin: the role of the forkhead transcription factor FKHRL1. *The Biochemical Journal*, *366*(1), 289-97.

Nakai, J., Ohkura, M., & Imoto, K. (2001). A high signal-to-noise Ca(2+) probe composed of a single green fluorescent protein. *Nature Biotechnology*, *19*(2), 137-41.

Nässel, D. R. (1993). Neuropeptides in the insect brain: a review. *Cell and Tissue Research*, *273*(1), 1-29.

Nässel, D. R., Enell, L. E., Santos, J. G., Wegener, C., & Johard, H. A. (2008). A large population of diverse neurons in the Drosophila central nervous system expresses short neuropeptide F, suggesting multiple distributed peptide functions. *BMC Neuroscience*, *9*(1), 90.

Nässel, D. R., & Winther, Å. M. (2010). Drosophila neuropeptides in regulation of physiology and behavior. *Progress in Neurobiology*, *92*(1), 42-104.

Nässel, D. R., Kubrak, O. I., Liu, Y., Luo, J., & Lushchak, O. V. (2013). Factors that regulate insulin producing cells and their output in Drosophila. *Frontiers in Physiology*, 4, p. 252.

Nijhout, H. F., & Williams, C. M. (1974). Control of moulting and metamorphosis in the tobacco hornworm, *Manduca sexta* (L.): cessation of juvenile hormone secretion as a trigger for pupation. *Journal of Experimental Biology*, *61*(2), 493-501.

Nikolaev, V. O., Bünemann, M., Hein, L., Hannawacker, A., & Lohse, M. J. (2004). Novel single chain cAMP sensors for receptor-induced signal propagation. *Journal of Biological Chemistry*, *279*(36), 37215-37218.

Nitabach, M. N., & Taghert, P. H. (2008). Organization of the Drosophila circadian control circuit. *Current Biology*, *18*(2), 84-93.

Offermanns, S., Iida-Klein, A., Segre, G. V., & Simon, M. I. (1996). G alpha q family members couple parathyroid hormone (PTH)/PTH-related peptide and calcitonin receptors to phospholipase C in COS-7 cells. *Molecular Endocrinology*, *10*(5), 566-574.

Okamoto, N., Yamanaka, N., Yagi, Y., & Nishida, Y. (2009). A fat body-derived IGF-like peptide regulates postfeeding growth in Drosophila. *Developmental Cell*, *17*(6), 885-891.

Okamoto, N., Nakamori, R., Murai, T., Yamauchi, Y., Masuda, A. & Nishimura, T. (2013). A secreted decoy of InR antagonizes insulin/IGF signaling to restrict body growth in Drosophila. *Genes and Development*, *27*, 87-97.

Palanche, T., Ilien, B., Zoffmann, S., Reck, M. P., Bucher, B., Edelstein, S. J., & Galzi, J. L. (2001). The neurokinin A receptor activates calcium and cAMP responses through distinct conformational states. *Journal of*

Biological Chemistry, *276*(37), 34853-34861.

Park, J. H., Helfrich-Förster, C., Lee, G., Liu, L., Rosbash, M., & Hall, J. C. (2000). Differential regulation of circadian pacemaker output by separate clock genes in Drosophila. *Proceedings of the National Academy of Sciences of the United States of America*, *97*(7), 3608-3613.

Park, D., Veenstra, J. A., Park, J. H., & Taghert, P. H. (2008). Mapping peptidergic cells in Drosophila: where DIMM fits in. PloS One, 3(3), e1896.

Pavelka, J., Shimada, K., & Kostal, V. (2003). Timeless: A link between fly's circadian and photoperiodic clocks? *European Journal of Entomology*, *100*(2), 255-265.

Pegoraro, M., Zonato, V., Tyler, E. R., Fedele, G., Kyriacou, C. P., & Tauber, E. (2017). Geographical analysis of diapause inducibility in European *Drosophila melanogaster* populations. *Journal of Insect Physiology*, *98*, 238-244.

Peng, Y., Stoleru, D., Levine, J. D., Hall, J. C., & Rosbash, M. (2003). Drosophila free-running rhythms require intercellular communication. *PLoS Biology*, *1*(1), e13.

Pengelley, E. T., & Fisher, K. C. (1957). Onset and cessation of hibernation under constant temperature and light in the golden-mantled ground squirrel (*Citellus lateralis*). *Nature*, *180*, 1371–1372.

Persson, M. G., Eklund, M. B., Dircksen, H., Eric Muren, J., & Nässel, D. R. (2001). Pigment-dispersing factor in the locust abdominal ganglia may have roles as circulating neurohormone and central neuromodulator. *Journal of Neurobiology*, *48*(1), 19-41.

Peschel, N., & Helfrich-Förster, C. (2011). Setting the clock - By nature: Circadian rhythm in the fruitfly *Drosophila melanogaster*. *FEBS Letters*, *585*(10), 1435-1442.

Petryk, A., Warren, J. T., Marqués, G., Jarcho, M. P., Gilbert, L. I., Kahler, J., … & O'Connor, M. B. (2003). Shade is the Drosophila P450 enzyme that mediates the hydroxylation of ecdysone to the steroid insect molting hormone 20-hydroxyecdysone. *Proceedings of the National Academy of Sciences of the United States of America*, *100*(24), 13773-13778.

Poelchau, M. F., Reynolds, J. A, Elsik, C. G., Denlinger, D. L., & Armbruster, P. A. (2013). RNA-Seq reveals early distinctions and late convergence of gene expression between diapause and quiescence in the Asian tiger mosquito, *Aedes albopictus*. *The Journal of Experimental Biology*, *216*(21), 4082-90.

Price, E. O. (1999). Behavioral development in animals undergoing domestication. *Applied Animal Behaviour Science*, *65*(3), 245-271.

Price, M. D., Merte, J., Nichols, R., Koladich, P. M., Tobe, S. S., & Bendena, W. G. (2002). *Drosophila melanogaster* flatline encodes a myotropin orthologue to *Manduca sexta* allatostatin. *Peptides*, *23(*4), 787-794.

Puig, O., Marr, M. T., Ruhf, M. L., & Tjian, R. (2003). Control of cell number by Drosophila FOXO: downstream and feedback regulation of the insulin receptor pathway. *Genes & Development*, *17*(16), 2006-2020.

Rajan, A., & Perrimon, N. (2012). Drosophila cytokine unpaired 2 regulates physiological homeostasis by remotely controlling insulin secretion. *Cell*, *2*(151), 123-137.

Readio, J., Chen, M. H., & Meola, R. (1999). Juvenile hormone biosynthesis in diapausing and nondiapausing *Culex pipiens* (Diptera: Culicidae). *Journal of Medical Entomology*, *36*(3), 355-360.

Renn, S. C. ., Park, J. H., Rosbash, M., Hall, J. C., & Taghert, P. H. (1999). A *pdf* neuropeptide gene mutation and ablation of PDF neurons each cause severe abnormalities of behavioral circadian rhythms in Drosophila. *Cell*, *99*(7), 791-802.

Richard, D. S., Gilbert, M., Crum, B., Hollinshead, D. M., & Scheswohl, D. (2001). Yolk protein endocytosis by oocytes in *Drosophila melanogaster*: immunofluorescent localization of clathrin, adaptin and the yolk protein receptor. *Journal of Insect Physiology*, *47*, 715-723.

Richard, D. S., Rybczynski, R., Wilson, T. G., Wang, Y., Wayne, M. L., Zhou, Y., … & Harshman, L. G. (2005). Insulin signaling is necessary for vitellogenesis in *Drosophila melanogaster* independent of the roles of juvenile hormone and ecdysteroids: Female sterility of the *chico*^{1} insulin signaling mutation is autonomous to the ovary. *Journal of Insect Physiology*, *51*(4), 455-464.

Richard, D. S., Watkins, N. L., Serafin, R. B., & Gilbert, L. I. (1998). Ecdysteroids regulate yolk protein uptake by *Drosophila melanogaster* oocytes. *Journal of Insect Physiology*, *44*(7), 637-644.

Riddiford, L. M. (1994). Cellular and molecular actions of juvenile hormone. I. General considerations and premetamorphic actions. *Advances in Insect Physiology*, *24*, 213-274.

Rieger, D., Shafer, O. T., Tomioka, K., & Helfrich-Förster, C. (2006). Functional analysis of circadian pacemaker neurons in *Drosophila melanogaster*. *Journal of Neuroscience*, *26*(9), 2531-2543.

Rieger, D., Fraunholz, C., Popp, J., Bichler, D., Dittmann, R., & Helfrich-Förster, C. (2007). The fruit fly *Drosophila melanogaster* favors dim light and times its activity peaks to early dawn and late dusk. *Journal of Biological Rhythms*, *22*(5), 387-399.

Riihimaa, A. J., & Kimura, M. T. (1988). A mutant strain of *Chymomyza costata* (Diptera, Drosophilidae) insensitive to diapause-inducing action of photoperiod. *Physiological Entomology*, *13*(4), 441-445.

Rocheville, M., Lange, D. C., Kumar, U., Patel, S. C., Patel, R. C., & Patel, Y. C. (2000). Receptors for dopamine and somatostatin: formation of hetero-oligomers with enhanced functional activity. *Science, 288*(5463), 154-157.

Root, C. M., Ko, K. I., Jafari, A., & Wang, J. W. (2011). Presynaptic facilitation by neuropeptide signaling mediates odor-driven food search. *Cell, 145*(1), 133-144.

Rosato, E., Trevisan, A., Sandrelli, F., Zordan, M., Kyriacou, C. P., & Costa, R. (1997). Conceptual translation of timeless reveals alternative initiating methionines in Drosophila. *Nucleic acids research*, *25*(3), 455-457.

Rountree, D. B., & Bollenbacher, W. E. (1986). The release of the prothoracicotropic hormone in the tobacco hornworm, *Manduca sexta*, is controlled intrinsically by juvenile hormone. *Journal of Experimental Biology*, *120*(1), 41-58.

Rozenfeld, R., & Devi, L. A. (2010). Receptor heteromerization and drug discovery. *Trends in Pharmacological Sciences*, *31*(3), 124-130.

Ruan, Y., Chen, C., Cao, Y., & Garofalo, R. S. (1995). The Drosophila insulin receptor contains a novel carboxyl-terminal extension likely to play an important role in signal transduction. *Journal of Biological Chemistry*, *270*(9), 4236-4243.

Rulifson, E. J., Kim, S. K., & Nusse, R. (2002). Ablation of insulin-producing neurons in flies: growth and diabetic phenotypes. *Science*, *296*(5570), 1118-1121.

Salminen, T. S., Vesala, L., Laiho, A., Merisalo, M., Hoikkala, A., & Kankare, M. (2015). Seasonal gene expression kinetics between diapause phases in *Drosophila virilis* group species and overwintering differences between diapausing and non-diapausing females. *Scientific reports*, *5*, 11197.

Sandrelli, F., Tauber, E., Pegoraro, M., Mazzotta, G., Cisotto, P., Landskron, J., ... & Costa, R. (2007). A molecular basis for natural selection at the timeless locus in *Drosophila melanogaster*. Science, *316*(5833), 1898-1900.

Sano, H., Nakamura, A., Texada, M. J., Truman, J. W., Ishimoto, H., Kamikouchi, A., … & Kojima, M. (2015). The nutrient-responsive hormone CCHamide-2 controls growth by regulating insulin-like peptides in the brain of *Drosophila melanogaster*. *PLoS Genetics*, *11*(5), e1005209.

Saunders, D. S., Richard, D. S., Applebaum., S. W., Ma, M., & Gilbert, L. I. (1990). Photoperiodic diapause in *Drosophila melanogaster* involves a block to the juvenile hormone regulation of ovarian maturation. *General and Comparative Endocrinology*, *79*(2), 174-84.

Saunders, D. S. (1990). The circadian basis of ovarian diapause regulation in *Drosophila melanogaster*: is the period gene causally involved in photoperiodic time measurement? *Journal of Biological Rhythms*, *5*(4), 315-331.

Saunders, D. S., Henricht, V. C., & Gilbert, L. I. (1989). Induction of diapause in *Drosophila melanogaster*: photoperiodic regulation and the impact of arrhythmic clock mutations on time measurement. *Proceedings of the National Academy of Sciences*, *86*(10), 3748-3752.

Schiesari, L., Andreatta, G., Kyriacou, C. P., O'Connor, M. B., & Costa, R. (2016). The insulin-like proteins dILPs-2/5 determine diapause inducibility in Drosophila. *PLoS One*, *11*(9), e0163680.

Schiesari, L., Kyriacou, C. P., & Costa, R. (2011). The hormonal and circadian basis for insect photoperiodic timing. *FEBS Letters*, *585*(10), 1450-1460.

Schlichting, M., Menegazzi, P., Lelito, K. R., Yao, Z., Buhl, E., Dalla Benetta, E., ... & Shafer, O. T. (2016). A neural network underlying circadian entrainment and photoperiodic adjustment of sleep and activity in Drosophila. *Journal of Neuroscience*, *36*(35), 9084-9096.

Schmidt, P. S., Matzkin, L., Ippolito, M., & Eanes, W. F. (2005a). Geographic variation in diapause incidence, life-history traits, and climatic adaptation in *Drosophila melanogaster*. *Evolution*, *59*(8), 1721-32.

Schmidt, P. S., Paaby, A. B., & Heschel, M. S. (2005b). Genetic variance for diapause expression and associated life histories in *Drosophila melanogaster*. *Evolution*, *59*(12), 2616-2625.

Schmoll, D., Walker, K. S., Alessi, D. R., Grempler, R., Burchell, A., Guo, S., … Unterman, T. G. (2000). Regulation

of glucose-6-phosphatase gene expression by protein kinase Bα and the forkhead transcription factor FKHR: Evidence for insulin response unit (IRU)-dependent and independent effects of insulin on promoter activity. *Journal of Biological Chemistry*, *275*(46), 36324-36333.

Schneider, L. E., Sun, E. T., Garland, D. J., & Taghert, P. H. (1993). An immunocytochemical study of the FMRFamide neuropeptide gene products in Drosophila. *Journal of Comparative Neurology*, *337*(3), 446-460.

Schoofs, L., Clynen, E., Cerstiaens, A., Baggerman, G., Wei, Z., Vercammen, T., … & Tanaka, S. (2001). Newly discovered functions for some myotropic neuropeptides in locusts. *Peptides*, *22*(2), 219-227.

Selcho, M., Millán, C., Palacios-Muñoz, A., Ruf, F., Ubillo, L., Chen, J., ... & Ewer, J. (2017). Central and peripheral clocks are coupled by a neuropeptide pathway in Drosophila. *Nature Communications*, 8: 15563.

Seluzicki, A., Flourakis, M., Kula-Eversole, E., Zhang, L., Kilman, V., & Allada, R. (2014). Dual PDF signaling pathways reset clocks via TIMELESS and acutely excite target neurons to control circadian behavior. *PLoS Biology*, *12*(3), e1001810.

Sha, K., Choi, S. H., Im, J., Lee, G. G., Loeffler, F., & Park, J. H. (2014). Regulation of ethanol-related behavior and ethanol metabolism by the corazonin neurons and corazonin receptor in *Drosophila melanogaster*. *PLoS One*, *9*(1). e87062.

Shafer, O. T., Kim, D. J., Dunbar-Yaffe, R., Nikolaev, V. O., Martin, J., & Taghert, P. H. (2008). Widespread receptivity to neuropeptide PDF throughout the neuronal circadian clock network of Drosophila revealed by real-time cyclic AMP imaging. *Neuron*, *58*(2), 223-237.

Shang, Y., Donelson, N. C., Vecsey, C. G., Guo, F., Rosbash, M. & Griffith, L. C. (2013). Short neuropeptide F is a sleep-promoting inhibitory modulator. *Neuron*, *80*(1), 171-183.

Shiga, S., Davis, N. T., & Hildebrand, J. G. (2003). Role of neurosecretory cells in the photoperiodic induction of pupal diapause of the tobacco hornworm *Manduca sexta*. *Journal of Comparative Neurology*, *462*(3), 275-285.

Shiga, S., & Numata, H. (2007). Neuroanatomical approaches to the study of insect photoperiodism. *Photochemistry and Photobiology*, *83*(1), 76-86.

Shiga, S., & Numata, H. (2009). Roles of PER immunoreactive neurons in circadian rhythms and photoperiodism in the blow fly, *Protophormia terraenovae*. *The Journal of Experimental Biology*, *212*(6), 867-77.

Sim, C., & Denlinger, D. L. (2008). Insulin signaling and FOXO regulate the overwintering diapause of the mosquito *Culex pipiens*. *Proceedings of the National Academy of Sciences of the United States of America*, *105*(18), 6777-81.

Sim, C., & Denlinger, D. L. (2013). Insulin signaling and the regulation of insect diapause. *Frontiers in Physiology*, *4*, 189.

Skrzydelski, D., Lhiaubet, A. M., Lebeau, A., Forgez, P., Yamada, M., Hermans, E., ... & Pelaprat, D. (2003). Differential involvement of intracellular domains of the rat NTS1 neurotensin receptor in coupling to G

proteins: a molecular basis for agonist-directed trafficking of receptor stimulus. *Molecular Pharmacology*, *64*(2), 421-429.

Slaidina, M., Delanoue, R., Gronke, S., Partridge, L., & Léopold, P. (2009). A Drosophila insulin-like peptide promotes growth during nonfeeding states. *Developmental Cell*, *17*(6), 874-884.

Socha, R., Šula, J., Kodrík, D., & Gelbič, I. (1991). Hormonal control of vitellogenin synthesis in *Pyrrhocoris apterus* (L.) (Heteroptera). *Journal of Insect Physiology*, *37*(11), 805-816.

Söderberg, J. A., Birse, R. T., & Nässel, D. R. (2011). Insulin production and signaling in renal tubules of Drosophila is under control of tachykinin-related peptide and regulates stress resistance. *PLoS One*, *6*(5), e19866.

Spielman, A. (1974). Effect of synthetic juvenile hormone on ovarian diapause of *Culex pipiens* mosquitoes. *Journal of Medical Entomology*, *11*(2), 223-225.

Stanley, C. E., & Kulathinal, R. J. (2016). Genomic signatures of domestication on neurogenetic genes in *Drosophila melanogaster*. *BMC Evolutionary Biology*, *16*(1), 6.

Stewart, B. A., Atwood, H. L., Renger, J. J., Wang, J., & Wu, C. F. (1994). Improved stability of Drosophila larval neuromuscular preparations in haemolymph-like physiological solutions. *Journal of Comparative Physiology A*, *175*(2), 179-191.

Stoleru, D., Peng, Y., Agosto, J., & Rosbash, M. (2004). Coupled oscillators control morning and evening locomotor behaviour of Drosophila. *Nature*, *431*(7010), 862-868.

Talsma, A. D., Christov, C. P., Terriente-Felix, A., Linneweber, G. A., Perea, D., Wayland, M., … & Miguel-Aliaga, I. (2012). Remote control of renal physiology by the intestinal neuropeptide pigment-dispersing factor in Drosophila. *Proceedings of the National Academy of Sciences*, *109*(30), 12177-12182.

Taniguchi, C. M., Emanuelli, B., & Kahn, C. R. (2006). Critical nodes in signalling pathways: insights into insulin action. *Nature reviews Molecular Cell Biology*, *7*(2), 85-96.

Tatar, M., Chien, S. A., & Priest, N. K. (2001). Negligible senescence during reproductive dormancy in *Drosophila melanogaster*. *The American Naturalist*, *158*(3), 248-258.

Tatar, M., Bartke, A., & Antebi, A. (2003). The endocrine regulation of aging by insulin-like signals. *Science*, *299*(5611), 1346-1351.

Tatar, M., Kopelman, A., Epstein, D., Tu, M. P., Yin, C. M., & Garofalo, R. S. (2001). A mutant Drosophila insulin receptor homolog that extends life-span and impairs neuroendocrine function. *Science*, *292*(5514), 107-10.

Tauber, E., Zordan, M., Sandrelli, F., Pegoraro, M., Osterwalder, N., Breda, C., … & Costa, R. (2007). Natural selection favors a newly derived *timeless* allele in *Drosophila melanogaster*. *Science*, *316*(5833), 1895-8.

Tauber, M. J., Tauber, C. A., & Masaki, S. (1986). *Seasonal Adaptations of Insects*. (Oxford University Press, USA.

Tawfik, A. I., Tanaka, S., De Loof, A., Schoofs, L., Baggerman, G., Waelkens, E., … & Pener, M. P. (1999). Identification of the gregarization-associated dark-pigmentotropin in locusts through an albino mutant. *Proceedings of the National Academy of Sciences of the United States of America*, *96*(12), 7083-7087.

Teleman, A. A. (2010). Molecular mechanisms of metabolic regulation by insulin in Drosophila. *Biochemical Journal*, *425*(1), 13-26.

Tian, L., Hires, S. A., Mao, T., Huber, D., Chiappe, M. E., Chalasani, S. H., ... & Bargmann, C. I. (2009). Imaging neural activity in worms, flies and mice with improved GCaMP calcium indicators. *Nature Methods*, *6*(12), 875-881.

Tran, H., Brunet, A., Griffith, E. C., & Greenberg, M. E. (2003). The Many Forks in FOXO's Road. *Science's STKE*, *2003*(172), RE5.

Tu, M. P., Yin, C. M., & Tatar, M. (2005). Mutations in insulin signaling pathway alter juvenile hormone synthesis in *Drosophila melanogaster*. *General and Comparative Endocrinology*, *142*(3), 347-356.

Truman, J. W., & Riddiford, L. M. (2002). Endocrine insights into the evolution of metamorphosis in insects. *Annual Review of Entomology*, *47*(1), 467-500.

Vanin, S., Bhutani, S., Montelli, S., Menegazzi, P., Green, E., Pegoraro, M., … Kyriacou, C. (2012). Unexpected features of Drosophila circadian behavioural rhythms under natural conditions. *Nature*, *484*(7394), 371-375.

Vecsey, C. G., Pírez, N., & Griffith, L. C. (2014). The Drosophila neuropeptides PDF and sNPF have opposing electrophysiological and molecular effects on central neurons. *Journal of Neurophysiology*, *111*(5), 1033-45.

Veenstra, J. A. (1989). Isolation and structure of corazonin, a cardioactive peptide from the American cockroach. *FEBS Letters*, *250*(2), 231-234.

Veenstra, J. A., Agricola, H. J., & Sellami, A. (2008). Regulatory peptides in fruit fly midgut. *Cell and Tissue Research*, *334*(3), 499-516.

Villablanca, A. C., Murphy, C. J., & Reid, T. W. (1994). Growth-promoting effects of substance P on endothelial cells in vitro. Synergism with calcitonin gene-related peptide, insulin, and plasma factors. *Circulation research*, *75*(6), 1113-1120.

Wang, J. W., Wong, A. M., Flores, J., Vosshall, L. B., & Axel, R. (2003). Two-photon calcium imaging reveals an odor-evoked map of activity in the fly brain. *Cell*, *112*(2), 271-282.

Williams, C. M., & Adkisson, P. L. (1964). An endocrine mechanism for the photoperiodic control of pupal diapause in the oak silkworm, *Antheraea pernyi*. *Biological Bulletin*, *127*(3), 511-525.

Williams, K. D., Busto, M., Suster, M. L., So, A. K. C., Ben-Shahar, Y., Leevers, S. J., & Sokolowski, M. B. (2006). Natural variation in *Drosophila melanogaster* diapause due to the insulin-regulated PI3-kinase. *Proceedings of the National Academy of Sciences*, *103*(43), 15911-15915.

Winther, Å. M., Acebes, A., & Ferrús, A. (2006). Tachykinin-related peptides modulate odor perception and

locomotor activity in Drosophila. *Molecular and Cellular Neuroscience*, *31*(3), 399-406.

Wise, S., Davis, N. T., Tyndale, E., Noveral, J., Folwell, M. G., Bedian, V., … & Siwicki, K. K. (2002). Neuroanatomical studies of *period* gene expression in the hawkmoth, *Manduca sexta*. *Journal of Comparative Neurology*, *447*(4), 366-380.

Wu, V., Yang, M., McRoberts, J. A., Ren, J., Seensalu, R., Zeng, N., ... & Walsh, J. H. (1997). First intracellular loop of the human cholecystokinin-A receptor is essential for cyclic AMP signaling in transfected HEK-293 cells. *Journal of Biological Chemistry*, *272*(14), 9037-9042.

Wülbeck, C., Grieshaber, E., & Helfrich-Förster, C. (2008). Pigment-dispersing factor (PDF) has different effects on Drosophila's circadian clocks in the accessory medulla and in the dorsal brain. *Journal of Biological Rhythms*, *23*(5), 409-424.

Yang, C. H., Belawat, P., Hafen, E., Jan, L. Y., & Jan, Y. N. (2008). Drosophila egg-laying site selection as a system to study simple decision-making processes. *Science, 319*(5870), 1679-83.

Yasuyama, K., Hase, H., & Shiga, S. (2015). Neuroanatomy of pars intercerebralis neurons with special reference to their connections with neurons immunoreactive for pigment-dispersing factor in the blow fly *Protophormia terraenovae*. *Cell and Tissue Research*, *362*(1), 33-43.

Yoshii, T., Wülbeck, C., Sehadova, H., Veleri, S., Bichler, D., Stanewsky, R., & Helfrich-Förster, C. (2009). The neuropeptide pigment-dispersing factor adjusts period and phase of Drosophila's clock. *Journal of Neuroscience*, *29*(8), 2597-2610.

Zhao, X., Bergland, A. O., Behrman, E. L., Gregory, B. D., Petrov, D. A., & Schmidt, P. S. (2016). Global transcriptional profiling of diapause and climatic adaptation in *Drosophila melanogaster*. *Molecular Biology and Evolution*, *33*(3), 707-720.

Zhou, L., Schnitzler, A., Agapite, J., Schwartz, L. M., Steller, H., & Nambu, J. R. (1997). Cooperative functions of the reaper and head involution defective genes in the programmed cell death of Drosophila central nervous system midline cells. *Proceedings of the National Academy of Sciences*, *94*(10), 5131-5136.

Zheng, X., Yang, Z., Yue, Z., Alvarez, J. D., & Sehgal, A. (2007). FOXO and insulin signaling regulate sensitivity of the circadian clock to oxidative stress. *Proceedings of the National Academy of Sciences of the United States of America*, *104*(40), 15899-15904.

Zonato, V., Collins, L., Pegoraro, M., Tauber, E., & Kyriacou, C. P. (2017). Is diapause an ancient adaptation in Drosophila? *Journal of Insect Physiology*, *98*, 267-274.

Zupanc, G. K. (1996). Peptidergic transmission: from morphological correlates to functional implications. *Micron*, *27*(1), 35-91.

ACKNOWLEDGEMENTS

First and foremost, I would like to thank my Supervisor, Prof. Rodolfo Costa, for giving me the opportunity to work in his lab as a PhD student. I am grateful for his ideas and guidance during this research work. I would also like to express my gratitude to Dr. Gabriella Mazzotta for being second supervisor of this project, for her comments and suggestions on my work.

Special thanks to Dr. Gabriele Andreatta, for teaching me how to work on diapause in flies. His constructive recommendations on this project have been really useful.

I am grateful for the assistance given by Dr. Stefano Bastianello, who greatly helped me with all the experiments with the semi-natural conditions.

Special thanks to Prof. Charlotte Förster who kindly hosted me in her lab for a period of 5 months. I appreciate her insightful comments and I am thankful for her for providing me with important directions. I am very thankful to Dr. Christiane Hermann-Luibl for the continuous support of my imaging experiments during my stay in Würzburg.

My sincere thanks also go to Prof. Charalambos Kyriacou, for his contribution and continuous help with my project. I would also like to thank Dr. Ezio Rosato for his useful recommendations on my work. My grateful thanks are also extended to Ane Martin Anduaga for all the enjoyable and enlightening conversations we shared while working on closely related projects.

I gratefully acknowledge the opportunity of doing my PhD in the INsecTIME Marie Curie ITN and having been involved in a network led by great experts of the field. I wish to thank all the members of this nice consortium for their contribution to my project. I would like to acknowledge the help provided by Prof. Paul H. Taghert whose comments, suggestions and useful critiques were much appreciated.

I also would like to thank my lab colleagues at the University of Padua for all their help during these last years. I am also grateful to all the members of Charlotte Förster's group for their support and hospitality during the time I spent working in her lab.

Last but not least, I would like to thank my family and friends for their support and encouragement throughout this PhD.

APPENDIX

Table 1. The timeless background of the Drosophila strains used in this study, determined by genotyping PCR.

ls = long and short isoforms, s = short variant

Strain	***timeless isoform***
Crz_1-Gal4	*ls*
Crz_2-Gal4	*ls*
dilp2(p)-Gal4	*s*
elav-Gal4	*ls*
gal1118	*ls*
han	*ls*
Hu-S	*s*
Hu-LS	*ls*
Insp3-Gal4	*s*
oregon-R	*ls*
Pdf-Gal4	*s*
R6-Gal4	*s*
UAS-2xsNPF	*ls*
UAS-Crz-$RNAi_1$	*ls*
UAS-Crz-$RNAi_2$	*ls*
UAS-hid	*s*
UAS-kir2.1	*s*
UAS-Na^+ChBac	*s*
UAS-Ork	*s*
UAS-Pdf	*s*
UAS-sNPFR1-DN	*s*
WTALA-S	*s*
WTALA-LS	*ls*

Table 2. Summary table of results obtained in diapause assays.

Data are shown in the order they appear in the Results chapter.

Genotype	***Diapause level*** *mean ± SD (%)*	***Diapause protocol****	***Age*** *(days)*	***Figure***
Pdf>Na$^+$ChBac	8.3 ± 5.1	*PROTOCOL 1*	11	*Figure 15A (page 58)*
+>Na$^+$ChBac	51.2 ± 6.5			
Pdf>Pdf	16.0 ± 5.4			
+>Pdf	37.3 ± 5.4			
Pdf>+	68.2 ± 1.6			
elav>2xsNPF	6.6 ± 3.2	*PROTOCOL 1*	11	*Figure 15B (page 58)*
elav>+	67.5 ± 6.6			
+>2xsNPF	43.8 ± 1.4			
Pdf>2xsNPF	4.3 ± 1.7	*PROTOCOL 1*	11	*Figure 15C (page 58)*
Pdf>+	59.8 ± 2.7			
R6>2xsNPF	13.5 ± 5.1			
R6>+	52.7 ± 6.2			
+>2xsNPF	29.8 ± 4.6			
Pdf>kir2.1	49.5 ± 6.3	*PROTOCOL 1*	11	*Figure 16A (page 59)*
+>kir2.1	40.9 ± 2.0			
Pdf>hid	65.5 ± 2.3			
+>hid	38.6 ± 5.6			
Pdf>+	40.3 ± 4.4			
Pdf>Ork	55.7 ± 10.9	*PROTOCOL 1*	11	*Figure 16B (page 59)*
Pdf>+	31.8 ± 4.7			
+>Ork	19.4 ± 5.9			
dilp2(p)>sNPFR1-DN	34.6 ± 12.7	*PROTOCOL 1*	11	*Figure 16C (page 59)*
dilp2(p)>+	26.5 ± 8.2			
Insp3>sNPFR1-DN	77.1 ± 9.9			
Insp3>+	57.1 ± 4.2			
+>sNPFR1-DN	16.4 ± 6.0			
Crz_1>Na$^+$ChBac	26.8 ± 6.7	*PROTOCOL 1*	11	*Figure 17B (page 62)*
Crz_1>+	24.3 ± 6.7			
+>Na$^+$ChBac	65.4 ± 6.7			
Crz_2>2xsNPF	46.1 ± 5.8	*PROTOCOL 1*	11	*Figure 17C (page 62)*
Crz_2>+	70.5 ± 2.7			
+>2xsNPF	43.1 ± 1.4			
Crz_1>Crz-RNAi$_1$	81.4 ± 2.7	*PROTOCOL 1*	11	*Figure 17D (page 62)*
Crz_1>Crz-RNAi$_2$	52.6 ± 5.4			
Crz_2>Crz-RNAi$_1$	83.3 ± 4.2			
Crz_2>Crz-RNAi$_2$	79.8 ± 4.6			
Crz_1>+	42.8 ± 4.8			
Crz_2>+	74.0 ± 10.7			
+> Crz-RNAi$_1$	68.6 ± 2.0			
+>Crz-RNAi$_2$	52.0 ± 7.0			

Genotype	***Diapause level*** *mean ± SD (%)*	***Diapause protocol****	***Age*** *(days)*	***Figure***
gal1118>Na^{+}ChBac	9.1 ± 6.3	*PROTOCOL 1*	11	*Figure 20B (page 71)*
+>Na^{+}ChBac	44.6 ± 8.2			
gal1118>Pdf	19.7 ± 8.2			
+>Pdf	41.6 ± 7.5			
gal1118>Ork	25.3 ± 10.2			
+>Ork	29.9 ± 9.9			
gal1118>+	45.1 ± 12.1			
Hu-S	6.6 ± 3.0	*PROTOCOL 1*	11	*Figure 21A (page 73)*
Hu-S Pdf^{01}	14.2 ± 3.6			
Hu-LS	34.8 ± 3.6			
Hu-LS Pdf^{01}	38.3 ± 6.1			
Hu-S	23.6 ± 7.3	*PROTOCOL 2*	11	*Figure 21B (page 73)*
Hu-S Pdf^{01}	9.2 ± 1.8			
Hu-LS	43.9 ± 7.6			
Hu-LS Pdf^{01}	51.9 ± 4.6			
Hu-S	6.4 ± 2.4		30	*Figure 21D (page 73)*
Hu-S Pdf^{01}	1.8 ± 1.5			
Hu-LS	72.1 ± 3.1			
Hu-LS Pdf^{01}	6.3 ± 1.8			
han	22.2 ± 7.3	*PROTOCOL 2*	11	*Figure 21F (page 73)*
control	57.4 ± 11.6			
han	11.4 ± 2.3		30	
control	41.7 ± 8.2			

* Flies were grown either at 23°C in LD 12:12 (PROTOCOL 1) or at 18°C in LD 18:6 (PROTOCOL 2) before being exposed to diapause inducing conditions (12°C, LD 8:16).

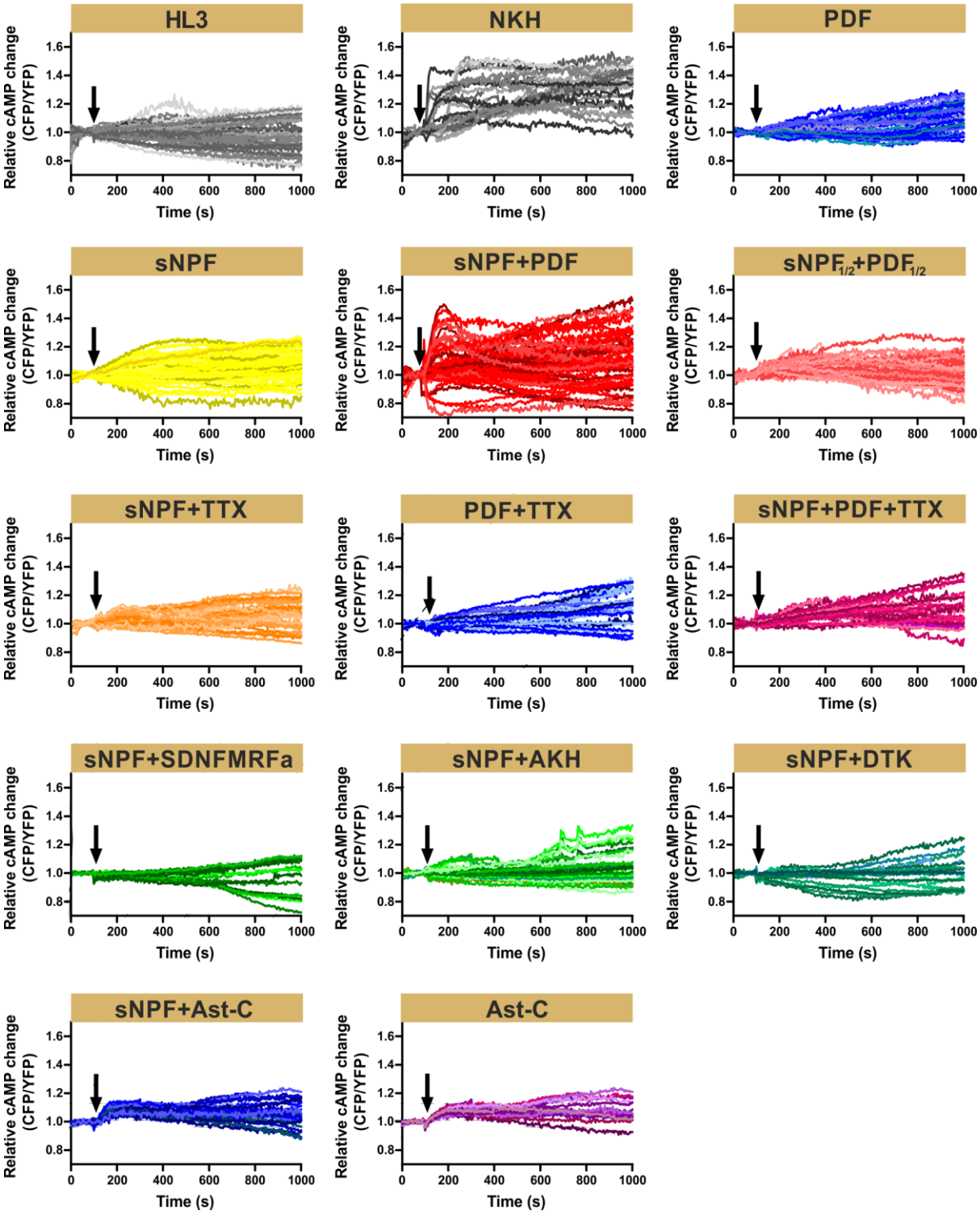

Figure 1. Single neuron traces recorded during live optical imaging in the insulin producing cells. Inverse FRET traces (CFP/YFP) of IPCs reflecting intracellular cAMP changes. Black arrow indicates the application point of the different substances at ~100 s. HL3: hemolymph-like saline (negative control); NKH: forskolin derivate (positive control); PDF: pigment dispersing factor; sNPF: short neuropeptide F; AKH: adipokinetic hormone; DTK: Drosophila tachykinin; Ast-C: allatostatin-C; TTX: tetrodotoxin (sodium channel blocker).

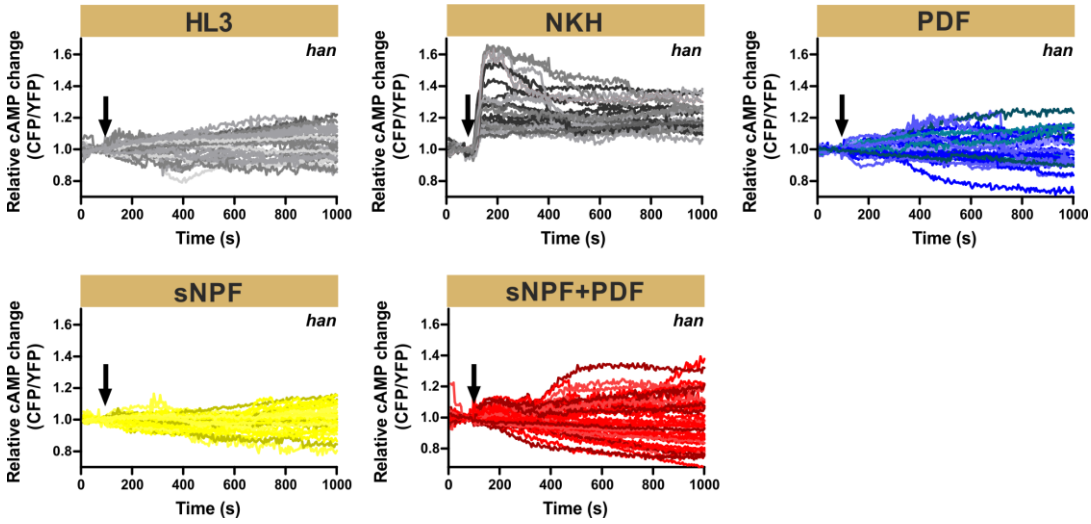

Figure 2. Single neuron traces recorded during live optical imaging in the insulin producing cells - PDFR null mutant (han) background. Inverse FRET traces (CFP/YFP) of IPCs reflecting intracellular cAMP changes. Black arrow indicates the application point of the different substances at ~100 s. HL3: hemolymph-like saline (negative control); NKH: forskolin derivate (positive control); PDF: pigment dispersing factor; sNPF: short neuropeptide F; TTX: tetrodotoxin (sodium channel blocker).

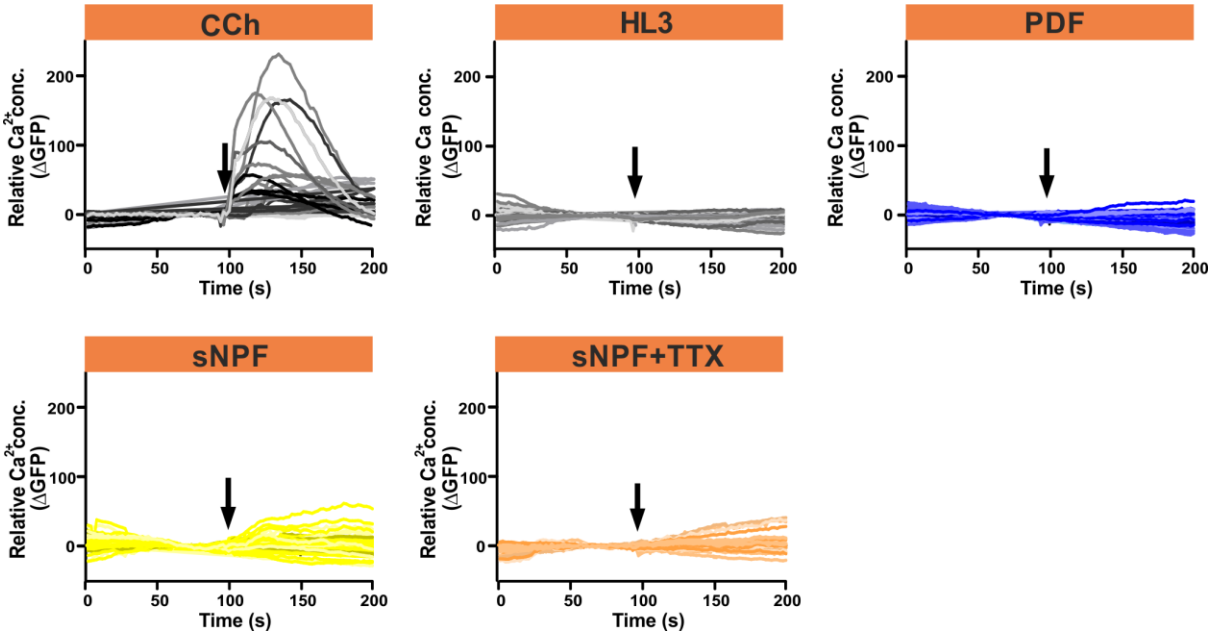

Figure 3. Single neuron traces recorded during calcium imaging in the insulin producing cells. Average changes in GFP fluorescence of IPCs reflecting intracellular changes in Ca^{2+} levels. Black arrow indicates the application point of the different substances at ~100 s. HL3: hemolymph-like saline (negative control); CCh: carbamylcholine (positive control); PDF: pigment dispersing factor; sNPF: short neuropeptide F; TTX: tetrodotoxin (sodium channel blocker).